National Research Council Canada

Conseil national de recherches Canada

NRC·CNRC

Canadian Journal of Fisheries and Aquatic Sciences

Journal canadien des sciences halieutiques et aquatiques

http://cjfas.nrc.ca

http://jcsha.cnrc.ca

ISSN 0706-652X / CJFSDX 60(10) 1177–1306 (2003)

The *Canadian Journal of Fisheries and Aquatic Sciences*, previously published as *Contributions to Canadian Biology* 1901–1925, *Contributions to Canadian Biology and Fisheries* 1926–1934, *Journal of the Biological Board of Canada* 1934–1937, and *Journal of the Fisheries Research Board of Canada* 1938–1979, is issued monthly to form annual volumes of 12 numbers plus supplements.

Editorial policy. The Journal publishes original research articles, perspectives (syntheses, critiques, re-evaluations), discussions (comment and reply), and rapid communications. Manuscripts may concern cells, organisms, populations, communities, ecosystems, or processes that affect aquatic systems. They may cover a range of disciplines including biology and ecology of marine and freshwater organisms, limnology, oceanography, physiology, toxicology, genetics, economics, disease, and management. Preference will be given to manuscripts that emphasize understanding of observed phenomena and interpretation of experimental results. The Journal encourages papers that lead from clearly stated purpose or rationale and from testable hypotheses, concepts, or questions to identifiable conclusions or syntheses. Such papers may amplify, modify, question, or redirect accumulated knowledge embodied in contemporary perceptions of a particular state of aquatic sciences. The Journal discourages papers that are essentially descriptive, except in emerging disciplines; have only site-specific or local applications (a certain year, place, taxon, chemical compound, etc.); only confirm previously established principles; or apply standard techniques without breaking new methodological ground.

Manuscripts for publication should be submitted to the Senior Editor, *Canadian Journal of Fisheries and Aquatic Sciences*, Department of Zoology, University of Guelph, Guelph, ON N1G 2W1, Canada (519-824-4120 ext. 52646; fax: 519-767-9798; e-mail: cjfas@uoguelph.ca).

Submissions in either English or French are acceptable. The information must be original, that is, not copyrighted, published, or submitted elsewhere except in abstract form or unless by written consent of the Editor.

Correspondence concerning accepted manuscripts and corrected proofs should be sent to NRC Research Press, National Research Council of Canada, Ottawa, ON K1A 0R6, Canada (fax: 613-952-7656; e-mail: research.press@nrc.gc.ca).

Instructions to Authors are published once a year in the first issue of each volume. Copies are available from NRC Research Press or at http://cjfas.nrc.ca. The **Publication Policy** of NRC Research Press is available at http://cjfas.nrc.ca.

Microfilm. Issues from 1934 through the current volume can be purchased on 16- or 35-mm microfilm. Photocopies of individual articles or issues can be purchased from University Microfilms International, 330 North Zeeb Road, Ann Arbor, MI 48106, U.S.A.

U.S. periodical postage paid at Champlain, N.Y., and at additional mailing offices. Attention U.S. POSTMASTER: Send address changes to **Canadian Journal of Fisheries and Aquatic Sciences**, c/o USACAN Media Distribution Center, P.O. Box 2888, Plattsburg, NY 12901, U.S.A.

Publié sans interruption depuis 1901, le *Journal canadien des sciences halieutiques et aquatiques* a paru sous plusieurs titres : *Contributions to Canadian Biology* 1901–1925, *Contributions to Canadian Biology and Fisheries* 1926–1934, *Journal of the Biological Board of Canada* 1934–1937, et *Journal of the Fisheries Research Board of Canada* 1938–1979. Le Journal paraît tous les mois, formant ainsi un volume de 12 numéros, et offre en plus jusqu'à deux suppléments par année.

Politique éditoriale. On publie, dans le Journal, des articles rendant compte de recherche originale, des perspectives (synthèses, critiques et réévaluations), des discussions (commentaires et réponses) et des communications rapides. Les documents peuvent porter sur les cellules, organismes, populations, communautés, écosystèmes ou processus qui affectent les systèmes aquatiques. Ils peuvent relever de divers domaines y compris la biologie et l'écologie des organismes marins et d'eau douce, la limnologie, l'océanographie, la physiologie, la toxicologie, la génétique, l'économie, la pathologie et la gestion. On accorde la préséance aux articles qui contribuent à la compréhension de phénomènes observés et à l'interprétation de résultats expérimentaux. On invite les auteurs à soumettre des articles ayant des objectifs précis ou relevant d'hypothèses, de concepts ou de questions vérifiables et se terminant par de solides conclusions ou d'utiles synthèses. Ces articles enrichissent, changent, mettent en question ou réorientent les connaissances acquises sur divers aspects des sciences aquatiques. On décourage toutefois la soumission d'articles simplement descriptifs (à moins qu'il ne s'agisse de nouvelles disciplines), d'application très limitée (applicables à une seule année, une seule région ou un seul taxon, portant sur un unique composé chimique, etc.); d'articles qui ne font que reprendre les principes énoncés dans des articles précédents; et d'articles rendant compte de l'application de normes sans gain de méthodologie.

Les auteurs voudront adresser leurs **manuscrits** à la directrice scientifique principale, *Journal canadien des sciences halieutiques et aquatiques*, Department of Zoology, University of Guelph, Guelph, ON N1G 2W1, Canada (519-824-4120 poste 52646; télécopieur : 519-767-9798; courriel : cjfas@uoguelph.ca).

Les contributions peuvent être en anglais ou en français. Elles doivent être originales, c.-à.-d. qu'elles ne doivent pas avoir fait l'objet d'un copyright, avoir été publiées ou soumises ailleurs, sauf sous forme abrégée ou avec le consentement du rédacteur. Le CNRC ne se tient en aucune façon responsable des opinions exprimées par un collaborateur ou des déclarations qui pourrait faire ce dernier.

La correspondance ayant trait aux manuscrits acceptés et les **épreuves corrigés** doivent être envoyées aux Presses scientifiques du CNRC, Conseil national de recherches du Canada, Ottawa, ON K1A 0R6, Canada (télécopieur : 613-952-7656; courriel : presses.scientifiques@cnrc.gc.ca).

Les Recommandations aux auteurs sont publiées une fois par année dans le premier numéro de chaque volume. Des copies sont disponibles auprès du Bureau de la rédaction aux Presses scientifiques du CNRC ou au http://jcsha.cnrc.ca. **La Politique de publication** est disponible auprès des Presses scientifiques du CNRC ou au http://jcsha.cnrc.ca.

Microfilms. On peut acheter sur microfilms de 16 ou 35 mm tous les numéros depuis 1934. Des photocopies d'articles ou de numéros individuels sont aussi en vente auprès de University Microfilms International, 330 North Zeeb Road, Ann Arbor, MI 48106, É.-U.

This Journal is indexed or abstracted in / Cette revue est signalée ou résumée dans
ABSEARCH, Aquatic Sciences and Fisheries Abstracts, Biological Abstracts, Biological & Agricultural Index, CAB Abstracts, Chemical Abstracts, Current Contents, Elsevier BIOBASE, Environmental Abstracts, Environmental Periodicals Bibliography, GEOBASE, GeoRef, Internationale Bibliographie der Zeitschriftenliteratur, Life Sciences Collection, Meteorological and Geoastrophysical Abstracts, Oceanic Abstracts, PASCAL Database, and Science Citation Index.

Volume 60, Number 10, October 2003

Canadian Journal of Fisheries and Aquatic Sciences

Published by the National Research Council of Canada

Volume 60, numéro 10, octobre 2003

Journal canadien des sciences halieutiques et aquatiques

Publié par le Conseil national de recherches du Canada

Senior Editor / Directrice scientifique principale **Moira M. Ferguson**

Editors / Directeurs

Jeffrey A. Hutchings, *Dalhousie University, Halifax*
Pierre Pepin, *Northwest Atlantic Fisheries Centre, DFO/MPO, St. John's, Newfoundland*
W. Gary Sprules, *University of Toronto at Mississauga*
Assistant to the Editors / Adjointe aux directeurs scientifiques **Holly Foster**

Associate Editors / Directeurs scientifiques associés

M.T. Arts, *Environment Canada, Burlington*
D. Boisclair, *Université de Montréal*
U. Borgmann, *Environment Canada, Burlington*
S.E. Campana, *DFO/MPO, Dartmouth*
R. Carignan, *Université de Montréal*
J.J. Dodson, *Université Laval*
G.T. Evans, *DFO/MPO, St. John's, Newfoundland*
K.T. Frank, *DFO/MPO, Dartmouth*
M.M. Hansen, *Danish Institute for Fisheries Research, Silkeborg, Denmark*
R. Hilborn, *University of Washington*
A. Hontela, *Université du Québec à Montréal*
D.F. Houlihan, *University of Aberdeen*
F.A. Huntingford, *University of Glasgow*
G.S. Jamieson, *DFO/MPO, Nanaimo*
B. Jonsson, *Norwegian Institute for Nature Research, Oslo, Norway*
P. Magnan, *Université du Québec à Trois Rivières*
C.T. Marshall, *University of Aberdeen*
R.B. Millar, *University of Auckland, New Zealand*
Y.T. Prairie, *Université du Québec à Montréal*
T.J. Quinn II, *University of Alaska–Fairbanks, Juneau, Alaska*
T.P. Quinn, *University of Washington*
R.D. Robarts, *Environment Canada, Saskatoon*
B. Sainte-Marie, *DFO/MPO, Mont-Joli*
D.W. Schindler, *University of Alberta*
R.E.H. Smith, *University of Waterloo*
S.J. Smith, *DFO/MPO, Dartmouth*
W.F. Vincent, *Université Laval*
R.D. Vinebrooke, *University of Regina*
C.J. Walters, *University of British Columbia*
R.D. Ward, *CSIRO Marine Research, Australia*
B. de Young, *Memorial University of Newfoundland*

NRC Research Press / Presses scientifiques du CNRC

Editor-in-chief / Directeur général **Bruce P. Dancik**
Assistant Editor-in-chief / Directeur général adjoint **Iain E.P. Taylor**

Journals Program / Programme des revues

(Fax / Télécopieur : 613-952-7656; e-mail: research.press@nrc.gc.ca / courriel : presses.scientifiques@cnrc.gc.ca; URL: http://pubs.nrc-cnrc.gc.ca)
Director / Directrice **Aldyth Holmes**
Business Manager / Gestionnaire des affaires **Paul McClymont**
Manager, Journals Program / Gestionnaire, Programme des revues **Carolyn Brown**
Managing Editor / Rédactrice administrative **Cecily M. Pearson** (613-993-9099)
Publication Officers / Agentes de publication **Jennifer McColl**
Advertising / Annonces publicitaires **Judy Gorman** (613-993-0151)
Reprints / Tirés à part **Roxanne Landriault** (613-990-2254)
Subscriptions / Abonnements **Eileen Evans-Nantais** (613-990-7873)

The National Research Council of Canada accepts no responsibility for statements or opinions expressed by a contributor. Acceptance of an advertisement, announcement, or other material does not imply endorsement by either the Journal's Senior Editor or the National Research Council.

© National Research Council of Canada 2003. All rights reserved.

No part of this publication may be reproduced, stored, or transmitted in any form or by any means, without the written permission of the publisher, except as stated below.

The National Research Council of Canada grants **permission*** to individuals to make single copies of articles for personal use. Any person may reproduce short excerpts from articles in the journal for any purpose that respects the moral rights of authors, provided that the source is fully acknowledged. As a courtesy, the consent of authors of such material should be obtained directly from the author.

Authorization to reproduce items for other than personal use, as stated above, is granted by the National Research Council of Canada provided that the copyright fee of $7.00 per copy is paid directly to CANCOPY, One Yonge Street, Suite 1900, Toronto, ON M5E 1E5, Canada.

*The above permission does not extend to other kinds of copying, such as copying for general distribution, for advertising, or promotional purposes, for creating new collective works, or for resale. For such copying, arrangements must be made with the publisher, National Research Council of Canada, Ottawa, ON K1A 0R6, Canada.

Subscription information

The *Canadian Journal of Fisheries and Aquatic Sciences* (ISSN 0706-652X) is published monthly by the National Research Council of Canada. The 2003 annual subscription rates (second class postage) for Canada are $830CAN institutional and $257CAN personal, for US & foreign $830US institutional and $257US personal. For air mail add $175US to foreign rate. Canadian customers please include 7% GST (business no. 12149 1807 RT 0275). Subscriptions are entered for the calendar year. Remittances should be made payable to the Receiver General for Canada credit NRC. Price for regular single issues: institutional, $105.00; personal, $35.00. Supplements will be priced separately. Special rates apply to members of Canadian scientific and engineering societies if they subscribe through their respective societies.

There are no refunds on cancelled subscriptions once delivery has begun. Claims for missing issues should be made within four months (N. America) or six months (outside N. America) following the date of publication. The publisher expects to supply missing issues only when losses have occurred in transit and when the reserve stock will permit. For change of address and subscription enquiries: Subscription Office, NRC Research Press, National Research Council of Canada, Ottawa, ON K1A 0R6, Canada; tel.: 613-993-9084; fax: 613-952-7656; e-mail: research.press@nrc.gc.ca.

Microform backfiles are available from UMI, P.O. Box 1346, Ann Arbor, MI 48106-1346, U.S.A., and Micromedia Ltd., 20 Victoria St., Toronto, ON M5C 2N8, Canada.

All issues of the *Canadian Journal of Fisheries and Aquatic Sciences* since 1996 are available on the Web. Pricing information can be found at http://cjfas.nrc.ca.

Le Conseil national de recherches du Canada ne se tient en aucune façon responsable des opinions exprimées par un collaborateur ou des déclarations que pourrait faire ce dernier. La publication d'annonces publicitaires, d'avis et autres n'implique pas l'endossement de leur contenu par la directrice principale de la Revue ou le CNRC.

© Conseil national de recherches du Canada 2003. Tous droits réservés.

Il est interdit de reproduire, de sauvegarder ou de transmettre quelque partie de la présente publication dans quelque format ou de quelque façon sans le consentement écrit de l'éditeur, à l'exception des conditions suivantes.

Le Conseil national de recherches du Canada accorde aux particuliers le droit de faire des copies individuelles pour leur usage personnel. Toute personne peut reproduire de courts extraits des articles de la Revue pour autant que les droits moraux de l'auteur soient respectés et que la mention de provenance soit clairement indiquée. Il est de convenance de demander le consentement de l'auteur avant de faire mention de son travail.

On obtiendra l'autorisation de reproduire des articles à d'autres fins que l'usage personnel (tel qu'on l'a décrit ci-dessus) auprès du Conseil national de recherches du Canada pour autant que des redevances de droits d'auteurs de 7,00 $/copie soient versées au CANCOPY, 1, rue Yonge, bureau 1900, Toronto, ON M5E 1E5, Canada.

*La permission ci-dessus ne s'applique pas à la reproduction à grande échelle, telle que la reproduction aux fins de distribution générale, publicitaire ou promotionnelle, de compilation de nouveaux ouvrages collectifs ou de revente. Dans de tels cas, il faudra ratifier une entente particulière avec l'éditeur, le Conseil national de recherches du Canada, Ottawa, ON K1A 0R6, Canada.

Renseignements sur l'abonnement

Journal canadien des sciences halieutiques et aquatiques (ISSN 0706-652X) est une publication mensuelle du Conseil national de recherches du Canada. Le prix de l'abonnement annuel au Canada (courrier de deuxième classe) est de 830 $CAN pour les organismes et de 257 $CAN pour les particuliers. À l'étranger (y compris les É.-U.), le prix de l'abonnement est de 830 $US pour les organismes et de 257 $US pour les particuliers. L'expédition par avion exige des frais de 175 $US en sus du prix d'abonnement à l'étranger. Les clients du Canada doivent ajouter la TPS de 7% (numéro d'entreprise 12149 1807 RT 0275). Les abonnements sont pour l'année civile. Tout paiement doit être adressé au Receveur général du Canada, crédit du CNRC. Le prix par numéro est de 105 $ pour les organismes et de 35 $ pour les particuliers. Le prix des hors-série varie. Les membres des sociétés canadiennes de sciences et de génie bénéficient de taux préférentiels en s'abonnant via leurs sociétés respectives.

Aucun remboursement ne sera accordé ni aucune annulation acceptée une fois que les livraisons auront commencé. Les réclamations de numéros manquants devront être soumises dans les quatre mois (Amérique du Nord) ou dans les six mois (à l'extérieur de l'Amérique du Nord) suivant la date de publication. L'éditeur ne fournira de numéros manquants que si le document a été perdu pendant l'expédition et que si le stock le permet. Adressez tout changement d'adresse ou toute question quant à l'abonnement au : Bureau des abonnements, Presses scientifiques du CNRC, Conseil national de recherches Canada, Ottawa, ON K1A 0R6, Canada; téléphone : 613-993-9084; télécopieur : 613-952-7656; courriel : presses.scientifiques@cnrc.gc.ca.

On peut obtenir les fichiers rétrospectifs sur **microforme** auprès de UMI, P.O. Box 1346, Ann Arbor, MI 48106-1346, É.-U., et auprès de Micromedia Ltée, 20, rue Victoria, Toronto, ON M5C 2N8, Canada.

À partir de 1996, tous les numéros de *Journal canadien des sciences halieutiques et aquatiques* sont accessibles sur le Web. On trouvera des renseignements sur les tarifs à http://jcsha.cnrc.ca.

Sedimentary Cladoceran remains and their relationship to nutrients and other limnological variables in 53 lakes from British Columbia, Canada

Darren G. Bos and Brian F. Cumming

Abstract: To develop models to predict past lake-water nutrient levels, the sedimentary remains of Cladocera were sampled from 53 lakes in central British Columbia, Canada. At the same time, the lakes were sampled for a suite of chemical variables. In addition, a host of physical and spatial explanatory variables were collected from each site. Canonical correspondence analysis showed that total phosphorus (TP), which ranged from 5 to 146 $\mu g \cdot L^{-1}$, was the measured environmental variable that best described the differences in species composition among the lakes. Additionally, lake depth and surface water temperature were also important in explaining the distribution of cladoceran taxa. *Chydorus brevilabris*, *Daphnia ambigua*, *Daphnia* cf. *pulex*, and *Graptoleberis testudinaria* had a preference for eutrophic lakes, whereas *Acroperus harpae*, *Alonella nana*, *Alonella excisa*, *Chydorus piger*, *Daphnia* cf. *dentifera*, and *Eubosmina* spp. were found in the less productive lakes. Predictive models to estimate TP from species abundance data were developed using weighted averaging techniques. This research has produced strong and significant inference models, which can now be used to reconstruct past changes in lake trophic status from remains of Cladocera in sediment cores.

Résumé : Des prélèvements de restes de cladocères dans les sédiments de 53 lacs du centre de la Colombie Britannique, Canada, nous ont servi à mettre au point des modèles pour évaluer les concentrations passées des nutriments dans l'eau des lacs. Au même moment, nous avons aussi mesuré une série de variables chimiques et noté plusieurs variables explicatives physiques et spatiales à chacun des sites. Une analyse canonique des correspondances révèle que le phosphore total (TP), qui varie de 5 à 146 $\mu g \cdot L^{-1}$, est la variable environnementale mesurée qui explique le mieux les différences de composition en espèces entre les lacs; la profondeur du lac et la température de surface de l'eau sont aussi des facteurs explicatifs importants de la répartition des taxons de cladocères. *Chydorus brevilabris*, *Daphnia ambigua*, *Daphnia* cf. *pulex* et *Graptoleberis testudinaria* préfèrent les lacs eutrophes, alors que *Acroperus harpae*, *Alonella nana*, *Alonella excisa*, *Chydorus piger*, *Daphnia* cf. *dentifera* et *Eubosmina* spp. se retrouvent dans les lacs moins productifs. Nous avons développé des modèles prédictifs qui permettent d'estimer TP d'après l'abondance des espèces à l'aide de techniques des moyennes pondérées. Ces modèles d'inférence solides et significatifs peuvent servir à déterminer le statut trophique antérieur des lacs, à partir des restes de cladocères dans des carottes de sédiments.

[Traduit par la Rédaction]

Introduction

Significant advances have been made over the last several decades in reconstructing past nutrient conditions using siliceous algal remains (Hall and Smol 1999). Improvements in core retrieval, extraction, and sectioning, along with improvements in statistical techniques, have allowed for increasingly accurate estimates of past nutrient conditions (e.g., Reavie et al. 1995; Hall and Smol 1999). However, the development of Cladocera as paleolimnological indicators has lagged in this field, even though they may provide an additional and strong technique to study past nutrient conditions in lakes. With the exception of one study from Denmark in which Brodersen et al. (1998) developed a quantitative model to infer total phosphorus (TP), the Cladocera have only been used qualitatively to infer nutrient conditions (e.g., Whiteside 1970; Boucherle and Zullig 1983; Hann et al. 1994). In North America, very little quantitative data exist describing the distribution of cladocerans in relation to measured environmental variables. However, experimental evidence from planktonic Cladocera (mainly *Daphnia* and *Bosmina*) shows that Cladocera can be directly affected by phosphorous availability in their environment (Urabe et al. 1997) and that differences exist between different genera in their phosphorus

Received 8 October 2002. Accepted 31 July 2003. Published on the NRC Research Press Web site at http://cjfas.nrc.ca on 30 October 2003.
J17131

D.G. Bos.[1] Parks Canada Western Service Centre, 300–300 West Georgia St., Vancouver, BC V6B 6B4, Canada.
B.F. Cumming. Paleoecological Environmental Assessment and Research Lab (PEARL), Biology Department, Queen's University, Kingston, ON K7L 3N6, Canada.

[1]Corresponding author (e-mail: Darren.Bos@pc.gc.ca).

 doi: 10.1139/F03-097 © 2003 NRC Canada

requirements (Schulz and Sterner 1999). These differences in mineral limitation likely contribute to changes in species composition seen across trophic gradients. Along with these direct effects, differences in nutrient levels may also affect the Cladocera by changing their food quality (Sterner et al. 1993; Plath and Boersma 2001) and habitat (Whiteside 1970; Hann 1990).

This research was undertaken to develop predictive models that could infer TP based on the relationship between the present-day distributions of cladoceran assemblages and lake-water TP in British Columbia, Canada. In a paleolimnological context, these models will be useful in examining past changes in lake phosphorus levels through analysis of subfossil remains of cladocerans in sediment cores and thus may be used in setting realistic remediation goals in anthropogenically influenced ecosystems. Additionally, this research provides valuable ecological information on the distribution and environmental preferences for many of the cladoceran species of British Columbia, Canada.

Materials and methods

Study area

Research was conducted in central British Columbia, Canada (Fig. 1). This part of British Columbia's interior plateau lies within the subboreal spruce biogeoclimatic zone, which is characterized by white spruce (*Picea glauca* (Moench) Voss) and lodgepole pine (*Pinus contorta* var. *latifolia* (Engelm.) Critchfield). Average rainfall is 620 mm, occurring predominantly between May and October with an additional 230 cm of snowfall usually between November and March (Valentine et al. 1978). Generally, the plateau is underlain by fine to medium-fine glacial till derived from base-rich volcanics. Grey luvisolic soils derived from the till are dominated by sand and silt with a thin organic layer on top (Valentine et al. 1978). Cattle ranching, farming, and forestry are present within many of the lake catchments, and cottage development is expanding, although many lakes remain unsettled. Lakes in the study region vary from oligotrophic to hypereutrophic, with the majority being mesotrophic in character. A wide variety of limnological conditions are present; there is an abundance of warm shallow polymictic lakes, although deep dimictic lakes are also common.

Sampling

Using spring TP values collected by the Prince George Ministry of Environment as a guide to lake trophic status, 27 lakes were selected that varied considerably in their spring TP values (Fig. 2). An additional 26 lakes without previous TP data were also included to increase the number of lakes available for calibrating the relationship between cladoceran species composition and a gradient of TP. All 53 lakes were sampled for water chemistry (including TP) between 6 July and 8 August 1997. Surface sediment samples (the uppermost 1 cm of the cores) were collected from the study lakes using a miniature gravity corer (Glew 1991). Contemporaneously, surface water samples were taken from both the pelagic and littoral zone; these were immediately shipped to the Pacific Environmental Science Center in Vancouver for analysis of dissolved solutes including Ba, Be, Ca, Cl, Cd, Co, Cr, Cu, Fe, Fl, K, Mg, Mn, Mo, Na, Ni, Pb, Si, SO_4, Sr, Zn, dissolved organic carbon (DOC), dissolved inorganic carbon (DIC), total nitrogen (TN), nitrate, nitrite, ammonia, and TP. While at each lake, measurements of conductivity, dissolved oxygen, pH, and temperature were taken with a Hydrolab® water-quality data transmitter (Hydrolab-Hach Co., Loveland, CO 80539-0389), as well as an Orion® model 240A pH meter (Thermo Orion, Beverly, MA 01915). Secchi disk measurements and net tows of plankton were also taken. Reference samples of the meiobenthic Cladocera were taken using a dip net with a 100-µm mesh. Lake area was calculated using 1 : 50 000 scale topographic maps. The percentage of the lake area that was littoral habitat was defined by using bathymetric maps from the Prince George Ministry of Environment to calculate the area that was shallower than the measured Secchi disk depth. Geographic coordinates were recorded at each lake using a Magellan 6-channel handheld global positioning system (GPS; Magellan GPS, Santa Clara, CA 95050-4300), coordinates were confirmed using 1 : 50 000 scale maps.

Submicrofossil preparation

Following sample preparation methods outlined by Frey (1986), 3 mL of wet sediment was taken from each sample and treated with 200 mL of 10% KOH. Samples were heated at 80 °C in a water bath for 1 h to defloculate the sediment. After defloculation, samples were placed on a 34-µm screen and rinsed with distilled water. Material retained on the screen was then rinsed into a small vial and topped up to 5 mL with distilled water. One drop of formaldehyde was added to prevent fungal growth.

Before plating cladoceran remains on slides, each vial was shaken until the contents were homogenized. A 100-µL aliquot of this slurry was removed and plated onto a microscope slide on a slide warmer to reduce the amount of water. When almost all of the water had evaporated, a drop of molten glycerin jelly was placed on the sample and mixed with a pin. A coverslip was then placed on each slide and the sample was allowed to set overnight at 35 °C on a slide warmer.

Remains were identified and enumerated at 400× magnification using a Leica DMRB microscope equipped with phase-contrast optics (Leica Microsystems Canada Inc., Richmond Hill, ON L4B 1L5, Canada). Entire coverslips were counted to avoid bias that could occur from an unequal distribution of remains on the slide. For each lake, slides were counted until at least 100 individuals had been enumerated. To determine the number of individuals, remains were adjusted to reflect the numbers produced from each individual (e.g., each individual cladoceran has two sides to its carapace and two postabdominal claws, so the number of these remains are divided by two, whereas each individual has only one headshield). For each species, only the most abundant remains counted (after the adjustment described above) were used as the number of individuals (Goulden 1969; Frey 1986). For most lakes, it was necessary to count more than one coverslip to enumerate a sufficient number of remains to obtain a stable relative abundance.

Taxonomy

Taxonomy followed Bos (2001), Chengalath and Hann (1981), De Melo and Hebert (1994), Frey (1959, 1960, 1962,

© 2003 NRC Canada

Fig. 1. Map of British Columbia showing the 53 study lakes. Inset map shows location of British Columbia (BC) in Canada.

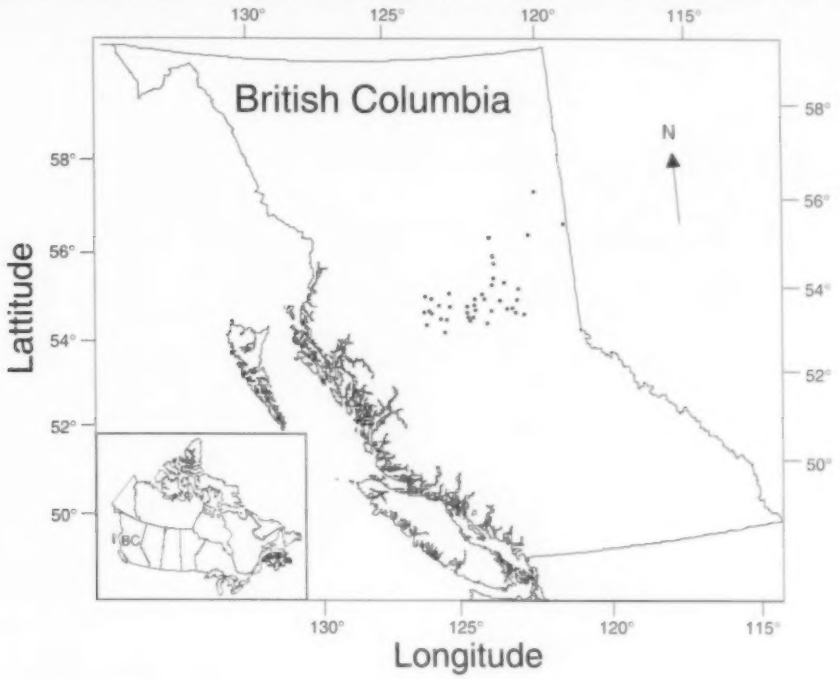

Fig. 2. Spring total phosphorus (TP) values provided by the Prince George Ministry of the Environment for 26 lakes that were sampled in this study.

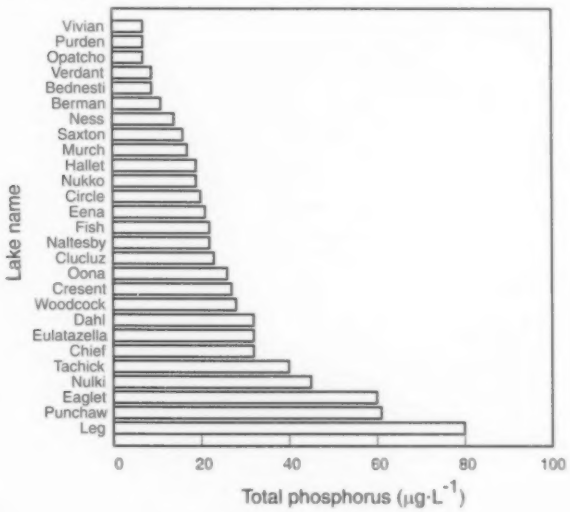

1965 1980, 1985), Hann (1981), Hebert (1995), Megard (1967), and Smirnov (1974, 1996). Samples taken from plankton tows and dip nets were also used to confirm the identification of the cladoceran species.

Taxonomy for Cladocera from North American (particularly the benthic forms) is still not complete. As outlined by Frey (1980, 1987) and Korovchinsky (1996), many of the North American species are morphologically similar to their European counterparts but differ in fine taxonomic detail. Unfortunately, the remains of Cladocera preserved in the sediments do not have sufficient detail to distinguish the important features that could be used to separate these species (e.g., leg morphology can be critical to separating species, yet these remains are never recovered from lake sediments). However, because a calibration approach is used here, it is sufficient to be able to separate the North American species from one another and to be cognizant that ecological tolerances described here may not be applicable to species that are distant from our study area.

Statistical analysis

Rare species, defined as those taxa that had a relative abundance of less than 1% in three sites, were deleted from the data files before the analysis because of the difficulty in determining the reliability of such low counts and the disproportionate effect that rare species have on ordination (Shi 1993). Environmental variables were also screened to check that they had an even or normal distribution across the data set (Jongman et al. 1995). Environmental variables that showed a skewed distribution were transformed using a square-root, log, or $\log(n + 1)$ transformation. For use in ordination, geographic coordinates were expanded using a cubic polynomial equation to account for the possibility of nonlinear patterns (such as patches or gaps) in the species over space (Legendre 1990).

Detrended correspondence analysis (DCA) was used to determine whether unimodal or linear statistical techniques would be most appropriate to model the species responses across the calibration set (Birks 1995). Following this initial step, correspondence analysis (CA) was then used to investigate the distribution of the species across the study lakes.

© 2003 NRC Canada

Fig. 3. Distribution of the 49 study lakes along a trophic gradient. Trophic categories are after Wetzel (1983). Water samples were taken between 6 July and 8 August 1999.

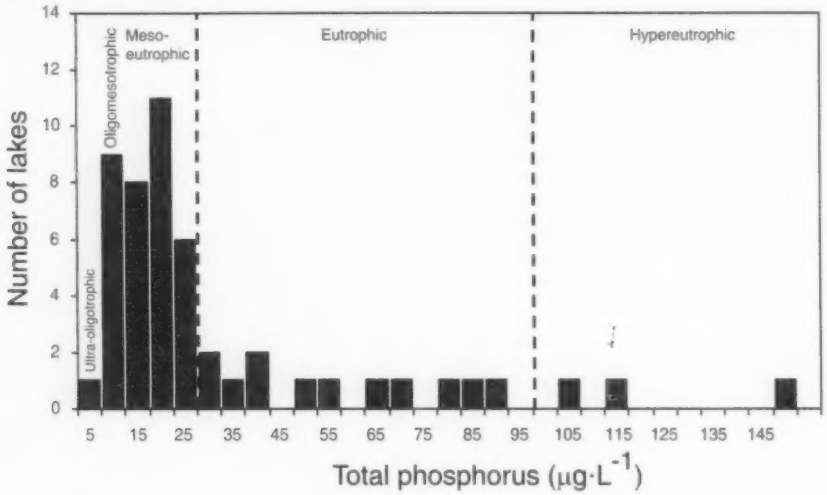

CA is useful to elucidate species clustering and to represent the full variance in species composition across the calibration set. Because CA is an indirect ordination technique, it is often difficult to ascertain the amount of variation that can be explained by measured environmental variables. Instead, canonical correspondence analysis (CCA), a direct ordination technique, was used. Because CCA constrains the ordination of species to a space defined by a linear combination of the measured variables, it allows the variables that best describe the species distribution to be selected, along with determining the amount of variation in the species data that can be described by those variables. Further, a comparison between CA and CCA ordinations allows the investigator to determine if the measured environmental variables can account for the main directions of variability in the species data. Following CCA, detrended canonical correspondence analysis (DCCA) was used to check the length of the environmental gradient. When constrained to a single environmental variable, DCCA may be used to ensure that the gradient length for that single variable is still long enough for unimodal inference models to be developed (Birks 1995).

Following Borcard et al. (1992), variance partitioning was used to investigate the relative importance of spatial versus chemical and physical environmental variables in describing the variation in species composition across sites. To avoid artificially increasing the explained variation, both the environmental and spatial variables were subjected to forward selection, and only significant variables were retained for further analyses (ter Braak 1988). Partially constrained ordinations (ter Braak 1990) were done using the following steps: (1) only the forward-selected chemical and physical environmental variables; (2) only the forward-selected spatial variables; (3) the forward-selected spatial variables with the forward-selected environmental variable as covariables; and (4) the forward-selected environmental variables with the forward-selected spatial variables as covariables. This allows the determination of the amount of variance in the species data that is (*a*) described by the environmental variables alone (sum of canonical eigenvalues from step 4), (*b*) described by the spatial variables alone (step 3), or (*c*) shared by the environmental and spatial variables (steps 1–3 or steps 2–4).

Models to quantitatively infer TP were developed using weighted averaging (WA) and weighted averaging with tolerance downweighting (WA(tol)) using the program WACALIB v. 3.3 (Line et al. 1994). Weighted averaging uses the abundance of a species at each site to determine the contribution of the environmental value at that site to the species optimum. The more abundant a species is at a site, relative to the other sites at which it occurs, the more the environmental value at that site contributes to the optimum (Birks et al. 1990). Similarly, the estimate of the tolerance of a species is obtained by calculating a weighted standard deviation (Birks 1995). After the optimum and tolerance for each species has been calculated, these parameters can then be used to infer environmental conditions based on the species composition of the taxa in that sample. An inverse deshrinking step was used to expand the inferred values (Line et al. 1994). The bootstrapped root-mean-squared error ($RMSE_{boot}$) and the bootstrapped coefficient of determination (r^2_{boot}) were used as the criteria for assessing the predictive ability of the models (Birks 1995). Because planktonic species respond to both TP and fish predation (Jeppesen et al. 1996, 2002), models were also developed using only the littoral taxa, which suffer relatively little predation by fish (Goulden 1971).

Results and discussion

Lake selection and species recovery

Generally, cladoceran remains were abundant and well preserved. Forty-nine of the original 53 lakes were suitable to be used in the planktonic and littoral (full species) model. Bednesti, Pittoney, and Grizzly West lakes were removed from the calibration set because the density of remains was too low to recover sufficient numbers. Jakes Lake was omitted because of a suspect TP value. Although most lakes

© 2003 NRC Canada

Fig. 4. Canonical correspondence analysis ordinations for (*a*) sites, (*b*) environmental variables, and (*c*) species. Species scores are scaled to be a linear combination of site scores. Axes are derived from the variation in the species data set; vectors for the environmental variables are their correlation to the axes and have no influence on the placement of the species or sites.

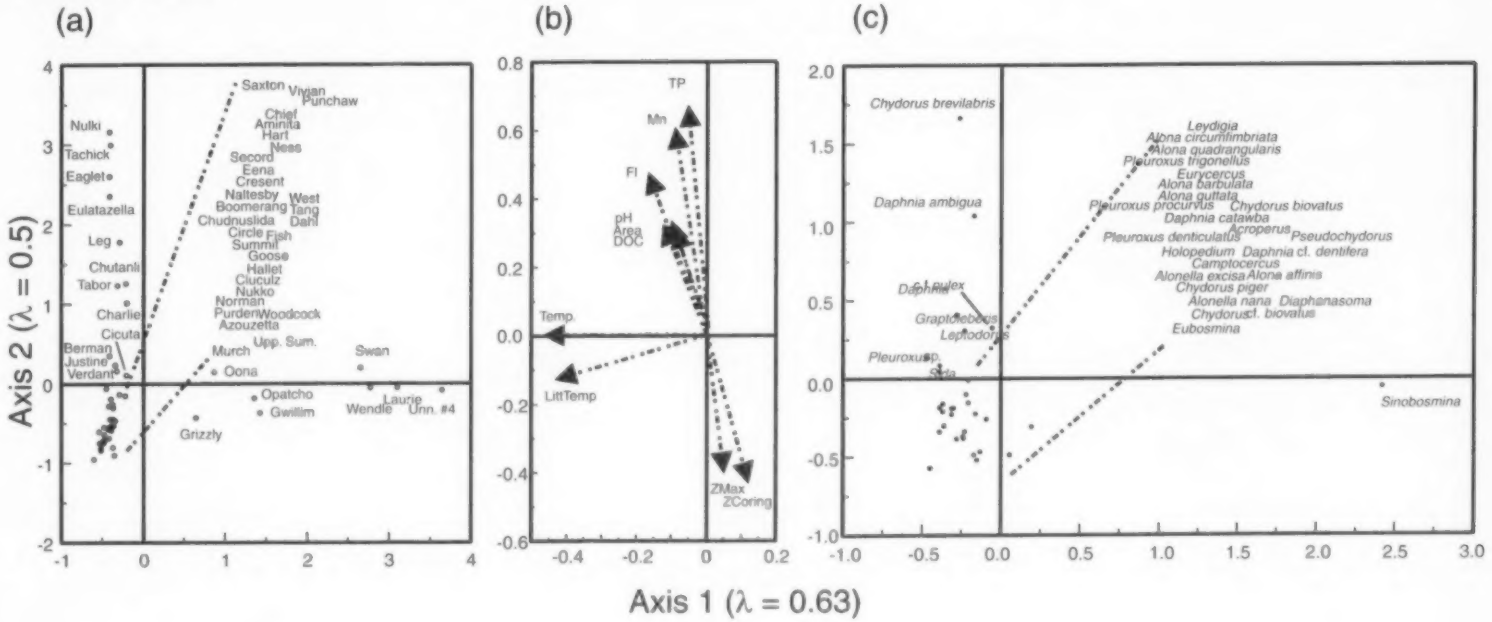

© 2003 NRC Canada

Table 1. Environmental data for the 53 sampled lakes.

Lake	Maximum depth (m)	Mean depth (m)	Secchi depth (m)	Surface area (ha)	Littoral area (%)	pH	Surface temperature (°C)	Specific conductance (μS)	Chl. *a* ($mg \cdot L^{-1}$)
Jakes	15	6.5	4.4	57	32	7.6	19.4	57.1	6.7
Goose	26	8.5	7	78	53	7.9	18.1	178.1	1.3
Aminita	18.9	5	7	36	77	6.1	21.8	7.9	5.6
Upper Summit	6.4	3.5	3.6	96	48	7.6	19.5	78.1	3.6
Opatcho	23	7	5.1	41	46	7.6	19.3	61.6	3
Woodcock	15	6.8	4.4	134	30	7.8	17.7	118.1	7.1
Purden	52.4	20.2	6.5	780	31	7.6	20.6	74.2	4.8
Chudnuslida	16.2	6.6	2.9	60	22	7.0	18	42.2	3.5
Ness	18.3	6.1	5.1	333	44	7.7	18.9	165.5	2.9
Eena	24	7.7	4.9	50	60	7.3	19.6	36.1	2.2
Laurie	23	9.9	3.4	97	25	7.6	13.6	65.4	7.4
Tang	10.9	5.7	2.7	44	25	7.4	19	47	8
Summit	16	6.4	2.25	1317	8	7.4	18.4	59.3	8.3
Gwillim	45		6	1121		7.9	16.4	233	11.2
Azouzetta	29.9		9	21	39	7.8	16.4	157	9.4
Grizzly East	5.8	5.2	2.2	73	54	6.7	19.9	15.2	10.7
Murch	13.1	5.4	2.9	128	30	7.4	18.6	62.8	12.5
Circle	15	4.7	4	71	57	7.5	18.4	90.8	4.8
Wendle	11.1	4.9	2.8	51	31	7.3	16.2	32.2	13.8
Secord	8	3	4	41	76	7.0	16.3	55	7
Boomerang	11	2.5	2.9	60	71	7.1	15.7	50	7.4
Pitoney	20.1	8.6	2.3	181	12	6.7	19.1	30	3.7
Nukko	17.1	7.2	3.1	421	12	7.4	18.8	83	5.6
Saxton	16	9.9	3.8	680	16	7.7	17.8	78.9	7.5
Hart	8.7	4.9	7	55	74	7.9	18.4	147.1	6.9
Unnamed No. 4	19.5	6.9	5.3	79	11	7.5	14.5	67.6	5.7
Naltesby	20.1	11.1	4.3	824		7.8	18.5	170.8	2.1
Verdant	7.6	3	3.9	30	61	8.0	19.1	174.6	10.2
Hallet	31	17.3	3.5	559	24	7.5	17.7	91.5	4.8
Vivian	8.2	4	3.9	49	47	7.8	19.1	169.6	6.9
Fish	13.1	4.7	3.4	50	45	7.6	21.7	96.5	6.7
Chutanli	9	4.1	2.7	180	24	7.8	18.1	141.2	5.3
Dahl	23.5	4.5	3.5	251	57	7.8	19.8	135.3	2.9
Oona	23.2	9.7	2.6	336	15	7.3	17.6	61	11
Norman	23.8	12	2.1	514	8	7.7	18.9	127	5.3
Bednesti	20.7	8.3	4.5	265	31	7.8	20.2	143.1	8.8
Berman	16.5	2.6	3.6	43	73	7.8	20.2	146.5	6.9
Justine	10	5.7	1.85	247	38	7.1	15.5	58.9	12
Cresent	14.3	6.5	1	62	3	7.6	18.7	98.1	25.1
Cluculz	61	29.6	2.7	1964	12	8.5	20.2	160.4	50.6
Tabor	9.2	5.4	3.6	346	33	7.8	18.4	182.7	9.6
Eulatazella	13.1	5.8	1.2	479	9	8.1	19.4	106.9	17.8
Chief	6.1	3.8	1.3	715	3	7.5	18.5	77.5	82.9
Swan	6		1.6	612		7.7	19.9	204	23.5
Grizzly West	6.5	3	0.6	138	9	8.1	18.3	89.5	38.5
Cicuta	12	5.1	0.6	184	6	8.6	17.6	84.6	104
Tachick	7.6	4.4	1.6	2110	12	8.3	17.1	199.7	53.5
Nulki	7.6	4.5	2.1	1597	17	8.2	17.3	154	24.1
Leg	5.2	1.8	1	35	37	7.4	20.6	170.4	20.5
Charlie	10		1.7			7.8	18.4	166.5	41.2

Note: Samples were taken from a depth of 0.5 m in the pelagic zone of the lake. Lakes are arranged in order of total phosphorus. Sampling began on 6 and Gwillim represent coring depth, as bathymetric maps were unavailable. Chl. *a*, chlorophyll *a*; DIC, dissolved inorganic carbon; DOC, dissolved organic

© 2003 NRC Canada

Alkalinity ($mg \cdot L^{-1}$)	DIC ($mg \cdot L^{-1}$)	DOC ($mg \cdot L^{-1}$)	Total nitrogen ($mg \cdot L^{-1}$)	Total phosphorus ($mg \cdot L^{-1}$)
29.35	6.3	6.7	<0.02	0.001
98.1	21.9	4.6	0.17	0.005
1.2	0.25	2.9	0.17	0.005
40.3	8.5	12.1	0.4	0.006
32.5	6.9	8.8	0.4	0.006
63.9	14	10.2	0.36	0.007
30.5	6.6	6	0.26	0.007
22.5	4.5	9.5	0.3	0.008
85.1	19.5	6.9	0.39	0.008
18.2	4.2	6.8	0.48	0.009
27.6	6	9.4	0.33	0.011
23.8	4.7	12.4	<0.02	0.011
28.4	6.1	10.9	<0.02	0.011
116	28.1	6.7	0.26	0.011
77	18.8	1.5	0.34	0.011
3.8	0.7	13.3	0.47	0.012
32	6.9	9	0.48	0.013
46.4	10.5	8.9	0.52	0.014
16.5	3.5	4.7	0.2	0.015
21.5	4.4	12.3	0.35	0.015
25.3	4.9	15.3	0.41	0.015
15.4	2.9	10	0.29	0.015
38.7	8.3	11.1	0.59	0.017
39.7	9	8.7	0.43	0.017
77.7	17.6	3.4	0.34	0.017
34	7.4	6.9	0.32	0.018
90.9	20.7	13.6	0.46	0.018
94	20.1	8.7	0.59	0.019
45.4	10.1	11.7	0.33	0.019
90.4	19.5	11	0.51	0.02
40.9	9.2	14.4	0.44	0.02
70.8	15.7	10.9	0.29	0.021
71.8	15.7	18.4	0.54	0.022
29.8	6.1	14.8	0.44	0.022
65.8	14.7	19.7	0.51	0.023
72.5	16.6	12.4	0.4	0.023
73	16.7	12.1	0.38	0.025
26.8	5.5	17	0.47	0.027
46.8	10.3	19.9	0.95	0.031
86	17.9	11.9	0.76	0.036
74.7	16.7	10.8	0.56	0.039
54.7	11.5	20.6	0.75	0.045
34.8	7.7	16.9	0.82	0.053
100	23.3	24.1	1	0.06
46.5	9.9	17.2	0.88	0.063
41.4	6	24.5	1.5	0.069
111	23.3	13.6	1.1	0.083
82.8	18.2	14.5	0.94	0.088
87.2	19.7	34.7	1.1	0.112
73.7	16.8	14.1	1.5	0.146

July and ended on 8 August 1997. Maximum depth for Swan Charlie carbon.

showed close agreement between measures of TP from the littoral zone and from the pelagic zone (data not shown). Jakes Lake had a value of 1 $\mu g \cdot L^{-1}$ in the pelagic zone and 29 $\mu g \cdot L^{-1}$ in the littoral zone.

The original species data were also divided into littoral and planktonic groups for the littoral-only model. However, for many lakes, the density of littoral species was very low in the sediments. For some lakes, the number of remains for littoral species was increased by counting additional slides. However, for Tang, Swan, Cicuta, Eena, Naltesby, Secord, Unnamed No. 4, Boomerang, Laurie, Gwillim, and Azouzetta lakes, the density of littoral species was extremely low (mean = 2 remains/coverslip or 33 remains/mL wet sediment). Making slides with higher concentrations was also not possible because the cladoceran remains become hidden in the sediment matrix. Thus, only 38 lakes had sufficient littoral taxa for model development. However, many of these lakes still had very low numbers of remains, and lakes with counts as low as 20 individuals were retained. This number is low and imparts considerable noise to the species data. However, it allows a preliminary analysis into the potential of the littoral-only model to determine if developing new methods to better separate the Cladocera from the sedimentary matrix would be profitable.

Water chemistry and ordination

The 49 lakes spanned a wide range of TP (Fig. 3) and ranged from oligotrophic (5 $\mu g \cdot L^{-1}$ TP) to hypereutrophic (146 $\mu g \cdot L^{-1}$). These lakes also encompassed significant variations in other limnological factors (Table 1).

Results from the DCA ordination gave a gradient length of 3.0, which suggests that unimodal statistical techniques (CA, CCA, and WA) are most appropriate. The CA shows a clear separation of the sites (Fig. 4*a*) and species (Fig. 4*c*) in the calibration set lakes. The large number of lakes near the origin shows that although a considerable range of lake types was sampled, they are not evenly spread across the gradient, but instead are more common around the mean (Fig. 4*a*). Two main gradients are shown in the CA. Axis 1 ($\lambda = 0.63$), which represents the greatest direction of variability in the data set, was most strongly correlated to temperature (Fig. 4*b*). Lakes such as Unnamed No. 4, Laurie, Wendle, and Swan showed the most dispersion on the first axis and had some of the coldest measured water temperatures in the calibration set (Table 1). Axis 2 ($\lambda = 0.5$) was most strongly correlated with TP and depth. Nulki, Tachick, Eaglet, and Eulatzella lakes showed the greatest dispersion on the second axis and were lakes that had some of the highest TP values and also tended to be relatively shallow. Although Unnamed No. 4, Laurie, Wendle, and Swan lakes stand out most as being the extreme sites on axis 1, it is also important to see that they also have some of the lowest TP values in the calibration set. This can be seen by extending the vector for TP on the diagram and connecting it orthogonally to the points for these lakes (Jongman et al. 1995). There is a pattern in the calibration set of a continuum of lakes that range from colder, deeper, oligotrophic lakes to warmer, shallower, hypereutrophic lakes. This is not unusual in that it would be surprising to find cold, deep, hypereutrophic lakes or warm, shallow, oligotrophic lakes (Hutchinson 1975). Although the

© 2003 NRC Canada

Fig. 5. Canonical correspondence analysis of (*a*) species and (*b*) sites. Axes are derived from a linear combination of total phosphorus (TP), depth, and temperature.

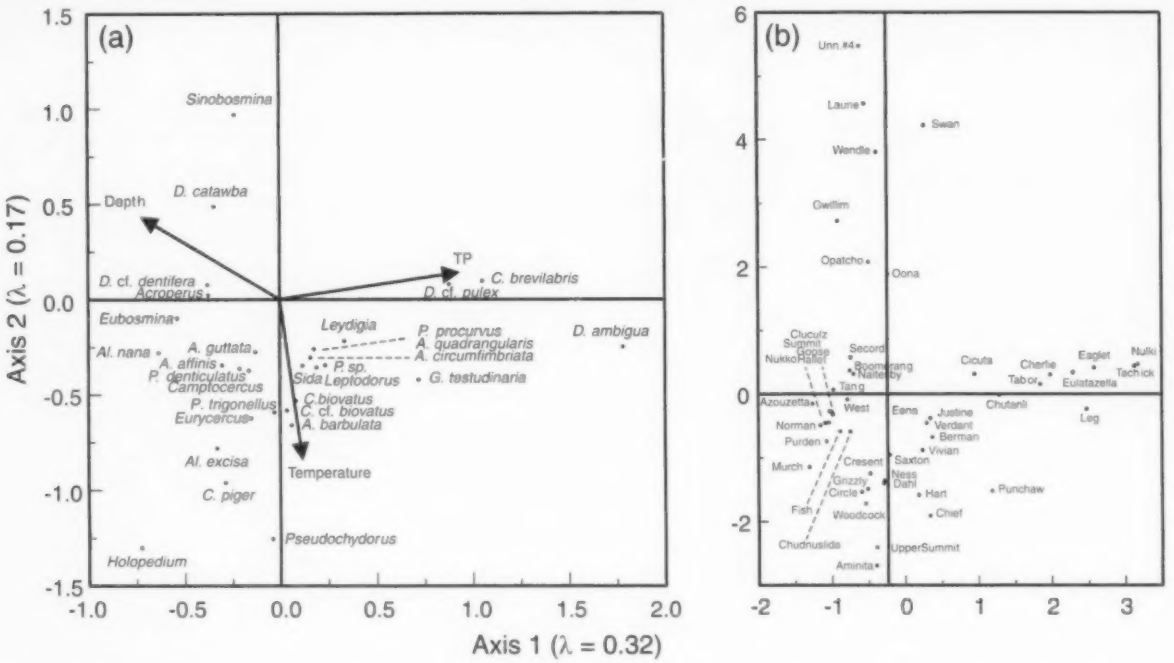

CA analysis is very useful in that it finds the maximum directions of variation in the data set and can show how environmental variables correlate to that variation, it is difficult to determine species–environmental relationships from indirect techniques. To show how species composition changes with different environmental conditions, it is more instructive to use a direct gradient analysis technique, such as CCA.

The most striking change between the CA and the CCA is that axes 1 and 2 are switched (Figs. 4 and 5). The relative position of species, environmental variables, and sites remain the same, but those that scored high on CA axis 1 now score high on CCA axes 2 ($\lambda = 0.17$), and those that scored high on CA axis 2 now score high on CCA axis 1 ($\lambda = 0.32$). Thus, the measured environmental variables are better able to describe the second greatest direction of variation in the species data (CA axis 2) than the largest direction of variation (CA axis 1). Although the CA shows that temperature is correlated to the largest direction of variation in the data set, when it is used as a descriptor in the CCA, it is not as good at representing the largest direction of variation as TP is at describing the second-greatest direction of variation. In summary, TP is the environmental variable that describes the most variation in the species data in the CCA; however, this is not the largest direction of variation in the species data. The greatest source of variation in the species data is correlated to temperature, but temperature itself is not the best descriptor of this variation.

As with the above CCA, TP, depth, and temperature were forward-selected for the environmental variables in the partially constrained ordinations. For the spatial variables, x^2 (longitude squared) and xy (longitude × latitude) were the only significant variables from forward selection. The variance partitioning showed that the forward-selected physical and chemical environmental variables described 23% of the variance in the species data, whereas forward-selected spatial variables described 13% of the variance. Five percent of this variance is shared between the environmental and spatial variables. Thus, 64% of the variation in the species data among sites is unexplained, 18% is described by TP, depth, and temperature, and 8% is purely spatial. Although the shared component (5%) may be due to variation in TP, depth, and temperature over the study region, the remaining 8% of the spatial variation is currently unknown but may be due to unmeasured environmental variables. Other factors that are not related to spatial distribution of sites, or the measured environmental variables, are strongly contributing to the variance in the species data. However, of the known variables, TP is the single strongest descriptor of variation in the cladoceran assemblages within this data set.

TP is the variable that directly describes the most significant amount of the variation in the species data (Fig. 5). This is probably related to changes in cladoceran habitat that occur along the TP gradient. The largest variation in the species data is not well accounted for but is related to temperature. This could be an effect of the changes in the fish communities along the continuum of lake temperature, depth, and oxygen saturation.

Species distribution

This study provides quantitative information on the distribution of Cladocera in relation to TP (Fig. 6). Many of the species are found across a range of TP. *Daphnia* cf. *dentifera* Forbes was one of the most common species found in the

© 2003 NRC Canada

Fig. 6. Relative abundance of species (%). Species are sorted by their total phosphorus (TP) optimum, shown in brackets after the species name. Sites are sorted by their measured TP, shown in parentheses after the site name. TP values are in $\mu g \cdot L^{-1}$. Because of the wide range of relative abundance for the species, different scales are used; values shown are the maximum value for each graph.

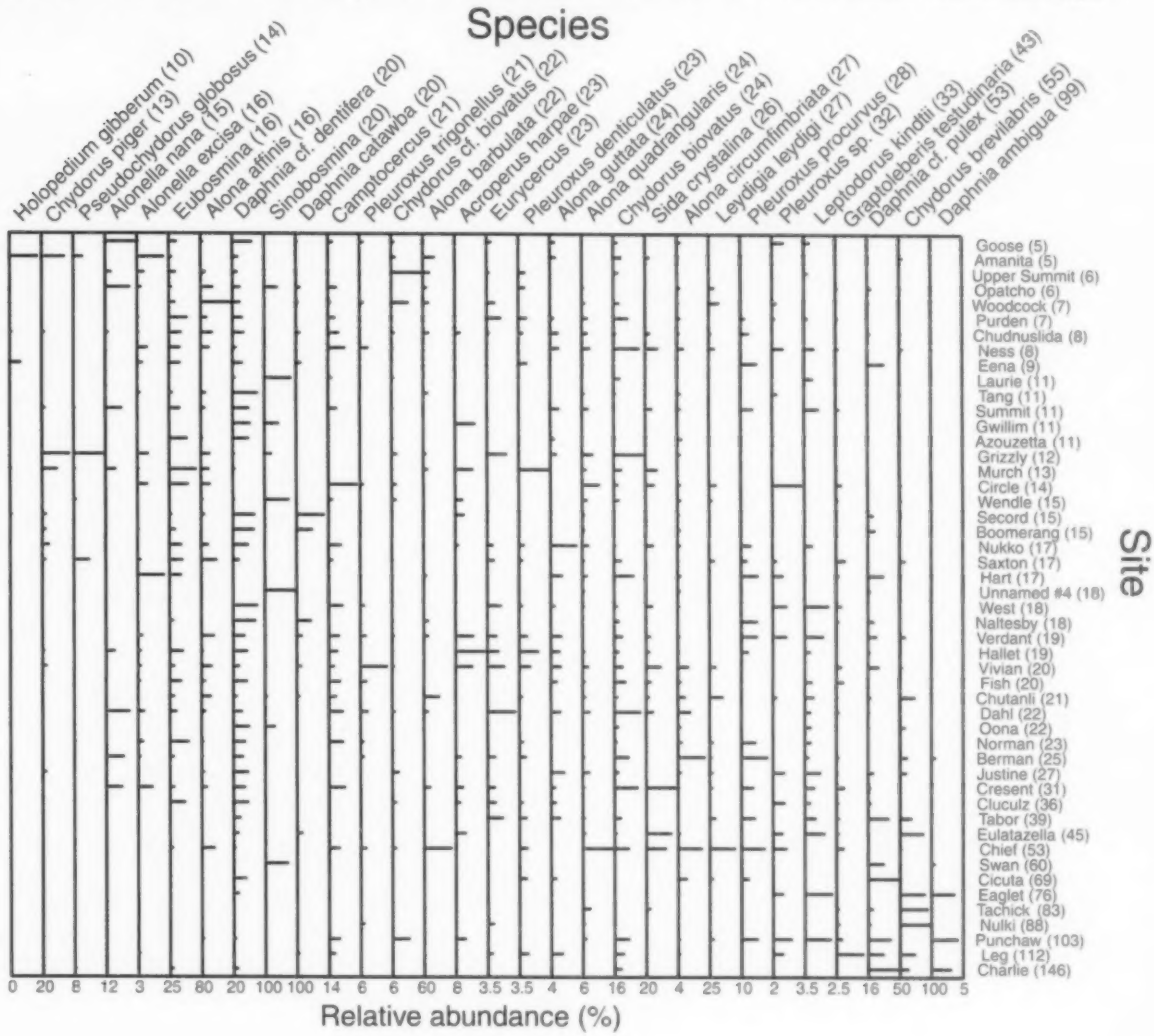

calibration set; it was not only found across a wide range of TP, but was also dominant in the relative abundance counts for many lakes. Despite having one of the widest distributions in the calibration set, *D.* cf. *dentifera* was not found in the hypereutrophic lakes. One reason why *D.* cf. *dentifera* is found across such a wide range of TP may be that it is not one species but a collection of species. Unfortunately, *D. dentifera*, *D. mendotae* Hebert, and *D. thorata* Forbes all share a similar postabdominal claw morphology, and it is currently not possible to separate them based on this microfossil remain.

Eubosmina and *Alona affinis* Leydig were also abundant in many of the lakes. *Eubosmina* and *A. affinis* were common in oligomesotrophic to mesotrophic lakes but were largely absent from lakes with TP greater than 30 $\mu g \cdot L^{-1}$. *Sinobosmina* was found over a similar range of TP to *Eubosmina*. However, it was much less common and was found in only eight lakes. Temperature may be more important than TP in determining the distribution of *Sinobosmina*. Although *Sinobosmina* was found from oligomesotrophic to eutrophic lakes, all of these lakes had lower water temperatures (Figs. 5, 6 and Table 1).

Chydorus biovatus Frey and *C.* cf. *biovatus* were often found in high relative abundance and were most common in the mesotrophic lakes. *Chydorus* cf. *biovatus* occurred less frequently than *C. biovatus* and, except for one lake, was more abundant in sites with lower TP. *Chydorus biovatus* was nearly ubiquitous in the calibration set, although it was less abundant in both the oligotrophic and hypereutrophic lakes. *Chydorus* cf. *biovatus* may be a form of *C. biovatus* but was identified separately by the striking difference in fovea on the headshield and carapace (Bos 2001).

© 2003 NRC Canada

Fig. 7. Weighted averaging regression model for total phosphorus (TP). (*a*) The apparent coefficient of determination ($r^2_{apparent}$) is based on using the entire calibration set to develop the model and then testing the inferred value for each lake against the measured value. (*b*) The bootstrapped coefficient of determination (r^2_{boot}) is produced by using a bootstrapping procedure to iteratively form the model from a subset of the calibration lakes and then testing the model using lakes that were not included in the model for that iteration. The mean value for each site from 9999 iterations was then regressed against the measured summer TP value to give the r^2_{boot}.

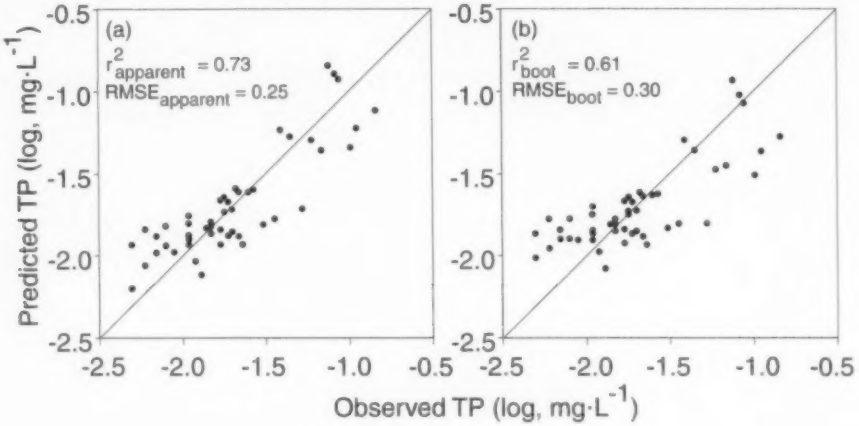

Fig. 8. Weighted averaging regression model for total phosphorus (TP) using only littoral species. (*a*) The apparent coefficient of determination ($r^2_{apparent}$) is based on using the entire calibration set to develop the model and then testing the inferred value for each lake against the measured value. (*b*) The bootstrapped coefficient of determination (r^2_{boot}) is produced by using a bootstrapping procedure to iteratively form the model from a subset of the calibration lakes and then testing the model using lakes that were not included in the model for that iteration. The mean value for each site from 9999 iterations was then regressed against the measured summer TP value to give the r^2_{boot}.

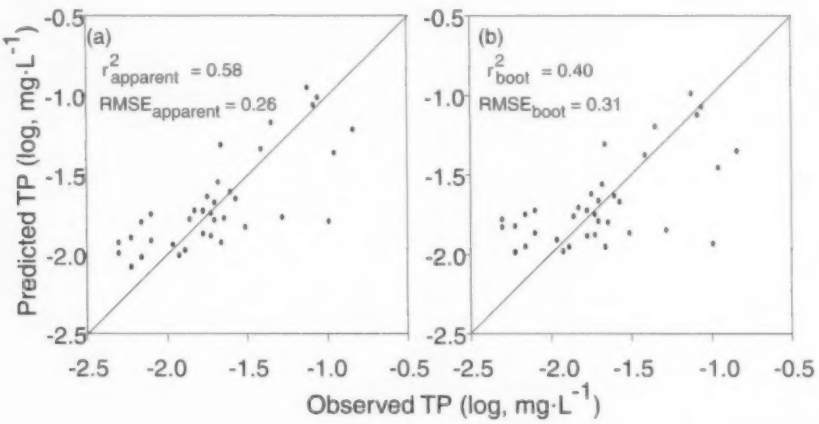

Unlike *C. biovatus*, *C. brevilabris* Frey had a more restricted distribution. *Chydorus brevilabris* had its greatest relative abundance in eutrophic and hypereutrophic lakes. Although *C. biovatus* is likely the same species described by Frey (1980) from Revelstoke, Alberta, *C. brevilabris* is interesting in that these lakes are considerably further north than what Frey (1980) described as a distribution limit for *C. brevilabris*. The strong preference of *C. brevilabris* for lakes with higher TP levels may provide a clue as to the differences in distribution of *C. biovatus* and *C. brevilabris* described by Frey (1985).

Alona circumfimbriata Megard also had high relative abundance in many of the lakes. It was present in lower abundance in oligotrophic to mesotrophic lakes but only achieved high relative abundance in eutrophic lakes. *Sida crystallina* Muller and *Leydigia leydigi* Schoedler are distributed similarly to *A. circumfimbriata*, although both of these species occur at much lower relative abundance in all of the lakes. *Graptoleberis testudinaria* Fischer and *Daphnia* cf. *pulex* Leydig were also widespread across the calibration set and had a similar distribution to *A. circumfimbriata* with the exception that *G. testudinaria* and *D.* cf. *pulex* were most abundant in hypereutrophic lakes.

Many of the less common species also showed a relationship to lake trophic condition. *Holopedium gibberum* Zaddach, *C. piger*, and *Pseudochydorus globosus* Baird were largely restricted to oligotrophic and oligomesotrophic lakes and generally accounted for less than 10% of the counts for a

© 2003 NRC Canada

lake. *Daphnia catawba* Coker occurred across a larger range of TP but also was usually low in relative abundance. *Camptocercus*, *Pleuroxus trigonellus* O.F. Muller, *Alona barbulata* Megard, *Acroperus harpae* Baird, *Eurycercus* spp., *Pleuroxus denticulatus* Birge, *Alona guttata* Sars, and *Alona quadrangularis* O.F. Muller were found across a wide range of TP but never had high relative abundance in any samples. More specialized littoral habitat preferences, which are not strongly related to TP, may be important in controlling the distribution of these species. The distribution of *Daphnia ambigua* Scourfield was largely restricted to hypereutrophic lakes and was never found in a relative abundance greater than 5%.

Overall planktonic species had a much greater relative abundance in most lakes compared with the littoral species. This is probably due to the much greater volume of planktonic habitat relative to the amount of littoral habitat in most of the study lakes.

Planktonic and littoral species TP model

DCCA showed that when constrained to only TP, there was still sufficient length in the gradient to continue using unimodal techniques (gradient length = 2.4) (Birks 1995). Reconstruction of TP with WA gave an apparent r^2 of 0.73 (Fig. 7). Using bootstrapping to evaluate the robustness of this value causes a drop in the r^2 to 0.61. Currently, our full-species model is capable of discriminating between oligo-mesotrophic, eutrophic, and hypereutrophic lakes (Fig. 7). However, reconstructions at the upper end of the TP range tend to be too low, and reconstructions at the lower end of the TP range tend to be too high. The small number of oligotrophic and hypereutrophic lakes in the data set result in an underestimate of TP optima for species at the high end of the gradient, whereas TP optima for species at the low end of the gradient are overestimated. Consequently, when these species are present, there is bias at the ends of the TP gradient. Because the bootstrapping procedure eliminates some lakes for each bootstrap cycle, it is likely that the under-representation at the extreme ends of the TP spectrum is further exaggerated during bootstrapping. Addition of ultra-oligotrophic and hypereutrophic lakes to the data set should improve the predictive abilities of these models. Because of a slight skew to lower TP values in the distribution of TP in our data set (Fig. 7), we assessed the impact of this on our inference models by creating a smaller data set with an optimal distribution of lakes. To form this new data set, we removed 19 lakes, randomly within blocks, from the lower end of the gradient to give an approximately even distribution of lakes along the log(TP) gradient. Results from this analysis were very similar ($r^2_{\text{apparent}} = 0.70$, $\text{RMSE}_{\text{apparent}} = 0.23$, $r^2_{\text{boot}} = 0.51$, $\text{RMSE}_{\text{boot}} = 0.30$) to the model using all lakes, with the exception that the smaller number of lakes results in a greater drop in the r^2 when using the bootstrapping procedure.

Littoral-only TP model

Results from the littoral-only model for TP reflect the problems with using a smaller number of lakes and lower counts of species. The littoral-only model has lower predictive ability and higher error (Fig. 8) than those of the full-species model (Fig. 7). Because the bootstrapping procedure can be strongly affected by the lack of redundancy in a small calibration set, the apparent r^2 and RMSE are probably better indicators of how the littoral-only model might perform with a larger number of calibration lakes. Given the inadequacies in the data, these results suggest that there is still potential in developing stronger littoral-only TP models.

Comparison to other TP models

Comparison to other models using diatoms and Cladocera to reconstruct TP shows that our models are comparable given the range of TP that they cover (2–146 $\mu g \cdot L^{-1}$). The full-species cladoceran model has a better predictive ability ($r^2_{\text{boot}} = 0.61$, $\text{RMSE}_{\text{boot}} = 0.30$, $n = 49$) than the Reavie et al. (1995) model based on diatom remains in 59 lakes over a similar TP gradient (5–138 $\mu g \cdot L^{-1}$) in British Columbia ($r^2_{\text{boot}} = 0.46$, $\text{RMSE}_{\text{boot}} = 0.48$, $n = 59$). Results from Brodersen et al. (1998) using Cladocera to reconstruct TP in Danish lakes ($r^2_{\text{boot}} = 0.79$, $\text{RMSE}_{\text{boot}} = 0.24$, $n = 32$) that cover a much larger gradient of TP (16–538 $\mu g \cdot L^{-1}$) than our study suggest that the predictive ability of our model should increase with the addition of ultra-oligotrophic and hypereutrophic lakes.

Cladoceran species composition changes over a gradient of TP in our study lakes. Models that use these changes in species composition are capable of reconstructing TP and can currently differentiate between the oligomesotrophic, eutrophic, and hypereutrophic lakes. Including more ultra-oligotrophic and hypereutrophic lakes in the model should make the model more generally applicable, improve estimates of TP optima and tolerance for the species, and increase the accuracy of TP estimates for sites at the ends of the current gradient. Even in environments where the density of cladoceran remains is very low, it will still be possible to do high-resolution paleolimnological analyses using Cladocera. However, given that the density of littoral species can be as low as 33 mL^{-1} wet sediment at the sediment–water interface, it is important to use a large-diameter corer so that a sufficient amount of material will be available for analysis. Alternatively, many smaller surficial samples could be taken. In lakes where the density of remains is very low, it will also be necessary to find a more efficient means to separate the Cladocera from the sedimentary matrix to make enumeration of remains efficient enough to be practical. Currently, no techniques have been perfected to achieve this. However, we are experimenting with densitometric techniques similar to those that have been used with live Cladocera (e.g., Goulden 1971). The Cladocera are a useful paleolimnological indicator for past changes in TP, along with being an independent indicator of TP from diatoms.

Acknowledgments

We thank Bruce Carmichael and Greg Warren of the British Columbia Ministry of Environment for logistical and technical support during fieldwork. We also thank Rick Nordin for providing funding for water chemistry analyses. This project was funded by a Natural Sciences and Engineering Research Council of Canada (NSERC) research grant to B.F.C., as well as a Queen's University E.G. Baumann Fellowship and an Ontario Graduate Student award to D.G.B.

© 2003 NRC Canada

References

Birks, H.J.B. 1995. Quantitative palaeoenvironmental reconstructions. *In* Statistical modeling of Quaternary science data. *Edited by* D. Madday and J.S. Brew. Technical Guide 5, Quaternary Research Association, Cambridge. pp. 161–254.

Birks, H.J.B., Line, J.M., Juggins, S., and Ter Braak, C.J.F. 1990. Diatoms and pH reconstruction. Philos. Trans. R. Soc. Lond. B Biol. Sci. **327**: 263–278

Borcard, D., Legendre, P., and Drapeau, P. 1992. Partialling out the spatial component of ecological variation. Ecology, **73**: 1045–1055.

Bos, D.G. 2001. Sedimentary cladoceran remains, a key to interpreting past changes in nutrients and trophic interactions. Ph.D. thesis, Queen's Univesity, Kingston, Ont.

Boucherle, M.M., and Zullig, H. 1983. Cladoceran remains as evidence of change in trophic state in three Swiss lakes. Hydrobiologia, **103**: 141–146.

Brodersen, K.P., Whiteside, M.C., and Lindegaard, C. 1998. Reconstruction of trophic state in Danish lakes using chydorid (Cladocera) assemblages. Can. J. Fish. Aquat. Sci. **55**: 1093–1103.

Chengalath, R., and. Hann, B.J. 1981. Two new species of *Alona* (Chydoridae, Cladocera) from western Canada. Can. J. Zool. **59**: 377–389.

De Melo, R., and Hebert, P.D.N. 1994. A taxonomic reevaluation of the North American Bosminidae. Can. J. Zool. **72**: 1808–1825.

Frey, D.G. 1959. The taxonomic and phylogenetic significance of the head pore of the Chydoridae (Cladocera). Int. Rev. Gesamten Hydrobiol. **44**: 27–50.

Frey, D.G. 1960. The ecological significance of cladoceran remains in lake sediments. Ecology, **41**: 684–699.

Frey, D.G. 1962. Supplement to the taxonomic and phylogenetic significance of the head pores of the Chydoridae (Cladocera). Int. Rev. Gesamten Hydrobiol. **47**: 603–609.

Frey, D.G. 1965. Differentiation of *Alona costata* Sars from two related species (Cladocera, Chydoridae). Crustaceana, **8**: 159–173.

Frey, D.G. 1980. On the plurality of the *Chydorus sphaericus* (O.F. Müller) (Cladocera, Chydoridae), and designation of a neotype from Sjaelsø, Denmark. Hydrobiologia, **69**: 83–123.

Frey, D.G. 1985. A new species of the *Chydorus sphaericus* group (Cladocera, Chydoridae) from western Montana. Int. Rev. Gesamten Hydrobiol. **70**: 3–20.

Frey, D.G. 1986. Cladocera analysis. *In* Handbook of Holocene palaeoecology and palaeohydrology. *Edited by* B.E. Berglund. John Wiley and Sons, New York. pp. 667–692.

Frey, D.G. 1987. The taxonomy and biogeography of the Cladocera. Hydrobiologia, **145**: 5–17.

Glew, J.R. 1991. Miniature gravity corer for recovering short sediment cores. J. Paleolimnol. **5**: 285–287.

Goulden, C.E. 1969. Interpretive studies of cladoceran microfossils in lake sediments. Mitt. Int. Ver. Limnol. **17**: 43–55.

Goulden, C.E. 1971. Environmental control of the abundance and distribution of the chydorid Cladocera. Limnol. Oceanogr. **16**: 320–321.

Hann, B.J. 1981. Occurrence and distribution of littoral Chydoridae (Crustacea, Cladocera) in Ontario, Canada, and taxonomic notes on some species. Can. J. Zool. **59**: 1465–1474.

Hann, B.J. 1990. Cladocera. *In* Methods in Quaternary ecology. *Edited by* B.G. Warner. Geoscience Canada Reprint Ser. No. 5. pp. 81–90.

Hann, B.J., Leavitt, P.R., and Chang, P.S.S. 1994. Cladocera community response to experimental eutrophication in Lake 227 as recorded in laminated sediments. Can. J. Fish. Aquat. Sci. **51**: 2312–2321.

Hall, R.I., and Smol, J.P. 1999. Diatoms as indicators of lake eutrophication. *In* The diatoms: applications to the environmental and earth sciences. *Edited by* E.F. Stoermer and J.P. Smol. Cambridge University Press, Cambridge, U.K.

Hebert, P.D.N. 1995. The *Daphnia* of North America — an illustrated fauna. University of Guelph, Guelph, Ont. [CD-ROM.]

Hutchinson, G.E. 1975. A treatise on limnology. *In* Geography and physics of lakes. Vol. I. Part I. *Edited by* Y.H. Edmonson. John Wiley & Sons, Inc., New York.

Jeppesen, E., Madasen, E.A., Jensen, J.P., and Anderson, N.J. 1996. Reconstructing the past density of planktivorous fish and trophic structure from sedimentary zooplankton fossils: a surface sediment calibration data set from shallow lakes. Freshw. Biol. **36**: 115–127.

Jeppesen, E., Jensen, J.P., Amsinck, S., Landkildehus, F., Lauridsen, T., and Mitchell, S.F. 2002. Reconstructing historical changes in Daphnia mean size and planktivorous fish abundance in lakes from the size of *Daphnia ephippia* in the sediment. J. Paleolimnol. **27**: 133–143.

Jongman, R.H.G., Ter Braak, C.J.F., and Tongeren, O.F.R. 1995. Data analysis in community and landscape ecology. Cambridge University Press, Cambridge.

Korovchinsky, N.M. 1996. How many species of Cladocera are there? Hydrobiologia, **321**: 191–204.

Legendre, P. 1990. Quantitative methods and biogeographic analysis. *In* Evolutionary biogeography of the marine algae of the North Atlantic. NATO ASI Series, Vol. G 22. *Edited by* D.J. Garbary and R.R. South. Springer-Verlag, Berlin, Germany.

Line, J.M., ter Braak, C.J.F., and Birks, H.J.B. 1994. WACALIB version 3.3 — a computer program to reconstruct environmental variables from fossil assemblages by weighted averaging and to derive sample-specific errors of prediction. J. Paleolimnol. **10**: 147–152.

Megard, R.O. 1967. Three new species of *Alona* (Cladocera, Chydoridae) from the United States. Int. Rev. Gesamten Hydrobiol. **52**: 37–50.

Plath, K., and Boersma, M. 2001. Mineral limitation of zooplankton: stoichiometric constraints and optimal foraging. Ecology, **82**: 1260–1269.

Reavie, E.D., Hall, R.I., and Smol, J.P. 1995. An expanded weighted-averaging model for inferring past total phosphorous concentrations from diatom assemblages in eutrophic British Columbia (Canada) lakes. J. Paleolimnol. **14**: 49–67.

Schulz, K.L., and Sterner, R.W. 1999. Phytoplankton phosphorus limitation and food quality for *Bosmina*. Limnol. Oceanogr. **44**: 1549–1556.

Shi, G.R. 1993. Multivariate data analysis in palaeoecology and palaeobiogeography — a review. Palaeogeogr. Palaeoclimatol. Palaeoecol. **105**: 199–234.

Smirnov, N.N. 1974. Fauna of the U.S.S.R., Crustacea. Academy of Sciences of the U.S.S.R. 1(2). Translated from Russian, Israel Program for Scientific Translations, Jerusalem, 1974, New Series No. 101.

Smirnov, N.N. 1996. Cladocera: the Chydorinae and Sayciinae (Chydoridae) of the world. SPB Academic Publishing, Amsterdam.

Sterner, R.W., Hagemeier, D.D., Smith, W.L., and Smith R.F. 1993. Phytoplankton nutrient limitation and food quality for Daphnia. Limnol. Oceanogr. **38**: 857–871.

ter Braak, C.J.F. 1988. CANOCO: an extension of DECORANA to analyze species–environment relationships. Vegetatio, **75**: 159–160.

ter Braak, C.J.F. 1990. Update notes: CANOCO version 3.10. Agricultural Mathematics Group, Wageningen.

Urabe, J., Clasen, J., and Sterner, R.W. 1997 Phosphorus limitation in *Daphnia* growth: is it real? Limnol. Oceanogr. **42**: 1436–1443.

© 2003 NRC Canada

Valentine, K.W.G., Sprout, P.N., Baker, T.E., and Lavkulich L.M. (*Editors*). 1978. The soil landscapes of British Columbia. B.C. Ministry of Environment, Victoria, B.C.

Wetzel, R.G. 1983. Limnology. Saunders College Publishing, Toronto, Ont.

Whiteside, M.C. 1970. Danish chydorid Cladocera: modern ecology and core studies. Ecol. Monogr. **40**: 79–118.

© 2003 NRC Canada

Change-in-ratio estimates of lobster exploitation rate using sampling concurrent with fishing

Ross Claytor and Jacques Allard

Abstract: We present a continuous change-in-ratio (CIR) method for estimating lobster exploitation rate using data from monitoring traps continuously sampled during fishing. The exploitation rate is estimated by fitting a nonlinear model to ratios of exploited catch over total catch (exploited plus an unexploited reference class) as a function of the cumulative exploited catch. Confidence intervals are obtained by bootstrapping. The method is applied to data collected by nearly 100 lobster fishers who sampled monitoring traps in fishing areas of Nova Scotia, Canada, from 1999 to 2001, and to simulated data. Best estimates are obtained where the exploited and the reference length classes are adjacent and narrow. A method to predict the impact of season length restriction on exploitation rate is presented. Simulations demonstrate that the method displays some robustness relative to departures from the model's assumptions. Exploitation rate estimates decline for length classes in which the minimum legal carapace length has been increased. The continuous CIR method can provide daily, local, and length-specific estimates of exploitation rate. For similar sample sizes, continuous CIR estimates are better than CIR estimates based on pre- and post-season sampling. A continuous CIR method is cost efficient because the data can be collected during regular fishing activity.

Résumé : On trouvera ici une méthode CIR (changement de proportions) en continu pour estimer le taux d'exploitation du homard à partir de données obtenues de pièges de surveillance échantillonnés continuellement durant la période de pêche. Le taux d'exploitation s'estime en ajustant un modèle non linéaire aux rapports des captures exploitées sur les captures totales (la classe de homards exploités plus une classe témoin non exploitée) en fonction des captures exploitées cumulées. Les intervalles de confiance sont calculées par bootstrap. La méthode a été utilisée avec les données récoltées par environ une centaine de pêcheurs de homards qui ont échantillonné les pièges de surveillance sur les zones de pêche en Nouvelle-Écosse, Canada, de 1999 à 2001, mais aussi avec des données simulées. Les meilleures estimations ont été obtenues lorsque les classes de longueur exploitées et les classes de référence sont adjacentes et étroites. Nous présentons une méthode pour prédire l'impact de la restriction de la durée de la saison de la pêche sur le taux d'exploitation. Des simulations démontrent que la méthode affiche une certaine robustesse lorsque des conditions préalables du modèles ne sont pas réalisées. Les estimations du taux d'exploitation diminuent chez les classes de longueur lorsqu'on accroît la longueur de la carapace minimale permise. La méthode CIR en continu peut fournir des estimations du taux d'exploitation en fonction du jour, de l'endroit et de la taille. Pour des échantillons de même taille, les estimations par la méthode CIR en continu sont plus précises que celles obtenues à partir d'échantillonnages faits avant et après la saison de pêche. La méthode CIR en continu est économiquement rentable car les données peuvent être récoltées durant les activités régulières de la pêche.

[Traduit par la Rédaction]

Introduction

Many fishery and wildlife management actions are designed to control or reduce the exploitation rate. Therefore, estimating the exploitation rate is necessary to plan these measures and evaluate their success.

In the Atlantic Canada lobster (*Homarus americanus*) fisheries, doubling egg-per-recruit has been the management target since 1997. To achieve this target, fishery managers have considered and (or) adopted regulations to reduce exploitation rates, including restrictions on the minimum carapace length and on the landing of female lobster.

Changes in catchability are a major source of difficulty in estimating lobster exploitation rates (McLeese and Wilder 1958; Miller and Mohn 1993; Tremblay and Smith 2001). Incorporating temperature in a catchability model improves exploitation rate estimates but increases the number of parameters (Paloheimo 1963; Pollock et al. 1984; Yamakawa et al. 1994). Mark–recapture experiments (Frusher and Hoenig 2001*a*, 2001*b*) have been successful but are costly to implement. Change-in-ratio (CIR) methods (Pollock and Hoening 1998) overcome some of these difficulties.

CIR methods use the change in proportions of the catch of two or more classes of animals to estimate population num-

Received 4 November 2002. Accepted 23 June 2003. Published on the NRC Research Press Web site at http://cjfas.nrc.ca on 30 October 2003.
J17169

R. Claytor.[1] Department of Fisheries and Oceans, P.O. Box 1006, Dartmouth, NS B2Y 4A2, Canada.
J. Allard. Département de mathématiques et de statistique, Université de Moncton, Moncton, NB E1A 3E9, Canada.

[1]Corresponding author (e-mail: claytorr@mar.dfo-mpo.gc.ca).

 doi: 10.1139/F03-102 © 2003 NRC Canada

bers (Paulik and Robson 1969; Udevitz and Pollock 1995) and, less often, other parameters. These methods have weak assumptions and few parameters. Classical CIR methods are based on before- and after-season ("end-point") samples and have been used to estimate exploitation rate in snow crab (*Chionoecetes opilio*) fisheries (Dawe et al. 1993; Chen et al. 1998). Frusher et al. (1998) proposed an extension to accommodate an added midseason sample and applied this method to estimate the exploitation rate of Tasmanian rock lobster (*Jasu edwardsii*) fisheries.

We propose an extension of the CIR method to estimate exploitation rate based on continuous sampling concurrent with fishing. The statistical treatment necessarily differs from that developed for end-point sampling for population estimates (Paulik and Robson 1969; Udevitz and Pollock 1995) and for end-point plus midpoint sampling for exploitation rate estimates (Frusher et al. 1998).

Consider the time series of ratios of the exploited class catch over the total of the exploited and reference class catches for each monitoring day. The estimate is obtained by modeling the sequence of ratios. Confidence intervals are obtained using bootstrap methods (in all cases, we use a 95% confidence level). Monte Carlo experiments are used to explore the robustness of the estimate.

We assume (1) that the population is closed, (2) that the ratio of catchability between the classes is constant throughout the season for all traps, (3) that the ratio of catchability by the monitoring traps and by the commercial traps is constant over the season for all classes, and (4) that the ratio of the fleet effort to the monitoring trap effort is either constant over the season or can be estimated up to a constant factor.

We will apply the continuous-sampling CIR method to a Canadian lobster fishery using two classes, an exploited class and a nonexploited reference class. Sampling is carried out by fishers using standardized monitoring traps. We estimate the exploitation rate in two areas for three fishing seasons and in six areas for two fishing seasons. The data, collected annually by 90 participating fishers, come from 27 000 trap hauls collected during 1700 fishing days over all seasons and areas combined.

Materials and methods

Model definition

Sampling method, CIR class definition, and assumptions

We examine a continuous monitoring sampling program carried out during the commercial fishing season. The sampling program includes protocols for measuring and recording the catch of exploited and unexploited length classes.

CIR methods require that the population be subdivided into two or more classes. It is ideal, but not necessary, that one of these is unexploited (Paulik and Robson 1969; Udevitz and Pollock 1991). We concentrate on the case in which two classes are used, an unexploited reference class and an exploited class. In the fishery that we examined, all lobster smaller than the minimum legal carapace length (MLCL) must be returned to the water. Hence, the MLCL defines the unexploited reference class and exploited classes.

Applying CIR methods to estimate exploitation rate or population number requires a closed population assumption. We study the effect of departure from this assumption using simulation as described below.

We assume that the ratio of catchability between the classes is constant over the season (Udevitz and Pollock 1995). For example, the above assumption could be violated if temperature affects the two classes differently or if depletion of the exploited class increases catchability of the reference class.

We also assume that the ratio of catchability of the monitoring traps and of the commercial fishery traps is constant over the season for the exploited classes. This assumption could be violated if fishing conditions were very different for the monitoring traps and the commercial fishery traps.

Finally, we assume that the ratio of the commercial effort to the monitoring effort is either constant over the season or can be estimated up to a constant factor. The latter means that the daily value of α(commercial effort/monitoring effort) is known for some fixed but possibly unknown constant α. Given that the monitoring effort is known, this will occur if, for example, an index, $I_{\text{commercial effort}} = \alpha$(commercial effort), of the commercial effort is available. In our case, logbook data provide such an index. Finally, we also examine the effect of incorrectly assuming that this ratio is constant by comparing estimates using this assumption with those using the estimated ratio.

All of the assumptions will be better satisfied if the exploited and reference classes are biologically as similar as possible. In the case of lobster, two narrow, adjacent length classes will better satisfy the assumptions than either two wide classes or nonadjacent classes.

Exploitation rate

The usual or "strict exploitation" rate during a fishing season is defined as $u = C/N$, where C is the fleet catch during the season and N is number of lobsters in the exploited population before the fishery starts. The exploited population is the base population for this definition.

The strict exploitation rate can be misleading if it is the only measure of exploitation rate used to evaluate the effectiveness of regulations that increase the minimum legal size. For example, a change in regulation that increases the minimum legal size can result in a smaller exploited population and, therefore, an increase in exploitation rate, even if catch is constant. As a consequence, we defined the extended exploitation rate, $u^* = C/(N + N^*)$, where N is as above and N^* is the number of lobsters in some nonexploited length class, allowing a consistent base population between years, independent of changes in regulations. Notice that the nonexploited length class referred to here may overlap with the reference class.

Model development

We present deterministic equations first, neglecting random variation. Let $i = e$ denote an exploited length class and $i = r$ denote a reference length class. Let $j = 1,\ldots, J$ refer to the J individual sequential fishing events that occurred during the fishing season. Let E_j denote the fleet effort at fishing event j and e_j denote the corresponding monitoring effort. Let c_{ij} denote the monitoring trap catch of length class i at event j. Finally, let $p_j = c_{ej}/(c_{ej} + c_{rj})$.

Under our assumptions, it can be shown (Appendix A) that the following relationship holds for each j:

© 2003 NRC Canada

Fig. 1. Locations of monitoring traps for the three spring seasons and two fall–spring seasons analyzed. The first two numbers preceding the hyphen refer to the lobster fishing area (LFA) number. The number after the hyphen refers to the subarea within the LFA.

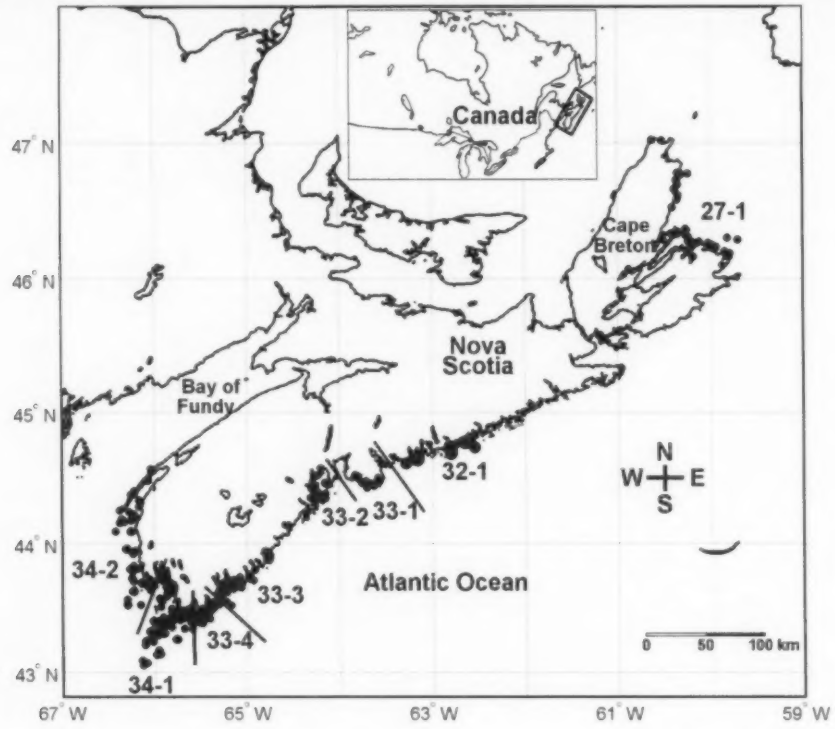

$$(1)\qquad p_j = \frac{1}{1 + \dfrac{1}{A + B\sum_{i=1}^{j-1}\left(E_i/e_i\right)c_{ei}}}$$

where A and B are constants.

To introduce random variation, let $p_j = \hat{p}_j + \varepsilon_j$. Then the above equation applies to the expected value $\hat{p}_j$ of p_j:

$$(2)\qquad \hat{p}_j = \frac{1}{1 + \dfrac{1}{A + B\sum_{i=1}^{j-1}\left(E_i/e_i\right)c_{ei}}}$$

Given a series of observations c_{ej} and $p_j = c_{ej}/(c_{ej} + c_{rj})$, we estimate A and B using nonlinear regression with the loss function:

$$(3)\qquad \Sigma_j(c_{ej} + c_{rj})\varepsilon_j^2$$

The weight is close to the inverse variance weight $(c_{ej} + c_{rj})/(\hat{p}_j(1 - \hat{p}_j))$. However, because $\hat{p}_j$ normally remains away from 0 (no exploited population catch) and 1 (no reference population catch), $(\hat{p}_j(1 - \hat{p}_j))$ does not vary much and has been ignored, allowing for simpler computations.

Finally, following Paulik and Robson (1969), we obtain an estimator of exploitation rate up to event j:

$$(4)\qquad \widehat{\mathrm{ER}}_j = 1 - \left(\frac{\hat{p}_j}{1 - \hat{p}_j}\right)\Big/\left(\frac{\hat{p}_0}{1 - \hat{p}_0}\right)$$

The special case $j = J$ gives the season exploitation rate. This estimate depends, therefore, on the sequence of observations. By comparison, typical end-point CIR methods would use only the first and last observations:

$$(5)\qquad \widehat{\mathrm{ER}}_{\text{End Points}} = 1 - \left(\frac{p_J}{1 - p_J}\right)\Big/\left(\frac{p_0}{1 - p_0}\right)$$

Confidence intervals for $\widehat{\mathrm{ER}}$ were estimated using bootstrapping. Consider the set of lobsters observed during a season. A sample with replacement of these lobsters was generated, and fishing events with no catch were removed. $\widehat{\mathrm{ER}}$ was computed using the reference/exploited and fishing event information for these lobsters. The confidence interval was obtained using the percentile method (Efron and Tibshirani 1993).

An estimate of the extended exploitation rate is obtained from the estimate of the strict exploitation rate by

$$(6)\qquad \widehat{\mathrm{XER}}_{ej} = \left(\frac{c_{e1}}{c_{e1} + c_{r1}^*}\right)\widehat{\mathrm{ER}}_{ej}$$

where c_r^* is the catch from the nonexploited portion of the base population (defined above as N^*).

© 2003 NRC Canada

Table 1. Fishery conditions during the study.

LFA	Season	Average landings (t)	Licenses	Traps per license	MLCL (mm)	Season
27	Mid-May to mid-July	1 300	486	275	73	1999 to 2000
					74.5	2001
32	19 April to 20 July	300	167	250	84	1999
					82.5	2000 to 2001
33	Last Monday in Nov. to 31 May	2 000	723	250	81	1999–2000
					82.5	2000–2001
34	Last Monday in Nov. to 31 May	12 000	992	375 Fall	81	1999–2000
				400 Spring	82.5	2000–2001

Note: LFA, lobster fishing area; MLCL, minimum legal carapace length.

Table 2. Average number of monitoring trap program participants, traps, trap hauls, and fishing days occurring in each area during the three spring fishery (1999–2001) and two fall–spring fishery (1999–2000, 2000–2001) seasons.

Area	Fishery	Participants	Traps	Trap hauls	Fishing days
27-1	Spring	19	75	2983	56
32-1	Spring	12	23	945	62
33-1	Fall–spring	6	19	836	108
33-2	Fall–spring	5	20	643	78
33-3	Fall–spring	13	40	2215	147
33-4	Fall–spring	6	18	735	94
34-1	Fall–spring	15	35	1759	129
34-2	Fall–spring	12	29	1562	140

Table 3. Fishermen and Scientists Research Society (FSRS) defined length classes.

Length class	Size definition (mm)
1	<51
2	51–60
3	61–70
4	71–75
5	76–80
6	81–90
7	91–100
8	>100

Partial-season exploitation rate estimates

We refer to the exploitation rate reached up to a moment before the end of the season as a partial-season exploitation rate. The continuous CIR method allows both in- and post-season estimates of the partial-season exploitation rate. Given some target exploitation rate, in-season estimates could be used to trigger an immediate change in season length, whereas post-season estimates could be used for forward planning.

The stability of in-season estimates of the partial-season exploitation rate is examined by obtaining estimates after each fishing event. We examine the stability of in-season exploitation rate estimates obtained after each fishing event. Visual examination of the estimates and of the bootstrapped confidence intervals were used to determine when the estimates stabilized. The number of events and exploitation rates required for stabilization can be used to make a judgement on the applicability of this method for in-season management decisions. The patterns from the data are compared with Monte Carlo simulations to provide insight into the major factors influencing the estimate.

Post-season estimates of partial-season exploitation rates are obtained using the model fitted with the full season data set. The estimates of $\hat{p}_0$ and $\hat{p}_j$ were then used to obtain $\widehat{\mathrm{ER}}_j$ (eq. 4). A confidence interval can be computed using the A and B parameter estimates associated with the upper and lower confidence limits of the final estimate or, equivalently, by running a new bootstrap.

Exploring the model

Null exploitation rate

Testing the hypothesis that the exploitation rate is 0 can be useful in regulation enforcement activities. Furthermore, not rejecting the null hypothesis when it is known to be true is a desirable property of a statistical method. We examine such a case using a range of lengths newly excluded from the fishery, where the exploitation rate is expected to be 0, as the exploited class.

Comparison of end-point versus concurrent sampling estimates

To compare the quality of end-point and concurrent sampling to estimate the exploitation rate and the extended exploitation rate, we carried out Monte Carlo simulations in the following manner. Data collection from a spring (April to July) and a fall–spring (November to May) lobster fishery were simulated. The estimated exploitation rate, observed landings and effort, and temperature recordings from observed fisheries (described below) were used to set up the simulation. Temperature-dependant catchability was then

© 2003 NRC Canada

Table 4. Number of lobster observed in monitoring traps by Fishermen and Scientists Research Society (FSRS) length class.

(*a*) Cases in which reference class is included in FSRS length-class 4

		Length class			
		Reference	Exploited		
		4	4	5	6
Area	Season	(71–MLCL)	(MLCL–75)	(76–80)	(81–90)
Males					
27-1	1999	338	303	405	314
27-1	2000	268	249	432	327
27-1	2001	418	248	469	389
Females					
27-1	1999	343	273	381	241
27-1	2000	245	275	391	233
27-1	2001	430	208	486	348

(*b*) Cases in which reference class is included in FSRS length-class 5

		Reference	Exploited		
		5	6	7	8
Area	Season	(76–80)	(MLCL–90)	(91–100)	(>100)
Males					
33-1	1999–2000	144	145	64	23
33-2	1999–2000	96	87	26	22
33-3	1999–2000	595	397	174	44
33-4	1999–2000	199	206	73	23
34-1	1999–2000	688	392	143	61
34-2	1999–2000	414	272	86	19
Females					
33-1	1999–2000	124	94	44	12
33-2	1999–2000	97	67	33	3
33-3	1999–2000	418	221	62	16
33-4	1999–2000	207	161	67	21
34-1	1999–2000	526	298	86	15
34-2	1999–2000	488	247	56	4

(*c*) Cases in which reference class is included in FSRS length-class 6

		Reference	Exploited		
		6	6	7	8
Area	Season	(81–MLCL)	(MLCL–90)	(91–100)	(>100)
Males					
32-1	1999	20	82	54	37
32-1	2000	22	144	122	78
32-1	2001	26	103	116	56
33-1	2000–2001	18	83	72	19
33-2	2000–2001	9	103	47	18
33-3	2000–2001	148	476	342	83
33-4	2000–2001	19	143	94	32
34-1	2000–2001	197	527	419	148
34-2	2000–2001	245	802	322	78
Females					
32-1	1999	32	60	42	22
32-1	2000	27	116	94	75
32-1	2001	34	103	87	41
33-1	2000–2001	18	43	37	11
33-2	2000–2001	23	98	32	11
33-3	2000–2001	102	264	97	28
33-4	2000–2001	20	113	76	10
34-1	2000–2001	200	416	306	71
34-2	2000–2001	255	702	202	26

Note: Length-class codes and carapace length boundaries (mm) for length classes are provided. Reference class for areas in lobster fishing areas (LFAs) 33 and 34 for the 1999–2000 season include 81- to 82.5-mm lobster monitored during the spring portion of the 1999–2000 season, when the minimum legal carapace length (MLCL) changed.

© 2003 NRC Canada

Fig. 2. Simulation examples demonstrating the data patterns for reference (solid circles) and exploited (open circles) classes at (*a*) a high exploitation rate (ER; ER ≈ 0.80), (*b*) a lower ER (ER ≈ 0.40), and (*c*) the steeper decline of the estimator $\hat{p}$ at the higher ER (broken line) compared with lower ER (solid line).

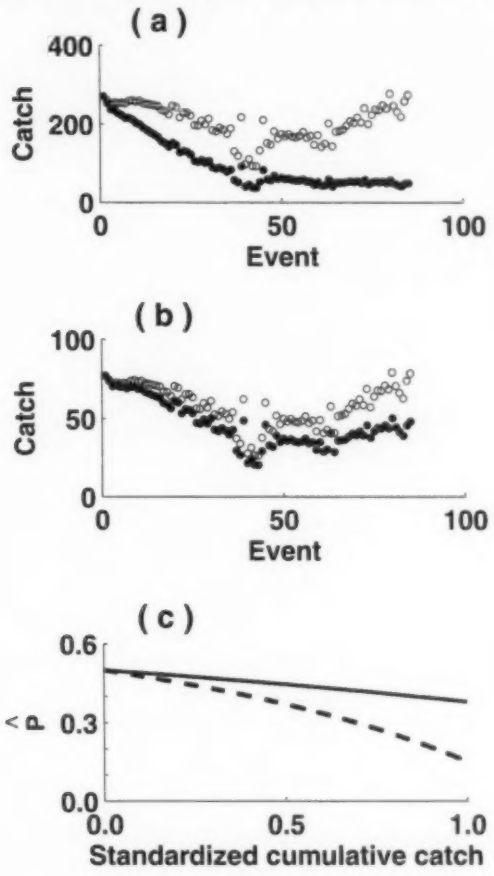

computed using Paloheimo's (1963) model, $q_t = q_{ref}(t - t_{ref})$, where q_t is catchability for temperature t, t_{ref} is the temperature at which lobsters become active, and q_{ref} was chosen to give the season catchability as $\widehat{ER}/E$. Random sampling from a binomial distribution at each fishing event simulated monitoring trap sampling of the reference and exploited classes.

Robustness

We investigate the consequences of violating assumption 1, that the population is closed, using simulations with perfect knowledge of natural mortality (migration would have similar effects on the estimator). Results of the following simulations were compared: annual instantaneous natural mortality of 0.1 for both classes, of 0.5 for the reference class and 0.1 for the exploited class, and of 0.1 for the reference class and 0.5 for the exploited class.

We evaluate the consequences of violating assumption 2, that the catchability ratio between the reference and exploited classes is constant, by Monte Carlo simulations with perfect knowledge of temperature effects. Paloheimo's model (1963) was used as above. First, results where t_{ref} was below the minimum observed temperature (2.6 °C, fall–spring fishery; 3.1 °C, spring fishery) were examined. Simulations using t_{ref} = 0 °C for the reference class and t_{ref} = 2 °C for the exploited classes were compared with results for the opposite attribution. Second, results in which t_{ref} was above the minimum observed temperatures were examined. Simulations using t_{ref} = 4 °C for the reference class and t_{ref} = 6 °C for the exploited classes were compared with results for the opposite attribution. Cases in which exploitation rates were high (≈0.80) and low (≈0.40) were examined. Simulated effort was constant, but catchability changed in response to the various levels of t_{ref}. Residuals were plotted against temperature to determine if there was a diagnostic pattern characteristic of violating assumption 2.

Fig. 3. Temperature trends for each day of data collection for all years and areas of monitoring trap data collection for fall–spring (1999–2000 and 2000–2001 seasons; solid circles) and spring fisheries (1999–2001 seasons; open circles).

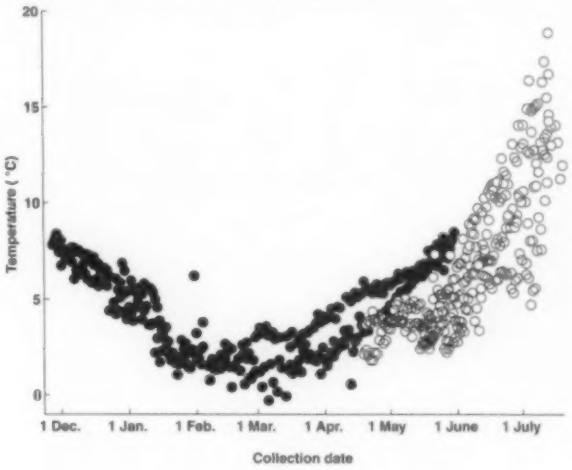

There are no data available to test assumption 3, that the ratio of catchability by the monitoring and commercial traps is constant. Given the differences in mesh sizes and escape mechanisms (described below) between the monitoring and commercial traps, the catchability by the monitoring and commercial traps is certainly different. However, given that these length classes are relatively narrow, that fishing is simultaneous, that the traps are fished in the same area, and that the same baits are used, an influential change in the ratio appears unlikely.

Assumption 4, that the ratio of the fleet effort to the monitoring effort is constant or can be estimated up to a constant factor, is examined empirically. We estimated the exploitation rate assuming a constant ratio, as well as using the estimated ratio of fleet effort to monitoring effort obtained from logbooks.

Data

Fishery

The Nova Scotia, Canada, Atlantic Coast lobster fisheries take place from the Bay of Fundy to the east coast of Cape

© 2003 NRC Canada

Fig. 4. Examples of (*a*) fall–spring and (*b*) spring exploited class (solid circles) and reference class (open circles) catches, (*c*) fall–spring and (*d*) spring observed (solid circles) and estimated ratios ($\hat{p}$), and (*e*) fall–spring and (*f*) spring residuals versus temperature. Fall–spring fishery examples are for males, size 6, area 33-3, in 1999–2000 season. Examples for spring fishery are for males, size 4, area 27-1, in 2000 season. Variable size symbols refer to relative number of total lobsters caught to indicate influence on loss function (eq. 3).

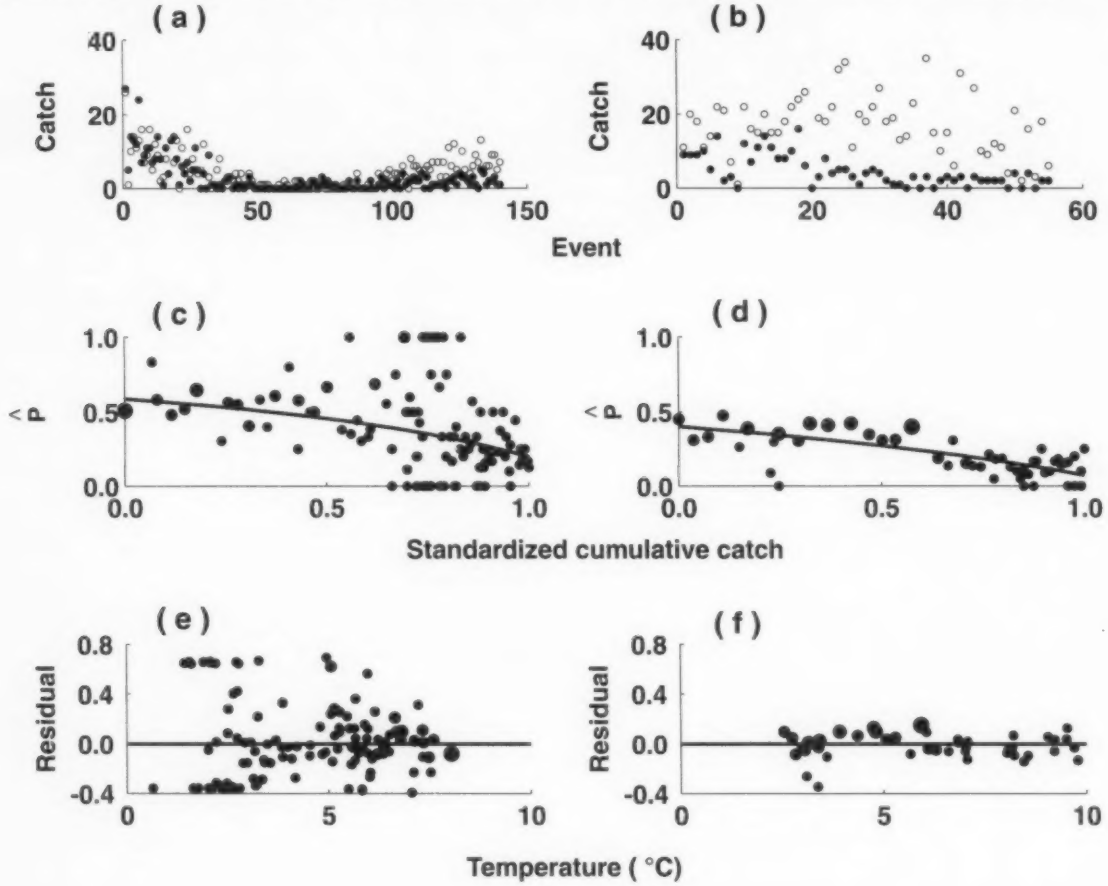

Breton. This area is subdivided into 11 lobster fishing areas (LFAs). In a program to develop a recruitment index for juvenile lobster, fishers belonging to the Fishermen and Scientists Research Society (FSRS) began in 1999 to collect data from a set of standardized monitoring traps located in every LFA.

We use data from eight study areas (27-1, 32-1, 33-1 to 33-4, 34-1, and 34-2) that are portions of LFAs 27, 32, 33, and 34 (Fig. 1). Each study area corresponded to a group of relatively similar ports (Campbell and Mohn 1983; Hudon 1994; Miller 1997) for which there were sufficient data (Fig. 1). The fishery conditions and regulations varied among the LFAs during the study (Table 1).

Monitoring program

The monitoring program used standardized 101.6 cm × 53.3 cm × 35.6 cm traps with a 2.5-cm mesh and a 12.7-cm entrance. To prevent small lobsters from leaving, the traps did not have escape vents. In comparison, commercial traps were a similar size but had mesh sizes ranging from 3.81 cm to 5.08 cm and an escape vent (Miller 1990). Participants placed the monitoring traps within their fishing ground where they expected to catch juvenile lobster. The traps remained at the same location during a given fishing period for spring fisheries but may have been moved between the fall and spring period for fall–spring fisheries. During a fishing period, monitoring occurred on a daily basis unless weather or other factors prevented it.

During the study, five to 19 fishers participated in each study area, and each one fished from two to five monitoring traps per season. Monitoring trap hauls ranged from about 600 to 3000 per area (Table 2).

Fishers recorded the number of lobster of each sex, the FSRS-defined length class (Table 3), and whether or not the length was above the MLCL in each monitoring trap on each fishing day. The FSRS-defined length classes relevant to our study were classes 4 to 8 (Table 4). An automated temperature recorder placed on one monitoring trap from each par-

© 2003 NRC Canada

Fig. 5. Point exploitation rate estimates (solid circles) and 95% confidence intervals (vertical lines) for (*a*) males and (*b*) females for length class containing the first exploited length class, (*c*) males and (*d*) females of the second largest exploited length class, and (*e*) males and (*f*) females from the largest exploited length class in each fishery examined.

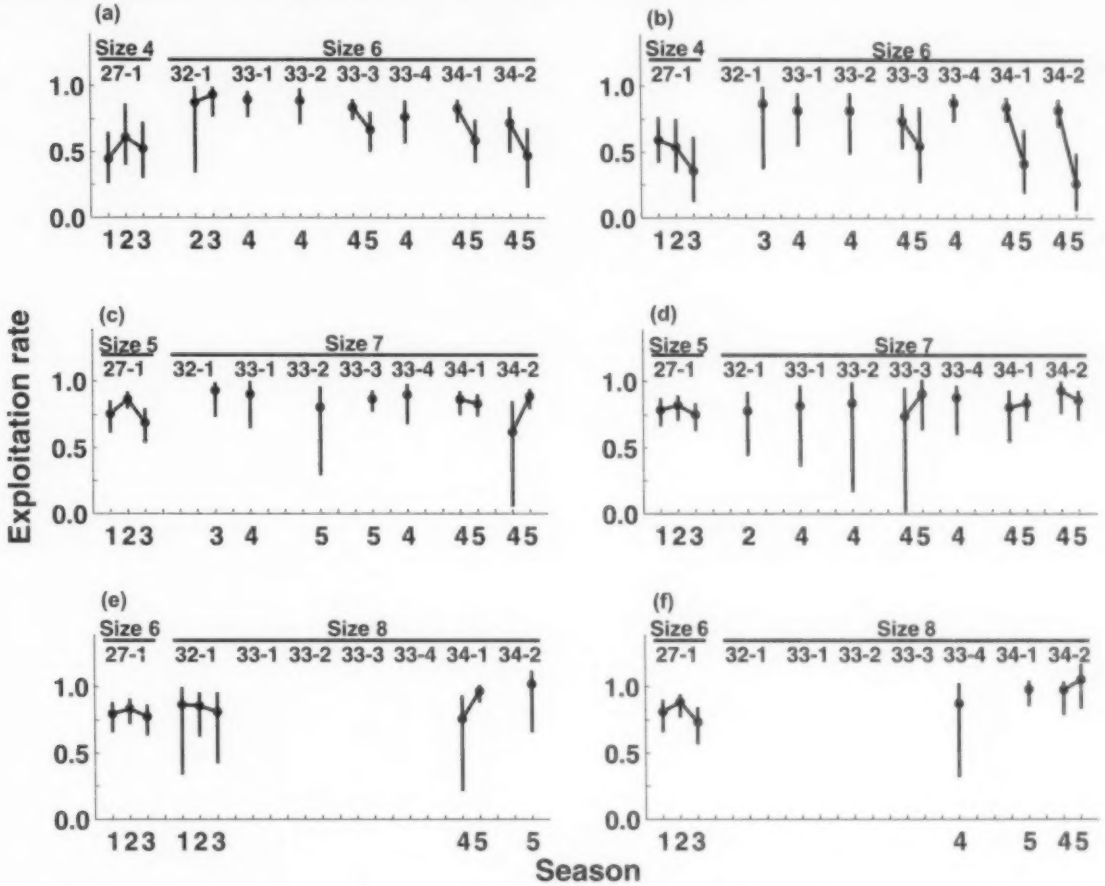

ticipant recorded temperature at 30-min intervals. Average daily temperatures were based on recordings from midnight to midnight.

Commercial effort

An index of commercial effort was obtained from logbooks that are mandatory in LFA 34 and voluntary in the other LFA study areas. In LFA 34, where number of trap hauls must be recorded, we obtained an exact measure of effort. In the other LFAs, effort from fishers who voluntarily recorded their daily number of trap hauls was used. The use of these voluntarily recorded trap hauls as an index of effort required the assumption that volunteers and nonvolunteers fished in a similar manner in these LFAs.

Results

Estimation

Illustration of method

For illustration purposes, consider the results of simple simulations for high (0.80) and low (0.40) exploitation rates for a fall–spring fishery (Figs. 2*a*, 2*b*). Catches from the reference and the exploited classes decrease as the temperature decreases (Fig. 3). Catches from the unexploited reference class recover to pre-season levels when temperature increases, whereas catches from the exploited class recover to a level lower than their pre-season level because of depletion. The amount of recovery is dependent on exploitation rate. The decline in the proportion of exploited to total catches (eq. 4) shows the difference in these exploitation rates (Fig. 2*c*).

In observed data from a fall–spring fishery (Figs. 3, 4*a*, 4*c*) and from a spring fishery (Figs. 3, 4*b*, 4*d*), we obtain similar patterns. Residuals do not show any particular pattern relative to temperature (Figs. 4*e*, 4*f*).

Estimated exploitation rates

Across all areas and seasons studied, exploitation rate estimates varied from 35% to 100% (Fig. 5). The 95% confidence interval length varied from 0.02 to 0.97, depending mostly on the number of lobsters observed.

In areas 27-1, 33-3, 34-1, and 34-2, the MLCL was increased between the last two seasons of the FSRS project so

© 2003 NRC Canada

Fig. 6. In-season exploitation rate estimates by event (solid line) with bootstrap 95% confidence limits (broken lines) for observed data from (*a*) fall–spring (1999–2000) fishery, area 34-1, size-6 females and (*b*) spring (2000) fishery, area 27-1, size-4 females. Lower confidence limit has been cut off at –1.0 in both cases to better illustrate the trend towards stability in the estimates.

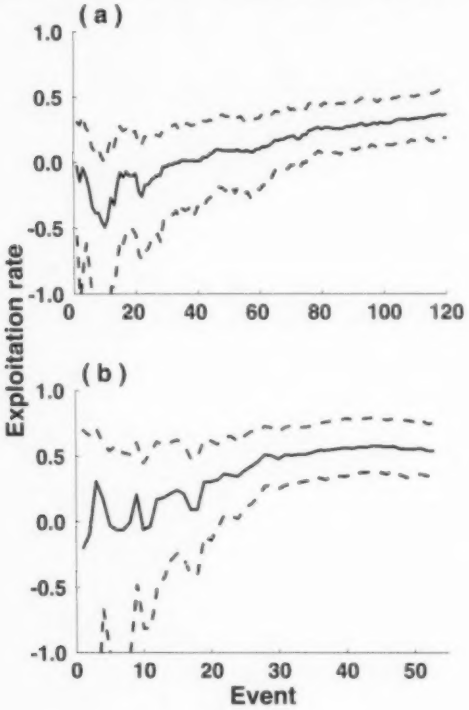

Fig. 7. Post-season exploitation rate estimates by fishing event (solid line) with 95% confidence limits (broken lines) for (*a*) fall–spring (1999–2000), area 33-3, size-6 females and (*b*) spring (1999), area 27-1, size-4 females. The solid horizontal and vertical lines show the relationship between a hypothetical target of 0.70 exploitation rate and the corresponding season date.

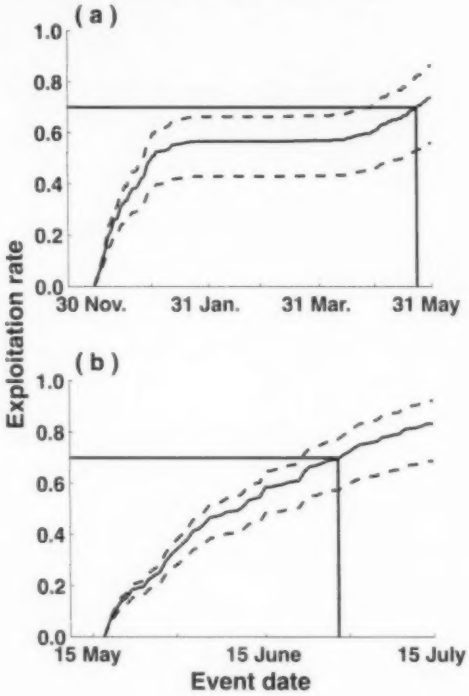

that a part of the first exploited length class became sublegal. The point estimate of the extended exploitation rate declined accordingly for males and females (Figs. 5*a*, 5*b*), but the difference is only significant for females in 34-1 and 34-2. During the same period, the MLCL remained unchanged in 32-1, and the point estimate of the exploitation rate increased for males in this area (Figs. 5*a*, 5*b*), but again the difference is not significant.

Estimated extended exploitation rates generally remained similar or increased during the last two seasons for the second and third exploited length classes regardless of area and minimum carapace length regulations. The exception was the trend for 27-1, which showed an increase from 1999 to 2000 followed by a decline from 2000 to 2001 (Figs. 5*c*, 5*d*, 5*e*, 5*f*).

Partial-season estimates

In-season estimates of the partial-season exploitation rate are highly unstable at the beginning of the season when the exploitation rate is still low (Fig. 6*a*, 6*b*). We conclude that an in-season estimate is useful only after the exploitation rate has reached 25% to 30%.

Post-season estimates of the partial-season exploitation rate show that in the fall–spring fishery, a 1-week reduction of the season would be required for area 33-3 (Fig. 7*a*) to reach a target exploitation rate of 70%, whereas in the spring fishery, a 2-week reduction would be needed (Fig. 7*b*).

Exploring the model

Null exploitation rate

In LFAs 33 and 34, changes in the MLCL removed the 81- to 82.5-mm lobsters from the legal catch range. The confidence interval for the exploitation rate for that class contains 0 for each subarea, as one would expect (Table 5). Equivalently, we would not reject the null hypothesis that the exploitation rate is 0 with a 5% significance level, based on these data.

Comparison of end-point versus concurrent sampling estimates

Concurrent sampling provided superior exploitation rate and extended exploitation rate estimates compared with end-point sampling when the number of traps was constant for individual events. For example, concurrent sampling at 73 traps per event provided estimates with less bias and smaller ranges than end-point sampling using 73 traps for each sampling event. The same results were found for 500 traps (Fig. 8). Concurrent sampling had to be at the lowest level tested (73 traps) and end-point sampling had to be at the highest

© 2003 NRC Canada

Table 5. Exploitation rates estimated for original and newly excluded reference classes (mm) for the 2000–2001 fall–spring season with 95% confidence intervals from bootstrap estimates.

	Reference class		Exploitation rate		
Area	Original (mm)	Newly excluded (mm)	Confidence interval: lower limit	Estimate	Confidence interval: upper limit
33–1	76–80	81–82.5	–1.06	0.03	0.50
33–2	76–80	81–82.5	–2.70	–0.86	0.05
33–3	76–80	81–82.5	–0.05	0.20	0.38
33–4	76–80	81–82.5	–0.94	0.06	0.51
34–1	76–80	81–82.5	–0.42	–0.12	0.09
34–2	76–80	81–82.5	–0.05	0.13	0.27

Fig. 8. Simulation tests of (*a*) strict exploitation rate (ER) and (*b*) extended exploitation rate (XER) estimates using sampling concurrent with fishing and pre- and post-sampling. Solid circles represent concurrent sampling and open circles represent end-point sampling mean estimates from simulated data. Vertical lines are minimum and maximum simulated estimates. Horizontal lines are true simulated exploitation rates.

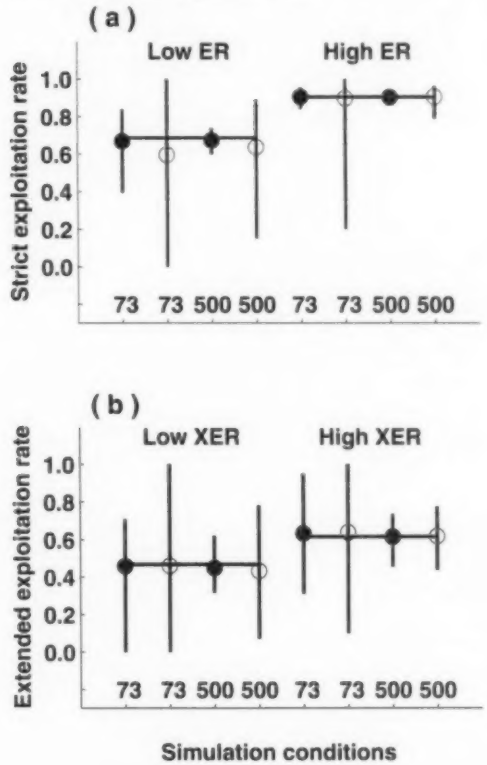

trap level (500) for end-point sampling to be superior to concurrent sampling (Fig. 8).

Robustness

When violating assumption 1, differences in natural mortality and (or) migration between the exploited and reference classes create a small bias (below 10%) in the estimate of the exploitation rate if the exploitation rate is high (above 90%). However, when the exploitation rate is low (≈40%), a difference in natural mortality and (or) migration rates of 40% between classes can create a bias of 20% in the estimate of the exploitation rate.

Table 6. Bias in simulated exploitation rate (ER) estimates when t_{ref} (°C) for reference and exploited lobster is below and above the minimum temperature observed in a simulated fishery.

		Percent bias	
Reference t_{ref} (°C)	Exploited t_{ref} (°C)	Fall–spring	Spring
High ER			
0	2	4	–17
2	0	–3	3
4	6	335	Failed
6	4	Failed	37
Low ER			
0	2	25	Failed
2	0	–18	55
4	6	1575	Failed
6	4	Failed	290

Note: Minimum observed temperature was 2.6 °C for fall–spring fishery and 3.1 °C for spring fishery. An estimate failed when the confidence interval for the parameter estimates contained 0.

In the violation of assumption 2, the estimation procedure performed better for fall–spring fisheries when simulated t_{ref} was less than the minimum temperature (2.6 °C) for reference and exploited classes. At high exploitation rates, bias in estimates was within ±5%, and at low exploitation rates, it was within ±25%. In contrast, when simulated t_{ref} was greater than the minimum temperature, the estimation procedure either failed or produced an unacceptably high bias (Table 6).

For spring fisheries, the bias was within 20% only when exploitation rate was high and simulated t_{ref} was less than the minimum temperature for reference and exploited classes. In all other cases, the estimation procedure either failed or produced an unacceptably high bias (Table 6). Therefore, the impact of the violation was greater for spring fisheries. The dispersion pattern of residuals as a function of temperature differed depending on t_{ref} for the reference and exploited class (Fig. 9).

Graphical analysis verified that assumption 4 was met in most cases (e.g., Fig. 10*a*) but was violated in a few cases (e.g., Fig. 10*b*). We examined the consequences of violating assumption 4 by estimating the exploitation rate using the estimated ratio of fleet effort to monitoring effort obtained from logbooks and also assuming a constant ratio. Most ex-

© 2003 NRC Canada

Fig. 9. Residuals versus temperature plots for simulation trials examining the effect of differing t_{ref} for reference and exploited classes: (*a*) t_{ref} for reference (0 °C) and exploited class (2 °C) is below the minimum observed temperature (2.6 °C); (*b*) t_{ref} for reference (4 °C) and exploited class (6 °C) is above the minimum observed temperature (2.6 °C).

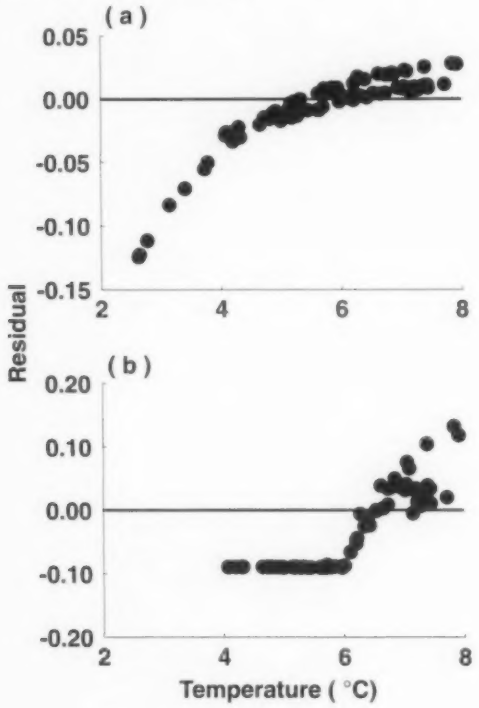

Fig. 10. An example of a data set in which assumption of a constant ratio between commercial effort and monitoring effort (*a*) was met, lobster fishing area (LFA) 27-1, 2001 season, and (*b*) was not met, LFA 33-4, 2000–2001 season.

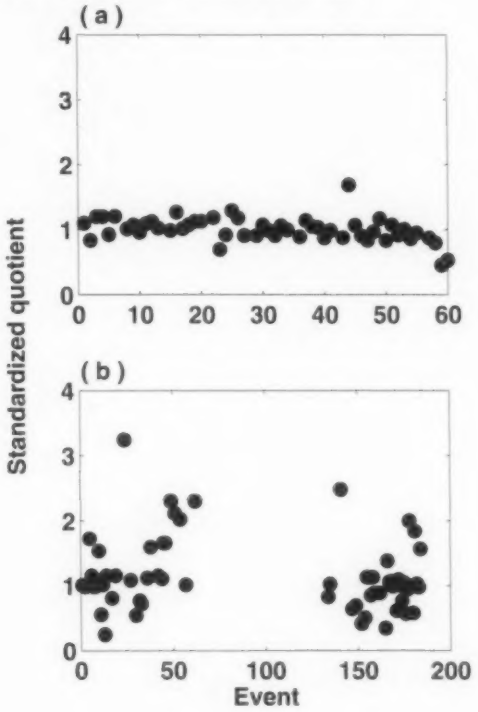

ploitation rate estimates differed by less than ±5%, and most bootstrapped confidence interval lengths differed by less than ±20% (Fig. 11).

Discussion

Advantages of the continuous CIR method

The main statistical advantage of the continuous CIR method is that it will give better results than the end-point CIR method except when the end-point sampling effort is much larger than the concurrent sampling effort. Furthermore, a small continuous sampling effort by fishers may be easier to implement than two or three large surveys by technical staff or fishers. A continuous sampling effort may also be less susceptible to accidental failures from such things as equipment malfunction or poor weather. Finally, the continuous CIR method allows both in-season and post-season estimates of partial-season exploitation rates.

Assumption consequences

We have made four basic assumptions. All assumptions will be better satisfied if the reference and exploited classes are adjacent and narrow. We have shown that the method displays some robustness relative to departures from these assumptions. We have also shown that the ratio of fleet to monitoring effort is constant for most of the data set studied.

The ratio of lobster catchability for the exploited and reference classes may vary as a consequence of agonistic behaviour among lobsters of differing sizes. For example, the depletion of the large lobsters from the exploited class may progressively increase catchability of the small lobsters from the reference class, therefore changing the ratio. Frusher and Hoenig (2001*c*) found a negative correlation between the catch of rock lobsters <90 mm carapace length and that of rock lobsters >109 mm carapace length in research traps. Ziegler et al. (2002) found a similar relationship between the catch of rock lobster males 81–100 mm compared with males >140 mm, and between the catch of females 81–90 mm and females >120 mm. The estimated correlation coefficients ranged from approximately 0 to –0.5. On one hand, these results confirm that nonadjacent, wide reference, and exploited classes must be avoided. On the other hand, given these results for widely spaced classes and that the correlation must be 0 within length classes, interpolation of these results suggests that the agonistic effect would be small for adjacent classes.

Jury et al. (2001) used video cameras to observe 8023 American lobster approaches to traps, 331 trap entries, and 310 trap escapes. They report that if a lobster entering the trap was larger than the current occupant, it chased the smaller one from the entrance portion of the trap. Similarly,

© 2003 NRC Canada

Fig. 11. Distribution in differences between exploitation rate (ER) estimates and confidence limit (CL) lengths for analyses using the ratio of commercial effort to monitoring traps compared with those assuming that the ratio is constant. Bins at the extremes represent all values greater than the value indicated if positive and all values less than the value indicated if negative.

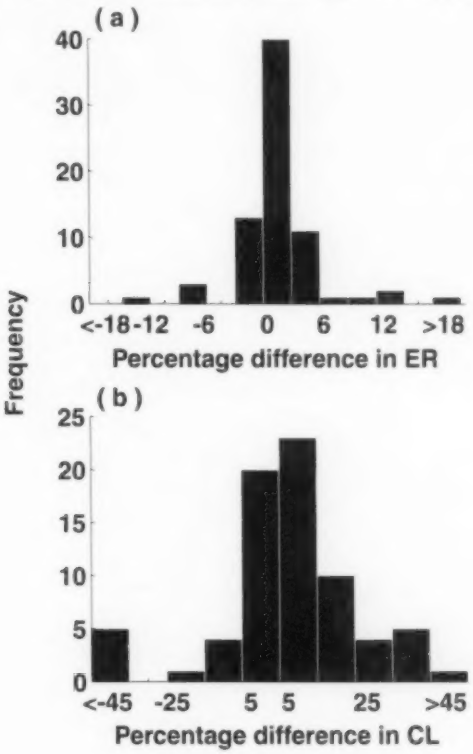

larger lobsters already in a trap excluded smaller lobsters from entry. They do not relate these behaviours to precise lobster size differences.

Molting season for lobster in LFAs 27 to 34 is from mid-July to early September (Waddy et al. 1995; Department of Fisheries and Oceans (DFO) 1998*a*, 1998*b*). For LFA 33 and 34, the fishing season and the molting season do not intersect. For LFAs 27 and 32, the fishing season, from April or May to mid-July, and the molting season, which begins in mid-July, have a very small intersection. Thus, molting should not influence exploitation rate estimates for either fishery.

Sampling guidelines

The successful use of the continuous CIR approach requires a well-designed sampling program. Usual care in sampling design must be applied, including ensuring the reliability of the participating fishers and the accuracy of the data acquisition. Measuring lobster to the nearest mm, rather than in 5-mm or 10-mm classes would assist in defining adjacent and narrow reference classes. Efforts should be made to cover the geographic range of the fishery to minimize any change in the relationship between the behaviour of the exploited and reference classes. A short-term tagging experiment coincident with a continuous monitoring program would provide alternative data for testing model assumptions and estimating partial-season exploitation rates (S. Martell and C. Walters, Fisheries Centre, University of British Columbia, Vancouver, BC V6T 2Z1, unpublished data).

Some minimum sample size is required. Paulik and Robson (1969) found that 500 or more animals were sufficient for most purposes. Between 100 and 500 animals, sufficient reference and exploited catches and a high exploitation rate are necessary to ensure useful results. Difficulties in interpreting estimates usually occur when <100 animals are sampled. Frusher et al. (1998) found that 100 lobster pots allowed them to detect a 25–30% reduction in exploitation rate. We found that useful estimates, as measured by the confidence limits, were obtained when the total catch of reference and exploited length classes was >200, a somewhat better result than that of Paulik and Robson (1969), which is consistent with the advantage of continuous sampling.

Improving assessment and management

Current DFO lobster stock assessments (DFO 1998*a*, 1998*b*, 2001) have provided exploitation rate estimates by sex for the entire exploited portion of lobster populations without quantifying statistical uncertainty. Furthermore, only LFA-wide estimates have been obtained, with the exception of LFA 27, which was split into north and south portions (DFO 1998*a*). The continuous CIR method presented here provides exploitation rate estimates by sex and length class, with confidence limits, and for smaller subareas of LFAs than would otherwise be possible.

We have shown that estimates of exploitation rates from data collected concurrently with fishing using monitoring traps are feasible. Our results also indicate that the method can be used to assess the impact of management measures. We have also described a method to predict the impact of season length restriction on exploitation rate, which adds to the range of management options available. For example, if it was decided to implement a shortening of the season to attempt to reduce exploitation rate, the method that we describe could be used to determine if it was as successful as intended. It is possible that fishing effort may shift to make up for early closure. For example, fishing may increase during marginal weather days or by some other mechanism to compensate for the closure days. Frusher et al. (1997) observed a shift in effort as the result of removing 17 days from a rock lobster fishery.

Our experience in other fisheries indicates that sampling concurrent with fishing is an effective way of incorporating local fishers into fish stock assessments (Claytor and Allard 2001) and providing a scientific basis for their participation in the assessment and management process (Claytor 2000).

Acknowledgements

We thank the executive of the Fishermen and Scientists Research Society (FSRS) for making the trap-monitoring data accessible. We especially thank the FSRS members who participated in the data collection. We thank Yong Chen, Carl MacDonald, Nora Macnee, Manon Mallet, Bob Miller, Bob O'Boyle, Stephen Smith, John Tremblay, and two anon-

© 2003 NRC Canada

ymous referees for comments and suggestions that improved the manuscript.

References

Campbell, A., and Mohn, R.K. 1983. Definition of American lobster stocks for the Canadian Maritimes by analysis of fishery-landing trends. Trans. Am. Fish. Soc. **112**: 744–759.

Chen, C-L., Hoening, J.M., Dawe, E.G., Brownie, C., and Pollock, K.H. 1998. New developments in change-in-ratio and index-removal methods, with application to snow crab (*Chionoecetes opilio*). *In* Proceedings of the North Pacific Symposium on Invertebrate Stock Assessment and Management. *Edited by* G.S. Jamieson and A. Campbell. Can. Spec. Publ. Fish. Aquat. Sci. No. 125. pp. 49–61.

Claytor, R.R. 2000. Conflict resolution in fisheries management using decision rules: an example using a mixed-stock Atlantic Canadian herring fishery. ICES J. Mar. Sci. **57**: 1110–1127.

Claytor, R.R., and Allard, J. 2001. Properties of abundance indices obtained from acoustic data collected by inshore herring gillnet boats. Can. J. Fish. Aquat. Sci. **58**: 2502–2512.

Dawe, E.G., Hoenig, J.M., and Xu, X. 1993. Change-in-ratio and index-removal methods for population assessment and their application to snow crab (*Chionoecetes opilio*). Can. J. Fish. Aquat. Sci. **50**: 1467–1476.

Department of Fisheries and Oceans. 1998*a*. Eastern Cape Breton lobster (LFAs 27–30). Department of Fisheries and Oceans Stock Status Report C3-59(1998).

Department of Fisheries and Oceans. 1998*b*. Eastern and south shore Nova Scotia lobster LFAs 31–33. Department of Fisheries and Oceans Stock Status Report C3-60(1998).

Department of Fisheries and Oceans. 2001. Southwest Nova Scotia lobster (Lobster Fishing Area 34). Department of Fisheries and Oceans Stock Status Report C3-62(2001).

Efron, B., and Tibshirani, R.J. 1993. An introduction to the bootstrap. Chapman & Hall, London, U.K.

Frusher, S.D., and Hoenig, J.M. 2001*a*. Strategies for improving the precision and natural mortality estimates from multiyear tagging models: a case study. Mar. Freshw. Res. **52**: 1649–1655.

Frusher, S.D., and Hoenig, J.M. 2001*b*. Estimating natural and fishing mortality and tag reporting rate of a southern rock lobster (*Jasus edwardsii*) from a multiyear tagging model. Can. J. Fish. Aquat. Sci. **58**: 2490–2501.

Frusher, S.D., and Hoenig, J.M. 2001*c*. Impact of lobster size on selectivity of traps for southern rock lobster (*Jasus edwardsii*). Can. J. Fish. Aquat. Sci. **58**: 2482–2489.

Frusher, S.D., Kennedy, R.B., and Gibson, I.D. 1997. Precision of exploitation-rate estimates in the Tasmanian rock-lobster fishery based on change-in-ratio techniques. Mar. Freshw. Res. **48**: 1069–1074.

Frusher, S.D., Kennedy, R.B., and Gibson, I.D. 1998. Preliminary estimates of exploitation rates in the Tasmanian rock lobster (*Jasus edwardsii*) fishery using the change-in-ratio and index-removal techniques with tag–recapture data. *In* Proceedings of the North Pacific Symposium on Invertebrate Stock Assessment and Management. *Edited by* G.S. Jamieson and A. Campbell. Can. Spec. Publ. Fish. Aquat. Sci. No. 125. pp. 63–71.

Hudon, C. 1994. Large-scale analysis of Atlantic Nova Scotia American lobster (*Homarus americanus*) landings with respect to habitat, temperature, and wind conditions. Can. J. Fish. Aquat. Sci. **51**: 1308–1321.

Jury, S.H., Howell, H., O'Grady, D.F., and Watson, W.H., III. 2001. Lobster trap video: *in situ* video surveillance of the behaviour of *Homarus americanus* in and around traps. Mar. Freshw. Res. **52**: 1125–1132.

McLeese, D.W., and Wilder, D.G. 1958. The activity and catchability of the lobster (*Homarus americanus*) in relation to temperature. J. Fish. Res. Board Can. **15**: 1345–1354.

Miller, R.J. 1990. Effectiveness of crab and lobster traps. Can. J. Fish. Aquat. Sci. **47**: 1228–1251.

Miller, R.J. 1997. Spatial differences in the productivity of American lobster in Nova Scotia. Can. J. Fish. Aquat. Sci. **54**: 1613–1618.

Miller, R.J., and Mohn, R.K. 1993. Critique of the Leslie method for estimating sizes of crab and lobster populations. N. Am. J. Fish. Manag. **13**: 676–685.

Paloheimo, J.E. 1963. Estimation of catchabilities and population sizes of lobsters. J. Fish. Res. Board Can. **20**: 59–88.

Paulik, G.J., and Robson, D.S. 1969. Statistical calculations for change-in-ratio estimators of population parameters. J. Wildl. Manag. **33**: 1–27.

Pollock, K.H., and Hoening, J.M. 1998. Change-in-ratio estimators. *In* Encyclopedia of statistical sciences update. Vol. 2. *Edited by* S. Kotz, C.B. Read, and D.L. Banks. John Wiley and Sons, Inc., New York. pp. 109–112.

Pollock, K.H., Hines, J.E., and Nichols, J.D. 1984. The use of auxiliary variables in capture–recapture and removal experiments. Biometrics, **40**: 329–340.

Ricker, W.E. 1975. Computation and interpretation of biological statistics of fish populations. Bull. Fish. Res. Board Can. No. 191.

Tremblay, M.J., and Smith, S.J. 2001. Lobster (*Homarus americanus*) catchability in different habitats in late spring and early fall. Mar. Freshw. Res. **52**: 1321–1331.

Udevitz, M.S., and Pollock, K.H. 1991. Change-in-ratio estimators for populations with more than two subclasses. Biometrics, **47**: 1531–1546.

Udevitz, M.S., and Pollock, K.H. 1995. Using effort information with change-in-ratio data for population estimation. Biometrics, **51**: 471–481.

Waddy, S.L., Aiken, D.E., and de Kleijn, D.P.V. 1995. Control of growth and reproduction. *In* Biology of the lobster *Homarus americanus*. *Edited by* Jan Robert Factor. Academic Press, New York. pp. 217–266.

Yamakawa, T., Matsumiya, Y., Nishimura, M., and Ohnishi, S. 1994. Expanded DeLury's method with variable catchability and its application to catch-effort data from spiny lobster gillnet fishery. Fish. Sci. **60**: 59–63.

Ziegler, P.E., Johnson, C.R., Frusher, S.D., and Garner, C. 2002. Catchability of the southern rock lobster *Jasus edwardsii*. II. Effects of size. Mar. Freshw. Res. **53**: 1149–1159.

Appendix A. Derivation of equations

We present deterministic equations first, neglecting random variation. We use the notation of the main text. We consider the fleet catches first. The exploited lobsters fleet catch C_{ej} depends on the depletion that occurred during fishing events 1,..., $j - 1$. Using the catch equation (Ricker 1975, p. 249) and ignoring natural mortality, we obtain

$$(1) \qquad C_{ej} = q_{ej} E_j \left(N_{e0} - \sum_{i=1}^{j-1} C_{ei} \right)$$

where terms are as defined above and N_{e0} is the initial population number.

Because reference lobsters are returned to the water, the reference lobster catch is

© 2003 NRC Canada

$$(2) \qquad C_{rj} = q_{rj} E_j N_{r0}$$

We will be interested in the ratio of fleet catches:

$$(3) \qquad \frac{C_{ej}}{C_{rj}} = \frac{q_{ej} E_j \left(N_{e0} - \sum_{i=1}^{j-1} C_{ei} \right)}{q_{rj} E_j N_{r0}}$$

We now consider the monitoring trap catch. We assume that the ratio of catchability by the fleet and by the monitoring traps is constant throughout the season. The number of lobsters available to the monitoring and fleet traps is equal. Applying the catch equation to the monitoring and to the fleet catches, we conclude that the relationship between the monitoring trap catch, c_{ij}, and the fleet catch, C_{ij}, is

$$(4) \qquad c_{ij} = \frac{C_{ij}}{(E_j / e_j)\kappa_i}$$

where e_j is monitoring trap effort at event j and κ_i is a constant independent of the fishing event j. Given that κ_i is a constant, the ratio E_j/e_j only needs to be known up to some constant factor.

Substituting in eq. 4, we obtain eqs. 5 and 6:

$$(5) \qquad \frac{c_{ej}}{c_{rj}} = \frac{C_{ej}/[(E_j/e_j)\kappa_e]}{C_{rj}/[(E_j/e_j)\kappa_r]}$$

$$= \frac{q_{ej} \left(N_{e0} - \sum_{i=1}^{j-1} (C_{ei}(E_i/e_i)\kappa_e \right)}{q_{rj} N_{r0}} \frac{\kappa_r}{\kappa_e}$$

$$(6) \qquad \frac{c_{ej}}{c_{rj}} = \frac{q_{ej} \left(N_{e0} - \left(\sum_{i=1}^{j-1} (E_i/e_i) c_{ei} \right) \kappa_e \right)}{q_{rj} N_{r0}} \frac{\kappa_r}{\kappa_e}$$

Because q_{ej}/q_{rj} is independent of j by assumption, we can rewrite the above as

$$(7) \qquad \frac{c_{ej}}{c_{rj}} = A - B \sum_{i=1}^{j-1} (E_i/e_i) c_{ei}$$

As in Paulik and Robson (1969), to accommodate observations with $c_{rj} = 0$, let $p_j = c_{ej}/(c_{ej} + c_{rj})$. After transforming eq. 7, we obtain the following nonlinear relationship:

$$(8) \qquad p_j = \frac{c_{ej}}{c_{ej} + c_{rj}} = \frac{1}{1 + \dfrac{1}{A + B \sum_{i=1}^{j-1} (E_i/e_i) c_{ei}}}$$

When the quotient E_i/e_i is assumed to be constant during the season, it is integrated into the constant B.

Again following Paulik and Robson (1969), using the relationship $c_{ij} = C_{ij}/\kappa_i$ and canceling the ratios κ_e/κ_r, we obtain the strict exploitation rate estimate for each j:

$$(9) \qquad \widehat{\mathrm{ER}}_j = 1 - \left(\frac{C_{ej}}{C_{rj}} \right) \Big/ \left(\frac{C_{e1}}{C_{r1}} \right)$$

$$\approx 1 - \left(\frac{c_{ej}}{c_{rj}} \right) \Big/ \left(\frac{c_{e1}}{c_{r1}} \right) = 1 - \left(\frac{p_j}{1 - p_j} \right) \Big/ \left(\frac{p_0}{1 - p_0} \right)$$

Now, we consider the extended exploitation rate:

$$(10) \qquad \mathrm{XER}_j = \frac{C_{ej}}{N_{e0} + N_0^*}$$

where N_0^* is the number of lobsters in the nonexploited class of the base population.

Using the previous relationship between ER_j and C_{ej} we have

$$(11) \qquad \mathrm{XER}_{ej} = \frac{N_{e0} \mathrm{ER}_{ej}}{N_{e0} + N_0^*}$$

Making the stronger assumption that $q_{ej} = q_{rj}$ for each j, we have the estimator of the extended exploitation rate:

$$(12) \qquad \widehat{\mathrm{XER}}_{ej} = \left(\frac{c_{e1}}{c_{e1} + c_{r1}^*} \right) \widehat{\mathrm{ER}}_{ej}$$

© 2003 NRC Canada

Estimation of recruitment in catch-at-age models

Mark N. Maunder and Richard B. Deriso

Abstract: Management strategies must be designed to take into account the uncertainty inherent in fish populations and their assessments. Annual recruitment variation is an important component of uncertainty. Several methods that allow the estimation of annual recruitment in statistical catch-at-age models are described: (*a*) maximum likelihood estimation with no penalty on the annual recruitment residuals, (*b*) maximum likelihood estimation with a lognormal penalty on the annual recruitment residuals, (*c*) importance sampling to numerically approximate the marginal likelihood with a lognormal penalty on the annual recruitment residuals, and (*d*) full Bayesian integration using Markov Chain Monte Carlo with a lognormal prior on the annual recruitment residuals. Simulation analysis is used to test the performance of these methods. All four methods perform similarly at estimating quantities that are based on averaging or summing multiple estimates of annual recruitment; however the marginal likelihood method (*c*) and Bayesian integration (*d*) perform best at estimating annual recruitment and the standard deviation in annual recruitment residuals (σ_R) when catch-at-age data is missing for some years. The ability to estimate σ_R can be important for defining uncertainty when developing management strategies. The methods are applied to a New Zealand snapper (*Pagrus auratus*) stock and the estimate of σ_R is approximately 0.6.

Résumé : Les stratégies de gestion doivent être élaborées de manière à tenir compte de l'incertitude inhérente aux populations de poissons et à leurs évaluations. La variation annuelle du recrutement est une composante importante de cette incertitude. On trouvera ici la description de plusieurs méthodes qui permettent d'estimer le recrutement annuel à l'aide de modèles statistiques basés sur les captures en fonction de l'âge : (*a*) une estimation de vraisemblance maximale sans pénalité pour les résiduels du recrutement annuel, (*b*) une estimation de vraisemblance maximale avec une pénalité de type lognormal sur les résiduels du recrutement annuel, (*c*) un échantillonnage pondéré pour obtenir une approximation de la vraisemblance marginale avec une pénalité de type lognormal sur les résiduels du recrutement annuel et (*d*) une intégration bayésienne complète à l'aide de la méthode de Monte Carlo par chaîne de Markov avec un a priori de type lognormal sur les résiduels du recrutement annuel. Une analyse de simulation permet de vérifier la performance de ces méthodes. Les quatre méthodes fonctionnent de manière semblable dans l'estimation de valeurs basées sur la somme ou la moyenne d'estimations multiples du recrutement annuel; cependant, la méthode de vraisemblance marginale (*c*) et l'intégration bayésienne (*d*) sont les meilleures pour estimer le recrutement annuel et l'écart type des résiduels du recrutement annuel (σ_R), lorsque les données de captures en fonction de l'âge sont absentes pour certaines des années. La capacité d'estimer σ_R peut être importante pour définir l'incertitude dans l'élaboration de stratégies de gestion. Ces méthodes sont appliquées à un stock de dorades royales (*Pagrus auratus*) et l'estimation de σ_R est d'approximativement 0.6.

[Traduit par la Rédaction]

Introduction

Annual recruitment variation is an important component for the management of fish stocks. Management strategies must be designed to take into account the uncertainty inherent in fish populations and their assessments. Uncertainty can be divided into estimation uncertainty and future uncertainty. Estimation uncertainty encompasses all uncertainty about the model structure and the associated parameter estimates. Future uncertainty includes how processes may change in the future irrespective of how well we have estimated them in the past. Recruitment variation, a form of future uncertainty, can be a significant component of the total uncertainty, especially if the recruiting year class comprises a large proportion of the total population. Populations with different levels of recruitment variability have different probabilities of extinction and recovery. One method to determine uncertainty from recruitment variation is to assume that future recruitment will occur with a similar distribution and time-series structure to historical recruitment. Therefore, it is important to have good estimates of historic recruitment variability.

Is it appropriate to put distributional constraints on annual recruitment in a fisheries stock assessment model? Some analysts would argue that we should not include any prior information in the analysis and let the data provide information about the variability in recruitment. The problem with this argument is that many applications only have sporadic catch-at-age data for the early time period and the estimates of annual recruitment for this period fluctuate more than would be reasonable for a typical fish stock. The variability

Received 7 November 2002. Accepted 31 August 2003. Published on the NRC Research Press Web site at http://cjfas.nrc.ca on 31 October 2003.
J17174

M.N. Maunder[1] and R.B. Deriso. Inter-American Tropical Tuna Commission, 8604 La Jolla Shores Drive, La Jolla, CA 92037-1508, U.S.A.

[1]Corresponding author (e-mail: mmaunder@iattc.org).

 doi: 10.1139/F03-104 © 2003 NRC Canada

seen in the annual recruitment estimates is exaggerated by the uncertainty in these estimates, and any inferences based on the point estimates of recruitment would be invalid (e.g., stock–recruitment relationships, environmental correlations with recruitment, stochastic forward projections). The inclusion of estimates of uncertainty for the recruitments is essential for these analyses, but frequently they are not included. The above argument also assumed that we have not learned anything from the many years of fisheries research, which is inconsistent with the scientific method (Hilborn and Liermann 1998). From previous studies, we know that recruitment is usually lognormally distributed and that the average standard deviation of the logarithm of the annual recruitment residuals over many fish species is around 0.6 (Beddington and Cooke 1983).

The method that is often used to constrain annual recruitment variation in stock assessment models (e.g., Maunder and Starr 2001) is similar to methods used for random effects models (Davidian and Giltinan 1995). In contrast to the argument presented above, the methods used for random effects models make prior assumptions about the distribution of parameters to allow information to be shared between data sets. The annual recruitment is comprised of two components, a fixed effect that is common to all years and a random effect that is different for each year. The fixed effect is usually the average recruitment or the recruitment expected from a stock–recruitment relationship. The random effect is the annual residual and is constrained by a distributional assumption. The distribution that is used to constrain the random effect is usually lognormal with the standard deviation of the logarithm of the annual recruitment residuals fixed (often at 0.6, e.g., Smith and Punt 1998). In traditional random effects models, the standard deviation is estimated as a parameter in the model rather than being fixed at a predetermined value (Davidian and Giltinan 1995). The estimation methods used in fisheries stock assessment are often based on maximizing the full likelihood function (e.g., Smith and Punt 1998; Maunder and Starr 2001). However, the estimation methods used in traditional random effects models usually integrate over the random effects to produce a marginal likelihood function; this marginal likelihood is maximized to estimate the model parameters (Davidian and Giltinan 1995). The marginal likelihood is often a better choice because as the number of years in the model increases, the number of parameters does not increase. Therefore, asymptotic approximations work better for the marginal likelihood (Gelman et al. 1995). This is particularly true for annual recruitment residuals in years for which there are no catch-at-age data. Unfortunately, annual recruitment is nonlinearly intertwined in the likelihood functions for catch-at-age, catch-per-unit-effort (CPUE), and trawl survey data, so that analytical solutions for the integral are not possible. Therefore, numerical integration or an approximation is required to calculate the marginal likelihood function.

Full Bayesian integration is an alternative to maximizing the marginal distribution. Bayesian analysis integrates the probability distribution across all model parameters as opposed to just across the random effects. However, in Bayesian analysis, prior distributions are required for all model parameters. Bayesian analysis has been used in several fisheries applications (e.g., McAllister et al. 1994; Maunder et al. 2000; Maunder and Starr 2001) and has recently been reviewed by Punt and Hilborn (1997) and McAllister and Kirkwood (1998).

We use simulation analysis to investigate several estimation methods that incorporate annual recruitment residuals in a simple catch-at-age model: (*a*) maximum likelihood estimation with no penalty on the annual recruitment residuals, (*b*) maximum likelihood estimation with a lognormal penalty on the annual recruitment residuals, (*c*) importance sampling to numerically approximate the marginal likelihood (integrated across the annual recruitment residuals) with a lognormal penalty on the annual recruitment residuals, and (*d*) full Bayesian integration with a lognormal prior on the annual recruitment residuals. We also investigate the effect of using an informative prior for the standard deviation of the logarithm of the annual recruitment residuals for methods *b*–*d* and the effect of recruitment being uniformly distributed rather than lognormally distributed as assumed. We apply the methods to estimate the variation in recruitment for the snapper (*Pagrus auratus*) stock on the west coast of the North Island of New Zealand.

Estimation methods

Annual recruitment, R_y, is defined as average recruitment, $\bar{R}$, multiplied by an annual residual, ε_y, that is exponentiated and bias corrected (e.g., Maunder and Starr 2001):

$$(1) \qquad R_y = \bar{R} e^{\varepsilon_y - 0.5\sigma_R^2}$$

The annual residual is modified by a lognormal bias correction factor, $-0.5\sigma_R^2$, to ensure that $\bar{R}$ is equal to the mean recruitment (rather than the median), where σ_R is the standard deviation of the logarithm of the annual recruitment residuals.

The annual recruitment is assumed to come from a lognormal distribution so that $\varepsilon_y \sim N(0,\sigma_R)$. A penalty (eq. 2) is added to the negative log-likelihood function to constrain the annual recruitment residuals (ignoring constants):

$$(2) \qquad -\ln P(\boldsymbol{\varepsilon}|\sigma_R) = \sum_y \ln(\sigma_R) + \frac{\varepsilon_y^2}{2\sigma_R^2}$$

The estimates using the full likelihood function minimize the combined negative log-likelihood (the terms penalized negative log-likelihood or negative log-posterior probability are also used because of the distributional assumption included for the recruitment residuals) including, in a typical statistical catch-at-age model, the catch-at-age data (C@A) and the CPUE or trawl survey data (eq. 3). This method assumes that the annual recruitment residuals are unknown parameters to be estimated.

$$(3) \qquad -\ln L(\mathbf{y}|\boldsymbol{\theta}) = -\ln L(\text{CPUE}|\boldsymbol{\varphi},\boldsymbol{\varepsilon}) - \ln L(\text{C@A}|\boldsymbol{\varphi},\boldsymbol{\varepsilon}) - \ln P(\boldsymbol{\varepsilon}|\sigma_R)$$

where $\boldsymbol{\varphi}$ are the model parameters, including the process (σ_R) and observation error variances, excluding the annual recruitment residuals ($\boldsymbol{\varepsilon}$); $\boldsymbol{\theta} = \{\boldsymbol{\varphi},\boldsymbol{\varepsilon}\}$; and $\mathbf{y}$ is the full data set $\mathbf{y} = \{\text{CPUE, C@A}\}$.

Traditional random effects models assume that the random effects (annual recruitment residuals) are random variables

© 2003 NRC Canada

(nuisance parameters), and therefore, they are integrated out to form a marginal likelihood function, $P(\mathbf{y}|\boldsymbol{\varphi})$. To produce the marginal likelihood, the full likelihood is integrated over $\boldsymbol{\varepsilon}$ (eq. 4).

$$(4) \quad L(\mathbf{y}|\boldsymbol{\varphi}) = \int L(\text{CPUE}|\boldsymbol{\varphi},\boldsymbol{\varepsilon})L(\text{C@A})|\boldsymbol{\varphi},\boldsymbol{\varepsilon})P(\boldsymbol{\varepsilon}|\boldsymbol{\varphi})\partial\boldsymbol{\varepsilon}$$

Because of the nonlinear nature of the problem, a numerical solution or an approximation is needed for the integral. We use importance sampling (IS) to numerically approximate the integral. This method integrates across the random effects and therefore cannot be used directly to estimate the annual recruitments or other derived parameters that are functions of the annual recruitments. These parameters are estimated by fixing the variance parameters at the values estimated using the marginal likelihood (eq. 4) while estimating $\boldsymbol{\varepsilon}$ and remaining parameters using the full likelihood (eq. 3).

The previously mentioned methods only use the historical information that recruitment is usually lognormally distributed. There is also historical information on the value of the standard deviation for this distribution, $P(\sigma_R)$. This information can be combined with the negative log-likelihood function (in this case, we use the posterior probability notation (eq. 5)):

$$(5) \quad -\ln P(\boldsymbol{\theta}|\mathbf{y}) = -\ln L(\text{CPUE}|\boldsymbol{\varphi},\boldsymbol{\varepsilon}) - \ln L(\text{C@A})|\boldsymbol{\varphi},\boldsymbol{\varepsilon}) - \ln P(\boldsymbol{\varepsilon}|\sigma_R) - \ln P(\sigma_R)$$

The prior can be generated by using a parametric representation of the frequency distribution of σ_R from many fish stocks that have estimates of annual recruitment. For example, Smith and Punt (1998) suggest that $\mu_{\sigma_R} = 0.6$ based on Beddington and Cooke (1983). Assuming $\sigma_{\sigma_R} = 0.2$, σ_R is normally distributed, and ignoring constants,

$$(6) \quad -\ln P(\sigma_R) = 0.5\frac{(\sigma_R - 0.6)^2}{0.2^2}$$

Prior information is usually associated with full Bayesian integration, which requires integration over all model parameters (see Punt and Hilborn (1997) for a review of Bayesian analysis in fisheries stock assessment). However, it is not necessary to do full Bayesian integration to make use of prior information. For example, the mode of the joint posterior distribution, which can be found using a function optimizer, can be used as estimates of the model parameters (e.g., Maunder and Starr 2001). Statistical inference should not be solely based on one's ideological view (e.g., Bayesian vs. Frequentist), but based on practical methods that perform well (precise and accurate) and are robust to assumptions. Therefore, we test the penalized likelihood, IS, and full Bayesian integration methods that include a prior for σ_R. We now describe the details of each of the estimation methods.

Likelihood (MLE)

In this method, the full negative log-likelihood, excluding the annual recruitment penalty term,

$$(7) \quad -\ln L(\mathbf{y}|\boldsymbol{\theta}) = -\ln L(\text{CPUE}|\boldsymbol{\theta}) - \ln L(\text{C@A}|\boldsymbol{\theta})$$

is minimized to estimate all parameters of the model. In the implementation of this method, $\bar{R}$ is not estimated, as it would be a redundant parameter, and instead of estimating $\boldsymbol{\varepsilon}$, the R_y are estimated directly and

$$(8) \quad \bar{R} = \frac{1}{T}\sum_y R_y$$

$$(9) \quad \sigma_R = \left(\frac{\sum_y \left[\ln(R_y) - \frac{1}{T}\sum_y \ln(R_y)\right]^2}{T-1}\right)^{1/2}$$

Penalized likelihood (PL)

In this method, the full negative log-likelihood, including the annual recruitment penalty term (eq. 3), is minimized to estimate all parameters of the model, including the annual recruitment residuals, which are assumed to be unknown parameters to estimate. This is equivalent to finding the mode of the posterior distribution of a hierarchical Bayesian model with locally uniform priors on all model parameters except the annual recruitment residuals.

Importance sampling (IS)

The marginal likelihood function can be approximated with numerical integration using IS (Gelman et al. 1995, pp. 307–308). The importance function is a multivariate normal based on the estimates of the recruitment residuals, $\boldsymbol{\varepsilon}$, and the corresponding variance–covariance matrix $\mathbf{V}$ when the variance parameters are fixed. The algorithm alternates between updating the importance function (step 2) and performing the numerical integration (steps 3–4).

(1) Choose initial values for $\boldsymbol{\varphi}$.
(2) Use an iterative function minimizer to estimate $\hat{\boldsymbol{\varepsilon}}$ (and $\hat{\mathbf{V}}$), $\bar{R}$, and q, while keeping σ_R and σ_{CPUE} fixed at their current estimates using the full negative log-likelihood function (eq. 3).
(3) Draw n sets of parameters, indexed by i, from a joint normal distribution $N(\hat{\boldsymbol{\varepsilon}}, \hat{\mathbf{V}})$.
(4) Estimate $\hat{\boldsymbol{\varphi}}$: (*a*) use an iterative function minimizer to estimate $\hat{\boldsymbol{\varphi}}$; (*b*) for each function evaluation of the function minimizer, calculate the objective function as

$$-\ln\left[\frac{1}{n}\sum_i \frac{L(\text{CPUE}|\boldsymbol{\varphi},\boldsymbol{\varepsilon}^i)L(\text{C@A}|\boldsymbol{\varphi},\boldsymbol{\varepsilon}^i)P(\boldsymbol{\varepsilon}^i)}{g(\boldsymbol{\varepsilon}^i)}\right],$$

where $g(\boldsymbol{\varepsilon}^i) = N(\boldsymbol{\varepsilon}^i; \hat{\boldsymbol{\varepsilon}}, \hat{\mathbf{V}})$ and $P(\boldsymbol{\varepsilon}^i) = N(\boldsymbol{\varepsilon}^i; 0, \hat{\sigma}_R\mathbf{I})$.
(5) Repeat steps 2–4 several times.
(6) Use an iterative function minimizer to re-estimate $\hat{\boldsymbol{\varepsilon}}$ and $\hat{\mathbf{V}}$ conditioned on the current estimates of σ_R and σ_{CPUE} using the full negative log-likelihood function (eq. 3).

The estimates of $\hat{\boldsymbol{\varepsilon}}$ and estimates of the derived parameters that are functions of $\hat{\boldsymbol{\varepsilon}}$ are taken from step 6. Estimates of the other parameters are taken from step 4 the last time that it is completed.

We found that 10 iterations of steps 2–4 were sufficient for the algorithm to converge and 1000 samples in step 3 re-

© 2003 NRC Canada

stricted the variation in the estimates between iterations after convergence to acceptable levels. It is possible that the population can become negative for some of the samples of the recruitment residuals from step 3. This causes computational errors and we used a smooth function causing the population size to be always slightly above zero when it would normally be predicted to go below zero. In a standard stock assessment model, the objective function would be highly penalized by the difference between the new biomass level and the predicted level that is negative to aid the optimization routine. However, in the IS method, one random sample from step 3 may cause the biomass to go negative, causing divergent behavior. Therefore, we did not include this penalty, and its exclusion did not appear to cause any significant bias in the results.

Full Bayesian integration (BI)

The Markov Chain Monte Carlo (MCMC) method is used to sample from the posterior distribution (Gelman et al. 1995). We use the MCMC method supplied with the AD Model Builder software (Otter Research Ltd. 2000), which starts the MCMC algorithm at the mode of the joint posterior distribution and uses multivariate normal jumping rules based on the estimated variance–covariance matrix. One hundred thousand MCMC steps were used and every 100th step was saved. Other methods, such as sample importance resampling (McAllister and Ianelli 1997), could also be used. Parameter estimates are calculated as the mean of the marginal posterior distribution (i.e., averaged across all the other model parameters). Only the prior for $\boldsymbol{\varepsilon}$ is assumed to be informative, the priors for the other parameters are chosen to be uninformative or diffuse (Table 1).

Penalized likelihood (PL – σ_R), importance sampling (IS – σ_R), and full Bayesian integration (BI – σ_R) with a prior on σ_R

These methods are the same as PL, IS, and BI except eq. 5 is used which has a prior on σ_R.

Simulation analysis

We use simulation analysis to test the performance of each of the methods described above. A simple age-structured model (Appendix A) was set up to simulate a population for $T = 20$ years, starting from an unexploited equilibrium population (with no variation in the initial conditions). The effort trajectory was set to give contrast in the biomass time series; it increased in the first 10 years, decreased for the next 5 years, and stayed low for the last 5 years. The model was used to generate catch, CPUE, and catch-at-age data. The simulated recruitment was generated as being comprised of T random annual residuals with standard deviation = 0.6 and mean = 0. The standard deviation of the observation error in the CPUE index, σ_{CPUE}, was set at 0.3, and the sample size of the catch-at-age data was set to 50. The same age-structured model was then fit to the data to estimate the model parameters. The parameters estimated in the model were average recruitment ($\bar{R}$), the standard deviation of recruitment residuals (σ_R), the catchability coefficient (q), the standard deviation of the fit to the CPUE data (σ_{CPUE}), and the annual recruitment residuals ($\boldsymbol{\varepsilon}$). The estimation scheme was initiated with the true values for q and σ_{CPUE}. $\bar{R}$ was set to one and a half times the true value, $\boldsymbol{\varepsilon} = 0$, and $\sigma_R = 1.0$. The simulation analysis was repeated 500 times for two different scenarios: (1) using catch-at-age data for all years and (2) using catch-at-age data for the last 10 years only. We also generate simulated data using random recruitment that is uniform $(0, 2\bar{R})$.

Table 1. Prior distributions used for the model parameters in the Bayesian integration method.

Parameter	Prior
$\bar{R}$	$U(0, 2\bar{R}^{true})$
q	ln $U(-\infty, \infty)$
σ_{CPUE}	ln $U(-\infty, \infty)$
σ_R	ln $U(-\infty, \infty)$
$\boldsymbol{\varepsilon}$	$N(0, \sigma_R^2)$

For each simulation, we report the estimates of $\bar{R}$, the biomass in the last year of the simulation as a ratio of the biomass in the first year of the simulation (B_T/B_1), R_y, σ_R, and σ_{CPUE}. These estimates are compared with the true values by calculating the relative error $\frac{\theta_i - \theta_i^{true}}{\theta_i^{true}}$ and reporting the 10, 50, and 90 percentiles and the average absolute error. We only tested methods PL – σ_R, IS – σ_R, and BI – σ_R using simulated data with no catch-at-age data for the first 10 years.

Application

The methods are applied to the snapper stock on the west coast of the North Island of New Zealand. The data consist of total catch from 1931 to 1998, a CPUE relative abundance index from 1974 to 1991, and catch-at-age data for 1975–1976, 1979, 1986–1987, and 1989–1998 (Nick Davies, National Institute of Water and Atmospheric Research, P.O. Box 1043, Whangarei, New Zealand, personal communication). We estimate the variation in annual recruitment.

Results

The relative error in the estimates of $\bar{R}$ is similar for all the methods (Table 2). There is very little bias with or without the first 10 years of catch-at-age data, except for BI that gives a 8% positive bias when the first 10 years of catch-at-age data are not used. The average error (average of the absolute value of the relative error) is increased when the first 10 years of catch-at-age data are not used and is highest for the likelihood method.

The results for the relative error in the estimates of B_1/B_T are also similar for all methods (Table 3). There is very little bias with or without the first 10 years of catch-at-age data, except for PL, which gives a 5% positive bias when the first 10 years of catch-at-age data are not used, and BI, which gives a 4% and 6% positive bias with and without the first 10 years of catch-at-age data, respectively. Unlike the results for $\bar{R}$, the average error is not greatly increased when the

© 2003 NRC Canada

Table 2. Relative error in the estimate of average recruitment $\bar{R}$ from four estimation methods.

	Catch-at-age data used for all years				Catch-at-age data not used for first 10 years			
	Median	10%	90%	Average absolute	Median	10%	90%	Average absolute
MLE	0.00	–0.07	0.08	0.05	0.02	–0.15	0.36	0.16
PL	–0.01	–0.06	0.06	0.04	0.02	–0.10	0.20	0.09
IS	0.00	–0.06	0.08	0.05	0.01	–0.12	0.19	0.10
BI	0.02	–0.04	0.08	0.04	0.08	–0.06	0.27	0.12

Note: MLE, maximum likelihood estimates using the full likelihood function; PL, penalized likelihood; IS, importance sampling; BI, Bayesian integration.

Table 3. Relative error in the estimate of biomass in the last year as a ratio of the biomass in the first year B_1/B_T from the four estimation methods.

	Catch-at-age data used for all years				Catch-at-age data not used for first 10 years			
	Median	10%	90%	Average absolute	Median	10%	90%	Average absolute
MLE	–0.02	–0.25	0.27	0.17	0.01	–0.20	0.28	0.15
PL	0.01	–0.16	0.22	0.12	0.05	–0.16	0.35	0.17
IS	0.01	–0.16	0.23	0.12	0.01	–0.17	0.23	0.13
BI	0.04	–0.13	0.26	0.13	0.06	–0.12	0.29	0.14

Note: MLE, maximum likelihood estimates using the full likelihood function; PL, penalized likelihood; IS, importance sampling; BI, Bayesian integration.

first 10 years of catch-at-age data are not used, except for the PL method.

The estimates of σ_R differ substantially between the different estimation methods (Table 4). When all catch-at-age data were used, the MLE method gave moderately positively biased estimates of σ_R, and when the first 10 years of catch-at-age data were not used, the estimates of σ_R became extremely positively biased. This bias was due to many of the recruitment estimates in the first few years, in which there are no catch-at-age data, being estimated as either very large or close to zero. The PL method is highly negatively biased and this bias increases when the first 10 years of catch-at-age data are not used. For some of the simulated data sets, σ_R was estimated to be zero, implying that the recruitment is the same for each year. The percentage of data sets in which σ_R was estimated to be zero was much higher when the first 10 years of catch-at-age data are not used (41%) compared with when all catch-at-age data were used (2%). The IS and BI methods performed much better at estimating σ_R when the first 10 years of catch-at-age data were not used compared with the MLE and PL methods. These methods also perform better when all catch-at-age data were used.

The estimates of σ_{CPUE} all have similar levels of average error for the different methods, but different biases (Table 5). The MLE, PL, and IS methods have a negative bias and BI has a smaller, but positive, bias.

Estimates of the relative error in the annual recruitment are similar for all four methods when the catch-at-age data were used for all years (Fig. 1). The variance in relative error increased for the last 5 years because these cohorts are only observed in a limited number of catch-at-age data sets. The MLE method shows a very small negative bias for all years, and the other methods show a small positive bias. When the first 10 years of catch-at-age data were not used, these methods performed differently, particularly in the first half of the time period (Fig. 2). The MLE method cannot adequately estimate recruitment in the first few years. As mentioned previously, these recruitments are often estimated to be either unrealistically high or close to zero. The PL method is better than the likelihood method at estimating recruitment in the first few years but has higher average error in the recruitment estimates for the latter years. The IS method performs better than the MLE and PL methods. The IS method shows less average error for the first few years compared with the MLE method and less average error in the latter years compared with the PL method. The BI method performs similarly to the PL method.

When the true recruitment comes from a uniform distribution, the errors in the estimates of average recruitment, depletion, and σ_{CPUE} are all very similar to those from when the true recruitment comes from a lognormal distribution. There is higher average error in the recruitment estimates for all but the likelihood method (Fig. 3). For the scenario in which there is no catch-at-age data for the first 10 years, there is much more error in the estimates of recruitment for the PL, IS, and Bayesian methods compared with when the true recruitment is from a lognormal distribution (Fig. 4). The increase in error occurs mostly in the first 10 years.

The inclusion of a prior on σ_R did not change the ability to estimate $\bar{R}$ or σ_{CPUE}. Estimates of depletion were only slightly improved (the average of the absolute value of the relative error is 0.16, 0.12, and 0.13 for the PL, IS, and BI methods, respectively). However, it did considerably decrease the average error in the estimates of σ_R (the average of the absolute value of the relative error is 0.56, 0.13, and 0.13 for the PL, IS, and BI methods, respectively). It also slightly reduced the error in the estimates of recruitment for the BI method (Fig. 5). A misspecified prior ($\mu_{\sigma_R} = 0.3$) gave simi-

© 2003 NRC Canada

Table 4. Relative error in the estimate of the standard deviation of the annual recruitment residuals from the four estimation methods.

	Catch-at-age data used for all years				Catch-at-age data not used for first 10 years			
	Median	10%	90%	Average absolute	Median	10%	90%	Average absolute
MLE	0.09	–0.11	0.34	0.17	8.96	6.28	11.04	8.23
PL	–0.19	–0.45	0.04	0.23	–0.54	–1.00	–0.20	0.64
IS	–0.02	–0.22	0.21	0.14	–0.09	–0.35	0.18	0.19
BI	0.00	–0.23	0.23	0.15	–0.03	–0.33	0.28	0.20

Note: MLE, maximum likelihood estimates using the full likelihood function; PL, penalized likelihood; IS, importance sampling; BI, Bayesian integration.

Table 5. Relative error in the estimate of σ_{CPUE} from the four estimation methods.

	Catch-at-age data used for all years				Catch-at-age data not used for first 10 years			
	Median	10%	90%	Average absolute	Median	10%	90%	Average absolute
MLE	–0.05	–0.25	0.20	0.14	–0.11	–0.29	0.14	0.15
PL	–0.07	–0.26	0.16	0.14	–0.04	–0.24	–0.21	0.14
IS	–0.05	–0.24	0.19	0.14	–0.05	–0.24	0.19	0.14
BI	0.02	–0.19	0.27	0.14	0.02	–0.18	0.28	0.14

Fig. 1. Median (solid line), 10th percentile (lower broken line), and 90th percentile (upper broken line) for the relative error in annual recruitment for the (*a*) maximum likelihood estimate, (*b*) penalized likelihood, (*c*) importance sampling, and (*d*) Bayesian integration methods when using all the catch-at-age data.

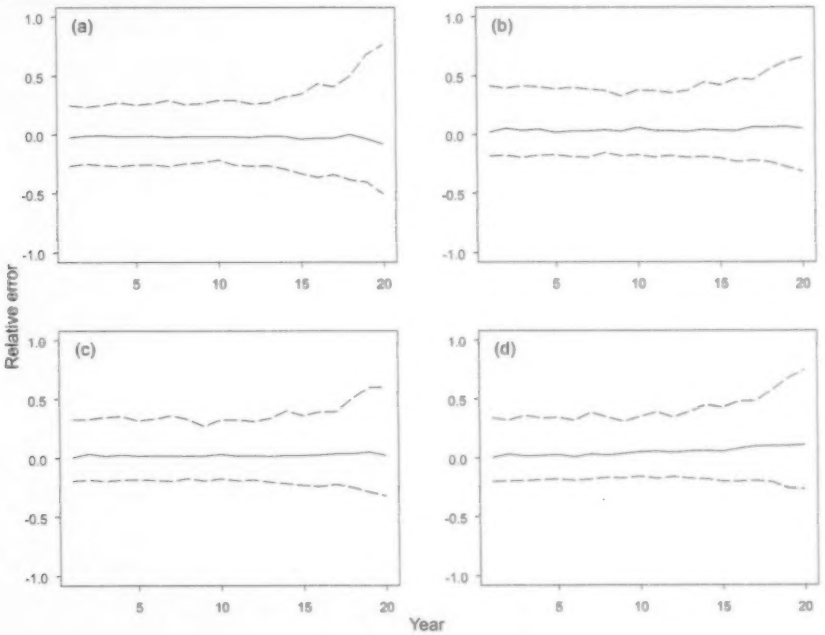

lar results, causing a considerable negative bias in σ_R for all methods and a considerable negative bias in annual recruitment estimates for the BI method.

For the application to the snapper stock on the west coast of the North Island of New Zealand, the MLE method had problems converging. The PL method produced an estimate of zero. The IS method produced an estimate around 0.6. The algorithm converged after about 10 iterations (Fig. 6). However, there is still variation in the estimates at each iteration. Increasing the number of samples from the importance function from 100 to 500 did not reduce this variation (Fig. 6). Therefore, a better estimate would be to take the average over a series of iterations rather than using the result after the final iteration. We use two averages, iterations 20

© 2003 NRC Canada

Fig. 2. Median (solid line), 10th percentile (lower broken line), and 90th percentile (upper broken line) for the relative error in annual recruitment for the (*a*) maximum likelihood estimate, (*b*) penalized likelihood, (*c*) importance sampling, and (*d*) Bayesian integration methods when not using the catch-at-age data for the first 10 years.

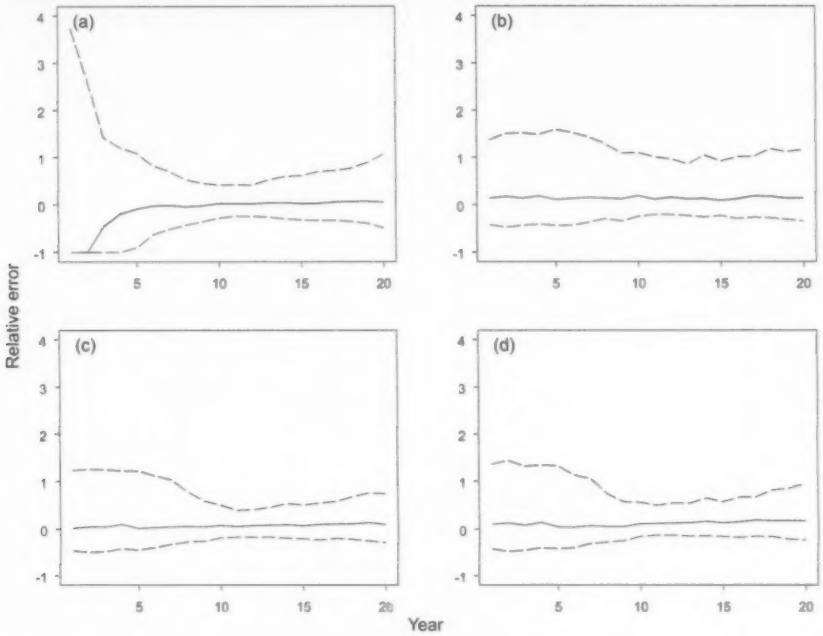

Fig. 3. Median (solid line), 10th percentile (lower broken line), and 90th percentile (upper broken line) for the relative error in annual recruitment for the (*a*) maximum likelihood estimate, (*b*) penalized likelihood, (*c*) importance sampling, and (*d*) Bayesian integration methods when using all the catch-at-age data and recruitment comes from a uniform distribution.

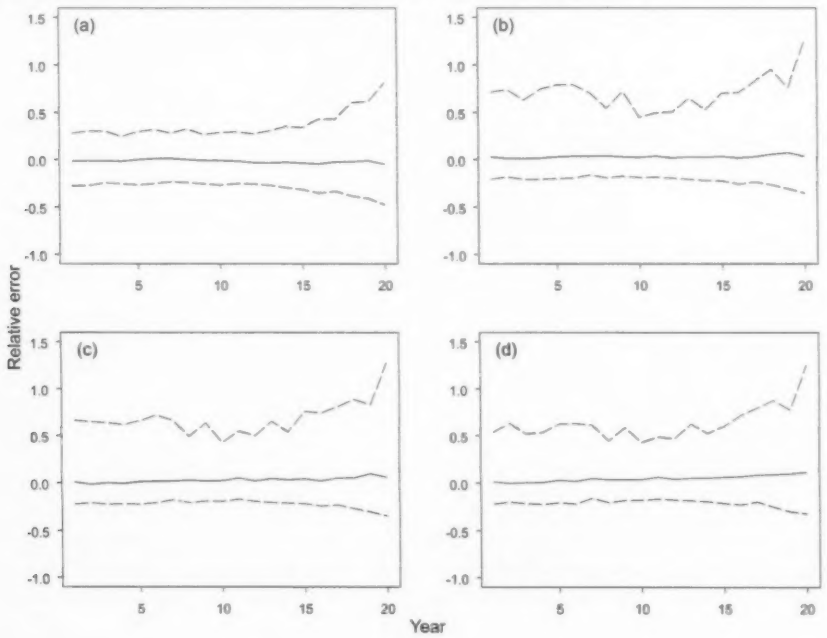

© 2003 NRC Canada

Fig. 4. Median (solid line), 10th percentile (lower broken line), and 90th percentile (upper broken line) for the relative error in annual recruitment for the (*a*) maximum likelihood estimate, (*b*) penalized likelihood, (*c*) importance sampling, and (*d*) Bayesian integration methods when not using the catch-at-age data for the first 10 years and recruitment comes from a uniform distribution.

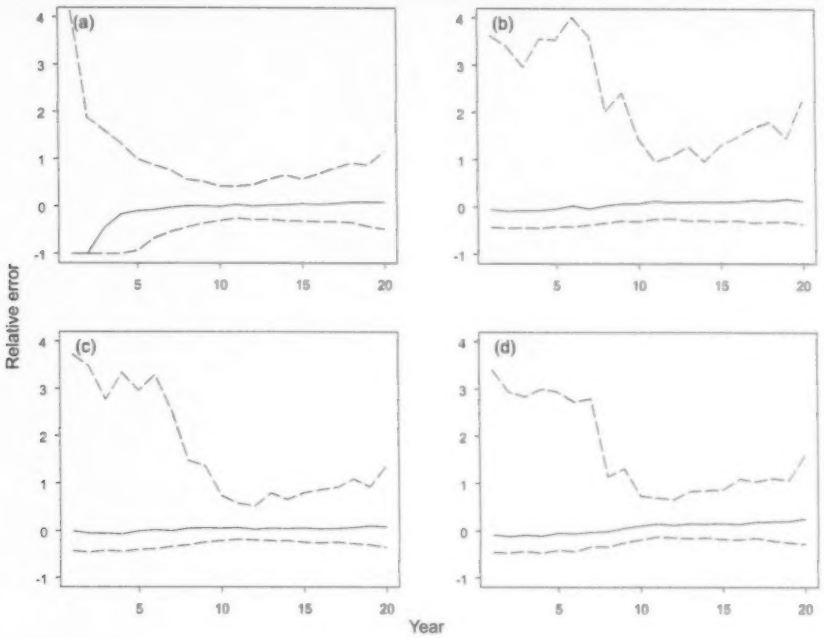

to 100 and 80 to 100. For 100 samples from the importance function, the estimates of σ_R are 0.597 and 0.584, respectively. For 500 samples from the importance function, the estimates of σ_R are 0.620 and 0.584, respectively. The BI method estimates σ_R equal to 0.668 and 0.699 using the mode of the marginal distribution and the average, respectively. The posterior distribution ranges from about 0.4 to 1.0 and is skewed to the right (Fig. 7).

Discussion

The methods presented in this paper for estimating annual recruitment in statistical catch-at-age models perform similarly when used to estimate quantities that are derived from a large number of annual recruitments (e.g., $\bar{R}$) or are a function of recruitments that have catch-at-age data associated with them (e.g., B_T/B_1). Average recruitment is unaffected by a lack of information (i.e., no catch-at-age data) for some annual recruitments because the CPUE time series covers the whole time period and the CPUE consists of the catches from several cohorts. Therefore, the individual annual recruitments can be incorrect, but the average of these recruitments must be close to the true average so that the predicted CPUE can be close to the observed CPUE. The methods also perform similarly for all quantities when the catch-at-age data are available for all years.

Annual recruitment and the standard deviation of the recruitment residuals are poorly estimated by the likelihood (MLE) and penalized likelihood (PL) methods when catch-at-age data are missing. The method based on the marginal likelihood (IS), which integrates across the recruitment residuals, and the full Bayesian integration (BI) method perform much better in estimating the standard deviation of the recruitment residuals and annual recruitments. This indicates that any analyses that use the standard deviation of the recruitment residuals for forward projections or other analyses should use the marginal likelihood or full Bayesian integration, particularly if catch-at-age data are not available for the whole time period or if, for some years, the catch-at-age data are uninformative. For example, we suggest that if an environmental correlation with recruitment or a stock–recruitment model is being considered, it should be integrated into the stock assessment as suggested by Maunder and Starr (2001) and Maunder and Watters (2003) and a marginal likelihood or Bayesian integration used.

It is interesting to discover that σ_R could be estimated using the PL method for nearly all artificial data sets when catch-at-age data were available for all years. The estimation problem is more complex than a traditional random effects application, which has multiple measurements for a quantity of interest for each individual. Each annual recruitment residual has information about it contained in multiple catch-at-age data sets. In addition, because biomass is the accumulation of multiple year classes, each annual recruitment residual is represented in multiple CPUE data points. The fit to the catch-at-age data is based on the multinomial distribution, and therefore, the observation error variance for the catch-at-age data is determined by the sample size. The only observation error variance that is estimated is for the CPUE data. It is interesting to look at the negative log-likelihood profile for σ_R when using catch-at-age data for all years, which has a local minimum around the true value and a global mini-

© 2003 NRC Canada

Fig. 5. Median (solid line), 10th percentile (lower broken line), and 90th percentile (upper broken line) for the relative error in annual recruitment for the (*a*) penalized likelihood with a prior on annual recruitment residuals (σ_R), (*b*) importance sampling with a prior on σ_R, and (*c*) Bayesian integration with a prior on σ_R methods when not using the catch-at-age data for the first 10 years.

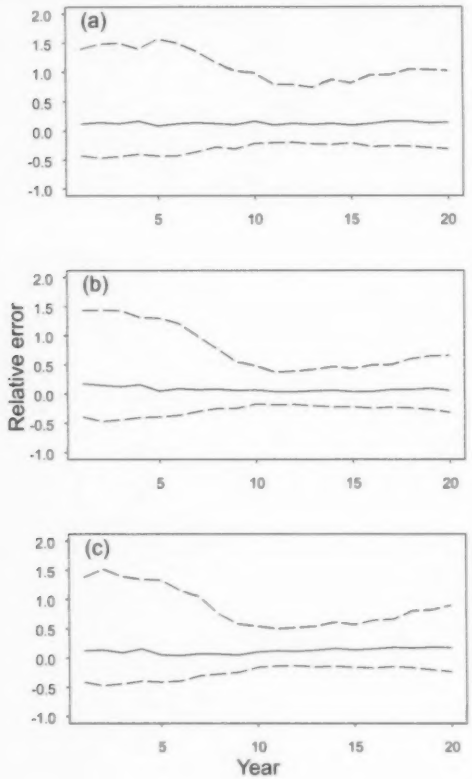

mum at zero (Fig. 8). The negative log-likelihood profile for σ_R when using catch-at-age only for the last 10 years only has a global minimum at zero (Fig. 8). However, if the estimates of $\sigma_R = 0$ are removed from the analysis, σ_R is still moderately negatively biased (median relative error is –0.17%) indicating that PL is still not a useful estimator for σ_R.

The results showed that estimates of annual recruitment have larger error if the true distribution of annual recruitment is different from that assumed in the analysis. However, the effect on the other quantities was small. The uniform distribution is an extreme sensitivity analysis compared with what empirical data suggest, therefore assuming a lognormal distribution is unlikely to cause large errors in the estimates for real applications.

Adding a prior on σ_R only improved the estimates of σ_R and not the other quantities. The PL method still estimated $\sigma_R = 0$ for a large proportion of the data sets. From these results, we conclude that putting a prior on σ_R is not particularly useful unless the data are very uninformative about annual recruitment. However, we did not investigate the influence on estimates of uncertainty (e.g., confidence intervals) because the marginal likelihood method is too computationally intense.

The application to the snapper stock gave values of σ_R about 10–15% higher for BI compared with IS. The estimates from the BI method are sensitive to what measure is used to derive the estimates (e.g., average, mode of the marginal, median) and also probably to the prior distribution for the other model parameters. The estimates from the IS method are sensitive to which iteration is used as the estimate and the random seed. It is probably best to use an average over several iterations to get a more stable estimate. The estimates of σ_R are consistent with those suggested or assumed for other fish stocks.

The methods described in this paper have different computational demands and different estimation efficiencies. The MLE and PL methods only require the maximization (or minimization if the negative log-likelihood is used) to be carried out once. If an accurate optimizer is used (i.e., one based on automatic derivatives, e.g., Otter Research Ltd. 2000) and convergence has been achieved, this should be the exact (local) solution. The only complication is that a local rather than a global maximum may have been found. In contrast, the other methods are only approximations (to the marginal likelihood and the posterior distribution) and are more computationally demanding. The IS algorithm requires a numerical approximation based on averaging the likelihood from random samples of $\boldsymbol{\varepsilon}$ from the normal distribution $N(\hat{\boldsymbol{\varepsilon}}, \hat{\mathbf{V}})$. Therefore, the likelihood function has to be evaluated for each sample. In addition, the IS method is also subject to the problem of local minima. The full Bayesian integration uses MCMC, which requires a large number of calculations of the objective function to approximate the posterior distribution. If too few iterations of the MCMC algorithm are performed, convergence may not be obtained, and if too many iterations are performed, the algorithm will take longer than needed. The priors used in the Bayesian analysis could be changed to see if other forms reduce the biases found for the Bayesian method when some of the catch-at-age data are missing. Medians or modes of the marginal posterior distributions could be used as alternative estimators. The MCMC algorithm started at the mode of the joint posterior distribution with jumping rules based on the covariance matrix. In initial simulations this caused bias in the estimates of σ_R because σ_R was estimated to be close to zero at the mode (see the PL results) and the estimated covariance matrix was inappropriate to cover the range of possible values for σ_R. To overcome this problem, we put a penalty on σ_R ($\mu_{\sigma_R} = 1.0$) while estimating the mode and the covariance matrix. The penalty was then removed when the MCMC algorithm was run. Sensitivity analyses suggested that this did not cause any significant biases in the results.

Simulated likelihood is a method that is becoming popular for implementing nonlinear random effects models (e.g., Harley 2002). Simulated likelihood involves taking random samples from the random effects distribution (this is the same as using the IS method with the importance sample equal to the random effects distribution). However, in applications like the one presented here in which the random effects parameters are combined in the model (i.e., the recruitments from multiple years are combined to determine the relative index of abundance and proportional catch-at-age data), all

© 2003 NRC Canada

Fig. 6. Estimates of σ_R (Rsd) for the snapper (*Pagrus auratus*) application after each iteration of the importance sampling method for two levels of the number of samples from the importance function (solid = 500, broken = 100).

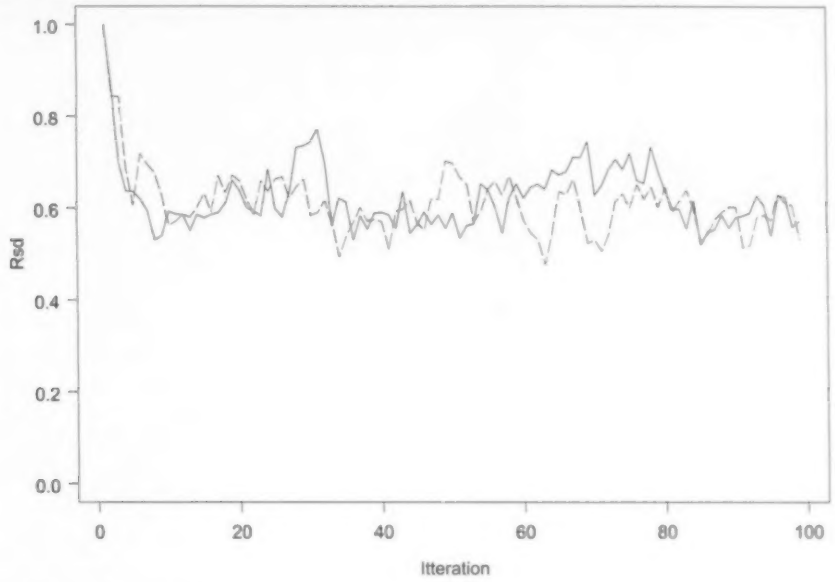

Fig. 7. Posterior distribution of σ_R (Rsd) for the snapper (*Pagrus auratus*) application from the Bayesian integration method.

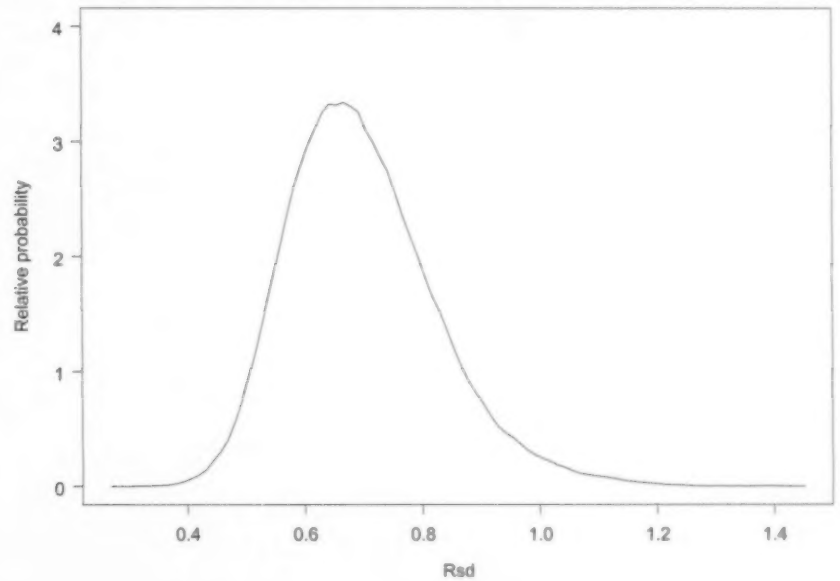

samples in an iteration have such small probability that the likelihood equals zero based on computer precision. The small probability occurs because the relative biomass in the last year, for a random sample of recruitments, is unlikely to be close to the observed index of abundance as it is a combination of all randomly sampled recruitments. Therefore, the minimization algorithm will not converge. This is our reason for using the IS algorithm. The IS algorithm generates samples that provide non-zero likelihoods because they are based on the importance function that has been derived from fitting the model to the data and therefore the samples produce predictions close to the observed data. The IS method is similar to the SIR algorithm used in Bayesian analysis (see Punt and Hilborn 1997).

The estimation of σ_R is very important for projecting the uncertainty in the consequences of future management strategies. For example, the probability of extinction for a population with an average population growth rate of zero is

© 2003 NRC Canada

Fig. 8. Scaled negative log-likelihood for different values of σ_R (Rsd) from a single simulated data set with catch-at-age data for all years (solid line) and catch-at-age data only for the last 10 years (broken line).

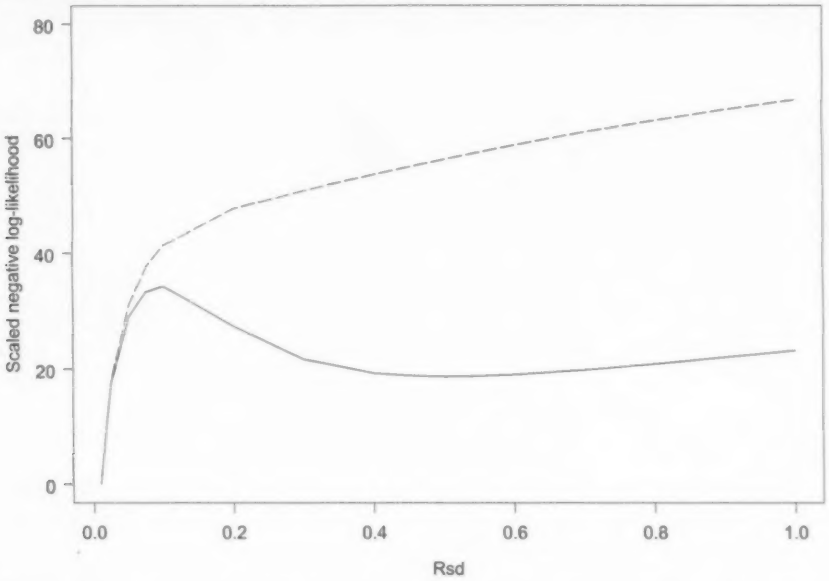

higher for a population that has a high σ_R than for a population that has low σ_R. Therefore, it is important to differentiate between temporal variation in recruitment and estimation error. The results of our analyses show that using a marginal likelihood or full Bayesian integration should be the preferred methods when σ_R is used to determine the temporal variation in recruitment for forward projections. However, we have not investigated if the improved estimates of σ_R would produce better management advice. Given the greater computational demands of the marginal likelihood or full Bayesian integration, further studies should be carried out to determine if the additional computational demands are worth the benefit they provide. This would require carrying out management policy simulations.

The methods presented in this paper could be extended to include a stock–recruitment relationship, environmental relationship, or other model parameters. A stock–recruitment relationship or an environmental relationship can easily be included in the analysis by replacing $\bar{R}$ in eq. 1 (see Maunder and Starr (2001) and Maunder and Watters (2003) for details). Process error for other model parameters can also be integrated out of the likelihood function. For example, fishing mortality is often modeled as a function of effort (E_y), catchability (q), and an annual residual (ε_y^E),

$$F_y = qE_y \exp(\varepsilon_y^E)$$

and a likelihood comparing the predicted and observed catch is included in the objective function. ε_y^E can be integrated out of the likelihood function in the same manner as ε_y is for recruitment. Meta-analysis, in which information is shared between stock assessments, could be carried out by modeling parameters (e.g., natural mortality) between populations as random effects and a marginal likelihood integrated across the random effects used for estimation.

In conclusion, if informative catch-at-age data are available for all years, then all of the methods perform well at estimating annual recruitment, average recruitment, and depletion level. In this case, the likelihood or penalized likelihood methods should be used because they are much less computationally intense, unless estimates of σ_R are needed. σ_R can be estimated using the penalized likelihood method if all years have informative catch-at-age data; however, σ_R is moderately negatively biased. The marginal likelihood and Bayesian integration methods perform best overall at estimating the model parameters when catch-at-age data are missing for some years.

Acknowledgements

Andre Punt provided comments on an earlier version of the manuscript and pointed out the local minima in the negative log-likelihood profile for σ_R.

References

Beddington, J.R., and Cooke, J.G. 1983. The potential yield of fish stocks. FAO Fish. Tech. Pap. **242**: 1–47.

Davidian, M., and Giltinan, D.M. 1995. Nonlinear models for repeated measurement data. Chapman and Hall, London.

Fournier, D.A., Hampton, J., and Sibert, J.R. 1998. MULTIFAN-CL: a length-based, age-structured model for fisheries stock assessment, with application to South Pacific albacore, *Thunnus alalunga*. Can. J. Fish. Aquat. Sci. **55**: 2105–2116.

Gelman, A., Carlin, J.B., Stern, H.S., and Rubin, D.B. 1995. Bayesian data analysis. Chapman and Hall, London.

Harley, S.J. 2002. Meta-analytical approaches to the study of fish population dynamics. Ph.D. thesis, Dalhousie University, Halifax, N.S.

© 2003 NRC Canada

Hilborn, R., and Liermann, M. 1998. Standing of the shoulders of giants: learning from experience in fisheries. Rev. Fish Biol. Fish. **8**: 273–283.

Maunder, M.N., and Starr, P.J. 2001. Bayesian assessment of the SNA1 snapper (*Pagrus auratus*) stock on the northeast coast of New Zealand. N.Z. J. Mar. Freshw. Res. **35**: 87–110.

Maunder, M.N., and Watters, G.M. 2003. A general framework for integrating environmental time series into stock assessment models: model description, simulation testing, and examples. Fish. Bull. **101**: 89–99.

Maunder, M.N., Starr, P.J.S., and Hilborn, R. 2000. A Bayesian analysis to estimate loss in squid catch due to the implementation of a sea lion population management plan. Mar. Mamm. Sci. **16**: 413–426.

McAllister, M.K., and Ianelli, J.N. 1997. Bayesian stock assessment using catch-age data and the sampling – importance resampling algorithm. Can. J. Fish. Aquat. Sci. **54**: 284–300.

McAllister, M. K., and Kirkwood, G. P. 1998. Bayesian stock assessment and policy evaluation: a review and example application using the logistic model. ICES J. Mar. Sci. **55**: 1031–1060.

McAllister, M.K., Pikitch, E.K., Punt, A.E., and Hilborn, R. 1994. A Bayesian approach to stock assessment and harvest decisions using the sampling/importance resampling algorithm. Can. J. Fish. Aquat. Sci. **51**: 2673–2687.

Otter Research Ltd. 2000. An introduction to AD Model Builder version 4.5 for use in nonlinear modeling and statistics. Otter Research Ltd., Box 2040, Sidney, BC V8L 3S3, Canada.

Punt, A.E., and Hilborn. R.1997. Fisheries stock assessment and decision analysis: the Bayesian approach. Rev. Fish Biol. Fish. **7**: 35–63.

Smith, A.D.M., and Punt, A.E. 1998. Stock assessment of gemfish (*Rexea solandri*) in eastern Australia using maximum likelihood and Bayesian methods. *In* Fisheries stock assessment models. *Edited by* T.J. Quinn II, F. Funk, J. Heifetz, J.N. Ianelli, J.E. Powers, J.F. Schweigert, P.J. Sullivan, and C-I. Zhang. Alaska Sea Grant College Program, AK-SG-98-01. pp. 245–286.

Appendix A. Description of simulator and estimator

The following is a description of the model equations used for the data simulator and for the estimator. The model is run from an unexploited state at the start of the fishery for 20 years. The model includes 10 age classes, with the 10th age class being a plus group.

Dynamics

$$N_{y,1} = \bar{R}\exp(\varepsilon_y - 0.5\sigma_R^2)$$

$$N_{y,a} = (N_{y-1,a-1}(1 - u_{y-1}s_{a-1}))e^{-M} \text{ for } a < A$$

$$N_{y,A} = (N_{y-1,A-1}(1 - u_{y-1}s_{A-1}))e^{-M} + (N_{y-1,A}(1 - u_{y-1}s_A))e^{-M}$$

$$u_y = \frac{C_y^*}{B_y}$$

$$B_y = \sum_a N_{y,a}s_a w_a$$

where $N_{y,a}$ are the numbers in age class a at the beginning of year y, $\bar{R}$ is the average recruitment, ε_y^R is the recruitment anomaly for year y, σ_R is the standard deviation for the recruitment residuals, $C_{y,a}$ is the catch in numbers of age a individuals in year y, M is the natural mortality rate, A is the maximum age used in the analysis, u_y is the exploitation rate in year y, s_a is the selectivity to the fishing gear for age a individuals, C_y^* is the total catch in weight for year y, B_y is the exploitable biomass for year y, and w_a is the weight for an individual of age a.

Initial conditions

$$N_{1,a} = \bar{R}e^{-M(a-1)} \text{ for } 1 < a < A$$

$$N_{1,A} = \frac{N_{1,A-1}e^{-M}}{1 - e^{-M}}$$

Simulation

$$\varepsilon_y \sim N(0, \sigma_R^2)$$

$$\varepsilon_y^{CPUE} \sim N(0, \sigma_{CPUE}^2)$$

$$CPUE_y = qB_y \exp(\varepsilon_y^{CPUE} - 0.5\sigma_{CPUE}^2)$$

$$n_{y,a} \sim \text{Multinomial}\left(\frac{C_{y,a}^{numbers}}{\sum_a C_{y,a}^{numbers}}, n = 50\right)$$

$$C_{y,a}^{numbers} = N_{y,a}u_y s_a$$

where q is the catchability coefficient for the CPUE index, ε_a^{CPUE} is the observation error in the CPUE index, σ_{CPUE} is the standard deviation of the error in the CPUE index, $n_{y,a}$ is the number of individuals of age a in the catch-at-age sample in year y, and n is the number in the catch-at-age sample.

Estimation

Likelihoods

CPUE

$$-\ln L(I|\theta) = \sum_y \left[\ln(\sigma_{CPUE}) + \frac{(\ln(CPUE_y) - \ln(qB_y))^2}{2\sigma_{CPUE}^2}\right]$$

Catch-at-age (modified from Fournier et al. 1998)

$$-\ln L(C@A|\theta) = -\ln\left[\exp\left\{\frac{-(P_{y,a} - \hat{P}_{y,a})^2}{2\sigma_{C@A}^2}\right\} + 0.001\right]$$

$$\sigma_{C@A}^2 = \frac{\left[(1 - P_{y,a})P_{y,a} + \frac{1}{A}\right]}{\sum_a n_{y,a}}$$

$$P_{y,a} = \frac{n_{y,a}}{\sum_a n_{y,a}}$$

© 2003 NRC Canada

$$\hat{P}_{y,a} = \frac{C_{y,a}^{\text{numbers}}}{\sum_a C_{y,a}^{\text{numbers}}} = \frac{N_{y,a} s_a u_y}{\sum_a N_{y,a} s_a u_y} = \frac{N_{y,a} s_a}{\sum_a N_{y,a} s_a}$$

where $n_{y,a}$ is the numbers of age a in the catch-at-age sample for year y.

Recruitment penalty

$$-\ln P(\varepsilon^R|\sigma_R) = \sum_y \left[\ln(\sigma_R) + \frac{(\varepsilon_y)^2}{2\sigma_R^2} \right]$$

Fixed parameters

$w_a = l_a^3$

$l_a = 1 - e^{-0.1a}$

$M = 0.2$

$s = 1$ for all a

© 2003 NRC Canada

Extending production models to include process error in the population dynamics

Andre E. Punt

Abstract: Four methods for fitting production models, including three that account for the effects of error in the population dynamics equation (process error) and when indexing the population (observation error), are evaluated by means of Monte Carlo simulation. An estimator that represents the distributions of biomass explicitly and integrates over the unknown process errors numerically (the NISS estimator) performs best of the four estimators considered, never being the worst estimator and often being the best in terms of the medians of the absolute values of the relative errors. The total-error approach outperforms the observation-error estimator conventionally used to fit dynamic production models, and the performance of a Kalman filter based estimator is particularly poor. Although the NISS estimator is the best-performing estimator considered, its estimates of quantities of management interest are severely biased and highly imprecise for some of the scenarios considered.

Résumé : Une simulation de Monte Carlo permet d'évaluer quatre méthodes d'ajustement des modèles de production, dont trois qui prennent en compte les effets des erreurs dans la dynamique de population (erreurs de processus) et dans l'indexation de la population (erreurs d'observation). Des quatre estimateurs examinés, l'estimateur NISS, qui représente la distribution de la biomasse de façon explicite et qui fait numériquement l'intégration des erreurs de processus inconnues, fonctionne le mieux; il n'est jamais le pire et est très souvent le meilleur en ce qui concerne les médianes des valeurs absolues des erreurs relatives. La méthode de l'erreur totale fonctionne mieux que celle de l'erreur d'observation couramment utilisée dans l'ajustement de modèles dynamiques de production; la méthode qui utilise un filtre de Kalman fonctionne particulièrement mal. Bien que la méthode NISS soit la meilleure des méthodes étudiées, les estimations d'intérêt pour la gestion qu'elle produit sont particulièrement faussées et très imprécises dans certains scénarios.

[Traduit par la Rédaction]

Introduction

Production (or biomass dynamics) models have a long history in quantitative fisheries science and have provided a key component of the basis that led to the popularity of maximum sustainable yield (MSY), and its associated biomass (B_{MSY}), as biological reference points for fisheries management. Production models are virtually the only method for stock assessment in situations in which the only data available are a time series of catches and some index of abundance. Historically, the index of abundance was fishery catch-per-unit-effort (CPUE), but the use of the results from fishery-independent resource surveys in production model assessments is more common now given the known limitations of CPUE as an index of abundance (e.g., Cooke and Beddington 1984).

Production models remain a useful tool for providing fisheries management advice in situations in which (*a*) there are insufficient age- and size-composition data to permit the use of assessment methods based on age- or size-structured models or (*b*) there is interest in biomass levels and surplus production before the years for which age- and size-composition data are available. The latter is particularly important when efforts are being made to rebuild overfished stocks to earlier levels that have not been observed since age- and size-composition data were collected.

The production models used for management purposes have changed over time from those assuming that each data point represents a population in dynamic equilibrium through those averaging the observed data over several years to approximate an equilibrium situation (e.g., Gulland 1961; Fox 1975) to those that do not make the assumption that the population is in equilibrium, i.e., dynamic production models (e.g., Pella and Tomlinson 1969).

Despite considerable evidence that methods based on the assumption that the population is in equilibrium are likely to lead to estimates of biological reference points that are substantially biased (e.g., Sissenwine 1978; Polacheck et al. 1993; Williams and Prager 2002), these methods are nevertheless still used today to some extent (e.g., Moses 2000; International Commission for the Conservation of Atlantic Tunas (ICCAT) 2000). The development of production models has, since the 1980s, been focused primarily on dynamic production models. Three main classes of dynamic production model have emerged. Conceptually, these three classes are special cases of the following generic production model:

$$(1a) \quad B_{y+1} = (B_y + g(B_y) - C_y)e^{\varepsilon_y}$$

$$(1b) \quad I_y = qB_y e^{\eta_y}$$

Received 5 November 2002. Accepted 31 August 2003. Published on the NRC Research Press Web site at http://cjfas.nrc.ca on 3 November 2003.
J17170

A.E. Punt. School of Aquatic and Fishery Sciences, Box 355020, University of Washington, Seattle, WA 98195-5020, U.S.A. (e-mail: aepunt@u.washington.edu).

 doi: 10.1139/F03-105 © 2003 NRC Canada

where B_y is the biomass at the start of year y ($y = 1,2,\ldots,n+1$); $g(B)$ is surplus production as a function of biomass; ε_y is the extent of process error during year y, $\varepsilon_y \sim N(0; \sigma_\varepsilon^2)$; I_y is the index of abundance for year y; q is the catchability coefficient; and η_y is the extent of measurement (or observation) error during year y, $\eta_y \sim N(0; \sigma_\eta^2)$.

The three classes of production-model estimator on which actual assessments have been based are (*i*) observation-error estimators ($\sigma_\varepsilon = 0$), (*ii*) process-error estimators ($\sigma_\eta = 0$), and (*iii*) total-error estimators (also known as errors-in-variables estimators; $\sigma_\varepsilon/\sigma_\eta = C$, where C is a prespecified constant). There are a variety of sources for process error, including variability in recruitment, growth, and natural mortality, whereas observation error arises from, for example, sampling error and (random) variation in the availability of the population to the sampling gear at the time of sampling. Although Hilborn (2001) calculates surplus production directly, most production model estimators assume $g(B)$ to be one of a small number of unimodal functions, the most common of which are the Schaefer (1954), Fox (1970), and Pella–Tomlinson (1969) forms.

Initially, process-error estimators were most popular because, for some choices for $g(B)$, parameter estimation could be achieved by means of multiple linear regression rather than nonlinear regression techniques (e.g., Schnute 1977; Hilborn 1979). However, simulation studies (e.g., Punt 1989*a*; Polacheck et al. 1993) have shown that process-error estimators tend to provide less precise estimates of model outputs such as current biomass and MSY than observation-error estimators. Although the total-error approach of Ludwig et al. (1988) has formed the basis for actual stock assessments (e.g., Punt 1989*b*), the bulk of recent applications of dynamic production models have been based on the observation-error formulation (Prager 1994, 2002; Williams and Prager 2002).

Simulation studies of the performance of production model estimators have shown that observation-error estimators provide biased and imprecise estimates in the presence of process error (Punt 1989*a*), which raises the question whether approaches that attempt to consider both observation and process error simultaneously might provide more satisfactory estimates. Apart from the approach of Ludwig et al. (1988), account can be taken when fitting production models of process and observation error by Kalman filter (Reed and Simons 1986; Pella 1993; Kimura et al. 1996) and, more generally, state–space models (de Valpine 2002). The latter two approaches differ from observation-error and total-error estimators in that a distribution for the biomass in year $y + 1$ is determined from a distribution for the biomass in year y by forecasting the distribution of biomass in year $y + 1$ using a population dynamics model and then updating this distribution based on the observed abundance index for year $y + 1$. Given a distribution for the initial biomass, this forecasting–updating process can be applied recursively to compute distributions of biomass for each year of interest. In essence, therefore, unlike observation-error and total-error estimators, the Kalman filter and general state–space models integrate over the unknown population biomasses and (or) process errors.

This paper outlines how production models can be based on each of the four types of estimators referred to above. Previous production model type estimators based on Kalman filters and general state–space models have tended to be based on population dynamics models that are linear in their parameters (possibly after transformation). The presentation below deals with a broader class of models for which no transformation exists that will make the population dynamics model linear. The paper then evaluates these estimators in terms of their likely bias and precision using simulations based on the 25-year catch history for hake (*Merluccis capensis*) off northern Namibia (Fig. 1).

Fig. 1. Catch history for northern Namibian hake (*Merluccis capensis*).

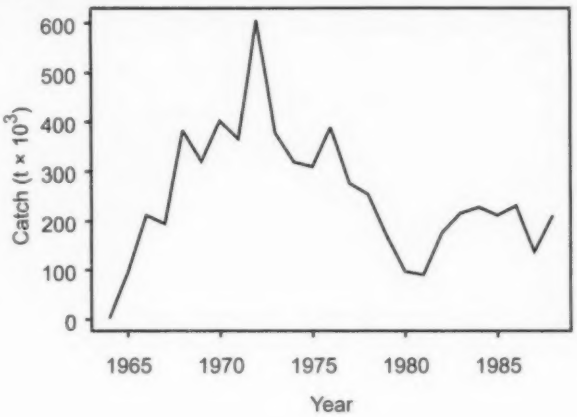

Materials and methods

The alternative estimators

The following sections outline production model estimators based on each of the four frameworks (observation error, total error, Kalman filter, and general state–space model) referred to above. Readers interested in a more general comparison of the four frameworks can consult de Valpine (2002).

The four estimators are all based on the population dynamics model and observation model given in eq. 1, where the function $g(B)$ is taken to be the Schaefer (or logistic) form of the production function, i.e., $g(B) = rB(1 - B/K)$, where r is the intrinsic growth rate and K is pre-exploitation population size (or carrying capacity). Applying these estimators to other forms for the production function or to delay-difference models (Deriso 1980; Schnute 1985) would involve straightforward modifications to the equations provided below.

For ease of comparison, it is assumed by all of the estimators that the population was at its pre-exploitation level at the start of the first year for which catches are available, i.e., $B_1 = K$. The parameters of interest are r, K, MSY, the ratio of the exploitation rate in the last year for which catches are available to the exploitation rate at which MSY is achieved, $F_n/F_{MSY} = (C_n/B_n)/(r/2)$, the biomass at the end of the modeled time horizon, B_{n+1}, and the relative biomass at the end of the modeled time horizon, $D_{n+1} = B_{n+1}/K$.

For all of the estimators, the likelihood of the abundance-index datum for year y, given the biomass for year y, is

© 2003 NRC Canada

Table 1. The specifications of the simulations trials.

Scenario	r	D_{n+1}	σ_ε	σ_η
Baseline	0.35	0.2, 0.4, 0.6, 0.8	0.2	0.2
No process error	0.35	0.2, 0.4, 0.6, 0.8	0.0	0.283
No observation error	0.35	0.2, 0.4, 0.6, 0.8	0.283	0.0
Alternative r values	0.15, 0.25, 0.45	0.4	0.2	0.2

Fig. 2. Time trajectories of "true" population size expressed relative to the pre-exploitation level for four choices for the 1989 relative biomass: (*a*) 0.2, (*b*) 0.4, (*c*) 0.6, and (*d*) 0.8.

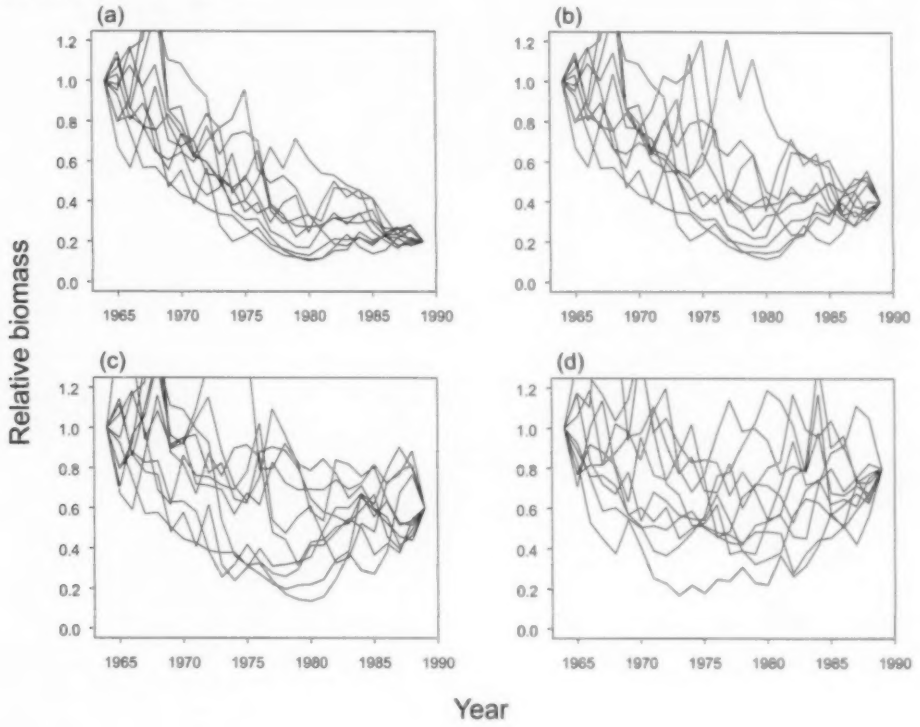

$$(2)\qquad L(I_y|q,B_y,\sigma_\eta) = \frac{1}{\sqrt{2\pi\sigma_\eta I_y}}\, e^{-\frac{(\ln I_y - \ln(qB_y))^2}{2\sigma_\eta^2}}$$

$$(3)\qquad -\ln L \propto n\ln\sigma_\eta + \frac{1}{2\sigma_\eta^2}\sum_y (\ln I_y - \ln(qB_y))^2 + n\ln\sigma_\varepsilon + \frac{1}{2\sigma_\varepsilon^2}\sum_y \varepsilon_y^2$$

The observation-error estimator

The estimates of r, q, and K for this estimator are obtained by minimizing the negative of the sum of the logarithms of eq. 2 over all years for which abundance-index information is available, where the biomass time series is obtained by projecting from $B_1 = K$ using eq. 1*a* under the assumption of deterministic dynamics, i.e., $\{\varepsilon_y = 0: y = 1,2,\ldots,n\}$.

The total-error estimator

The estimates of r, q, and K for this estimator are obtained by minimizing a negative log-likelihood function that includes contributions from the abundance indices and the process errors (which are treated as nuisance parameters when applying this estimator, i.e., the parameter vector for this estimator is $\{r, q, K, [\varepsilon_y: y = 1,2,\ldots n], \sigma_\varepsilon, \sigma_\eta\}$):

It is necessary to specify the relationship between σ_ε and σ_η to apply this estimator. For the purposes of this paper, $\sigma_\varepsilon = \sigma_\eta$. This assumption is arbitrary, but the results of applications of total-error production models to real data sets are seldom very sensitive to the ratio of σ_ε to σ_η unless this ratio strongly favors observation error or process error (Ludwig et al. 1988).

General state–space model

The general state–space model considered in this paper is implemented using the numerical integration state–space (NISS) approach of de Valpine (2002) and de Valpine and Hastings (2002). Unlike the total-error estimator, the NISS estimator and the Kalman filter estimator outlined below

© 2003 NRC Canada

Fig. 3. Relative error distributions for (*a*) intrinsic growth rate, (*b*) carrying capacity, (*c*) relative biomass in 1989, (*d*) biomass in 1989, (*e*) F_n/F_{MSY}, and (*f*) MSY (maximum sustainable yield) for four alternative estimators (observation error (Obs Err), NISS (numerical integration state–space), total error (Tot Err), Kalman filter).

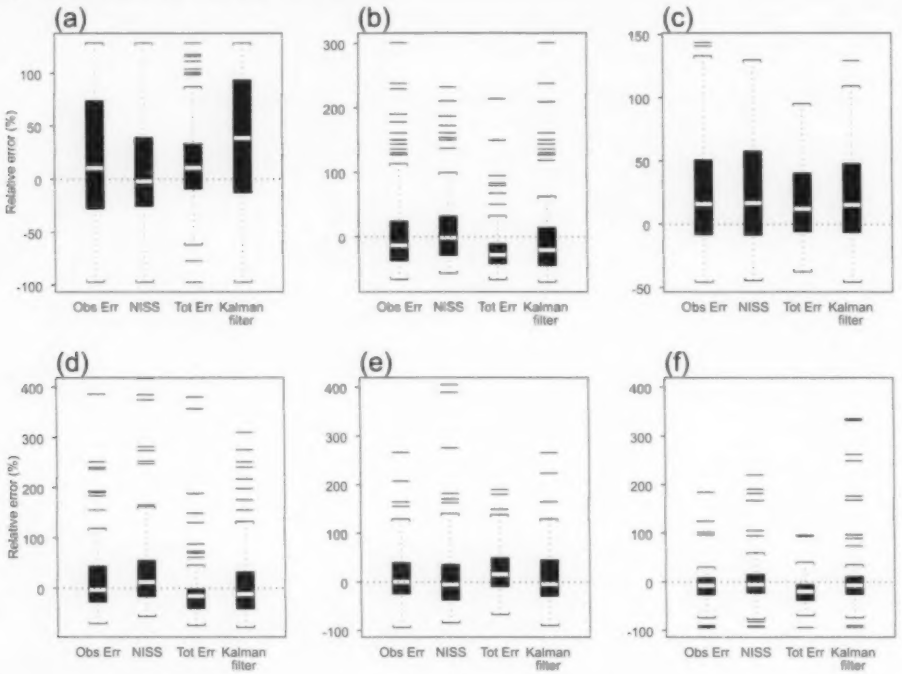

integrate over the process errors, as is appropriate given that the process errors are random effects in a nonlinear time-series model. Note that even though the process errors are integrated out, this is not a Bayesian estimator.

For this approach, therefore, the quantity maximized to determine the estimates for the model parameters and outputs (ignoring the conditioning on the model parameters) is

$$(4) \qquad L(\boldsymbol{I}^{(n)}) = P(I_1)\prod_{y>1} P(I_y|\boldsymbol{I}^{(y-1)})$$

where $\boldsymbol{I}^{(y)}$ is the vector $(I_1,I_2,\ldots,I_y)$.

The yth factor in the likelihood $P(I_y|\boldsymbol{I}^{(y-1)})$ is computed using the formula

$$(5) \quad P(I_y|\boldsymbol{I}^{(y-1)}) = \int \frac{1}{\sqrt{2\pi}\sigma_\eta I_y} e^{-\frac{(\ln I_y - \ln(qB_y))^2}{2\sigma_\eta^2}} P(B_y|\boldsymbol{I}^{(y-1)})dB_y$$

$$= \int P(I_y|B_y)P(B_y|\boldsymbol{I}^{(y-1)})dB_y$$

The distribution for the biomass at the start of year y, conditional on the data for years $y-1$ and earlier, $P(B_y|\boldsymbol{I}^{(y-1)})$, is updated from the distribution for the biomass at the start of year $y-1$ according to the "filtering" equation:

$$(6) \qquad P(B_y|\boldsymbol{I}^{(y-1)}) = \int P(B_y|B_{y-1})P(B_{y-1}|\boldsymbol{I}^{(y-1)})dB_{y-1}$$

where $P(B_{y-1}|\boldsymbol{I}^{(y-1)}) \propto P(I_{y-1}|B_{y-1})P(B_{y-1}|\boldsymbol{I}^{(y-2)})$ so that

$$(7) \qquad P(B_y|\boldsymbol{I}^{(y-1)}) = \int P(B_y|B_{y-1})\frac{P(I_{y-1}|B_{y-1})P(B_{y-1}|\boldsymbol{I}^{(y-2)})}{P(I_{y-1}|\boldsymbol{I}^{(y-2)})}dB_{y-1}$$

and $P(B_y|B_{y-1})$ is the probability

$$(8) \qquad P(B_y|B_{y-1}) = \frac{1}{\sqrt{2\pi}\sigma_\varepsilon} e^{-\frac{[\ln B_y - \ln(B_y + g(B_y) - C_y)]^2}{2\sigma_\varepsilon^2}}$$

The integrations (eqs. 5 and 7) cannot be evaluated analytically. Instead they are evaluated numerically by discretizing the range for the annual biomass.

The initial distribution of biomass, $P(B_1)$, is obtained by projecting an arbitrary probability distribution forward with zero catches until it reaches equilibrium. Determining the initial distribution of biomass therefore involves conducting integrals (eqs. 5 and 7) with $C_y = 0$ numerically until convergence occurs.

The expected biomass at the start of year y, $E(B_y)$, is computed using the equation

$$(9) \qquad E(B_y) = \int B_y P(B_y|\boldsymbol{I}^{(y-1)})dB_y$$

The Kalman filter

The traditional Kalman filter (e.g., Meinhold and Singpurwalla 1983; Harvey 1989) is a special case of the general state–space approach outlined above in which the state equation (i.e., the population dynamics model) is linear in its parameters. However, the Schaefer production model is nonlinear so it is necessary to by apply an extended Kalman

© 2003 NRC Canada

Fig. 4. Median absolute relative errors for four estimators (observation error (Obs Err), NISS (numerical integration state–space), total error (Tot Err), Kalman filter) and six model outputs (r, K, relative biomass (RelB), biomass (Bmass), F_n/F_{MSY} (F), MSY) for variants of the baseline trial in which the "true" 1989 relative biomass is modified. Relative biomass values depicted are (*a*) 0.2, (*b*) 0.4, (*c*) 0.6, and (*d*) 0.8.

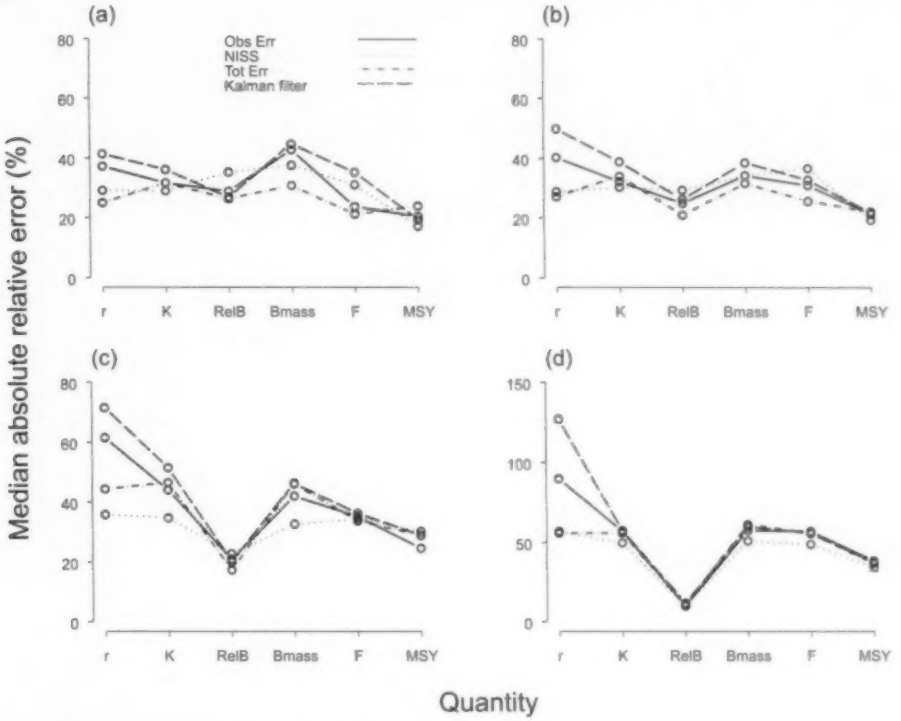

filter approach in which the nonlinear dynamics model is linearized (Pella 1993; Dereksdóttir and Magnusson 2003). In the case of a production model, the Kalman filter used here updates the expected value and variance of the logarithm of population biomass, i.e., $E(\ln B_y)$ and $\mathrm{Var}(\ln B_y)$ from the expected value and variance of the logarithm of the population biomass at the start of the previous year and the information contained in the abundance index for year $y-1$. The initial state, year $y = 1$, corresponds to a population distributed about its pre-exploitation level, i.e.,

$$(10)\quad E(\ln B_1) = \ln K \text{ and } \mathrm{Var}(\ln B_1) = \frac{\sigma_\varepsilon^2}{1-(1-r)^2}$$

The equations to update the expected value and variance of the logarithm of the population biomass are (Dereksdóttir and Magnusson 2003)

$$(11a)\quad E(\ln B_{y+1}) = \ln \tilde{B}_{y+1} + K_y[\ln(I_y/q) - \ln \tilde{B}_{y+1}]$$

$$(11b)\quad \mathrm{Var}(\ln B_{y+1}) = F_y^2(1-K_y)\mathrm{Var}(\ln B_y) + \sigma_\varepsilon^2$$

where K_y is the Kalman gain factor for year y:

$$(12)\quad K_y = \frac{\mathrm{Var}(\ln B_y)}{\mathrm{Var}(\ln B_y) + \sigma_\eta^2}$$

$\tilde{B}_{y+1}$ is the biomass at the start of year $y+1$ based on the deterministic component of the population dynamics model, i.e., the result of replacing B_y by $\exp(E(\ln B_y))$ in eq. 1*a*, and

$$(13)\quad F_y = \frac{\partial(\ln \tilde{B}_{y+1})}{\partial \ln B_y} = \frac{\exp(E(\ln B_y)) + r\exp(E(\ln B_y))(1-2\exp(E(\ln B_y))/K)}{\tilde{B}_{y+1}}$$

It is straightforward to show that the initial state (eq. 10) is the solution to eqs. 11*a* and 11*b* when $\sigma_\eta^2 \to \infty$.

The function maximized to obtain the estimates for the model parameters and outputs is

$$(14)\quad L(\boldsymbol{I}^{(n)}) = \prod_y \frac{1}{\sqrt{2\pi(\mathrm{Var}(\ln B_y) + \sigma_\eta^2)I_y}} \times \exp\left(-\frac{(\ln(I_y/q) - E(\ln B_y))^2}{2(\mathrm{Var}(\ln B_y) + \sigma_\eta^2}\right)$$

Evaluating the alternative estimators

In common with several previous studies that have evaluated the performances of production model estimators (e.g., Polacheck et al. 1993; Kimura et al. 1996), the four estimators outlined above are evaluated by means of Monte Carlo simulation. Each simulation trial consists of 100 simulations (results with a larger number of simulations were not qualitatively different from those based on 100 simulations). The "true" dynamics of the population are assumed to be gov-

© 2003 NRC Canada

Fig. 5. Median absolute relative errors for four estimators (observation error (Obs Err), NISS (numerical integration state–space), total error (Tot Err), Kalman filter) and six model outputs (r, K, relative biomass (RelB), biomass (Bmass), F_n/F_{MSY} (F), MSY) for simulation trials in which there is no process error. Relative biomass values depicted are (*a*) 0.2, (*b*) 0.4, (*c*) 0.6, and (*d*) 0.8.

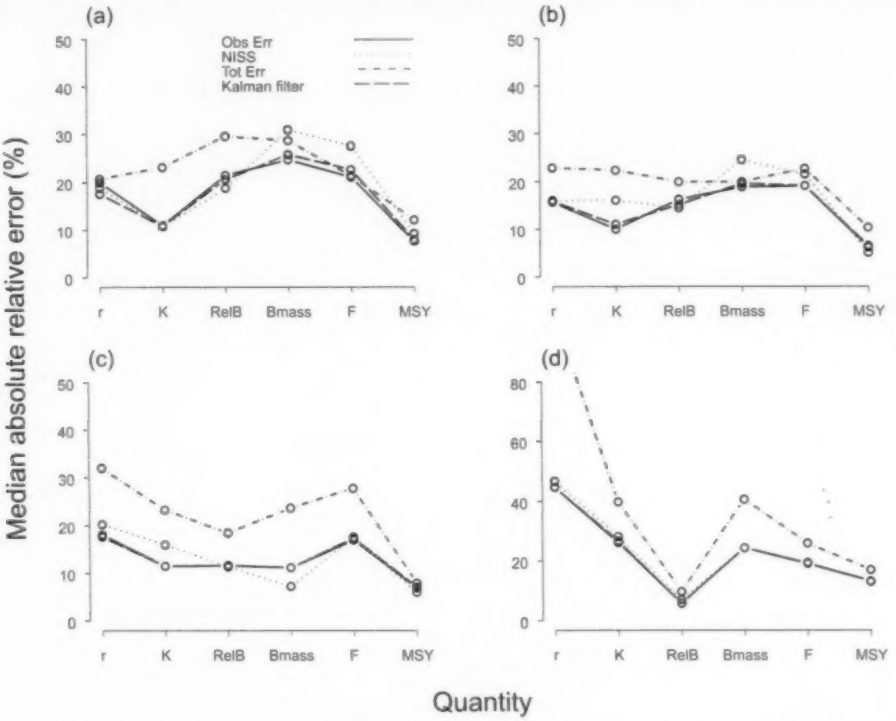

erned by eq. 1*a* and the historical sequence of catches is taken to be that for hake off northern Namibia (Fig. 1). In general, when evaluating estimators by means of simulation, consideration is given to models of the "truth" that are more complicated than those underlying the estimators being evaluated (e.g., Punt 1989*a*; Punt et al. 2002). However, for the purposes of this study, the "true" dynamics are taken to be the same as those underlying the four estimators so that any differences between the estimated and true values for the model parameters and outputs are due to the impact of the estimator rather than, say, model misspecification error.

Although the parameters of the Schaefer model are r and K, the "truth" for the simulation trials of this paper is based on specifying r and the relative biomass at the start of year $n + 1$, D_{n+1}, and solving for K. As the result, the initial relative biomass and that for year $n + 1$ are the same for all of the simulations, but because of the differences in process errors, the relative biomasses for the intervening years and the value of K differ among simulations. Alternative scenarios for the simulation experiment were created by varying the values for r, D_{n+1}, σ_ε, and σ_η (Table 1).

The results are summarized by the distribution for the relative error, i.e., for a quantity X:

$$(15) \quad R_i^X = \frac{X_i^{\text{True}} - X_i^{\text{Est}}}{X_i^{\text{True}}}$$

where R_i^X is the relative error for quantity X and simulation i, X_i^{True} is the "true" value of quantity X for simulation i, and X_i^{Est} is the estimate of quantity X for simulation i.

Results and discussion

The simulation scenarios

Ten time trajectories of "true" population biomass (expressed relative to the pre-exploitation equilibrium level (K)) are shown for each of the four baseline simulation trials (Fig. 2). The initial relative biomass (year 1964) is always 1, whereas the 1989 relative biomass differs among simulation trials but is the same for each simulation within a simulation trial. The information content of the "true" biomass trajectory is clearly determined to a large extent by the prespecified value for D_{n+1}, but there is also (substantial) intersimulation variability in the time trajectories of biomass due to the impact of process error. The time trajectories for the abundance index (not shown here) exhibit even greater variability due to the impact of measurement error.

Detailed results for a single simulation trial

The relative error distributions for the baseline trial in which the 1989 relative biomass equals 0.4 are plotted (Fig. 3). The "truth" underlying this simulation trial most closely mimics the results of the actual production model based assessments of Namibian hake in the late 1980s (e.g., Punt 1989*b*). However, those assessments were highly un-

© 2003 NRC Canada

Fig. 6. Median absolute relative errors for four estimators (observation error (Obs Err), NISS (numerical integration state–space), total error (Tot Err), Kalman filter) and six model outputs (r, K, relative biomass (RelB), biomass (Bmass), F_n/F_{MSY} (F), MSY) for simulation trials in which there is no observation error. Relative biomass values depicted are (*a*) 0.2, (*b*) 0.4, (*c*) 0.6, and (*d*) 0.8.

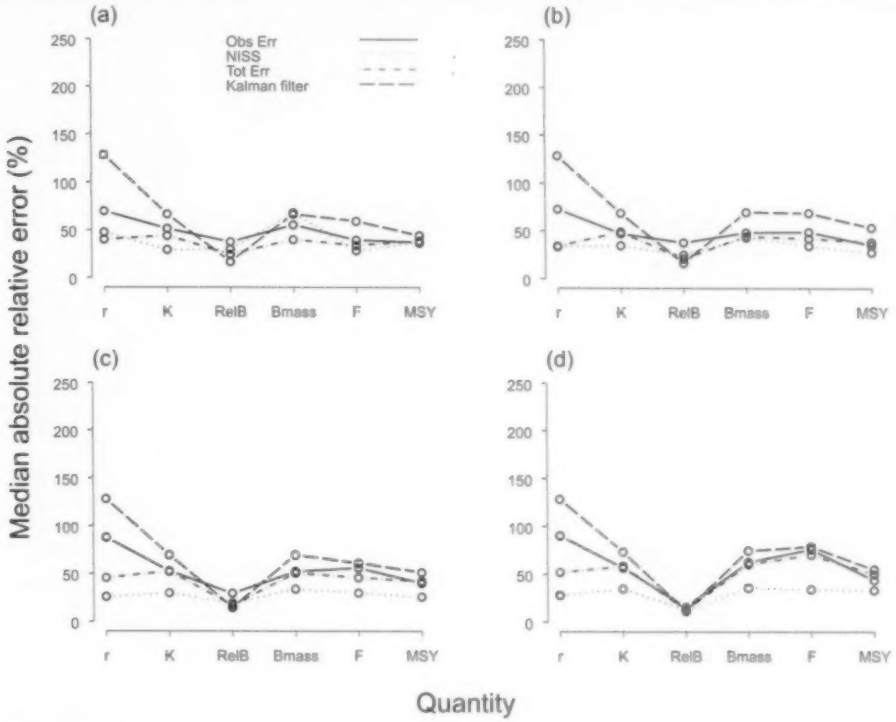

certain and so the sensitivity of the performance of the estimators to a variety of alternative scenarios needs to be examined.

The possibility of extreme estimates (relative errors >100%) is much greater for r (21% of simulations for the Kalman filter estimator), 1989 biomass, and F_n/F_{MSY} than for the 1989 relative biomass, K, and MSY. In terms of minimizing bias, the NISS estimator performs best for r, F_n/F_{MSY}, and MSY, whereas the total-error estimator performs best for 1989 biomass and 1989 relative biomass. The Kalman filter estimator provided the least biased estimates of K. The estimates provided by the total-error estimator exhibit the least inter-simulation variability, whereas those provided by the observation-error estimator vary the most among simulations.

It is clearly necessary to combine the effects of the bias and the imprecision of the estimates of the model outputs in any statistic for comparing overall performance among estimators. The root-mean-square-error (RMSE) is such a statistic. However, the RMSE is very sensitive to outliers. Therefore, a more robust performance statistic, the median of the absolute values of the relative errors (MARE), forms the basis for the comparisons among the four estimators in this paper.

For the baseline simulation trial (Fig. 4b), in terms of the MARE, the total-error estimator performs "best" for r, F_n/F_{MSY}, 1989 biomass, and 1989 relative biomass, whereas the NISS estimator performs best for MSY and K. The observation-error estimator performs better than the Kalman filter for all of the model outputs except MSY in terms of the MARE. Although the NISS and total-error estimators perform best, their estimates of absolute biomass are still relatively poor (MAREs of 32% and 34%, respectively). This result is, however, not unexpected given the outcomes from previous investigations into the performance of production model based stock assessment methods (e.g., Punt and Butterworth 1993). One of the implications of the uniformly poor performance of the estimators in terms of their ability to estimate absolute biomass is that were catch limits to be based on the estimates of biomass from any of these estimators, it would be appropriate to apply a precautionary reduction factor to reduce the probability of catch limits exceeding sustainable levels.

The estimates of 1989 biomass from the Kalman filter are negatively biased (Fig. 3*d*). One possible reason for this is that the estimate of the biomass in year y is taken to be the median of its distribution (i.e., $\hat{B}_y = \exp(E(\ln B_y))$ which is less than the mean of its distribution ($\bar{B}_y = \exp(E(\ln B_y) + 0.5\mathrm{Var}(\ln B_y))$). However, using the means of the distributions for biomass rather than medians did not reduce the extent of bias for 1989 biomass noticeably.

Sensitivity to alternative "true" model specifications

The MARE for each estimator and model output for various "true" levels for the 1989 relative biomass can be used to examine sensitivity to the value of this parameter (Fig. 4). The results for a 1989 relative biomass of 0.2 are qualitatively the same as those for a 1989 relative biomass of 0.4 in terms of the best-performing estimator. However, the NISS

© 2003 NRC Canada

Fig. 7. Distributions of relative error for relative biomass in 1989 (upper panels) and F_n/F_{MSY} (lower panels) for trials in which (*a* and *d*) $\sigma_\varepsilon = \sigma_\eta = 0.2$, (*b* and *e*) $\sigma_\varepsilon = 0$, and (*c* and *f*) $\sigma_\eta = 0.0$ for four estimators (observation error (Obs Err), NISS (numerical integration state–space), total error (Tot Err), Kalman filter).

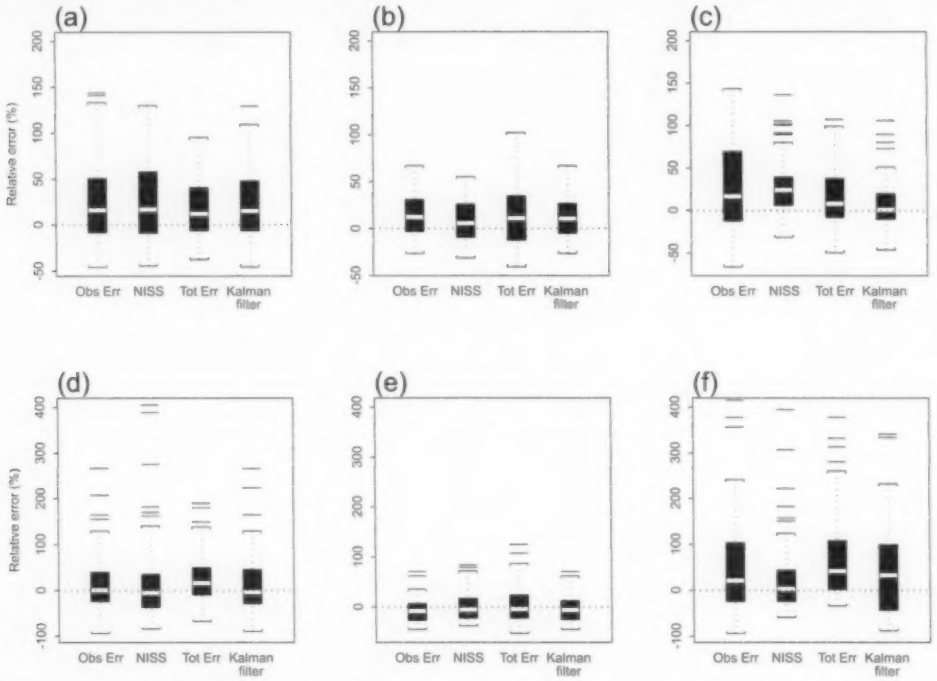

estimator outperforms the other three estimators for all but the 1989 relative biomass for "true" relative biomasses of 0.5 and larger. The size of the MARE increases as the "true" 1989 relative biomass increases. This is, however, not unexpected because higher 1989 relative biomasses correspond to lesser "contrast" in the data (Fig. 2), which, in turn, reduces the ability to adequately estimate quantities of management interest (Hilborn 1979). In contrast to when the 1989 relative biomass is 0.4 (Fig. 3), the estimates can be highly biased when the 1989 relative biomass is high; r tends to be positively biased, whereas K and 1989 biomass are negatively biased.

The observation-error estimator is based on the assumption that the amount of process error is negligible compared with the amount of observation error. Therefore, the performance of this estimator relative to those of the other estimators should be expected to improve markedly for simulation trials in which there are no process errors. As expected, the observation-error estimator generally does perform best when there is only observation error (Fig. 5). However, the performances of the Kalman filter and NISS estimators are virtually identical to that of the observation-error estimator. This occurs because the parameters related to the amounts of process and observation error are estimable parameters for these latter two estimators. In contrast, the performance of the total-error estimator is generally poorer (particularly for a 1989 relative biomass of 0.8). It should be noted that the MARE is lower in Fig. 5 than in Fig. 4 for similar scenarios, confirming the expectation from previous studies that, irrespective of the choice of estimation framework, increased process error leads to poorer performance of production-model estimators.

The NISS estimator is consistently the best performing of the four estimators when there is only process error (Fig. 6). The performance of the Kalman filter in this case is consistently poorest for quantities other 1989 relative biomass. Although the NISS estimator performs best in Fig. 6, its performance is, however, very poor when compared with Figs. 4 and 5.

The impact of the magnitude of process and observation error can be seen more clearly from the relative error distributions for 1989 relative biomass and F_n/F_{MSY} (Fig. 7). The estimates are less biased and more precise (leading to lower MAREs) when there is only observation error (Figs. 7*b* and 7*e*), and the chances of extreme estimates are markedly lower for this case. The estimates of 1989 relative biomass from the NISS estimator are positively biased when there is only process error (Fig. 7*c*), but the estimates from this estimator are also much more precise, which leads to the NISS estimator having the lowest overall MARE.

The relative performances of the different estimators are sensitive to the "true" value for the intrinsic growth rate (r) (Fig. 8). The NISS estimator performs best for the lower values for r (although performance is generally poorer the lower the "true" value for r) and the total-error estimator performs best for the higher values for r.

Other estimation methods and structural models

The approaches considered in this paper are not Bayesian. It is, however, possible to construct Bayesian production

© 2003 NRC Canada

Fig. 8. Median absolute relative errors for four estimators (observation error (Obs Err), NISS (numerical integration state–space), total error (Tot Err), Kalman filter) and six model outputs (r, K, relative biomass (RelB), biomass (Bmass), F_n/F_{MSY} (F), MSY) for simulation trials in which the "true" value of r is (*a*) 0.15, (*b*) 0.25, (*c*) 0.35, and (*d*) 0.45. The 1989 relative biomass is 0.4 for all of the simulations.

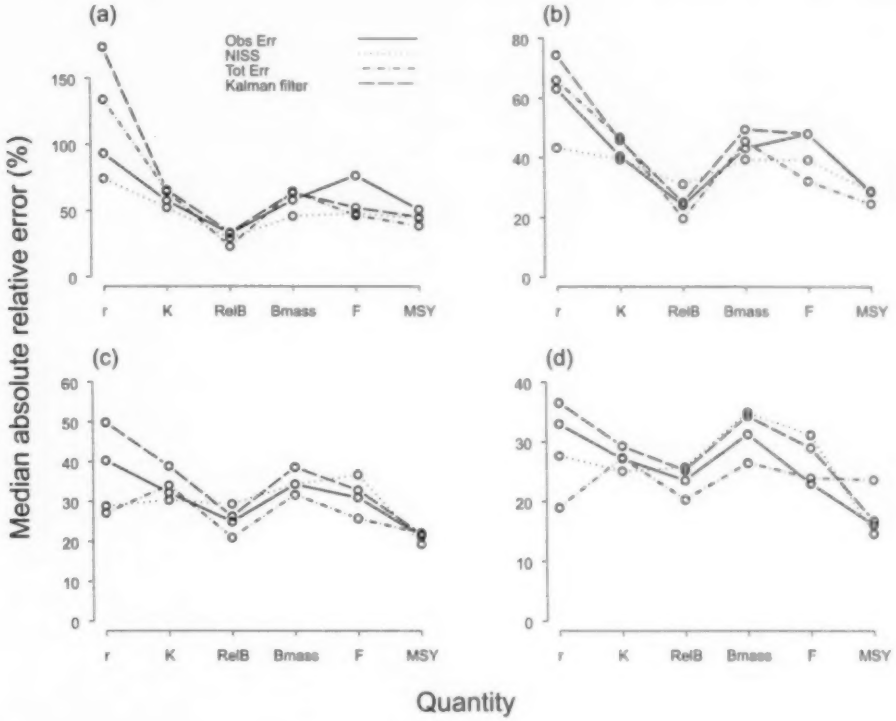

models (e.g., McAllister and Kirkwood 1998; Meyer and Millar 1999; McAllister et al. 2001). Although the ability of Bayesian estimators to provide more accurate and precise estimates of fisheries management related quantities than frequentist estimators has yet to be evaluated in depth (Nielsen and Lewy (2002) being a notable exception), the ability of Bayesian approaches to incorporate additional information through prior distributions makes this a key issue for future research.

Observation-error and total-error estimators are commonly used to fit age- and size-structured population dynamics models (e.g., Hilborn 1990; Methot 2000), whereas Kalman filter approaches have been applied to fit size-structured population dynamics models (e.g., Sullivan 1992). The ability to apply general state–space modeling techniques to fully age- and (or) size-structured fisheries models requires the development of more efficient numerical methods for computing the likelihood function than that used for the NISS estimator. This is because the computational requirements of eqs. 5–8 become prohibitive when there are many state variables. The use of Monte Carlo methods (e.g., Carlin et al. 1992; Shumway and Stoffer 2000) is therefore probably necessary to implement such models.

Choices among estimators

The four estimators considered in this paper are all candidates for use in actual stock assessments. All four estimators can make use of multiple time series of abundance indices, as well as series of absolute estimates of abundance. None of the estimators uniformally outperformed all of the others for all of the scenarios considered. However, overall, the NISS estimator is probably best as it is never the worst estimator and is often the best. The total-error estimator appears to be the next-best estimator. Although this points to the use of the NISS estimator in future production-model assessments, the very poor performance of this estimator in some of the simulation trials highlights that even the best-performing production model estimators may provide estimates of quantities of management interest that are severely biased and highly imprecise. It should also be recalled that the "true" model for the simulations was the same as that underlying the estimators. The level of error would have been even greater had a "true" model differing from the Schaefer model been used to represent reality.

One of the key assumptions underlying the simulations is that the biomass at the start of the first year for which catches are available equals K, i.e., $B_1 = K$, and that the estimators are aware of this. Although this assumption is unlikely to be greatly violated for hake off northern Namibia (Fig. 1), the sensitivity of the results to this assumption is examined by a simulation trial in which the "true" relative biomass at the start of the first year for which catches are available is set equal to 0.6 and the "true" relative biomass in year $n + 1$ is set equal to 40% of this, i.e., $D_{n+1} = 0.24$.

© 2003 NRC Canada

Fig. 9. Relative error distributions for (*a*) intrinsic growth rate, (*b*) carrying capacity, (*c*) relative biomass in 1989, (*d*) biomass in 1989, (*e*) F_{89}/F_{MSY}, and (*f*) MSY (maximum sustainable yield) for four alternative estimators (observation error (Obs Err), NISS (numerical integration state–space), total error (Tot Err), Kalman filter) when the relative biomass at the start of 1964 is 0.6 rather than 1.

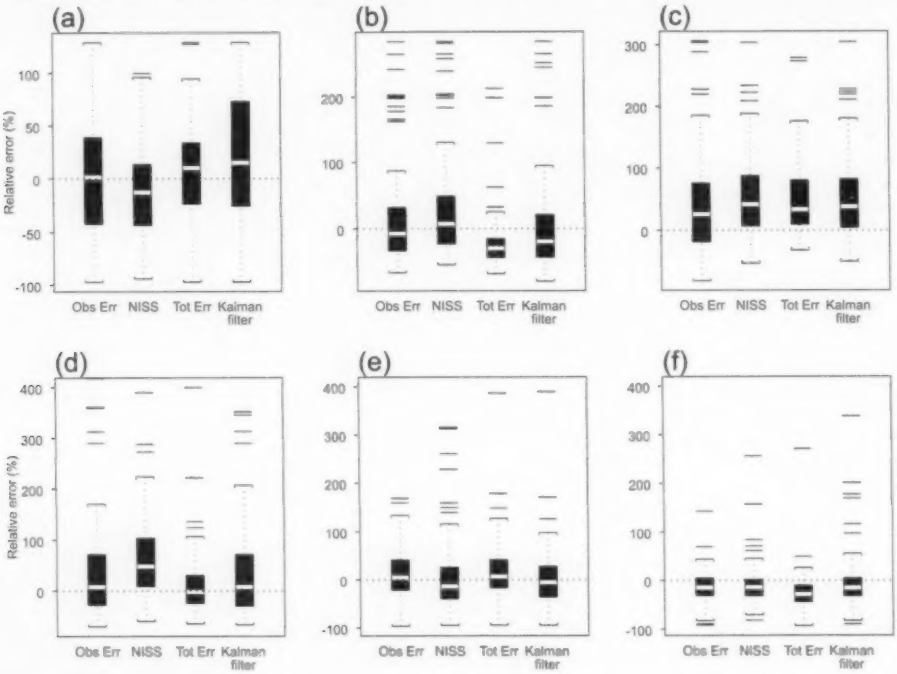

Fig. 10. Distribution of biomass for (*a*) 1964 and (*b*) 1989 from an application of the numerical integration state–space (NISS) estimator to one of the simulated data sets.

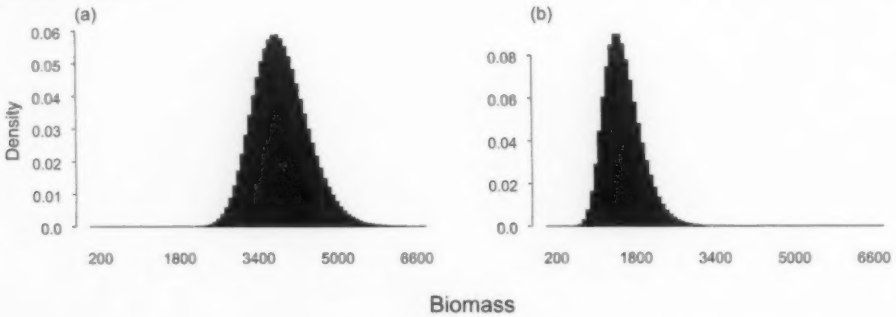

The relative error distributions for the four estimators when the initial relative biomass is treated as an estimable parameter by all four estimators rather than being assumed equal to 1 are shown (Fig. 9). The estimates of 1989 biomass and 1989 relative biomass are more biased and variable than is the case for the baseline trial. There is also a notable deterioration in the performance of the NISS estimator in terms of its ability to estimate 1989 biomass and F_{89}/F_{MSY} (Figs. 9*d*, 9*e*). The observation-error estimator again outperforms the Kalman filter estimator.

The relatively poor performance of the Kalman filter is perhaps surprising given that it would have been equivalent to the NISS estimator had the population dynamics model been linear. The extended Kalman filter considered in this paper is based on the assumption that the distribution of biomass is lognormal. However, the distributions of biomass from the NISS approach are not as skewed as might have been anticipated had biomass been lognormally distributed (see Fig. 10 for examples of biomass distributions from the NISS estimator), suggesting that, although beyond the scope of the present paper, a different formulation of the Kalman filer may have performed somewhat better. Another reason for the relatively poor performance of the Kalman filter may lie in the attempt to estimate the observation- and process-error variances and the error associated with linearizing the population dynamics model (see eq. 13).

It should be noted that there are factors other than performance under simulated conditions that need to be considered

© 2003 NRC Canada

when selecting an estimator for use in production-model assessments. In particular, the computational demands of the NISS estimator are substantial compared with those of the other three estimators. Also, this estimator involves approximating integrals numerically. The accuracy of the approximations depends on how fine the numerical grid used for integration is. However, there is a tradeoff between increased accuracy of integration and the time demands of the calculations.

Acknowledgements

This work was funded through NMFS grant NA07FE0473. The comments by two anonymous reviewers are greatly acknowledged.

References

Carlin, B.P., Polson, N.G., and Stoffer, D.S. 1992. A Monte Carlo approach to nonnormal and nonlinear state–space modeling. J. Am. Stat. Assoc. **87**: 493–500.

Cooke, J.G., and Beddington, J.R. 1984. The relationship between catch rates and abundance in fisheries. IMA J. Math. Appl. Med. Biol. **1**: 391–405.

Dereksdóttir, E., and Magnusson, K.G. 2003. A strike limit algorithm based on adaptive Kalman filtering with an application to aboriginal whaling of bowhead whales. J. Cetacean Res. Manag. **5**: 29–37.

Deriso, R.B. 1980. Harvesting strategies and parameter estimation for an age-structured model. Can. J. Fish. Aquat. Sci. **37**: 268–282.

de Valpine, P. 2002. Review of methods for fitting time-series models with process and observation error and likelihood calculations for nonlinear, non-gaussian state–space models. Bull. Mar. Sci. **70**: 455–471.

de Valpine, P., and Hastings, A. 2002. Fitting population models with process noise and observation error. Ecol. Monogr. **72**: 57–76.

Fox, W.W. 1970. An exponential surplus-yield model for optimizing exploited fish populations. Trans. Am. Fish. Soc. **99**: 80–88.

Fox, W.W. 1975. Fitting the generalized stock production model by least-squares and equilibrium approximation. Fish. Bull. **73**: 23–37.

Gulland, J.A. 1961. Fishing and the stocks of fish at Iceland. Fish. Invest. Min. Agric. Fish. Food U.K. (Ser. 2), **23**: 1–52.

Harvey, A.C. 1989. Forecasting, structural time series models, and the Kalman filter. Cambridge University Press, Cambridge.

Hilborn, R. 1979. Comparison of fisheries control systems that utilize catch and effort data. J. Fish. Res. Board Can. **36**: 1477–1489.

Hilborn, R. 1990. Estimating the parameters of full age-structured models from catch and abundance data. Bull. Int. North Pac. Fish. Comm. **50**: 207–213.

Hilborn, R. 2001. Calculation of biomass trend, exploitation rate, and surplus production from survey and catch data. Can. J. Fish. Aquat. Sci. **58**: 579–584.

International Commission for the Conservation of Atlantic Tunas. 2000. Report of the Standing Committee on Research and Statistics (SCRS). International Commission for the Conservation of Atlantic Tunas (ICCAT), Madrid, Spain.

Kimura, D.K., Balsiger, J.W., and Ito, D.H. 1996. Kalman filtering the delay-difference equation: practical approaches and simulations. Fish. Bull. **94**: 678–691.

Ludwig, D., Walters, C.J., and Cooke, J.G. 1988. Comparison of two models and two estimation methods for catch and effort data. Nat. Resour. Model. **2**: 457–498.

McAllister, M.K., and Kirkwood, G.P. 1998. Bayesian stock assessment: a review and example application using the logistic model. ICES. J. Mar. Sci. **55**: 1031–1060.

McAllister, M.K., Pikitch, E.K., and Babcock, E.A. 2001. Using demographic methods to construct Bayesian priors for the intrinsic rate of increase in the Schaefer model and implications for stock rebuilding. Can. J. Fish. Aquat. Sci. **58**: 1871–1890.

Meinhold, R.J., and Singpurwalla, N.D. 1983. Understanding the Kalman filter. Am. Stat. **37**: 123–127.

Methot, R.D. 2000. Technical description of the Stock Synthesis Assessment Program. NOAA Tech Memo NMFS-NWFSC-43.

Meyer, R., and Millar, R.B. 1999. Bayesian stock assessment using a state–space implementation of the delay difference model. Can. J. Fish. Aquat. Sci. **56**: 37–52.

Moses, B.S. 2000. A review of artisanal marine and brackishwater fisheries of south-eastern Nigeria. Fish. Res. **47**: 81–92.

Nielsen, A., and Lewy, P. 2002. Comparison of the frequentist properties of Bayes and maximum likelihood estimators in an age-structured fish stock assessment model. Can. J. Fish. Aquat. Sci. **59**: 136–143.

Pella, J.J. 1993. Utility of structural time series models and the Kalman filter for predicting consequences of fishery actions. *In* Proceedings of the International Symposium on Management Strategies for Exploited Fish Populations. *Edited by* G. Kruse, D.M. Eggers, R.J. Marasco, C. Pautzke, and T.J. Quinn II. Alaska Sea Grant College Prog. Rep. No. 92-02, University of Alaska, Fairbanks. pp. 571–593.

Pella, J.J., and Tomlinson, P.K. 1969. A generalized stock production model. Inter-Am. Trop. Tuna Comm. Bull. **13**: 421–458.

Polacheck, T., Hilborn, R., and Punt, A.E. 1993. Fitting surplus-production models: comparing methods and measuring uncertainty. Can. J. Fish. Aquat. Sci. **50**: 2597–2607.

Prager, M.H. 1994. A suite of extensions to a nonequilibrium surplus-production model. Fish. Bull. **92**: 374–389.

Prager, M.H. 2002. Comparison of logistic and generalized surplus-production models applied to swordfish, *Xiphias gladius*, in the North Atlantic Ocean. Fish. Res. **58**: 41–57.

Punt, A.E. 1989*a*. A further preliminary comparative investigation into the performance of catch–effort model estimation procedures used in the management of the ICSEAF hake stocks. Coll. Sci. Pap. Int. Comm. SE. Atl. Fish. **16**: 63–122.

Punt, A.E. 1989*b*. $f_{0.1}$ quotas for the ICSEAF hake stocks based on seven model-estimation procedures which perform best in simulation trials. Coll. Sci. Pap. Int. Comm. SE. Atl. Fish. **16**: 123–149.

Punt, A.E., and Butterworth, D.S. 1993. Variance estimates for fisheries assessment: their importance and how best to evaluate them. *In* Risk evaluation and biological reference points for fisheries management. *Edited by* S.J. Smith, J.J. Hunt, and D. Rivard. Can. Spec. Publ. Fish. Aquat. Sci. No. 120. pp. 145–162.

Punt, A.E., Smith, A.D.M., and Cui, G. 2002. Evaluation of management tools for Australia's South East Fishery. 2. How well do commonly used stock assessment methods perform? Mar. Freshw. Res. **53**: 631–644.

Reed, W.J., and Simons, C.M. 1986. Analyzing catch–effort data by means of the Kalman filter. Can. J. Fish. Aquat. Sci. **53**: 2157–2166.

Schaefer, M.B. 1954. Some aspects of the dynamics of populations important to the management of commercial marine fisheries. Inter-Am. Trop. Tuna Comm. Bull. **1**: 27–56.

Schnute, J. 1977. Improved estimates from the Schaefer production model: theoretical considerations. J. Fish. Res. Board Can. **34**: 583–603.

Schnute, J.T. 1985. A general theory for analysis of catch and effort data. Can. J. Fish. Aquat. Sci. **42**: 414–429.

© 2003 NRC Canada

Shumway, R.H., and Stoffer, D.S. 2000. Time series analysis and its applications. Springer Verlag, New York.

Sissenwine, M.P. 1978. Is MSY an adequate foundation for optimum yield? Fisheries, **3**: 22–42.

Sullivan, P.J. 1992. A Kalman filter approach to catch-at-length analysis. Biometrics, **48**: 237–257.

Williams, E.H., and Prager, M.H. 2002. Comparison of equilibrium and nonequilibrium estimators for the generalized production model. Can. J. Fish. Aquat. Sci. **59**: 1533–1552.

© 2003 NRC Canada

Horizontal and vertical distribution patterns, retention rates, and population dynamics of zooplankton on Western Bank, Scotian Shelf

Christian S. Reiss, Ian A. McLaren, and Patricia Avendaño

Abstract: We assess the importance of retention rates and local production to the concentration of zooplankton on Western Bank, Scotian Shelf, during September and October 1998. We do so using (*i*) particle retention rates derived from an array of 25 current meters and inferences from hydrographic structure; (*ii*) observations on the horizontal and vertical distribution of zooplankton and ichthyoplankton; and (*iii*) a simple projection-matrix model of the population dynamics of two copepod species, *Centropages typicus* and *Pseudocalanus* spp. Zooplankton biomass and adult stages of copepods were more abundant in surface waters on the bank ($p < 0.05$) at broad (25 km) spatial scales. Zooplankton was correlated with ichthyoplankton abundance at this scale ($r > 0.5$, $p < 0.001$), a result of local production of both zooplankton and fish on the bank. The time-dependent anticyclonic circulation around Western Bank was variable, and particle retention rates were 18 and 33% for 20 days at 12.5 and 28.5 m, respectively. The population model showed that both *C. typicus* and *Pseudocalanus* spp. are capable of increasing their population size despite advective loss and mortality rates approaching 10%·day^{-1}. We conclude that local production exceeding advective loss rates can explain the high concentrations of zooplankton on Western Bank.

Résumé : Nous avons évalué l'importance des taux de rétention et de la production locale pour expliquer les concentrations de zooplancton sur le banc occidental de la plate-forme néo-écossaise en septembre et en octobre 1998 au moyen (*i*) des taux de rétention des particules calculés d'après les données fournies par un réseau de 25 courantomètres et les inférences tirées de la structure hydrographique, (*ii*) des observations de la distribution horizontale et verticale du zooplancton et de l'ichtyoplancton et (*iii*) un modèle simple de matrice de projection de la dynamique de population de deux copépodes, *Centropages typicus* et *Pseudocalanus* spp. La biomasse du zooplancton et la densité des stades adultes des copépodes sont plus importantes dans les eaux superficielles sur le banc ($p < 0,05$) aux échelles spatiales larges (25 km). À cette échelle, il y a une corrélation ($r > 0,5$, $p < 0,001$) entre le zooplancton et l'abondance de l'ichtyoplancton, le résultat à la fois de la production de zooplancton et de celle de poissons sur le banc. La circulation anticyclonique reliée au temps autour du banc occidental est variable et les taux de rétention des particules sont respectivement de 18 et de 33 % après 20 jours à 12,5 et 28,5 m, respectivement. Le modèle démographique démontre que la taille des populations tant de *C. typicus* que de *Pseudocalanus* spp. peut s'accroître malgré des pertes par advection et des taux de mortalité qui atteignent presque 10 % par jour. En conclusion, la production locale qui dépasse les taux de pertes par advection peut expliquer les fortes concentrations de zooplancton sur le banc occidental.

[Traduit par la Rédaction]

Introduction

Shallow offshore banks are a feature of northwest Atlantic continental shelves and are known spawning locations for major stocks of commercial fish on the Scotian Shelf (Brander and Hurley 1992; Reiss et al. 2000). The survival of fish larvae on these banks may be linked to seasonal production cycles of their zooplankton prey following the spring bloom or to other processes that maintain high prey concentrations over the spawning and developmental grounds at other times of the year (O'Boyle et al. 1984; Taggart et al. 1996). Understanding the physical and biological processes that generate and maintain high prey concentrations against advection and mixing is critical for predictive modeling of growth and survival of larval fish (Lasker 1975, 1981).

On some larger banks (e.g., Georges Bank), the spatiotemporal abundance of zooplankton may be related both to entrainment of zooplankton within the prevailing circulation and to hydrographic fronts (Davis 1984*a*; McGillicuddy et al. 1998). As a result of advection within frontal currents,

Received 28 October 2002. Accepted 3 August 2003. Published on the NRC Research Press Web site at http://cjfas.nrc.ca on 3 November 2003.
J17153

C.S. Reiss.[1,2] Department of Oceanography, Dalhousie University, Halifax, NS B3H 4J1, Canada.
I.A. McLaren and P. Avendaño. Department of Biology, Dalhousie University, Halifax, NS B3H 4J1, Canada.

[1]Corresponding author (e-mail: christian.reiss@noaa.gov).
[2]Present address: Southwest Fisheries Science Center, National Oceanic and Atmospheric Administration, 8604 La Jolla Shores Drive, La Jolla, CA 92037, U.S.A.

 doi: 10.1139/F03-106 © 2003 NRC Canada

the ages and, therefore, sizes and developmental stages of fish larvae and zooplankton increase downstream of their entrainment sources (Davis 1984*a*; Townsend and Pettigrew 1996; McGillicuddy et al. 1998). On other banks (e.g., Western Bank on the central Scotian Shelf), concentrations of some species of copepods and fish larvae typically decrease from the bank to surrounding waters, suggesting that the bank is a source for both (McLaren and Avendaño 1995; Taggart et al. 1996). In such cases, there is little spatial structure in copepod developmental stages (McLaren and Avendaño 1995; McLaren et al. 1997), although there is for fish larvae (Jeffrey and Taggart 2000; Reiss et al. 2000).

Because of the relative spatial uniformity of copepod stage–frequency distributions, McLaren and Avendaño (1995) hypothesized that copepod developmental rates were similarly uniform and were probably temperature-dependent and not food-limited (Huntley and Boyd 1984; Huntley and Lopez 1992; Reiss et al. 1999). If so, spatial differences in zooplankton concentrations may be related to advective and mixing losses from Western Bank. A critical question then is how are the high zooplankton concentrations on the bank maintained against advective loss and mortality? Here we investigate this question by (*i*) calculating depth-specific advective loss rates for Western Bank based on a current-meter array deployed between August and October 1998; (*ii*) examining the horizontal and vertical distribution of copepod stages (nauplii through adults) on and around Western Bank in relation to physical features such as hydrographic fronts and water column stratification; and (*iii*) using published egg production rates to model population growth rates of two species of copepods (*Centropages typicus* and *Pseudocalanus* spp.). The latter is predominantly *Pseudocalanus newmani*, especially in late summer and autumn on both Browns Bank (McLaren et al. 1987) and Emerald Bank (McLaren et al. 1989), but with a small admixture of *Pseudocalanus moultoni*. As these species are difficult to distinguish in early stages, we use the genus name. The two copepod genera differ in important aspects of life histories that are relevant to this study.

Centropages typicus and *Pseudocalanus* have different seasonal peaks in reproduction and abundance on the Scotian Shelf and Western Bank. Several studies have shown that the abundance of *C. typicus* peaks between late summer and early autumn and precedes *Pseudocalanus*, which peaks between October and January (Tremblay and Roff 1983; McLaren et al. 1989; McLaren and Avendaño 1995). Additionally, *C. typicus* exhibits a typical bet-hedging spawning strategy by releasing many eggs (~15–50 per batch) into the water column throughout the spawning season, resulting in very high fecundities. In contrast, *Pseudocalanus* retains its eggs within eggs sacs attached to the metasome for a temperature-dependent period of some days before the eggs hatch. As a result, both its batch and lifetime fecundities are significantly lower than those of *C. typicus* (McLaren et al. 1989; Dagg 1978; Ohman et al. 2002).

These life history differences coupled with detailed physical oceanographic data led us to investigate whether the higher abundances of zooplankton on the bank are maintained because growth and production exceed advective loss and mortality, rather than by physical retention or concentration mechanisms.

Materials and methods

Plankton collections

Zooplankton and larval fish were collected during CCGS *Parizeau* cruise 98-058 from 29 September to 15 October 1998 on and around Western Bank, Scotian Shelf. Conductivity (*C*), temperature (*T*), and depth (*D*, from pressure) and fluorescence (Sea-Tech, Inc., Albuquerque, N.Mex.) were determined at biological sampling stations using a CTD instrument (model SBE-25; Sea-Bird Electronics, Inc., Bellevue, Wash.). Salinity (*S*) and density (ρ) were derived from these data using Sea-Bird supplied software.

First, a mesoscale survey (29 September to 5 October) assessed distributions of larval fish and zooplankton in relation to the circulation and hydrography. This survey consisted of 29 stations across the outer Scotian Shelf and over Western Bank (Fig. 1*a*, solid circles). Two oblique plankton tows were made at each of these stations using a bongo net (61 cm in diameter) equipped with 333-μm mesh. The first tow was made to the bottom of the pycnocline (surface samples; ~35 m depth), as determined from the CTD cast made at that station, the second tow was made to the sea bottom or to 200 m (oblique samples). Attached to each bongo cylinder was a 25-cm net with 64-μm mesh for collecting smaller zooplankton. A mechanical flowmeter (model 2030; General Oceanics, Inc., Miami, Fla.), placed in the mouth of each net, was used to estimate volumes of water filtered. The depth of each tow was estimated trigonometrically from wire angle and length and subsequently verified by an attached temperature–depth recorder (TDR; VEMCO, Inc., Shad Bay, N.S.). From each tow, the contents of the port 333-μm net were preserved in 5% buffered formaldehyde, and those of the starboard 333-μm net were preserved in ethanol for later examination of otoliths from larval fishes; estimated filtered volumes did not differ more than 8% between nets. For this study, we used only the abundance of larval silver hake (*Merluccius bilinearis*) and the wet-weight biomass of zooplankton from these large mesh nets. Preliminary analysis showed that the biomass concentrations (based on the large nets) of zooplankton in the surface layer (21.3 $g \cdot m^{-3} \pm 2.23$ standard deviation (SD)) averaged larger (Wilcoxon signed rank test, $p < 0.01$) than those obtained at the same stations by oblique hauls of the water column as a whole (14.7 $g \cdot m^{-3} \pm 1.78$ SD). From this, it can be inferred that concentrations averaged higher in waters above rather than below the pycnocline. Furthermore, high biomasses in off-bank oblique hauls consisted largely of deep-dwelling (>100 m), late-stage copepodids of *Calanus finmarchicus*, which did not occur in such concentrations over the bank at this time of year (see also McLaren et al. (2001)). Finally, because any exchanges off and onto the bank (which are a central concern of this study) must occur in upper waters (<100 m), we only focus here on samples from above the pycnocline, where relevant biomasses are most concentrated. The port and starboard contents from the 25-cm, 64-μm mesh nets were combined and preserved in 5% buffered formaldehyde and the volume was computed.

Second, to assess the potential importance of water column stratification to the retention and concentration of zooplankton, we examined the vertical distribution, abundance, and composition of zooplankton at stations on and off Western Bank (Fig. 1*a*, open diamonds). For these comparisons,

© 2003 NRC Canada

Fig. 1. Bathymetric chart of the Western Bank region indicating locations of the broadscale CTD/BONGO survey (solid circles), the locations of 64-μm mesh vertical net tows (open diamonds), the 36-h fixed sampling station (D), and the current-meter array (solid stars) used to estimate loss rates from the crest of the bank to the surrounding waters in the upper panel. The lower panel illustrates the initial starting distribution of particles on the crest (open triangles) and on the southern flank (open circles) on Western Bank used to calculate particle retention rates for the bank between August and October 1998. Isobaths are 50, 60, 80, 100, 200, 500, 1000, and 2000 m inclusive. EB, Emerald Bank; EBa, Emerald Basin; WB, Western Bank.

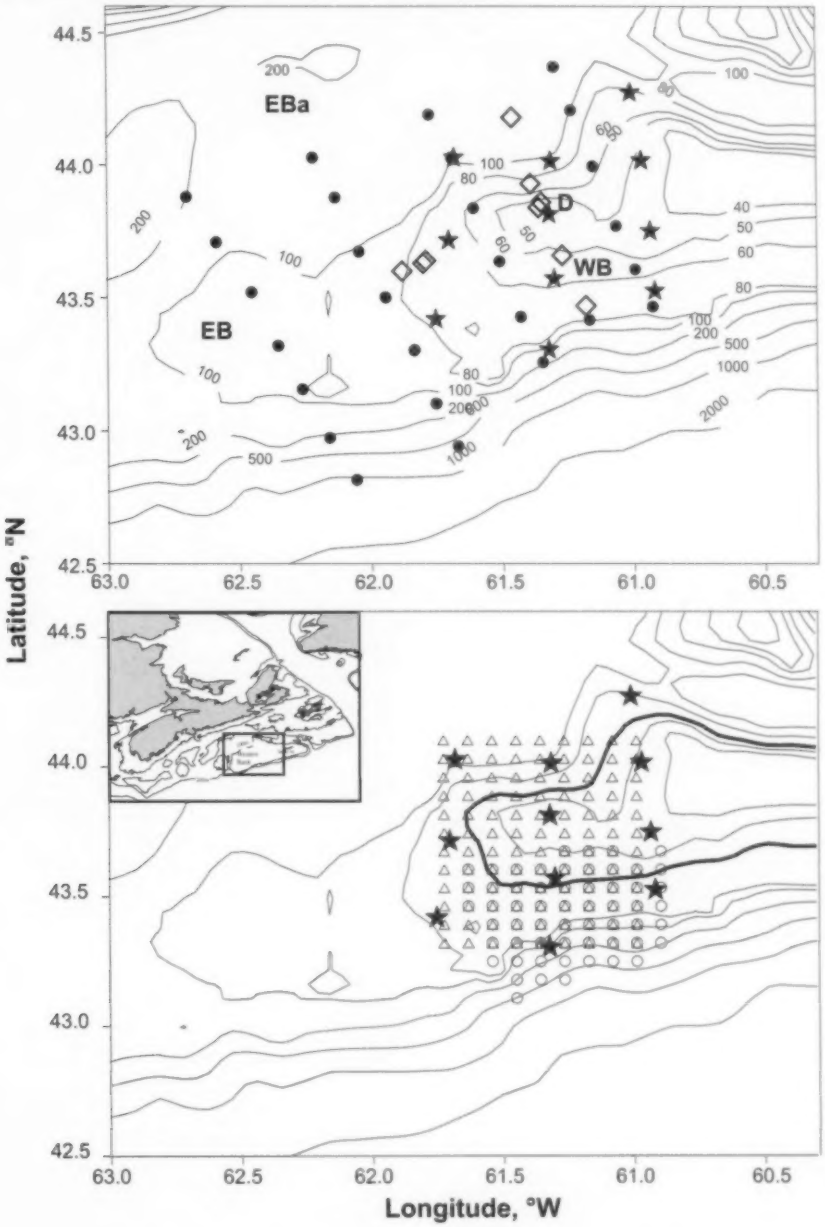

we define stations with bottom depths >75 m to be off the bank. A closing ring-net, 50 cm in diameter with 64-μm mesh and mechanical flowmeter (as above), was used to sample three to six depth strata at each station, including at least the mixed layer, a pycnocline layer (inferred from both the fluorescence maximum and the change in density with depth ($d\rho/dz$)), and the subpycnocline waters, on various dates throughout the cruise. The net was weighted and attached to a hydrowire for vertical sampling. It was retrieved at 1 $m \cdot s^{-1}$ and closed by a messenger at the upper limit of

© 2003 NRC Canada

Fig. 2. Hydrographic sections of temperature (°C; top panels), salinity (psu; middle panels), and density (σ_t; bottom panels) (*a*) across north to south and (*b*) along west to east Western Bank during October 1998. The hatched bar separates the northern and southern sections of the transect occupied on two different nights. Isotachs of temperature are shown in 2 °C increments, whereas those of salinity and density are shown in increments of 0.5 psu and σ_t, respectively.

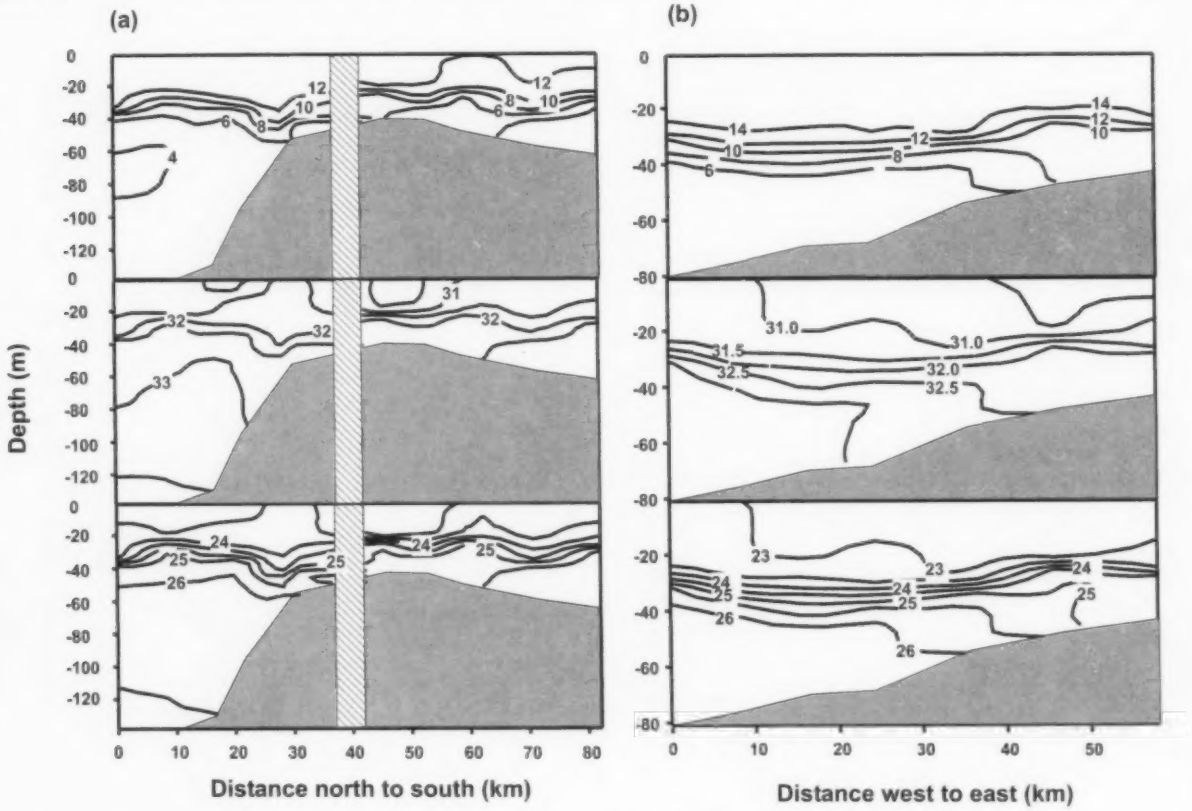

the stratum. It became evident that the flowmeter rotor revolved as the net was lowered. Therefore, theoretical volumes sampled were estimated from stratum depth and the area of the net; concentrations of zooplankton are expressed as number·L^{-1} of water filtered. Patterns of relative vertical concentrations of plankton did not exhibit any obvious differences using either the metered or theoretical volumes, although the concentrations of plankton were necessarily higher using the latter.

Third, to assess the potential importance of diel variation in vertical distribution in maintaining zooplankton concentrations over Western Bank, a series of vertically discrete plankton tows was made over a 36-h period (8–9 October) at a fixed station, 46 m deep, near the crest of Western Bank. At this station (Fig. 1*a*, "D"), samples were collected from five nominal depth strata (0–7, 7–14, 14–21, 21–28, 28–35 m) at approximately 3-h intervals using the closing 64-μm plankton net. Late-stage copepodids and adult copepods were combined and naupliar stages were combined for these analyses. Again, concentrations were estimated from net area and length of haul.

Two-way analysis of variance (ANOVA) was performed on $\log_e(x + 1)$-transformed abundance from both the on- and off-bank locations and the diel samples. In each case, vertical distribution, either stratum depth or depth zone (mixed layer, pycnocline, or bottom layer), was one factor and location (on or off bank) or time of day (day or night) were used as other factors. Fisher's least significance difference (LSD) procedure was used to assess multiple differences detected in ANOVAs. Interaction effects between depth and time of day were used to assess changes in vertical distribution with time of day.

Laboratory analyses

Wet weight (g·m^{-3}) of plankton samples (333-μm mesh) was determined gravimetrically after removal of larval fish and other large plankton (ctenophores, large euphausiids). The fine-mesh (64-μm) bongo samples were subsampled using a Folsom plankton splitter, and copepodid and adult copepods were identified to species and developmental stage (mainly from Lawson and Grice 1970; Diaz and Evans 1983; Frost 1989). The same process was used for the 64-μm, vertical net tows, except that nauplii and copepod eggs were also identified (McLaren 1965, 1966; Sazhina 1985) to lowest possible taxonomic category and enumerated. Other well-known planktonic taxa were identified to genus from a vari-

© 2003 NRC Canada

Fig. 3. Interpolated flowfields for three release dates of simulated particles showing the variability in the circulation around Western Bank during the current-meter deployment (2 August to 15 October 1998). Left and right columns represent currents at 12.5 m and 28 m, respectively. The 60-m isobath on Western Bank is represented by the polygon.

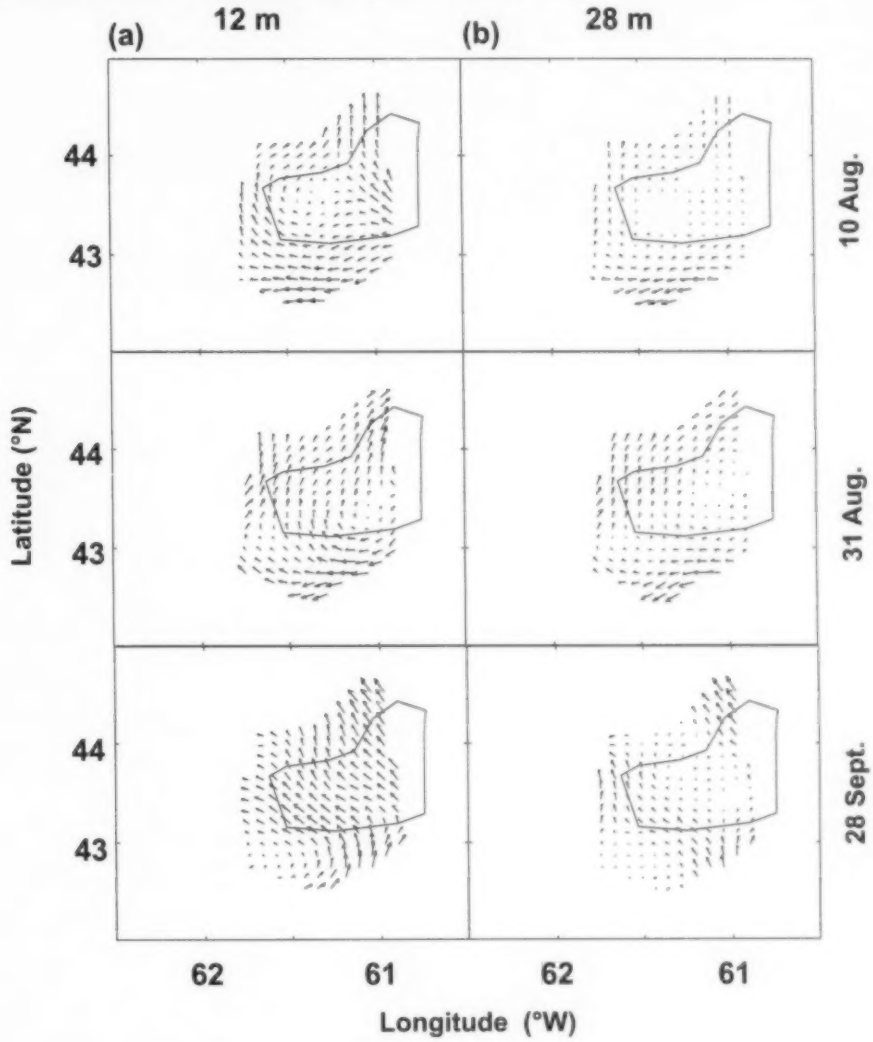

ety of sources. Throughout the study, we examine the overall patterns of distribution of copepod developmental stages but also focus on the naupliar and later stages (copepodids and adults) of *C. typicus* and *Pseudocalanus*.

Circulation and hydrography

The circulation around Western Bank was assessed using 25 current meters (RCM-7 and AANDERAA S4) arrayed on 11 moorings in a grid approximately 60 km × 60 km (Fig. 1). The meters were placed at ~12.5 m (the mixed layer), ~35 m, and ~50 m below the surface. Data collected between 2 August and 15 October were used to quantify the circulation around Western Bank before and during the cruise period (Hazen and Reiss 1999; Panteleev et al. 2000). The current-meter data were directly interpolated onto a three-dimensional grid (5 km × 5 km × 5 m) every 0.5 h using a variational interpolation algorithm (Panteleev et al. 2000). This provided a time-dependent flowfield for the calculation of retention rates at different depths on the bank. For this study, we chose two depths characterizing the upper mixed layer (12.5 m) and base of the mixed layer (28 m). Initial particle fields were centered at two locations: the crest (109 particles) and southern flank (97 particles) of Western Bank (Fig. 1*b*). Particles were released weekly beginning 2 August and concluding on 28 September (nine release dates). A polygon was defined by the 60-m isobath and was used to assess the percentage of particles remaining on Western Bank. Particle retention was calculated every 5 days for 20 days for each particle release date, with the exception of those from the last release date that were tracked for only 15 days, to the end of the data re-

© 2003 NRC Canada

Fig. 4. Particle retention trajectories for particles released within the 60-m isobath (*a*, *b*) near the crest of Western Bank and (*c*, *d*) on the southern flank near the shelf edge weekly beginning on 2 August and concluding on 28 September (nine releases) at 12- and 28-m depths.

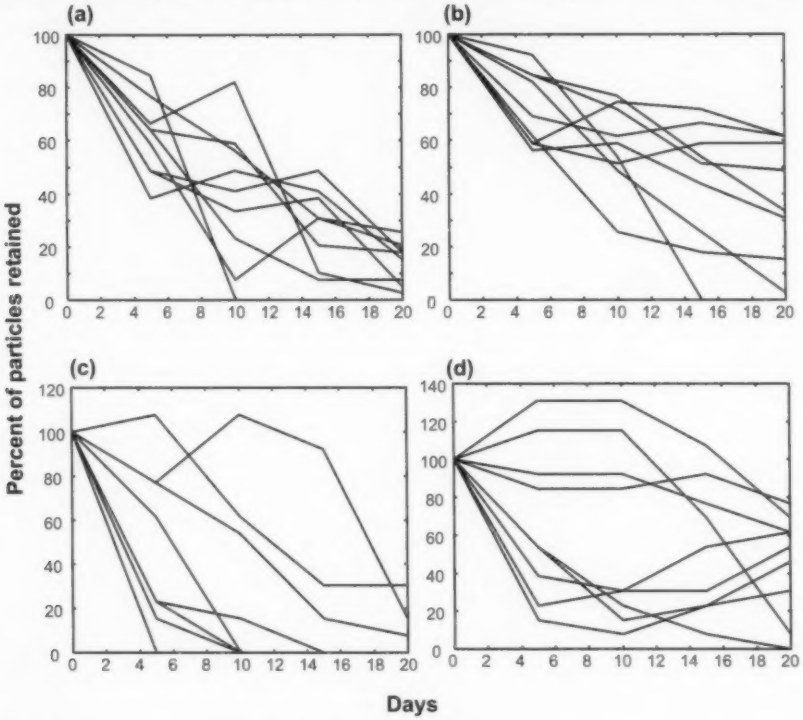

cords. At times, particle retention rates may exceed 100% simply because particles initialized very near the boundaries of the polygons may cross onto the bank before being advected around the bank. Such patterns may not necessarily indicate physical concentration.

The stability of the hydrographic structure (rather than its dynamics) on and around the bank was examined by constructing sections of T, S, and ρ for various time periods. In total, four hydrographic sections north to south and three hydrographic sections west to east across the bank were made over the 25-day study (Hazen and Reiss 1999). Only representative figures are included here.

Demography

The demographic model used here is close to that developed for *Pseudocalanus* and *Calanus pacificus* by Bollens (1988). The model is a modified stage-structured, projection-matrix model in which the inputs are stage duration and survival probability (loss rate and mortality) of nauplii and copepodids and egg production rates (number of female eggs·day^{-1}) and assumes a 1:1 sex ratio. To examine the importance of fecundity on the potential concentration of copepods on Western Bank, we use published egg production rates to model population growth rates of *Pseudocalanus* and *C. typicus*. Temperature-dependent stage durations of *C. typicus* are based on McLaren et al. (1989, their table 5) with an assumed water temperature of ~15 °C. The egg production rate of *C. typicus* was calculated from arguments in McLaren et al. (1989), in which egg production rates were either empirically derived or estimated as a percentage of female body weight, divided by the average egg weight. Temperature-dependent stage durations and egg production rates of *Pseudocalanus* were derived for females of known weight from Corkett and McLaren (1978) and McLaren (1965). The use of temperature-dependent rates for both development and egg production are a big assumption, and any reduction of these rates as a result of food shortages would have to be assumed arbitrarily. Although Huntley and Boyd (1984) concluded, based on literature review, that zooplankton in coastal waters are usually not food-limited, the subject remains controversial. Davis (1984*b*) also concluded that on Georges Bank, neither *Pseudocalanus* nor *Paracalanus parvus* was food-limited. On nearby Emerald Bank, McLaren et al. (1989) demonstrated that secondary production by smaller species of zooplankton (i.e., excluding *Metridia lucens* and *Calanus* spp.) was highest during the months of September through November. On Western Bank, the spatiotemporal patterns of nutrients and primary production (Dauchez et al. 1996), as well as lipid contents of copepods on and off the bank (Reiss et al. 1999; Reiss, unpublished data for October 1998), also support the conclusion that food was not limiting during September–October 1998. Taken together these observations support the use of temperature-dependent stage durations and egg production rates in this study. Mortality rates here are fixed at 6%·day^{-1}, associated with an unquantified but presumed invertebrate predation rate (after Ohman (1986) as in Bollens (1988)). Ohman et al. (2002) also showed that mortality rates were fairly constant across

© 2003 NRC Canada

Table 1. Ranked average concentration (number·L^{-1}) of zooplankton taxa collected during the broadscale survey conducted 29 September to 5 October 1998 over the outer Scotian Shelf and grouped according to location off (>75-m depth) and on (<75-m depth) Western Bank.

Off bank					On bank				
Taxon	Mean	Median	SD	CV	Taxon	Mean	Median	SD	CV
Oithona similis	11.7	8.96	8.42	0.71	*Oithona similis*	14.9	16.1	4.78	0.31
Placopecten sp.	10.0	0.35	2.85	2.84	*Centropages typicus*	7.1	7.7	4.46	0.62
Centropages typicis	3.5	0.23	3.21	0.91	*Microsetella norvegicus*	4.7	5.7	3.11	0.65
Paracalanus parvus	2.0	0.17	1.35	0.66	*Paracalanus parvus*	2.0	2.1	0.96	0.47
Microsetella norvegicus	1.5	0.11	1.32	0.89	*Pseudocalanus* spp.	1.5	1.5	0.65	0.43
Clausocalanus sp.	1.3	0.15	0.96	0.74	*Clausocalanus* sp.	1.0	0.9	0.29	0.29
Pseudocalanus spp.	1.0	0.64	0.91	0.92	*Microcalanus pusilis*	0.6	0.5	0.39	0.63
Microcalanus pusillis	0.6	0.33	0.70	1.22	*Placopecten* sp.	0.4	0.07	0.66	1.73
Limacina sp.	0.2	0.04	0.38	2.42	*Limacina* sp.	0.3	0.11	0.45	1.36
Unknown calanoid	0.01	0.04	0.15	1.81	Unknown calanoid	0.1	0.09	0.16	1.13
Calanus finmarchicus	0.06	0.04	0.10	1.55	Tintinids	0.1	0.06	0.15	1.14
Temora longicornis	0.02	0.0	0.04	1.89	*Temora longicornis*	0.1	0.07	0.16	1.28
Cladocera	0.01	0.0	0.04	2.49	*Calanus finmarchicus*	0.03	0.03	0.03	0.94
Tintinnid	0.01	0.0	0.02	2.17	Cladocera	0.02	0.0	0.05	2.23
Ctenophora	0.009	0.0	0.04	4.27	Unknown harpacticoid	0.01	0.0	0.03	2.82
Metridia lucens	0.009	0.0	0.02	2.57	*Metridia lucens*	0.01	0.0	0.01	2.13
Parathemisto sp.	0.007	0.003	0.01	1.65	*Thysanoessa* sp.	0.004	0.003	0.003	0.87
Oncaea sp.	0.006	0.0	0.01	2.26	*Sagitta* spp.	0.004	0.003	0.003	0.77
Sagitta spp.	0.004	0.001	0.01	2.93	*Parathemisto* sp.	0.001	2.0	0.001	0.67
Thysanoessa sp.	0.004	0.001	0.005	1.15	Salps	0.001	0.0	0.004	2.54
Tomopteris sp.	0.004	0.0	0.01	4.60	Ctenophora	0.0	0.2	0.0	1.10
Unknown harpacticoid	0.003	0.0	0.007	2.20	*Tomopteris* sp.	0.0	0.0	0.00	1.63
Salps	0.001	0.0	0.003	2.84	*Oncaea* sp.	0.0	0.0	0.00	

Note: Samples were collected with a 64-μm mesh net towed obliquely from the pycnocline. The median, standard deviation (SD), and coefficient of variation (CV) of the concentrations are also given.

developmental stages for *Pseudocalanus* and less so for *C. finmarchicus*. Moreover, McLaren et al. (2001) estimated mortality rates for *C. finmarchicus* on the Scotian shelf of ~6%·day^{-1} of overwintered animals (after reproduction) in March–May but only ~1%·day^{-1} among largely "resting" stages in June–February. Few other data from around Western Bank are available to estimate mortality rates of zooplankton.

The population projection model that we develop here can be used to extract standard population information such as the net population growth rate (Roughgarden 1997; Caswell 2000). Thus, we determined the finite rate of increase (λ) under several different conditions to investigate the importance of varying the loss and mortality rates for these two taxa with different reproductive strategies.

Results

Hydrographic structure and circulation

The water column over and around Western Bank was horizontally and vertically structured in *T*, *S*, and ρ (Fig. 2). Temperature varied from 15 °C in the surface mixed layer to <6 °C in bottom waters on the flanks of the bank. Salinity exhibited similar patterns to temperature across and along the bank. Vertical and horizontal variations in salinity ranged 3 psu, with weak salinity fronts at the surface and bottom on the southern and western flanks. Within the surface layer, a surface front was evident in both density and salinity over the 60-m isobath. Below the pycnocline, a subsurface front was also found near the 60-m isobath, where the 26.5-σ_t isopycnal and the 33-psu isohaline layers intersected the bottom. On the northern flank, only a weak bottom front was evident. On the west-to-east transect, fronts were evident in both salinity and density, intersecting the surface over the 75- to 80-m isobath and the bottom near the 60-m isobath. The pycnocline was coincident with both the thermocline and the halocline at ~30 m deep. Similar features were visible in the hydrographic sections of *T*, *S*, and ρ during different time periods of the cruise (Hazen and Reiss 1999). The final result is that the two frontal features (surface and bottom), along with the pycnocline, effectively separated water masses, both horizontally and vertically, especially on the southern and western flanks of the Western Bank.

The circulation around Western Bank varied over the course of the current-meter deployment (Fig. 3). On average, the circulation on and around Western Bank was predominantly anticyclonic, with a low-velocity area on the crest of the bank, and is consistent with other numerical (Hannah et al. 2001) and observational information (Panteleev et al. 2001). Along the southern flank, velocity of the westward current decreased onto the bank. Over the bank, there was a substantial decrease in the velocities between 12 m and 28 m under a variety of conditions. Events that moved water across the entire bank in a single direction (usually to the northwest)

© 2003 NRC Canada

Fig. 5. Spatial distribution of zooplankton in surface waters (to pycnocline) around Western Bank between 29 September and 5 October 1998: (*a*) biomass ($g \cdot m^{-3}$) retained by nets with 333-μm mesh; (*b*) concentrations ($number \cdot L^{-1}$) of early (C1–C2) and (*c*) late (C3–C5) copepodids; and (*d*) adult copepods retained by the small nets with 64-μm mesh.

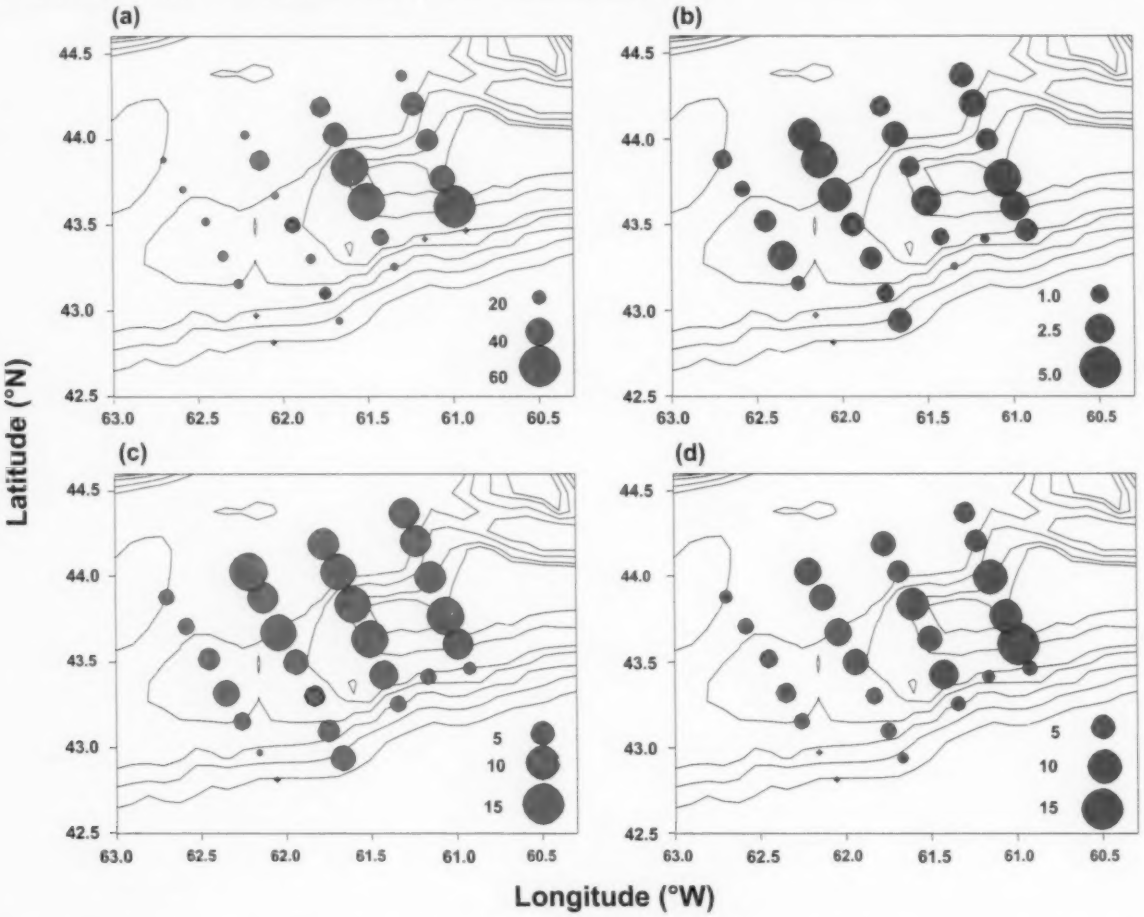

were observed during several time periods of the current-meter deployment. Rarely, if ever, were on-bank current flows observed at the northeasternmost current meter. Thus, a variety of advective conditions on Western Bank was captured during the current-meter deployment, including the sampling period of this field study.

Particle retention rates

Particle retention rates were calculated assuming exponential loss for 20 days with weekly starting intervals beginning 2 August and ending 28 September (Fig. 4). Particle retention on Western Bank was high and varied considerably with depth. For particles released on the crest of Western Bank, loss rates ranged from 6.5 to 14.1%·day^{-1} at 12.5 m and from 2.9 to 11.2%·day^{-1} at 28 m (Figs. 4*a*, 4*b*). Average particle retention, for particle releases centered on the bank, was between 18% at 12.5 m and 33% at 28 m after 20 days. Loss rates of particles released on the southern flank but within the 60-m isobath (9% of southern flank particles) varied from 14.4%·day^{-1} at 12.5 m to 4.8%·day^{-1} at 28 m. The average loss rate at 28 m is probably underestimated as some particles (about 5%) near the boundary of the 60-m isobath were advected onto the bank from the flank during certain iterations, and in fact, the exponential model is a bad fit to some of these loss trajectories. The advection of a few particles released on the flank, but very near the boundary of the polygon defining "on bank", resulted in retention rates exceeding 100%. In general, most particles released on Western Bank were lost off the northern flank, although some were advected off the western flank and were subsequently transported anticyclonically around the bank with the prevailing circulation. Particles released on the northern flank were mostly transported northeast out of the sampling area into northeastern Emerald Basin, whereas particles on the southern flank were lost to the shelf-slope current or were advected around Western Bank.

Zooplankton composition, distribution, and relative abundance

The zooplankton composition over and around Western Bank was dominated by common northwest Atlantic copepod species. Nine taxa of calanoid, two species of cyclopoid, and

© 2003 NRC Canada

Fig. 6. Frequency distributions of the developmental stages (C1 to C5, female and male adults) of *Centropages typicus* (circles) and *Pseudocalanus* (squares) on (solid symbols) and off (open symbols) Western Bank during October 1998.

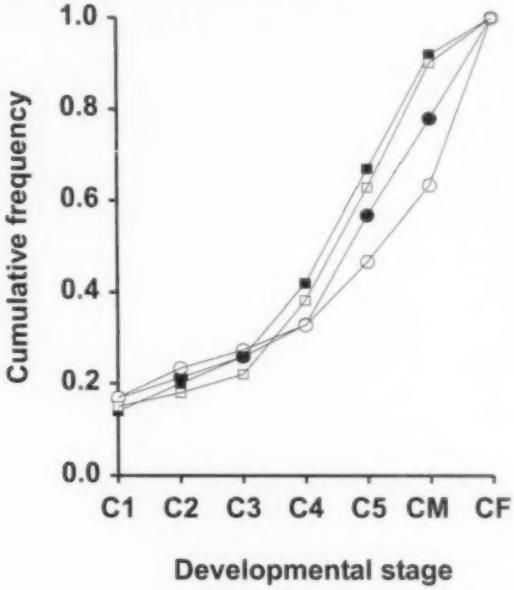

one species of harpacticoid copepod were enumerated from zooplankton samples from 64-μm mesh nets (Table 1). Numerically dominant species included *C. typicus*, *Pseudocalanus* spp. (both *moultoni* and *newmani*), *Oithona similis*, *Clausocalanus* sp., *Paracalanus parvus*, *Microcalanus pusillis*, and the harpacticoid *Microsetella norvegica*, all with average concentrations of at least 0.5 L^{-1} (Table 1). Most taxa averaged more abundant on (station depths <75 m) rather than off the bank, although there was significantly more variation among species off the bank (average coefficient of variation (CV) = 1.99) than on (average CV = 1.17) (Wilcoxon rank-sum test, $p < 0.01$).

Significant bank-scale variation in the distribution of zooplankton biomass and abundance of copepods was observed (Fig. 5). Zooplankton biomass (retained in a 333-μm mesh net) was on average higher (Mann–Whitney test, $p < 0.05$) on Western Bank (34.4 $g \cdot m^{-3}$) than off the bank (14.8 $g \cdot m^{-3}$). Total adult copepod concentration (all species combined) was also significantly higher (Mann–Whitney test, $p < 0.05$) on the bank ($\bar{x}$ = 7.5 L^{-1}) than off ($\bar{x}$ = 3.1 L^{-1}). This on-bank and off-bank difference was not significant for early- or late-stage copepodids (Mann–Whitney test, $p > 0.1$) because of high variability, although the mean abundances were higher on the bank than off for both groups. There were clear spatial differences between zooplankton biomass and copepod stage distributions. Three stations north of the crest had high concentrations of early- and late-stage copepodids (Figs. 5*b*, 5*c*) that were not expressed in the biomass estimates derived from 333-μm samples.

Zooplankton biomass and copepod concentrations (early- and late-stage copepodids and adults) were all positively correlated with larval fish abundance (Spearman r_s = 0.5 to 0.6, all $p < 0.001$). Eggs and larvae of fish (principally silver hake (*M. bilinearis*)) were more abundant on the bank than off (Mann–Whitney test, $p < 0.01$), indicating a broadscale overlap between larval fish and zooplankton abundance similar to that described by McLaren and Avendaño (1995) and McLaren et al. (1997).

The distribution of developmental stages may exhibit significant differences owing to restricted mixing between the bank and the surrounding flanks. Also, the frequency distributions of developmental stages should differ on and off the bank if mortality rates vary spatially, ontogenetically, and by species. They could also vary spatially from differences in timing of major reproductive periods. We tested both hypotheses for *C. typicus* and *Pseudocalanus* by comparing the stage–frequency distribution of each species on and off the bank (Fig. 6). Although they differed from one another, neither species exhibited significantly different cumulative stage–frequency distributions on vs. off the bank (Kolmogorov–Smirnov test, $p > 0.3$ for both). Thus, although absolute rates of mortality may vary spatially between species, there was little evidence for such variation in stage-specific mortality or timing of major reproduction within species. These patterns are found despite the fact that both ctenophores and *Sagitta* spp. are more abundant on the bank than off (Reiss, unpublished), whereas larger euphausiids are more common in the basins and along the shelf edge rather than on the bank (Cochran et al. 1994) and these predators should prey on different size classes of zooplankton.

Vertical distribution of copepods

The observed broadscale patterns in both copepods and larval fish, along with the vertical variation in the circulation on and around the bank, strongly suggest that the spatial patterns of zooplankton could be influenced by their vertical distribution. To examine this hypothesis, we assessed the vertical distributions of copepods at two spatial and temporal scales: on and off the bank over the study period and at a fixed station on the crest of the bank over a 36-h period. We pooled the estimated zooplankton concentrations from vertical net tows collected over the duration of the cruise into three depth zones (mixed layer, pycnocline, and bottom layer) and examined the patterns with ANOVA to compare broad spatial and temporal distributions.

A variety of mesoscale vertical distribution patterns of copepods was found on Western Bank (Fig. 7). Results of a two-way ANOVA of total naupliar abundance in relation to location and depth zone were marginally significant (Fig. 7*a*; two-way ANOVA, df = 1,2, $p = 0.06$). Multiple comparisons (Fisher's LSD, df = 80, $p < 0.05$) showed that nauplii were indeed more abundant on the bank than off, although there was no significant difference in their abundance among depth zones. Results of a two-way ANOVA on total copepod concentration on and off Western Bank and among depths zones revealed higher concentrations on Western Bank (Fig. 7*b*; two-way ANOVA, df = 1,2, $p = 0.04$) than off. On average, copepods were least abundant within the bottom layer, off the bank.

There were also species-specific patterns of abundance on and off the bank. *Centropages typicus* nauplii exhibited a complicated horizontal and vertical pattern in abundance on and off Western Bank (Fig. 7*c*; Table 2). These differences in abundance were consistent with both horizontal mixing

© 2003 NRC Canada

Fig. 7. Vertical distribution and abundance (number·L^{-1}) of (*a*) total nauplii, (*b*) total copepods, (*c*) nauplii and (*d*) copepodid and adult stages of *Centropages typicus*, (*e*) nauplii and (*f*) copepodid and adult stages of *Pseudocalanus* on (solid bars) and off (open bars) Western Bank among depth zones of the mixed layer (M), the pycnocline (P), and water below the pycnocline (L) collected between 29 September and 15 October 1998. Confidence limits are ±2 standard errors.

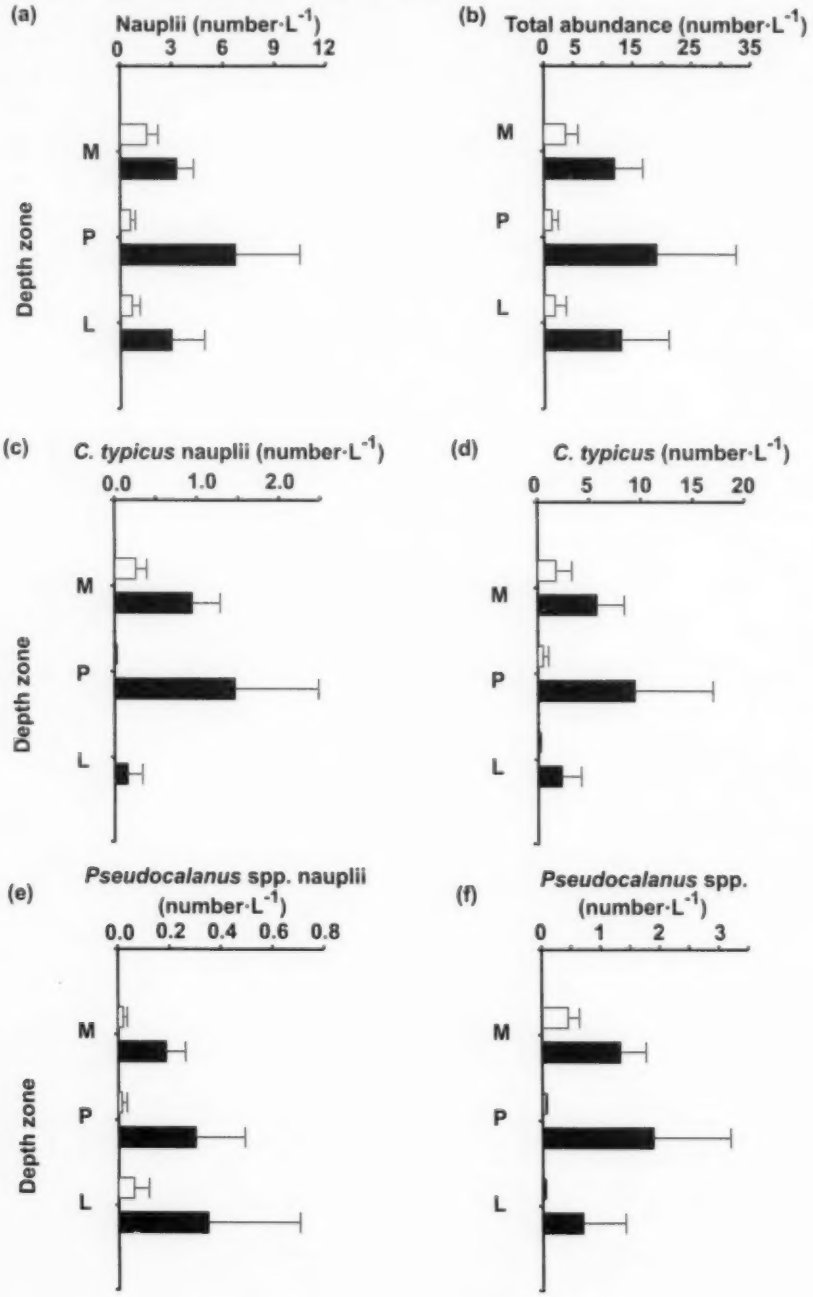

from the bank in surface waters and vertical segregation by water mass. ANOVA showed differing abundances between locations and among depth zones (df = 1,2, $p < 0.0001$), with a highly significant interaction between location and depth zone ($p < 0.002$). *Centropages typicus* nauplii were least abundant within subpycnocline waters both on and off the bank, but also within the pycnocline off the bank compared with on the bank. Advanced stages of *C. typicus* (C1

© 2003 NRC Canada

Table 2. Results of a two-way fixed factor analysis of variance (on or off bank) and depth zone (mixed layer, pycnocline, and subpycnocline) performed on $\log_e$-transformed abundances of naupliar stages of *Centropages typicus* and *Pseudocalanus* and later stages (C1 to adult) of *Pseudocalanus* over and around Western Bank between 28 September and 15 October 1998.

Source	df	Mean square	*F* ratio	*p* value
***C. typicus* nauplii**				
Location	1	87.6	18.49	<0.0001
Depth zone	2	80.16	16.92	<0.0001
Location × depth zone	3	32.5	6.86	<0.002
Error	80	4.7		
Total (adjusted)	85			
Total	86			
***Pseudocalanus* spp. nauplii**				
Location	1	77.9	19.67	<0.0001
Depth zone	2	5.18	1.31	0.276
Location × depth zone	2	5.68	1.43	0.244
Error	80	3.96		
Total (adjusted)	85			
Total	86			
***Pseudocalanus* spp.**				
Location	1	88.6	19.49	<0.0001
Depth zone	2	23.04	5.07	<0.01
Location × depth zone	2	16.54	3.64	<0.05
Error	80	4.54		
Total (adjusted)	85			
Total	86			

to adult) had a less complex distribution (Fig. 7*d*). Significant differences in abundance by location and depth zone (two-way ANOVA, df = 1,2, $p < 0.02$ for each factor) were not complicated by significant interaction among levels of the factors; *C. typicus* were more abundant on the bank and within surface or pycnocline waters than below the pycnocline, with the lowest concentrations found off the bank below the pycnocline.

Nauplii of *Pseudocalanus* were more abundant on Western Bank than off but exhibited no significant differences with depth (Fig. 7*e*; Table 2). In contrast to the fairly homogenous vertical distribution of nauplii on and off the bank, the horizontal and vertical distribution of patterns of later stages of *Pseudocalanus* were more complex (Fig. 7*f*). In general, later stages of *Pseudocalanus* were homogeneously distributed in the water column on the bank and were substantially less abundant within the pycnocline and subpycnocline waters off the bank. This pattern resulted in a significant location and depth-zone interaction (Table 2; two-way ANOVA, df = 2, $p < 0.05$).

We used a two-way ANOVA that explicitly accounts for both vertical distribution (surface to a depth of 31 m) and temporal (day–night) variation to assess the diel vertical distribution of both *C. typicus* and *Pseudocalanus* during a 36-h time series on the crest of Western Bank (Fig. 8). We specifically looked for an interaction between the depth and the time of day as an indication of a diel change in vertical distribution. Neither nauplii nor later stages of *C. typicus* or *Pseudocalanus* exhibited significant interactions between depth and time of day with date as a covariate (two-way ANCOVA, df = 4,1, $p > 0.5$ for nauplii and both species). Overall, late copepodids and adult stages of both *C. typicus* and *Pseudocalanus* increased in abundance with depth, and no maxima were observed (Figs. 8*b*, 8*d*). Naupliar stages of both species exhibited similar patterns to later stages, although *Pseudocalanus* tended to increase at depth, whereas *C. typicus* tended to decrease at depth (Figs. 8*a*, 8*c*).

Demography of dominant copepods

The 8 × 8 projection matrix of the population dynamics of *C. typicus* and *Pseudocalanus* incorporates eight developmental stages: egg production, nauplii, copepodids 1 to 5, and reproductively active adult females. All naupliar stages (N1 to N6) were combined into a single term with a developmental duration equal to the sum of the copepodid durations (~23 days) at 15 °C (McLaren et al. 1989). The main diagonal of the matrix, which is usually 0 in the standard Leslie matrix, is the survival probability (S_x) of the animals that have molted to that stage from the preceding stage (P_x). Advective loss (A_x) from the bank is proportional and so affects all stages equally. Under conditions where mortality $M_x = 0$, the survival probability is simply $1 - P_x$. Mortality and advective loss rates are incorporated into the survival probability along the main diagonal as $(1 - P_x + (-M_x) + (-A_x))$. Thus, stage-specific mortality rates can be incorporated into the basic projection matrix, and likewise, if stage-specific behaviors (vertical migration or ontogenetic vertical distributions) were resolved, A_x could vary among stages. As shown above (Fig. 6), we were unable to discern any significant differences in stage–frequency differences on and off the bank for each taxon. Thus, we used stage-specific probabilities of molting derived from temperature-dependent stage durations from McLaren et al. (1989) for *C. typicus* and located them along the first subdiagonal. We assumed that the reproductive life span of adults is 30 days; so an additional loss rate of 0.033 day^{-1} was added to the mortality term of the adult stages after Bollens (1988). Temperature-dependent egg production rates of *C. typicus* were taken as 5% of female dry weight per day from females averaging 19.6 µg dry weight during September 1980 with an individual egg weight of 0.03 µg (all per McLaren et al. 1989). This gives ~33 eggs·day^{-1} (one-half female for the models), which agrees with peak values of 25–35 eggs·day^{-1} at the same time of year in the southern North Sea (Halsband and Hirche 2001). For *Pseudocalanus*, egg production rates are much lower than *C. typicus* (Dagg 1978; McLaren et al. 1989). Given the similar lengths observed on Western bank during this study, we used the average mid-September weight of 7.4 µg for female *Pseudocalanus* on nearby Emerald Bank (McLaren et al. 1989) to estimate a late-summer egg production rate assuming a water temperature of 15 °C. The resulting egg production is ~5 eggs·day^{-1}. All models took as the starting population the average relative abundance of each stage estimated from the broadscale survey, although the starting vectors have little effect on the final outcomes. Five scenarios were examined. First, the model was run with an assumed survival probability of 100% (no mortality, no advective loss) giving a baseline from which to compare the effects of varying advective loss, mortality, and egg production rate. Second, the population model was run with an advective loss rate of 9%·day^{-1} (derived from the 12.5-m loss rates). Third,

© 2003 NRC Canada

Fig. 8. Vertical distribution and abundance (number·L^{-1}) of (*a*) nauplii and (*b*) copepodid and adult stages of *Centropages typicus* and (*c*) nauplii and (*d*) copepodid and adult stages of *Pseudocalanus* collected at a fixed 36-h sampling series near the crest of Western Bank collected during the day (open bars) and night (solid bars).

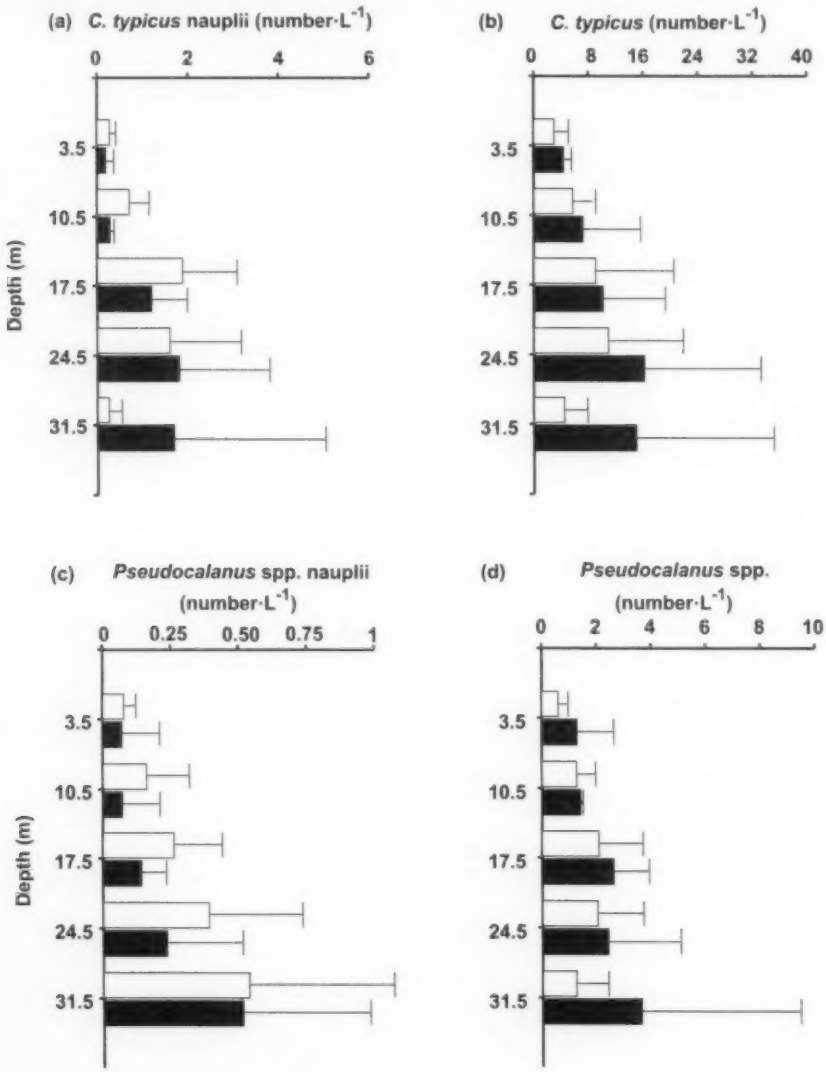

the population model was run with the loss rate (9%·day^{-1}) and a mortality rate of 6%·day^{-1}. This copepod mortality rate has been used by Ohman (1986) and is substantially higher than that for *C. finmarchicus* on the Scotian Shelf at the same time of year (McLaren et al. 2001). The fourth model run was performed with the 6% mortality and the loss rate associated with a 28-m depth (5.54%·day^{-1}). For each scenario, the projection matrix was evaluated after 60 days, and the eigenvalues and eigenvectors of the matrix were derived. The value of the largest eigenvalue determines the finite intrinsic rate (λ) of increase or decrease in population size, and the eigenvectors determine the relative proportions of each stage in the population (Caswell 2000). A population is growing exponentially when $\lambda > 1$, decreasing exponentially when $\lambda < 1$, and stationary when $\lambda = 1$ (Roughgarden 1997; Caswell 2000). Finally, we examined the effect of a 50% decrease in egg production and high retention for each genera.

In the absence of mortality or advective loss from the bank, the projection matrix indicates that the population of *C. typicus* and *Pseudocalanus* would grow at rates of 19% and 14%·day^{-1}, respectively (Table 3). Considerable deviations in the population growth rates of these two species are projected under the differing conditions of the model runs. Positive growth rates are projected for *C. typicus* under all conditions examined, whereas negative or very low population growth rates are projected for *Pseudocalanus* under many of the same conditions. For example, *C. typicus* under

© 2003 NRC Canada

Table 3. Demographic parameters used as input into a population projection model of (*a*) *Centropages typicus* and (*b*) *Pseudocalanus* life stages on Western Bank, Scotian Shelf, during September and October 1998.

	Mortality rate (%·day^{-1})	Loss rate (%·day^{-1})	Fecundity (female eggs·day^{-1})	Population growth rate (%·day^{-1})
(*a*) *Centropages typicus*				
Baseline	0	0	16	19
Low retention	0	9	16	9
Low retention + mortality	6	9	16	3
High retention + mortality	6	5.5	16	8
Low fecundity+ high retention + mortality	6	5.5	8	5
(*b*) *Pseudocalanus* spp.				
Baseline	0	0	5	14
Low retention	0	9	5	4.1
Low retention + mortality	6	9	5	–0.02
High retention + mortality	6	5.5	5	0.03
Low fecundity + high retention + mortality	6	5.5	2.5	0.005

conditions of high retention, 6%·day^{-1} mortality, and with both 100% and 50% of potential egg production rates is able to maintain higher growth rates than *Pseudocalanus* can maintain under conditions of low retention and no mortality. A slightly negative population growth rate is projected for *Pseudocalanus* under conditions of low retention rates plus mortality, suggesting that the vertical distributions of naupliar and copepodid stages could have significant impact on the potential population growth rates of this species compared with *C. typicus*.

Discussion

Retention rates on Western Bank are very high, still 18–33% after 20 days, depending on depth. This high retention rate has important implications for population growth rates of less fecund taxa such as *Pseudocalanus* and less influence for highly fecund taxa such as *C. typicus*. Our demographic model of these two dominant copepods suggests that zooplankton taxa with either reproductive strategy can persist and accumulate on Western Bank even with combined advective and mortality losses approaching 10%·day^{-1}. Simply stated, zooplankton concentrations are likely to increase under the conditions found on Western Bank during the summer and early autumn without the need of complicated behaviors interacting with hydrography (e.g., by using the vertical current shear) to maintain populations on the bank.

The interpolated flowfields, generated from an array of current meters, resolved the anticyclonic circulation on and around Western Bank as a recurring, but time-varying, feature that was influenced by bathymetry (Reiss et al. 2000; Panteleev et al. 2001). The strongest currents flowed southwest along the Scotian Shelf break with some transport northward between Emerald Bank and Western Bank. This bathymetrically steered flowfield created the relative null on Western Bank, ensuring a longer residence time of particles on the shoal. The spatial variation in current velocity was, in general, concurrent with hydrographic features, and this has important implications for the advective loss or gains of zooplankton from the flanks of the bank. For example, on the southern and western flanks of the Bank, surface and bottom fronts were present in the approximate location of the rapid change (shear) in the current. This inhibits loss of water off the bank from these flanks. On the northern flank, hydrographic features were weaker, and particles were more readily lost from the bank on this flank. Such a circulation pattern may explain the high concentrations of zooplankton off the northwest flank of Western Bank. Likewise, on-bank flow was rarely found from the northeastern flank of Western Bank, suggesting that high concentrations of zooplankton found there resulted from advection in the prevailing currents.

At many stations off Western Bank, very few smaller zooplankters (including *Pseudocalanus* and *C. typicus*) were found below the pycnocline, indicating that vertical water mass structure on the flanks of the bank, driven by the prevailing currents, partially structured the zooplankton community. Both observations and the particle-tracking simulations showed that some areas around Western Bank are not sources of zooplankton to the crest of the bank. For example, zooplankton concentrations decreased rapidly off the southern flank of the bank in both surface and near-bottom waters. Such rapid declines in biomass have been observed before (McLaren and Avendaño 1995; Reiss et al. 2000). Additionally, because particles released on the southern flank traveled mostly around rather than onto the bank, the flux of particles derived from the southern flank is minimal. This feature, combined with its low concentrations of copepods, limits the southern flank as a source of zooplankton for the crest.

The lack of day–night vertical differences in abundance of both copepod taxa suggests that motivations for diel vertical migrations were not strong on Western Bank. However, there were clear taxonomic and ontogenetic patterns of vertical distribution and evidence for elevated abundance of zooplankton within the pycnocline. These findings indicate that retention rates could be substantially higher than the average rates used in the population growth projections. For example, naupliar stages of *Pseudocalanus* were more abundant below the pycnocline on Western Bank and thus would likely exhibit higher retention rates than predicted. In contrast, *C. typicus* nauplii, copepodid, and adult stages were more abundant within the upper mixed layer where loss rates are higher. Yet, because of their high fecundity, the popula-

© 2003 NRC Canada

tion can still increase under most simulated conditions. For animals with lower fecundity, like *Pseudocalanus*, hatching eggs within or below the pycnocline would ensure higher retention rates. High concentrations of zooplankton at or just above pycnoclines are commonly observed in stratified water columns (Turner and Dagg 1983; Mullin et al. 1985; Incze et al. 1996). Although our results did not always show this pattern, the centers of mass of different taxa were near the base of the mixed layer, and this has important implications in the context of population growth and persistence on Western Bank. Zooplankton concentrated at depths greater than 12 m, for example, below or within the pycnocline will be subjected to significantly higher retention rates than animals concentrated above the pycnocline.

The matrix population projections provide a powerful technique to evaluate the relative importance of advective loss and the intrinsic rate of increase of zooplankton under different conditions. However, this model should not be construed as predictive, as it simply projects the population forward, assuming all other factors are held constant (Caswell 2000). For example, the population model always projected more nauplii than copepodids and more early than later copepodid stages. However, late-stage copepodids were considerably more abundant than early-stage copepodids and nauplii in the samples collected on and off Western Bank. There are several possible explanations for this result. Mortality rates between species must almost certainly vary, if only to balance differences in egg production. For example, Dagg (1978) showed that both *Pseudocalanus* and *C. typicus* exhibited approximately the same population sizes despite egg production rates that were orders of magnitude greater in *C. typicus* (Ohman et al. 2002). The differences in projected and observed abundances may result from a variety of other processes. For example, egg production rates in *C. typicus* vary with temperature and also with the number of clutches produced (Carlotti et al. 1997). Other low-frequency cycles may result from the production of relatively synchronous cohorts, commonly observed in zooplankton populations of temperate regions including the Scotian Shelf (e.g., McLaren et al. 1989, 2001), which would complicate comparisons between population projections and observed stage–frequency distributions. Overall, however, as shown earlier by Bollens (1988) and Davis (1984*a*), the method can assess possible scenarios. Monthly time series of abundance and distribution, coupled with knowledge of seasonal temperature cycles, could add realism to such models.

The general overlap between larval fish and zooplankton on Western Bank results from successful reproduction over the crest and subsequently advection off the bank over the period of 20 or so days. Similar patterns were found at other times (McLaren and Avendaño 1995; Taggart et al. 1996; Reiss et al. 2000). The observed differences in the size of some larval fishes around the bank are consistent with a single spawning location over the crest (Reiss et al. 2000). The lack of differences in the stage distributions of zooplankton around Western Bank is striking and may be explained by similar timings of major reproduction and temperature-dependent development and production rates of zooplankton everywhere on and around the bank. An interesting outcome of our observations and modeling study is that the abundance of zooplankton on the bank, and therefore the concentration of prey available for larval fish, could be dramatically reduced by both increased advective loss rates and lower water temperatures that increase stage durations, more so than by reduced egg production rates associated with the differing reproductive strategies (Kiorboe and Sabatini 1994).

Numerical simulations have shown that retention on banks can occur as a result of horizontal shear in the circulation, regardless of water mass properties (Cong et al. 1996). However, few studies have shown that zooplankton populations originate largely within recirculation systems. For example, work on Georges Bank (Davis 1984*a*; McGillicuddy et al. 1998) has shown that bank populations of both *Pseudocalanus* and *C. finmarchicus* are derived from non-local founding populations that are advected into and entrained within the bank-scale circulation. Our results and those of previous studies on Western Bank show a different pattern. We suggest that population sizes and stage distributions observed result from local production, rather than by transport of large numbers of copepods from off-bank or upstream areas onto the bank. We do not discount the possibility that other areas on or north of the bank may at times provide low concentrations of zooplankton to populate the bank; however, these innocula must successfully reproduce on the bank. It is also possible that local production from diapaused eggs may provide the initial population of some species early in the season. Such arguments have been proposed before (Marcus 1996). *Centropages typicus* nauplii have been hatched from sediments at least 1 year old (Lindley 1990), suggesting the possibility that local production is all that is necessary for the persistence of some zooplankton populations on Western Bank. Future studies should examine the possibility and importance of diapaused eggs in sediments to initial increases in populations of some copepod taxa to further elucidate population structuring mechanisms on Western Bank.

In conclusion, we have provided quantitative estimates of the retention rate for particles released at various depths on the crest of Western Bank. These estimates, coupled with a simple projection model of two taxa of copepods with differing life history strategies, indicate that population growth can be maintained in the face of mortality and advective loss. The data are consistent with the hypothesis that local production, exceeding loss, rather than physical concentration is the mechanism that maintains higher prey concentrations over Western Bank compared with surrounding waters.

Acknowledgements

We thank the Captain and crew of the CCGS *Parizeau* for their help and dedication to our research program. We also thank C.T. Taggart, B. deYoung, G. Panteleev, P. Groenkjaer, A. Bochdansky, J. Jeffrey, A. Pickle, and A. Vanderlaan, as well as W. Judge and D. Hazen, for all their help in the field. This work was sponsored by the Natural Sciences and Engineering Research Council of Canada by grants to the Canadian GLOBEC Western Bank Program through C. Taggart, I. McLaren, and B. deYoung. C. Reiss was a GLOBEC Canada Postdoctoral Fellow.

© 2003 NRC Canada

References

Bollens, S.M. 1988. A model of predatory impact of larval marine fish on the population dynamics of their zooplankton prey. J. Plankton Res. **10**: 887–906.

Brander, K., and Hurley, P.C.F. 1992. Distribution of early-stage Atlantic cod (*Gadus morhua*), haddock (*Melanogrammus aeglefinus*), and witch flounder (*Glyptocephalus cynoglossus*) eggs on the Scotia Shelf: a reappraisal of evidence on the coupling of cod spawning and plankton production. Can. J. Fish. Aquat. Sci. **49**: 238–251.

Carlotti, F., Rey, C., Javanshir, A., and Nival, S. 1997. Laboratory studies on egg and faecal pellet production of *Centropages typicus*: effect of age, effect of temperature, individual variability. J. Plankton Res. **19**: 1143–1165.

Caswell, H. 2000. Matrix population models. Sinauer Associates, Inc., Sunderland, Mass.

Cochrane, N.A., Sameoto, D.D., and Belliveau, D.J. 1994. Temporal variability of euphausiid concentrations in a Nova Scotia shelf basin using a bottom-mounted acoustic Doppler current profiler. Mar. Ecol. Prog. Ser. **107**: 55–66.

Cong, L., Sheng, J., and Thompson, K.T. 1996. A retrospective study of particle retention on the outer banks of the Scotian Shelf, 1956–1993. Can. Tech. Rep. Hydrogr. Ocean Sci. No. 170.

Corkett, C., and McLaren, I.A. 1978. The biology of *Pseudocalanus*. Adv. Mar. Biol. **15**: 1–231.

Dagg, M.J. 1978. Estimated, in situ rates of egg production for the copepod *Centropages typicus* (Krøyer) in the New York Bight. J. Exp. Mar. Biol. Ecol. **34**: 183–196.

Dauchez, S., Legendre, L., Fortier, L., and Levasseur, M. 1996. New production and production of large phytoplankton (>5 μm) on the Scotian Shelf (NW Atlantic). Mar. Ecol. Prog. Ser. **135**: 215–222.

Davis, C.S. 1984*a*. Interaction of a copepod population with the mean circulation on Georges Bank. J. Mar. Res. **42**: 573–590.

Davis, C.S. 1984*b*. Food concentrations on Georges bank: nonlimiting effect on development and survival of laboratory reared *Pseudocalanus* sp. and *Paracalanus parvus* (Copepoda: Calanoida). Mar. Biol. **82**: 41–46.

Diaz, W., and Evans, F. 1983. The reproduction and development of *Microsetella norvegica* (Boeck) (Copepod, Harpacticoida) in Northumberland coastal waters. Crustaceana, **45**: 113–130.

Frost, B.W. 1989. A taxonomy of the marine calanoid copepod genus *Pseudocalanus*. Can. J. Zool. **67**: 525–551.

Halsband, C., and Hirche, H.J. 2001. Reproductive cycles of dominant calanoid copepods in the North Sea. Mar. Ecol. Prog. Ser. **209**: 219–229.

Hannah, C.G., Shore, J.A., Loder, J.W., and Naimie, C.E. 2001. Seasonal circulation on the Western and Central Scotian Shelf. J. Phys. Oceanogr. **31**: 591–615.

Hazen, D.G., and Reiss C.S. 1999. Cruise summary: CCGS-PARIZEAU Cruise (98-058) to Western Bank, September 28 to October 22, 1998. GLOBEC-CANADA Western Bank Report 1997/7. Dalhousie University, Department of Oceanography, Halifax, N.S.

Huntley, M., and Boyd, C. 1984. Food limited growth of marine zooplankton. Am. Nat. **124**: 201–240.

Huntley, M., and Lopez, M.D.G. 1992. Temperature dependent production in marine copepods: a global synthesis. Am. Nat. **140**: 201–240.

Incze, L.S., Aas, P., and Ainaire, T. 1996. Distributions of copepod nauplii and turbulence on the southern flank of Georges Bank: implications for feeding by larval cod (*Gadus morhua*). Deep-Sea Res. II, **43**: 1855–1873.

Jeffrey, J.A., and Taggart, C.T. 2000. Growth variation and water mass associations of larval silver hake (*Merluccius bilinearis*) on the Scotian Shelf. Can. J. Fish. Aquat. Sci. **57**: 1728–1738.

Kiorboe, T., and Sabatini, M. 1994. Reproductive and life cycle strategies in egg carrying cyclopoid and free-spawning calanoid copepods. J. Plankton Res. **16**: 1353–1366.

Lasker, R. 1975. Field criteria for survival of anchovy larvae: the relation between inshore chlorophyll maximum layers and successful first feeding. Fish. Bull. **73**: 453–462.

Lasker, R. 1981. Factors contributing to variable recruitment of the northern anchovy (*Engraulis mordax*) in the California Current: contrasting years 1975–1978. Rapp. P.-V. Réun. Cons. Int. Explor. Mer, **178**: 375–388.

Lawson, T.J., and Grice, G.D. 1970. The development stages of *Centropages typicus* Krøyer (Copepoda, Calanoida). Crustaceana, **18**: 187–208.

Lindley, J.A. 1990. Distribution of overwintering calanoid copepod eggs in sea-bed sediments around southern Britain. Mar. Biol. **104**: 209–217.

Marcus, N. 1996. Ecological and evolutionary significance of resting eggs in marine copepods: past, present, and future studies. Hydrobiologia, **320**: 141–152.

McGillicuddy, D.J., Lynch, D.R., Moore, A.J., Gentleman, W.C., Davis, C.S., and Meise, C.J. 1998. An adjoint data assimilation approach to diagnosis of physical and biological controls on *Pseudocalanus* spp. in the Gulf of Maine – Georges Bank region. Fish. Oceanogr. **7**: 205–218.

McLaren, I.A. 1965. Some relationship between temperature and egg size, body size, development rate and fecundity of the copepod *Pseudocalanus*. Limnol. Oceanogr. **10**: 528–538.

McLaren, I.A. 1966. Predicting development rate of copepod eggs. Biol. Bull. **131**: 457–469.

McLaren, I.A., and Avendaño, P. 1995. Prey field and diet of larval cod on Western Bank, Scotian Shelf. Can. J. Fish. Aquat. Sci. **52**: 448–463.

McLaren, I.A., Labberge, E., Corkett, C.J., and Sevigny, J.M. 1987. Life cycles of four species of *Pseudocalanus* in Nova Scotia. Can. J. Zool. **67**: 552–558.

McLaren, I.A., Tremblay, M.J., Corkett, C.J., and Roff, J.C. 1989. Copepod production on the Scotian Shelf based on life-history analyses and laboratory rearings. Can. J. Fish. Aquat. Sci. **46**: 560–583.

McLaren, I.A., Avendaño, P., Taggart, C.T., and Lochmann, S.E. 1997. Feeding by larval cod in different water masses on Western Bank, Scotian Shelf. Fish. Oceanogr. **6**: 250–265.

McLaren, I.A., Head, E., and Sameoto, D. 2001. Life cycles and seasonal distributions of *Calanus finmarchicus* on the central Scotian Shelf. Can. J. Fish. Aquat. Sci. **58**: 659–670.

Mullin, M.M., Brooks, E.R., Reid, F.M.H., Napp, J., and Stewart, E.F. 1985. Vertical structure of nearshore plankton off southern California: a storm and a larval fish food web. Fish Bull. **83**: 151–170.

O'Boyle, R.N., Sinclair, M., Conover, R.J., Mann, K.H., and Kohler, A.C. 1984. Temporal and spatial distribution of ichthyoplanton communities of the Scotian Shelf in relation to biological, hydrological and physiographic features. Rapp. P.-V Reun. Cons. Int. Explor. Mer, **183**: 27–40.

Ohman, M.D. 1986. Predator-limited population growth of the copepod *Pseudocalanus* sp. J. Plankton Res. **8**: 673–713.

Ohman, M.D., Runge, J.A., Durbin, E.G., Field, D.B., and Niehoff, B. 2002. On birth and death in the sea. Hydrobiologia, **20**: 1–14.

© 2003 NRC Canada

Panteleev, G.G., Maximenko, N.A., deYoung, B., Reiss, C.S., and Yamagata, T. 2000. Anisotropic optimization of the current field with the variational method. Oceanology, **40**: 451–457.

Panteleev, G.G., deYoung, B., and Yaremchuk, M. 2001. The mean summer and fall circulation of Western Bank on the Scotian Shelf. Atmos. Ocean. **39**: 127–144

Reiss, C.S., McLaren, I., and Avendaño, P. 1999. Utility of storage lipid volumes in inferring recent trophic history of copepods. Can. J. Fish. Aquat. Sci. **56**: 2444–2449.

Reiss, C.S., Panteleev, G.G., Sheng, J., Taggart, C.T., and deYoung, B. 2000. Observations on larval fish transport and retention on the Scotian Shelf in relation to geostrophic circulation. Fish. Oceanogr. **9**: 195–213.

Roughgarden, J. 1997. Primer of ecological theory. Prentice-Hall, Upper Saddle River, N.J.

Sazhina, L.I. 1985. [Nauplii of widespread species of pelagic copepods of the world ocean.] Akad. Nauk. Yukrain. SSR, Inst. Biol. Southern Seas. [In Russian.]

Taggart, C.T., Thompson, K.R., Maillet, G.R., Lochmann, S.E., and Griffin, D.E. 1996. Abundance and distribution of larval cod (*Gadus morhua*) and zooplankton in a gyre-like water mass on the Scotian Shelf. *In* Proceedings of the International Workshop on Survival Strategies in Early Life Stages of Marine Resources. *Edited by* Y.Y. Watanabe and Y. Oozecki. A.A. Balkema Publishers, Rotterdam, Holland. pp. 155–173.

Townsend, D.A., and Pettigrew, N.G. 1996. Frontal currents and the transport of larval fish. Deep-Sea Res. **43**: 1773–1792.

Tremblay, M.J., and Roff, J.C. 1983. Production estimates for Scotian Shelf copepods based on mass specific P/B ratios. Can. J. Fish. Aquat. Sci. **40:** 749–753.

Turner, J.T., and Dagg, M. 1983. Vertical distributions of continental shelf zooplankton in stratified and isothermal waters. Biol. Oceanogr. **3**: 1–40.

© 2003 NRC Canada

Planktonic invaders of the St. Lawrence estuarine transition zone: environmental factors controlling the distribution of zebra mussel veligers

Christine Barnard, Jean-Jacques Frenette, and Warwick F. Vincent

Abstract: The St. Lawrence estuarine transition zone (ETZ) is a productive ecosystem supporting a larval fish nursery. Since 1994, *Dreissena polymorpha* veligers have become the dominant zooplankton (up to 260 individuals·L^{-1}). The environmental factors controlling their distribution across the ETZ and their potential impact on the plankton were determined. Their horizontal distribution was limited by salinity, with maximum decreases in concentration at 2‰. A sharp decline in prey availability at >2‰ may be a secondary stressor for the veligers, in addition to the direct effects of salinity. Their vertical distribution was homogeneous throughout the water column, even in the presence of a pycnocline. Redundancy analysis showed that veliger concentrations were positively correlated with temperature and turbidity and negatively correlated with salinity and total phosphorus. Veligers were also positively correlated with chlorophyll *a* and picophytoplankton concentrations, suggesting little effect on their phytoplankton prey. Moreover, the veligers were positively correlated with the sestonic ratio of particulate to total phosphorus, indicating their positive association with good food quality. The veligers appear to have no severe negative impacts on the ETZ plankton community and are restricted to favourable conditions for their survival in the upstream, low salinity region of the ETZ.

Résumé : La zone de transition estuarienne (ZTE) du fleuve Saint-Laurent est reconnue pour sa grande productivité, tel que démontré par son rôle de pouponnière de larves de poissons. Depuis 1994, les larves véligères de *Dreissena polymorpha* ont envahi le plancton de cette zone (jusqu'à 260 individus·L^{-1}). Cette étude documente les facteurs environnementaux contrôlant leur distribution dans la ZTE et leurs impacts sur la communauté phytoplanctonique. Leur distribution horizontale était limitée par la salinité avec une diminution abrupte de leur abondance à 2 ‰. Un déclin simultané de la bio-disponibilité de leurs proies à >2 ‰ fut observé, impliquant que cette chute de bio-disponibilité pourrait constituer un stress additionnel à l'effet de la salinité. Leur distribution était homogène dans toute la colonne d'eau, même lors de la présence d'un gradient vertical de densité. Une analyse de redondance révèle que les véligères sont positivement corrélées à la température et à la turbidité, mais négativement corrélées à la salinité et au phosphore total. Les véligères sont positivement corrélées à leurs proies, i.e., à la biomasse de chlorophylle *a* et au picophytoplancton, impliquant qu'elles ne semblent pas avoir d'impacts sévères sur leurs proies phytoplanctoniques. Les véligères étaient positivement corrélées au seston de bonne qualité alimentaire et semblaient être associées aux conditions favorables pour leur croissance qui caractérisent les eaux de faibles salinités de la ZTE.

Introduction

Zebra mussels, *Dreissena polymorpha*, have spread throughout North American aquatic ecosystems since their introduction to the Great Lakes in the late 1980s (Hebert et al. 1989). This exotic species is remarkably versatile and adept at exploiting new niches. In some areas, *D. polymorpha* can reach densities of 175 000 m^2 within 2 or 3 years of colonisation (Mellina and Rasmussen 1994). As unsurpassed competitors for habitat and food, they continually outcompete native bivalves (Ricciardi et al. 1998) and cause great physical disturbance. Their invasion is linked to a significant decrease in phytoplankton (Caraco et al. 1997), flagellated protozoa (Findlay et al. 1998), and zooplankton (Pace et al. 1998). Contamination of the food web by their bioaccumulation of chemicals has also been documented (de Kock and Bowmer 1993). A vast literature exists on the distribution, biology, and ecological impacts of adult zebra mussels (Strayer and Smith (1993) and references therein). However, the environmental factors controlling the successful development of the veliger larval stage and its potential impacts on the microbial food web are poorly documented (Sprung

Received 5 July 2002. Accepted 25 August 2003. Published on the NRC Research Press Web site at http://cjfas.nrc.ca on 3 November 2003.
J16978

C. Barnard and J.-J. Frenette.[1] Département de chimie-biologie, Université du Québec à Trois-Rivières, C.P. 500, Trois-Rivières, QC G9A 5H7, Canada.
W.F. Vincent. Département de biologie, Université Laval, Sainte-Foy, QC G1K 7P4, Canada.

[1]Corresponding author (e-mail: jean-jacques_frenette@uqtr.ca).

 doi: 10.1139/F03-103 © 2003 NRC Canada

1993), despite the fact that veligers can reach extremely high densities in the plankton of North American fresh waters (>400 individuals·L^{-1}; de Lafontaine et al. 1995).

Zebra mussels are well documented in North American rivers, and high proportions of veligers must be ultimately advected to the sea. However, little information is available on the physical factors limiting the horizontal and vertical distribution of veligers in estuaries. Although recognised as a freshwater species, the zebra mussel veligers are believed to tolerate salinities up to 4‰ for a short period of time, depending on water temperature and acclimation period (Strayer and Smith 1993; Kilgour et al. 1994; Wright et al. 1996). It remains unknown, however, how salinity may limit the downstream distribution of veligers in North American estuaries.

A few freshwater studies have found that veligers in lakes are situated within the upper few metres of the water column (Strayer and Smith 1993; Stoeckel et al. 1997). Fraleigh et al. (1993) found that their vertical distribution is controlled by water temperature, wind speed, and mixing rate. During the warmer month of July, the veligers were found at slightly lower temperatures in the deeper part of the epilimnion. Stratification was observed only when the wind speed was below 8 km·h^{-1}, and 64% of the individuals were found in the epilimnion between 4 and 6 m. In lakes, veligers are thus found slightly deeper in the water column when mixing rates are weak, probably owing to passive sedimentation (Garton and Haag 1993). Kern et al. (1994) observed that veligers are distributed evenly throughout the water column in the Rhine River, probably owing to higher mixing rates. *Dreissena* veligers have locomotive capacities, yet it is unknown if their vertical distribution is due to passive or active transport in estuaries where the water column may be stratified. A vertically stratified environment could prevent the veligers from crossing the density barrier (pycnocline) between the fresh and salt water, thereby resulting in a nonhomogeneous distribution.

Zebra mussel veligers are primarily herbivores with a preference for algae rich in polyunsaturated fatty acids (PUFA) (Vanderploeg et al. 1996), but they also consume photosynthetic picoplankton, bacteria, flagellates, and detritus (Sprung 1993; Wright et al. 1996). According to these authors, the size spectrum of their prey varies between 1 and 9 µm. In addition, Wright et al. (1996) observed that in laboratory experiments, the veligers also fed on the estuarine algae *Isochrysis galbana* and *Pavlova lutheri*. Veligers tend to have a significantly higher survival rate when they consume plankton containing long-chained PUFAs, in particular algae containing the long-chained (*n*-3) PUFA, docosahexaenoic acid (Wacker et al. 2002). Under favourable conditions, a veliger can increase roughly 10 times its weight during its 1- to 3-week planktonic period (Sprung 1993). The impact of adult zebra mussels on the plankton through their filter feeding is well documented; however, little is known about how feeding by the veliger stage of this organism may affect phytoplankton abundance.

The St. Lawrence estuarine transition zone (ETZ) is situated between Ile d'Orléans and Ile-aux-Coudres and contains high concentrations of microplankton and macroplankton that support a productive fish nursery (Vincent and Dodson 1999; Winkler et al. 2003). The recent arrival of *Dreissena polymorpha* in this region has raised concerns about their potential competition with herbivorous zooplankton that provide the food supply to the larval fish community. Zebra mussel veligers were absent from the ETZ plankton samples obtained during cruises in 1991 to 1993. However, in 1994, 1995, and 2000, this situation changed dramatically as they were among the dominant zooplankton, contributing to more than 80% of the total number of animals and achieving densities >200 individuals·L^{-1} (Vincent and Dodson 1999; G. Winkler, Université Laval, Département de biologie, Ste-Foy, QC G1K 7P4, unpublished data). The veligers are assumed to originate mainly from upstream and from the shores of the St. Lawrence, as adults are sparsely distributed on the fluvial bed of the ETZ (A. Casper, Département de biologie, Université Laval, Ste-Foy, QC G1K 7P4, unpublished data). Any impacts on the food web would therefore not be due to adult populations, but rather to the omnipresence of the veligers in the plankton. Hydrodynamic processes play a major role in controlling the distribution of organisms in this tidal estuary. For example, Frenette et al. (1995) documented the prolonged residence time for phytoplankton and protozoa in the ETZ and a combination of immigration and emigration pathways favouring larger particles and high taxon diversity. Hydrodynamic processes in combination with an abundant food supply from upstream similarly result in high populations of macrozooplankton in this region (Winkler et al. 2003). Zebra mussel veligers, in their most abundant stage, measure between 70 and 160 µm and also have the potential of being retained within the ETZ.

The overall aim of this study was to determine the role of several environmental variables in influencing the distribution of veligers in an estuarine transition zone. More specifically, the objectives were to determine the horizontal and vertical distribution of the veligers across the St. Lawrence ETZ and to assess the effects of salinity, depth, temperature, water column stratification, and temporal and tidal variation. In addition, we evaluated the potential impact of veligers on communities at the base of the food web by examining their relationship with total phytoplankton biomass (chlorophyll *a*), picophytoplankton cell concentrations, and the nutritional quality of the seston. The present study provides insights into the factors controlling the distribution and abundance of this invasive species in the upper estuary of a large river ecosystem.

Materials and methods

Sampling site

The ETZ of the St. Lawrence River is situated ca. 50 km downstream from Québec City (Canada) between the islands of Ile d'Orléans and Ile-aux-Coudres (Fig. 1). These waters are characterized by salinities ranging from 0.1‰ to 10‰. The freshwater discharge averages 10 000 $m^3 \cdot s^{-1}$ and current speeds may reach >2.5 m·s^{-1} (d'Anglejan and Smith 1973).

The bottom morphology of the ETZ consists of three channels, one following the north shore, one short channel in the middle, and one following the south shore. The north channel is used for maritime transport and is characterized by deeper waters and stronger currents. The middle channel consists of an archipelago of small islands with Ile d'Orléans and Ile-aux-Coudres being the largest islands and marking its eastern and western boundaries. Finally, the south channel has

© 2003 NRC Canada

Fig. 1. Estuarine transition zone (ETZ) of the St. Lawrence River, Québec, Canada. Summer 2000: stations are indicated by a letter representing the channel (N, north; S, south; M, middle) followed by numbers indicating the salinity (0, 0‰; 01, 0–1‰; 13, 1–3‰; 35, 3–5‰; 5+, 5+‰). Summer 2001: triangles (▲) mark the fixed stations.

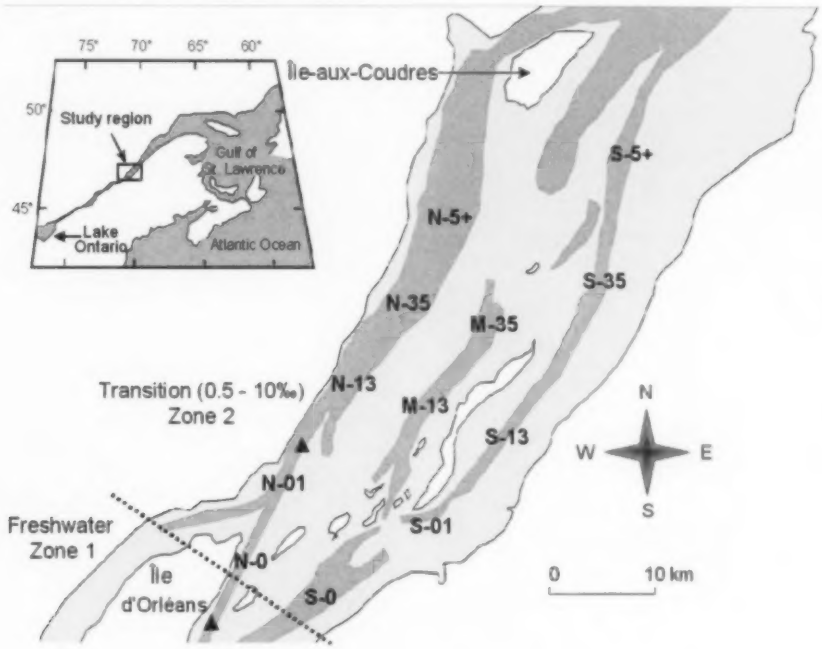

slower currents and shallower waters than the north channel. Large mudflats are found on the south shore near Montmagny, whereas vast intertidal marshes (3×10^6 m^2) are located on the shores of the north channel at Cap Tourmente (Lucotte and d'Anglejan 1986).

Sampling was conducted during the summers of 2000 and 2001. The research goals of the summer of 2000 were to determine the factors controlling the veligers' horizontal distribution across the ETZ and to assess the physical, chemical, and biological variables associated with veliger abundance. During the summer of 2001, the veligers' vertical distribution was assessed in the strictly freshwater zone of the ETZ (zone 1), as well as directly in the ETZ (zone 2) during different tidal regimes. Veliger abundance was evaluated as a function of depth and water column stratification.

Summer 2000 sampling

Five cruises were undertaken during the summer of 2000: 4 and 14 June, 15 and 28 July, and 8 August. During these cruises, 12 stations were sampled consisting of five in the north channel (N), two in the middle channel (M), and five in the south channel (S) (Fig. 1). Each station was chosen according to salinity, and therefore the geographical position of the station differed with every sampling period, depending on the tidal state. Five salinities were selected for the stations in the north and south channels: 0‰ (0), 0–1‰ (01), 1–3‰ (13), 3–5‰ (35), and finally 5‰ or more (5+). The salinity of the stations in the middle channel varied between 1–3 and 3–5‰. Because of unfavourable meteorological conditions, certain stations had to be eliminated during the first and last cruise, specifically S-13, N-0, N-01, N-13, and N-35 during the first cruise and M-13 and M-35 during the last cruise.

Physical variables

The site of each station was chosen according to surface salinity, which was determined with a salinometer (Yellow Springs Instrument Co., Yellow Springs, OH 45387). Water column salinity and temperature as a function of depth were recorded using a CTD (conductivity–temperature–depth meter; sea logger SBE-19; Sea Bird Electronics, Inc., Bellevue, WA 98005), which was lowered from the surface to 2 m from the bottom. At each station, water was collected at the surface (0–2 m) and near the bottom (2 m from the bottom) with a 5-L Go-Flo bottle (General Oceanics Inc, Miami, FL 33169). These water samples were stored cool and in the dark. Upon arrival at the laboratory, turbidity for each sample was recorded using a nephelometer (model DRT15-CE; HF Scientific, Inc., Fort Myers, FL 33916).

Veligers

To collect *D. polymorpha* veligers, a bottom-to-surface haul was made using a plankton net (63-μm mesh with a 50-cm diameter), and an additional haul was made from 2 m to the surface. The contents were filtered through a 63-μm screen to eliminate smaller particles and were then preserved in denatured ethanol (95%) at a final concentration of approximately 80%. Because of clogging of the net with sediments and subsequent loss of material during the haul, the veliger densities from the full water column hauls were equal to or lower than the veliger densities from surface hauls; hence, only surface data were used in the statistical analyses for

© 2003 NRC Canada

this year. To improve the method for the summer 2001 sampling, Go-Flo bottles were used to collect veligers.

Veliger counts were conducted in the laboratory using cross-polarisation according to Johnson (1995). This method renders the veligers visible and easily distinguishable from other zooplankton and detritus. The volume of the counts had to correspond to a minimum of 10% of the total sample volume. If 300 individuals were counted before reaching this 10%, another subsample was counted to use the average of the two counts.

Chlorophyll a

Upon arrival at the laboratory, the water collected with the Go-Flo bottles was passed through GF/F (Whatman plc, Kent, U.K.) 25-mm filters in duplicate. These filters were then frozen (–20 °C) and kept in the dark until extraction. They were subsequently ground in 90% acetone and extracted over 24 h. The extracts were then cleared by centrifugation and assayed by spectrofluorometry (Varian Cary-Eclipse; Varian, Inc., Palo Alto, CA 94304-1030) before and after acidification (0.001 mol·m^{-3} HCl). Chlorophyll *a* (Chl *a*) from *Anacystis nidulans* (Sigma-Aldrich Corp., St. Louis, MO 63103) was used for calibration.

Photosynthetic picoplankton

In a darkened room, immediately upon arrival in the laboratory, approximately 15–20 mL of water sample were filtered onto Anodisc (Whatman) filters, which were mounted on slides using Aquapolymount (Polysciences, Inc., Warrington, PA 18976). These slides were immediately stored in the dark at 4 °C for 24 h and then stored frozen (–20 °C). Within days of the slide preparation, counting was undertaken with an Olympus epi-fluorescence microscope (Olympus America Inc., Melville, NY 11747) with exchangeable blue and green excitation filters and 1000× oil immersion. When excited with a green light source, photosynthetic picoplankton with phycocyanin and (or) Chl *a* fluoresce bright red (PC), whereas phycoerythrin-rich photosynthetic picoplankton (PE) fluoresces bright orange (Lovejoy et al. 1993). Three hundred individuals were counted with a minimum of 15 fields. A minimum of 50 fields was counted when counts were low.

Protist communities

Samples for protists (phytoplankton and protozoa) were examined and prepared using the procedures outlined by Lovejoy et al. (1993). These samples were fixed immediately with 1% gluteraldehyde and 0.1% paraformaldehyde (final concentrations), stored in the dark at 4 °C, and later settled in Utermöhl chambers. The auto- and fluorochrome (DAPI) fluorescence allowed us to differentiate organisms from abiotic particles and to locate and characterize cells. The organisms were grouped into two broad categories: autotrophs (including mixotrophs) and heterotrophs.

Chemical variables

Particulate organic carbon (POC), nitrogen (PON), and phosphorus (PP) were obtained by filtering 20–100 mL (depending on turbidity) of water through precombusted and acid-washed GF/F filters. These were then stored frozen in the dark (–20 °C). For the dissolved components (NO_3^-, total nitrogen (TN), and soluble reactive phosphorus (SRP)), the water was filtered through precombusted GF/F filters and stored cool in the dark until analysis. For total phosphorus (TP), unfiltered water was immediately acidified (1 mL 30% H_2SO_4 per 100 mL sample) upon arrival at the laboratory. All analyses were conducted at the National Laboratory for Environmental Testing (NLET) in Burlington, Ontario, according to the standard methods (NLET 1994).

Summer 2001 sampling

Two cruises were undertaken to assess the short-term dynamics of veliger vertical abundance at fixed stations during different tidal states. Both cruises occurred during the spring tides of June and July 2001. One fixed station was located in the strictly freshwater zone (46°52′86″N, 70°55′60″W) and the other directly in the transition zone (47°06′71″N, 70°42′44″W) (Fig. 1). Each site was sampled at three high, three low, and four intermediate tides, thus a total of six high, six low, and eight intermediate tides for each station for both cruises.

The veligers were collected with two 5-L Go-Flo bottles. These bottles collected water at the surface (0–2 m), in the middle of the column (depending on the column depth), and near the bottom (1–2 m from the bottom). The water was then filtered through a 63-μm sieve and preserved and counted as described above.

Data analysis

Spatial autocorrelation was tested in the summer 2000 veliger data by constructing a correlogram obtained using Moran's *I* (Legendre and Fortin 1989). This correlogram was globally significant at the $\alpha = 5\%$ level because several individual values were significant at the Bonferroni corrected level (unpublished data) (Legendre and Fortin 1989). To account for the spatial structure in the data, spatial components were incorporated into the statistical analyses (Legendre 1993). For the summer 2001 data, the statistical model constructed took into account spatial and temporal autocorrelation (see below).

Water column stratification

A measure of water column stratification (Δs) was calculated as the difference between salinity at the surface and at the bottom of the water column for the stations in zone 2 (summer 2001). If veliger larvae are passively transported, the vertical stratification of their distribution (abundance at the bottom – abundance at the surface = Δ_{vel}) should be correlated with Δs. Because these values (Δ_{vel} and Δs) did not have normal distributions, Spearman's nonparametric test was used to evaluate the correlation.

Spatial and temporal distribution of the veligers

Temporal variation in veliger abundance between the four cruises undertaken in summer 2000 data was tested using a repeated measure ANOVA (analysis of variance, mixed-effect model) with SAS (version 8.2; SAS Institute Inc., Cary, NC 27513-2414). The date was a fixed effect and the station was a random effect. Temporal dependency was adjusted with heterogeneous compound symmetry based on the Akaike information criteria. Multivariate normality was verified using the Mardia Skewness and Kurtosis statistic. Multiple com-

© 2003 NRC Canada

parisons were made using the protected least significant difference (LSD) method.

For the vertical distribution assessed during the summer of 2001, a split–split plot ANOVA (mixed-effects model) was used to fit the veliger abundance data. The effects of zone (1 and 2), depth (surface, mid-column, and bottom), and tidal cycle (high, low, and intermediate) on veliger abundance were verified. In the main plot, the date (cruise) was a random effect and zone was a fixed effect. The effect of depth was in the subplot, whereas the effect of the tidal states was in the sub-subplot. This model took into account the possible correlations between observations in the same zone.

Relationships between environmental, spatial, and biological variables (RDA)

Redundancy analysis (RDA; CANOCO program 4.0, ter Braak 1998) was used to determine whether variation in species abundance was coordinated in response to environmental and spatial gradients. The variation in species abundance was partitioned into independent components: pure environmental, pure spatial, spatial component of environmental variation, and unexplained (Borcard et al. 1992). This method was used to partial out the intrinsic spatial component of community structure and to establish the relative contribution of environmental factors in controlling the species distribution.

To choose between a linear and nonlinear model, a detrended canonical correspondence analysis (DCCA) was employed, and RDA was chosen over canonical correspondence analysis (CCA) because the range of the ordination sample scores in a detrended correspondence analysis (with detrending by segments and nonlinear rescaling) was less than 1.5 standard deviation units (ter Braak 1998). This indicated that the application of a linear method was appropriate. This multivariate technique for direct gradient analysis graphically summarises the relationships between the species and the abiotic environmental and spatial variables.

Data from summer 2000 sampling were used whereby the species variables consisted of veliger and picophytoplankton (PE and PC categories) numerical densities and Chl *a* biomass. The environmental variables were salinity, temperature, turbidity, TP, Cl^-, SO_4^{2-}, SRP, NO_3^-, TN, and date (cruises 3, 4, and 5) to test for temporal variation in species abundance. Logarithmic and square root transformations were used to normalise the distribution of the data. To account for differences in units, the species data were centred and standardised (ter Braak 1998). The spatial component was a matrix of two-dimensional geographic coordinates including all of the terms of a cubic trend surface polynomial, as suggested by Legendre (1990, cited from Borcard et al. 1992). This surface regression was of the form $Z = b_1X + b_2Y + b_3XY + b_4X^2 + b_5Y^2 + b_6X^2Y + b_7XY^2 + b_8X^3 + b_9Y^3$, where X was the longitude and Y was the latitude in universal transverse mercator co-ordinates. This matrix represented the geographic surface over which the species were sampled, and the model tested its relative influence on the variation in species abundance.

Forward selection of environmental variables and polynomial terms was applied to select the set of variables that significantly explained the variation in abundance of the species ($p < 0.05$). To account for collinearity, environmental variables with variance inflation factors greater than 15 were eliminated. Once the significant environmental and spatial variables were identified, four analyses were conducted to partition the variance in the species data following Borcard et al. (1992): (1) RDA of the species matrix constrained by the environmental variables; (2) RDA of the species matrix constrained by the spatial variables; (3) like analysis 1 after removing the effect of the spatial variables; and (4) like analysis 2 after removing the effect of the environmental variables. In RDAs calculated using CANOCO, the sum of all canonical eigenvalues can be interpreted as the fraction of explained variation (r^2). Monte Carlo permutation tests (999 unrestricted permutations) were used to assess the statistical significance of the relationship between the species and independent variables. The total explained variation (r^2) was the sum of the explained variation in analyses 1 and 4 or in analyses 2 and 3. The "pure" environmental variation was defined by analysis 3, and the "pure" spatial variation was defined by analysis 4. The variation "shared" by the spatial and the environmental components was calculated by subtracting analysis 3 from analysis 1 or analysis 2 from analysis 4. The unexplained portion of the variation was obtained by subtracting the total variation explained from one.

Results

Horizontal and temporal distribution

Concentrations of veliger larvae dropped precipitously across the freshwater–saltwater gradient of the ETZ, and there was a negative exponential relationship with salinity (Fig. 2). For summers 2000 and 2001, the maximum decrease in veliger abundance occurred at approximately 2‰, which may correspond to a physiological threshold. For summer 2000, the highest densities were obtained during the second and fourth cruises, with densities reaching up to 260 individuals·L^{-1} at stations in the north channel and salinities between 0 and 1‰. For summer 2001, the highest densities were observed in the freshwater zone (240 individuals·L^{-1}). The greatest relative decrease in mean abundance occurred between salinity intervals 0–2 and 2–4‰, with decreases from 75.9 to 18.0 and from 75.2 to 13.2 individuals·L^{-1} for summers 2000 and 2001, respectively. The sampling undertaken during summer 2001 (spring tides of June and July) showed a sharp decline in veliger abundance with an increase in salinity from the freshwater zone 1 to the transition zone 2 (Fig. 3). Densities were lowest during high and ebbing tides. The strong influence of salinity on veliger abundance, rather than geographical position, was evident when sampling was conducted from the fixed stations.

The presence of veligers in early summer appears to be determined by the water temperature, as spawning occurs around 18 °C (Sprung 1993). During the first cruise (4 June 2000), their abundance was sparse, consistent with the low water temperatures between 12.5 and 15 °C. For the second cruise (26 June 2000) onwards, water temperatures were >18 °C and the veligers were abundant at low salinities (<2‰). Date had a significant effect on the variation in veliger concentrations (df = 3,31, $F = 5.58$, $p = 0.0035$). Veliger densities from cruise 2 were significantly higher than those

© 2003 NRC Canada

Fig. 2. Veliger larvae densities in the St. Lawrence estuarine transition zone (ETZ) as a function of salinity for (*a*) summer 2000 cruises (●, 14 June; ○, 15 July; ■, 28 July; □, 8 August) and (*b*) summer 2001 fixed stations in zones 1 and 2 (●, 25–29 June; ○, 23–27 July). The statistics are for an exponential fit (solid line) to the data.

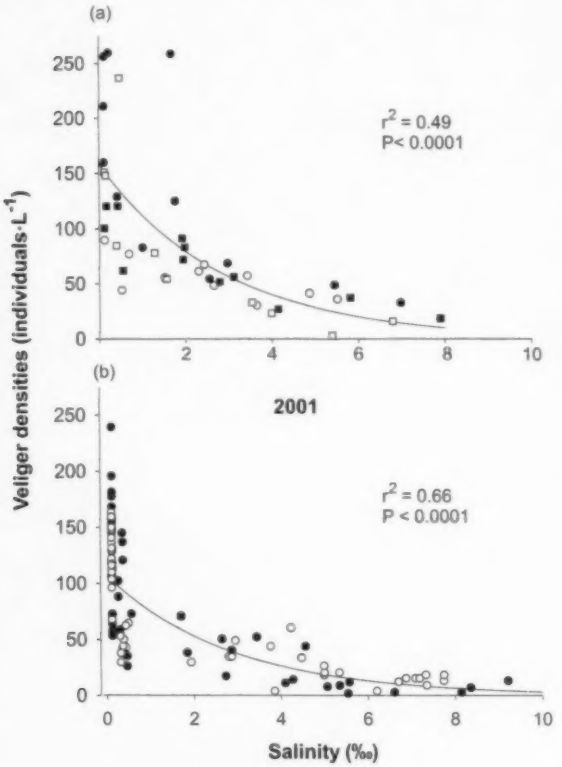

from cruises 3, 4, and 5. Densities from cruises 3, 4, and 5 were not significantly different. This was also evident in the RDA results with the near absence of correlation between veligers and cruises 3 and 5 (Fig. 4).

Vertical distribution (summer 2001)

Veligers in zones 1 and 2 were homogeneously distributed throughout the water column. No vertical stratification in distribution was observed (Table 1; Fig. 3), even in stratified water columns. However, the zone and tidal state affected veliger abundance. There was a sharp decline in veliger densities when going from zone 1 to zone 2, and tidal state played a significant role in influencing veliger densities in the transition zone only. Consistent with these results, there was no statistical relationship between Δ_{vel} and Δs when all transition zone stations were considered (Spearman's rho = 0.02, $p > 0.05$, $n = 19$) or when only stratified stations were considered (Spearman's rho = –0.02, $p > 0.05$, $n = 9$). These results underscore the homogeneous distribution of the veligers in the water column, regardless of stratification and mixing conditions.

Relationships between environmental, spatial, and biological variables (RDA)

Six of the nine environmental variables were selected using forward selection ($p < 0.05$): temperature, salinity, turbidity, TP, cruise 3, and cruise 5. After environmental variable selection, the Monte Carlo tests of significance for the first canonical axis of analysis 1 yielded an eigenvalue of 0.399 (F ratio = 17.926, $p = 0.001$) and of 0.630 for all canonical axes (Table 2). The first two axes explained 53.9% (39.9 + 14.0) of the total variance in the species data. The fraction of the species–environment variation that was jointly explained by the first two axes was high (0.855), thus little information on species–environment relationships was lost by discarding the additional axes. Because the eigenvalue of the third axis was small compared with the first two ($\lambda_1 = 0.399$, $\lambda_2 = 0.140$, $\lambda_3 = 0.074$), it can be ignored, as can the higher numbered ordination axes. Veliger densities, Chl *a* biomass, and PC picoplankton were positively cross-correlated, with temperature and turbidity strongly related to them (Fig. 4). For interpretations of the biplot diagram, arrows pointing in the same direction indicate positively correlated variables, perpendicular arrows indicate lack of correlation and arrows pointing in opposite directions indicate negatively correlated variables. The angles between environmental and species arrows and the length of the arrows can be used jointly to infer the direction and intensity of species responses to environmental variables (ter Braak 1998). However, RDAs only reveal the shared variation among species variables explained by the environmental variables. Thus the relationship between veliger abundance and the species variables was verified separately from this analysis and revealed that veligers were indeed positively correlated with Chl *a* (Pearson $r = 0.48$, $p = 0.004$) and PC picoplankton (Pearson $r = 0.45$, $p = 0.008$). Salinity and TP were negatively related to the veliger densities and Chl *a* biomass, but positively correlated to PE picoplankton. Turbidity and temperature were negatively correlated with salinity and TP.

Among the nine terms in the surface polynomial, the following ones were retained in the forwards selection: $Z = b_1X + b_2Y + b_3XY + b_4X^2 + b_5Y^2 + b_6X^2Y + b_7XY^2$. After variable selection, the Monte Carlo tests of significance for analysis 2 for all canonical axes yielded an eigenvalue of 0.239, which was not significant (Table 2). Variation partitioning indicated that the total variation explained by environmental and spatial variables together accounted for 74.4% of the total variation, whereas 25.6% was left unexplained. The environmental variables accounted for 63% of the total variation explained in the species matrix. Approximately 23% of this variation can also be predicted by the spatial matrix. Only 15% of the variation is attributable to spatial effects and cannot be related to the measured environmental variables (Table 2). This portion of variation acts partly as a descriptor of unmeasured underlying processes such as external causes or underlying biotic processes such as growth, reproduction, predation, input from various source populations, and stress-dependent mortality. The purely spatial effect was weak or insignificant. This statistical result is to be expected given that water masses are advected up and down the estuary by as much as several tens of kilometres over each semidiurnal tidal cycle, and rapid changes take place at any fixed *x*–*y* lo-

© 2003 NRC Canada

Fig. 3. Veliger larvae densities as a function of tidal state and salinity in the estuarine transition zone (ETZ) for (*a*) cruise 1 (25–29 June 2001) and (*b*) cruise 2 (23–27 July 2001). For the transition zone, tidal cycles were further divided into flood and ebb tides, as veliger densities varied significantly between the two tidal regimes. Values are the means ± standard deviation (when available). Solid bars, surface densities; open bars, mid-column densities; shaded bars, bottom densities; ▼, salinity.

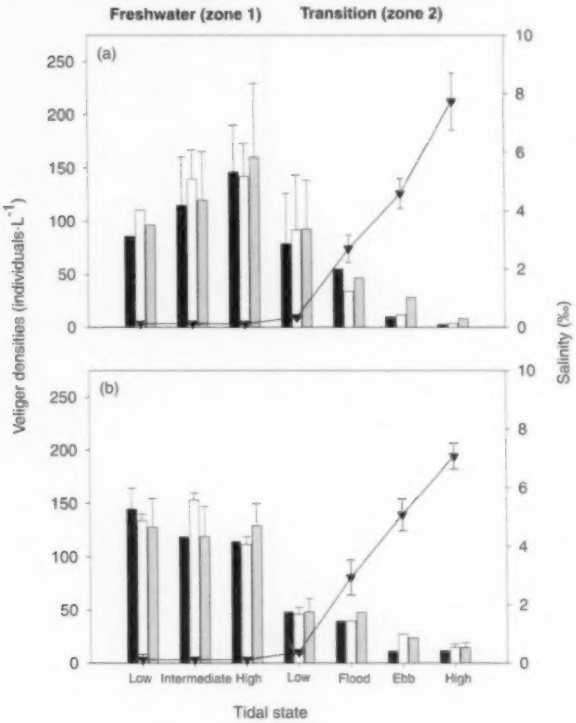

cus. Biological and chemical properties are therefore more closely related to the shifting salinity field rather than geographic position. As for the environmental variable component, 66% of the total variation is accounted for by the purely environmental effects, indicative of the selected variables being effective descriptors of the species data in the ETZ. This underscores the influence of the position of the salinity front in the transition zone and its subsequent effects on community composition.

Food quality

According to the approximate limits set by Healey and Hendzel (1980) and Hecky et al. (1993), the stoichiometric ratios obtained of the ETZ seston showed no apparent nutrient deficiencies (Fig. 5). The values for C:P, N:P and C:N (μmol:μmol) were consistently below the thresholds for limitation, with the exception of the C:N ratio, where N seemed moderately deficient. The C:Chl *a* ratios were exceptionally high, which may indicate general nutrient deficiency or high concentrations of heterotrophic organisms as well as detritus. Turbidity was highly positively correlated with particulate C, N, and P (Fig. 6). The C:N:P ratios (Table 3) lay well below the Redfield ratio of 106:16:1, which reveals the absence of nutrient limitation in the ETZ seston. In addition, SRP and nitrate were always at detectable levels (means = 0.011 ± 0.004 mg·L^{-1} and 0.28 ± 0.076 mg·L^{-1}, respectively), implying adequate nutrient supply for the phytoplankton. Finally, veliger densities were weakly but positively correlated with the PP/TP ratio (r^2 = 0.18, p = 0.0001, n = 46) as well as with PP (r^2 = 0.14, $p < 0.05$, n = 46), indicative of their association with good quality seston.

Particle aggregation

Particle size appears to be one aspect that affects the food availability for zebra mussel veligers (Sprung 1993; S. Bernier, Département de biologie, Université Laval, Ste-Foy, QC G1K 7P4, unpublished data). We therefore examined the extent of cell aggregation across the ETZ given the known flocculation characteristics of salinity gradients (Kranck 1979). We found a strong decrease in the bioavailability of the veligers' prey (Fig. 7). This effect was greatest for the autotrophs with a 2.9-fold increase of organisms within aggregates >10 μm from salinity interval 1–2‰ to 2–3‰. At this latter interval, up to 80% of the potential autotrophic prey were within aggregates and thus too large to be consumed by veligers.

Discussion

Spatial distribution of the veligers

The pattern of change in the veliger distribution across the ETZ showed several characteristics consistent with the joint effects of abiotic and biotic controlling factors. The changes in veliger density during the summer 2000 cruises can be explained by (1) salinity, (2) stress due to advective transport, (3) retention and turbidity, (4) bioavailability of the veligers' prey, and (5) predation.

Salinity

The longitudinal distribution of zebra mussel veligers in the St. Lawrence ETZ was a strong function of salinity and tidal state. The highest densities were found at salinities below 2‰, but individuals were found up to 10‰. The maximum decrease in veliger abundance occurred around 2‰, which corresponds to a lower tolerance threshold than that reported in the literature. These results are consistent with the recent findings of S. Bernier (Département de biologie, Université Laval, Ste-Foy, QC G1K 7P4, unpublished data), who noted a sharp decrease in filtration rates of veligers at salinities greater or equal to 2‰. Past studies have indicated that their lethal incipient tolerance to salinity is at ~4.5‰, and maximum growth rates have been observed up to 2‰ (Strayer and Smith 1993; Kilgour et al. 1994; Wright et al. 1996). Their tolerance to salinities between 4‰ and 5‰ is for a short period of time, depending on the water temperature and acclimation period. Veliger abundance was positively correlated to temperature, but this is likely to reflect the close negative correlation between temperature and salinity. Temperature is not likely to have had a strong negative impact on the veligers as it never dropped below 11.5 °C in the ETZ and veligers can tolerate temperatures between 0 and 29 °C (Sprung (1993) and references cited

© 2003 NRC Canada

Fig. 4. (*a*) Redundancy analysis biplot of the species matrix constrained by the environmental variables. Percent variance in species data for each axis is specified in parentheses. Species are indicated by solid arrows. Significance of axis 1 is $P = 0.001$, significance of overall test is $P = 0.001$. Environmental variables are indicated by dotted arrows (TP, total phosphorus; PC, photosynthetic picoplankton (phycocyanin-rich and (or) Chl *a*); PE, photosynthetic picoplankton (phycoerythrin-rich). (*b*) Chl *a* biomass and picoplankton (PC and PE) densities are stacked as a function of the station for each cruise. Note that picoplankton densities were available solely for cruises 3, 4, and 5. Cruises: cross-hatched bars, 14 June (cruise 2); solid bars, 15 July (cruise 3); open bars, 28 July (cruise 4); shaded bars, 8 August 2000 (cruise 5).

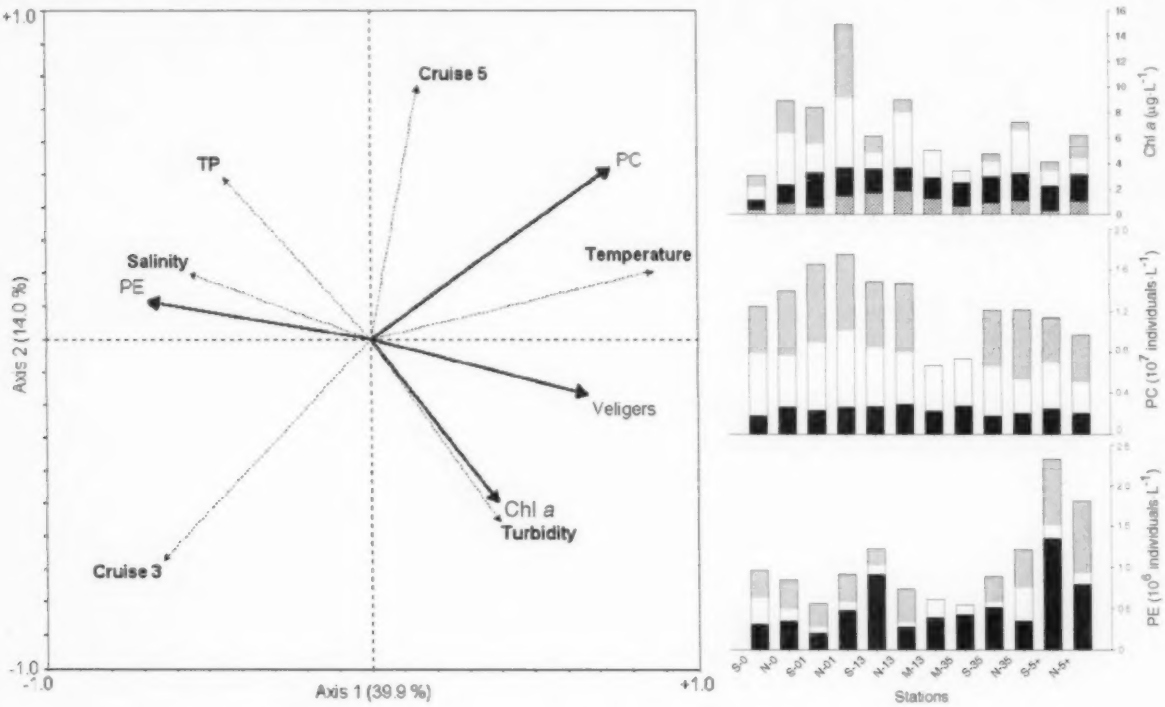

Table 1. The results from a split–split plot analysis of variance for the effects of depth (surface, mid-column, bottom), tidal state (high, intermediate, low), and zone (freshwater and transition) on veliger abundance for summer 2001 sampling from the two fixed stations in the St. Lawrence estuarine transition zone.

Source of variance	df	MS	*F* value	*P*
(*a*) Main plot				
Cruise	1	620.71	0.72	0.5524
Zone	1	224 609.99	259.88	**0.0394**
Error 1	1	864.27		
(*b*) Subplot				
Depth	2	321.40	5.87	0.0645
Zone × depth	2	202.14	3.69	0.1234
Error 2	4	54.72		
(*c*) Sub-subplot				
Tide	2	3 924.25	4.07	**0.0204**
Zone × tide	2	10 271.29	10.64	**<0.0001**
Depth × tide	4	309.96	0.32	0.8631
Zone × depth × tide	4	547.31	0.57	0.6871
Error 3	90	965.00		
Total	113			

Note: $n = 114$; results in bold are significant; df, degrees of freedom; MS, mean square; error 1 = cruise × zone; error 2 = (cruise × depth) + (cruise × zone × depth); error 3 = (cruise × tide) + (cruise × zone × tide) + (cruise × depth × tide) + (cruise × zone × depth × tide) + tidal replicates (cruise × zone × tide × depth).

© 2003 NRC Canada

Table 2. The results of variation partitioning in redundancy analysis.

	r^2	P
Analysis 1	0.630	**0.001**
Analysis 2	0.239	0.057
Analysis 3	0.488	**0.001**
Analysis 4	0.114	0.233
Total explained	0.744	
Pure environmental	0.488	
Pure spatial	0.114	
Shared	0.142	
Unexplained	0.256	

Note: The relative and shared contribution of the environmental and spatial components to the variation in the species data are indicated.

therein). At salinities exceeding 4‰, this freshwater species' physiological state deteriorates quickly and growth is inhibited (Sprung 1993). Zebra mussel veligers are extremely sensitive to sudden changes in salinity, but their tolerance to such changes increases significantly if these changes are gradual (Strayer and Smith 1993; Kilgour et al. 1994). In the ETZ, the prevailing high mixing rates may not allow for an appropriate acclimation period. The veligers may thus be exposed to abrupt changes in salinity associated with this mixing and the different tidal regimes, which may explain the sharp decrease in abundance at 2‰.

Stress due to advective transport

Horvath and Lamberti (1999) found that veligers were highly susceptible to damage by physical forces (i.e., shear and turbulence) and that mortality in high current streams (>1.0 $m \cdot s^{-1}$) could limit veliger survival during downstream transport. Veliger densities from summer 2001 cruises showed a significant decline from zone 1 to zone 2, even during low tide (salinity <0.5‰). This may imply that mortality due to advective transport could have come into play. As for the effect of turbulence on the veligers, those collected in the highly mixed waters of the ETZ were active, i.e., swimming and gut filled, at salinities varying between 1‰ and 3‰ (C. Barnard, unpublished data). The physiological state of the veligers was not thoroughly examined, yet their presence or absence appears to be representative of their abundance as the abundance dropped significantly from one fixed station to the other over a fairly short distance and few empty shells were observed. The decline from zone 1 to zone 2 could be indicative of the negative impact of hydrodynamic forcing, salinity, or other factors discussed below.

Retention and turbidity

Retention by hydrodynamic trapping can explain the high densities observed at stations N-0 and N-01. Frenette et al. (1995) documented a prolonged residence time for cells (2–200 µm) in the ETZ and pathways that favour retention of larger particles (>20 µm). Veligers could then be subjected to this hydrodynamic trapping, a consequence of opposing currents in stratified estuaries that position the organisms to be moved upstream on flooding tides and retained during ebbing tides (Frenette et al. 1995). This recirculation mechanism would tend to lower downstream advective losses in this stratified estuary.

Fig. 5. Particulate nutrient stoichiometry and the C:Chl *a* ratio of the seston in the St. Lawrence estuarine transition zone (ETZ) during summer 2000. Samples were taken from the surface (0–2 m). Indication of nutrient deficiency according to Healey and Hendzel (1980) and Hecky et al. (1993): P, P deficiency; N, N deficiency; G, general nutrient deficiency; single symbol indicates moderate deficiency; double symbols indicate severe deficiency. Stations are indicated by a letter representing the channel (N, north; S, south; M, middle) followed by numbers indicating the salinity (0, 0‰; 01, 0–1‰; 13, 1–3‰; 35, 3–5‰; 5+, 5+‰).

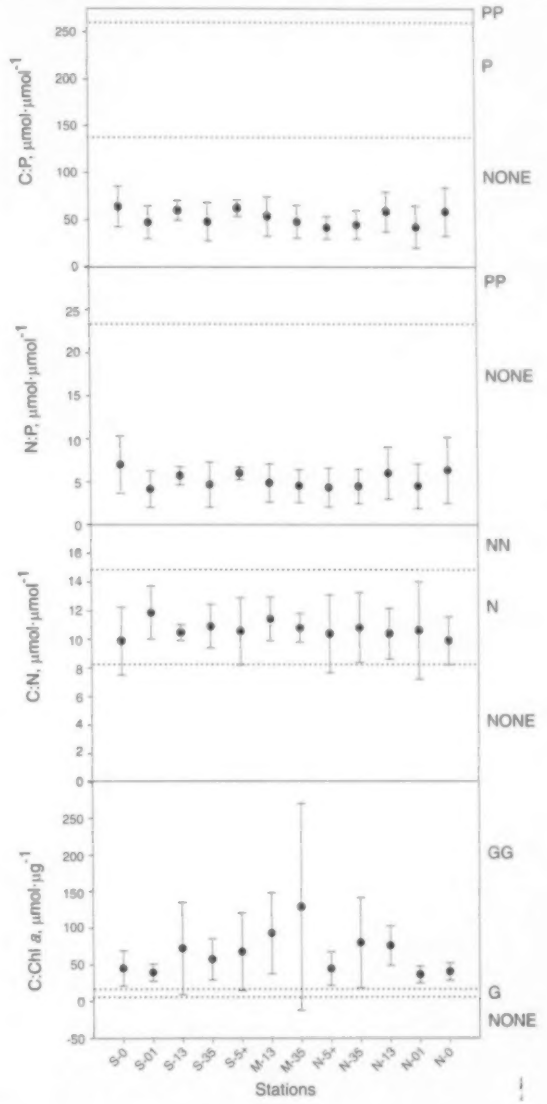

The veligers were positively correlated with turbidity, implying that turbidity can be used as an approximate guide to their distribution in the ETZ. The turbidity maximum present in this part of the estuary is the result of the recirculation

© 2003 NRC Canada

Fig. 6. Relationship between the log of (*a*) particulate organic carbon (POC), (*b*) nitrogen (PON), and (*c*) phosphorus (PP) as a function of turbidity (nephelometric turbidity units (NTU)) in the St. Lawrence estuarine transition zone (ETZ).

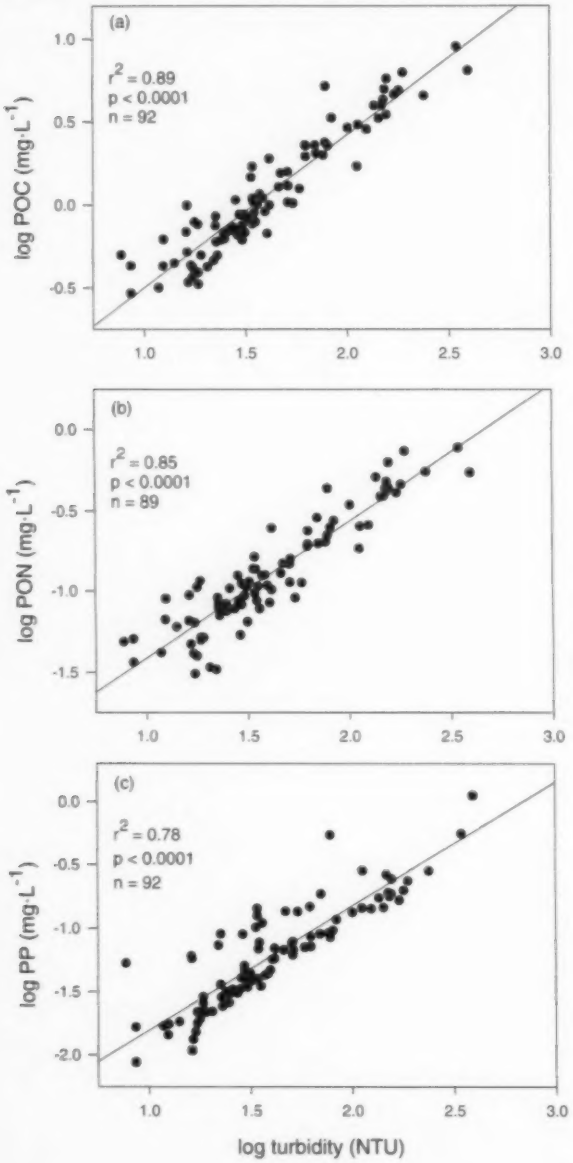

and retention mechanisms of suspended matter (Vincent and Dodson 1999). The stations where high veliger densities were found (N-0 and N-01) were situated directly in this maximum turbidity zone. Along with the potential accumulation of veligers due to vertical circulation and entrapment, these high densities could also be favoured by Coriolis effects and horizontal recirculation. These stations could also be receiving individuals originating from adult populations colonising the shores of Île d'Orléans.

Table 3. Molar ratios of particulate organic carbon to nitrogen to phosphorus (C:N:P) for the seston (0–2 m) at the 12 stations sampled during summer 2000.

Station	Cruise 2	Cruise 3	Cruise 4	Cruise 5
S-0	43:3:1	87:91:1	48:5:1	77:10:1
S-01	46:4:1	70:6:1	58:6:1	64:6:1
S-13	74:5:1	58:7:1	54:6:1	62:6:1
S-35	23:2:1	53:5:1	56:6:1	45:5:1
S-5+	16:1:1	50:6:1	34:5:1	68:6:1
M-13	28:2:1	61:6:1	54:6:1	NA
M-35	40:3:1	30:3:1	54:7:1	NA
N-5+	44:4:1	34:3:1	63:7:1	92:11:1
N-35	37:3:1	45:4:1	69:9:1	82:8:1
N-13	23:2:1	66:5:1	61:6:1	63:7:1
N-01	24:2:1	40:3:1	56:6:1	70:8:1
N-0	24:2:1	50:3:1	66:7:1	49:4:1

Note: Stations are indicated by a letter representing the channel (N, north; S, south; M, middle) followed by numbers indicating the salinity (0, 0‰; 01, 0–1‰; 13, 1–3‰; 35, 3–5‰; 5+, 5+‰). NA, not available.

Bioavailability of the veligers' prey

Kranck (1979) found that the particle size spectra of organisms in the maximum turbidity zone increases drastically from zone 1 to zone 2. According to this author, the majority of particles in the turbidity maxima (zone 2) appear to be >10 µm because of flocculation processes. Indeed, preliminary microscopic results on the protist community of the ETZ revealed that the veligers' prey become unavailable to them because of the formation of aggregates, thus causing mechanical interference. This sharp decrease in prey bioavailability at salinity >2‰ may be an important stressor to the veligers, in addition to salinity.

Predation

Previous studies conducted in the St. Lawrence ETZ observed sharp declines in Chl *a*, photosynthetic picoplankton, and protist concentrations between zones 1 and 2 (Lovejoy et al. 1993; Frenette et al. 1995). The authors attributed this effect to zooplankton grazing, as there is a large standing stock of zooplankton in the ETZ (Vincent and Dodson 1999; Winkler et al. 2003). Predation pressures could then also be partially responsible for the decrease in veliger abundance. Wright et al. (1996) observed that rotifer predation caused high mortality rates of their zebra mussel larvae culture. Mills et al. (1995) observed that alewife (*Alosa pseudoharengus*) and rainbow smelt (*Osmerus mordax*) prey upon veligers but concluded that predation did not substantially reduce the number of veligers because they were either resistant to predation pressures and (or) the predation rate was not high enough. In contrast, other authors have stressed the importance of predation on veligers by fish larvae (*Osmerus esperlanus*, *Lucioperca lucioperca*, *Acerina arnua*, and *Ruttilus rutilus*) (Sprung 1993).

Vertical distribution (summer 2001)

The veligers were evenly distributed throughout the water column, regardless of tidal state and zone. Even when the water column was stratified, no significant difference in abundance between surface, mid-column, and bottom samples was observed. Kern et al. (1994) also observed homoge-

© 2003 NRC Canada

Fig. 7. Protists within aggregates >10 μm as a function of salinity in the St. Lawrence estuarine transition zone (ETZ). The protist community was grouped into two functional groups: autotrophs, solid circles and solid line; heterotrophs, open triangles and dotted line. Samples were collected on 15 July 2000.

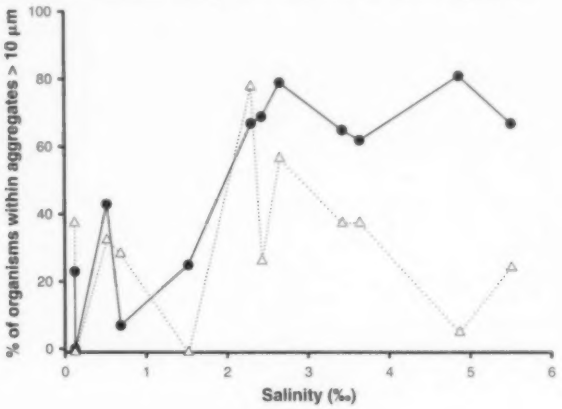

neous vertical distribution in the Rhine River, which most likely had higher mixing rates than lakes in which stratified distribution was observed under low wind conditions (Fraleigh et al. 1993; Garton and Haag 1993). With current speeds at ca. 2.5 $m \cdot s^{-1}$ and horizontal and vertical mixing, the ETZ hydrodynamics are much more complex and intense than in lakes. The veligers are most likely undergoing passive transport under these conditions. The elevated current speed and mixing rates of the ETZ throughout the water column and the constant influence of the salinity front on the hydrodynamics most probably does not allow the veligers to actively maintain their position in a density gradient or to passively settle. In this regard, veligers are also unlikely to have the capacity to actively move to areas of high productivity to feed.

Temporal distribution

Certain authors have documented that a single massive explosion of individuals during the summer characterizes veliger larvae abundance in the plankton, whereas other authors have observed several pulses of high abundances over the summer (Stoeckel et al. 1997). These authors suggested that upriver source populations spawned in frequent distinct bursts throughout the summer rather than just once or twice. Of the four cruises undertaken during summer 2000, our data revealed that veliger abundance was significantly higher during cruise 2 than during cruises 3, 4, and 5. Our data were not collected on a daily basis but show evidence of sporadic and distinct peaks in veliger abundance. This was consistent with the results obtained during the fixed station sampling of summer 2001, which showed large variation in veliger abundance between samples. Stoeckel et al. (1997) also observed the continual passage of pulses of individuals in a large river.

Food quality

Herbivores with high nutrient demands, such as the veligers, are frequently limited not by food quantity or available energy but by the quantity of mineral elements in their food, i.e., seston food quality (Sterner and Hessen 1994). It has been illustrated that food quality has a highly significant effect on the survival rates of *Dreissena* veligers (Wacker et al. 2002). Seston ratios have proven to be effective physiological indicators of the nutritional state of phytoplankton (Healey and Hendzel 1980). Veliger densities were weakly but positively correlated with the PP/TP ratio as well as with PP, indicating their association with good quality seston. The ratio PP/TP represents the amount of phosphorus within the particulate material (and potential prey items) relative to the total phosphorus. Under nutrient-poor or resource-limited conditions, organisms tend to have a high particulate carbon content relative to other nutrients (Sterner 1997). The seston throughout the ETZ has relatively low C:P, C:N, and N:P ratios, indicative of its good overall nutritional quality, and in this aspect is a favourable environment for veliger growth. According to pre-established criteria, the ratios suggest no severe limitation of single N or P of plankton in the water column (Healey and Hendzel 1980; Hecky et al. 1993), and SRP and nitrate were always at detectable levels, suggesting adequate nutrient supply for the algae. The C:N:P ratios were generally in agreement, suggesting no simultaneous deficiencies. In general, however, these did not correspond to the traditional Redfield ratio of 106:16:1. The concentrations of particulate matter in this dynamic estuary are presumably much higher and more variable than in typical oceanic environments. Redfield ratios tend to be an exception rather than the rule in fresh water (Hecky et al. 1993), and studies have shown that although this ratio is found in the ocean and large lakes, it can vary greatly according to transient effects on cellular physiology (Falkowski 2000).

The high C:Chl *a* ratios observed in the ETZ could potentially be interpreted as indicating a high general nutrient deficiency or as a substantial detrital influence (Healey and Hendzel 1980; Hecky et al. 1993). The first scenario is highly unlikely considering the values of seston elemental ratios. In the second scenario, some authors attempt to correct for the influence of detritus on particulate C, N, and P on the basis of a standard C:Chl *a* ratio (Hecky et al. 1993). Estimating the latter is difficult for the St. Lawrence ETZ where physical gradients are pronounced. Even the C:Chl *a* ratio of algae grown in culture varies significantly with varying degrees of nutrient stress and light conditions (Healey and Hendzel 1980). If detritus had an overriding influence on the ratios, we would expect to find an increase of particulate C in the ratios with an increase in turbidity, but this was not the case. Moreover, there were no differences between the surface and bottom ratios, despite higher turbidities near the bottom (C. Barnard, unpublished data).

Järvinen et al. (1999) also observed high C:Chl *a* ratios in large, turbid Lake Tanganyika, which is characterized by low Chl *a* concentrations. In the ETZ, Chl *a* concentrations are tidally variable, with lows occurring during high tide (Vincent and Dodson 1999). It has been shown that the phytoplankton in the ETZ are adapted to intermittent light rather than low light conditions (Vincent et al. 1994), which could result in lower cellular requirement for Chl *a* and thus a higher C:Chl *a* ratio.

Chl *a* biomass, veliger abundance, and particulate C, N, and P were all positively correlated with turbidity. It is interesting to note that the turbidity does not seem to negatively

© 2003 NRC Canada

affect Chl *a* biomass or seston quality. The positive relationship between turbidity and the biological variables is likely the result of the common influence of hydrodynamic retention on biotic particles, as well as on abiotic particles (Frenette et al. 1995). A similar peak in phytoplankton biomass, coincident with the turbidity maximum, has also been observed in the ETZ of the James River, U.S.A. (Moon and Dunstan 1990).

Impacts of veligers on the food web

The positive correlations between Chl *a*, PC picoplankton, and veliger concentrations imply that the veligers have no severe negative impacts on these food sources and that phytoplankton resources are not limiting for the veligers in the ETZ. These associations also suggest that veligers are subject to the same physical and chemical forces in the water column as the other biological variables. These biological variables had a negative relationship with salinity and TP but a positive relationship with temperature and turbidity. As shown with variance partitioning, the spatial component did not have a strong influence on the biological community. On the other hand, the environmental variables were highly significant explanatory variables, underlying the pivotal role that the salinity front plays in structuring the biological community. The zone of high veliger abundance, the upstream portion of the ETZ, seems to be a favourable environment (low salinity and abundant food resources) for their growth. Bertrand and Vincent (1994) observed that picoplankton could contribute from 6% to 56% of the total Chl *a* in the water column of the ETZ. This may imply that a high proportion of the Chl *a* biomass is edible by the veligers (prey size spectrum 1–9 μm) (Sprung 1993; Wright et al. 1996). In the present study, the mean photosynthetic picoplankton densities at <2‰ was 5.09 (standard deviation = 1.9) × 10^6 individuals·L^{-1}. This is similar to the photosynthetic picoplankton densities previously documented by Bertrand and Vincent (1994) before the invasion. No decrease in the photosynthetic picoplankton densities of the ETZ has thus been observed since the arrival of this new species.

In summary, we found that the larval veligers of *Dreissena polymorpha* were abundant in the low salinity waters of the St. Lawrence ETZ. Their concentrations decreased exponentially with increasing salinity, with the maximum decrease observed at 2‰, suggesting salinity-induced mortality, grazer, or other loss processes. The veligers were homogeneously distributed throughout the water column, under all tidal regimes, even when the water column was stratified. Despite their dominance in the ETZ plankton, the veligers have no severe effects on the lower food web because they are positively correlated with Chl *a* biomass, picoplankton densities, and good quality seston. The high productivity of the ETZ may explain why the ecosystem does not appear to be negatively impacted by their invasion, i.e., the ETZ may have a sufficient surplus of food resources to support the high population of zebra mussel veligers in addition to the usual zooplankton residents. The high abundance of veligers may have an impact on higher trophic levels, but this was not assessed in our analysis. The low salinity waters (<2‰) of the upper reaches of the St. Lawrence ETZ therefore provide a favourable environment for their survival. Future perspectives should investigate their impact on the biomass size spectrum of the microbial community and on higher trophic levels of this important larval fish nursery.

Acknowledgements

This research is a contribution of Québec-Océan (le groupe interinstitutionnel de recherches océanographiques du Québec) and CEN (Centre d'Études Nordiques). We thank Ladd Johnson, Connie Lovejoy, and Paul Hamilton for assistance and support at various stages of the project. We also thank Hugues Boulanger, Julie Harnois, Kim Huggins, Brigitte Laberge, Marie-Audrey Livernoche, Carl Martin, Sébastien Roy, Gesche Winkler, and the crews of the *Willie DeRaspe* and the *Marie-Karine D.* for their help in the field and in the laboratory. The first cruise of the summer of 2001, conducted on the *Willie DeRaspe*, was possible thanks to the support of the Department of Fisheries and Oceans (Canada). Finally, we thank Christian Salesse for the use of his microscope and Andrea Bertolo for many helpful discussions on statistics. This study was funded by a Natural Sciences and Engineering Research Council of Canada (NSERC) strategic grant led by Ladd Johnson, NSERC discovery grants to J.-J.F. and W.F.V., and a FCAR (Québec) postgraduate fellowship to C.B.

References

Bertrand, N., and Vincent, W.F. 1994. Structure and dynamics of photosynthetic picoplankton across the saltwater transition zone of the St. Lawrence River. Can. J. Fish. Aquat. Sci. **51**: 161–171.

Borcard, D., Legendre, P., and Drapeau, P. 1992. Partialling out the spatial component of ecological variation. Ecology, **73**: 1045–1055.

Caraco, N.F., Cole, J.J., Raymond, P.A., Strayer, D.L., Pace, M.L., Findlay, S., and Fischer, D.T. 1997. Zebra mussel invasion in a large river, turbid river: phytoplankton response to increased grazing. Ecology, **78**: 588–602.

d'Anglejan, B., and Smith, E. 1973. Distribution, transport, and composition of suspended matter in the St. Lawrence Estuary. Can. J. Earth Sci. **10**: 1380–1396.

de Kock, W.C., and Bowmer, C.T. 1993. Bioaccumulation, biological effects, and food chain transfer of contaminants in the zebra mussel (*Dreissena polymorpha*). *In* Zebra mussels: biology, impacts and control. *Edited by* T. Nalepa and D. Schloesser. Lewis Publishers, Boca Raton, Fla. pp. 503–533.

de Lafontaine, Y., Lapierre, L., Henry, M., and Grégoire, Y. 1995. Abondances des larves de moule zébrée (*Dreissena polymorpha*) et de Quagga (*Dreissena bugensis*) aux abords des centrales hydroélectriques de Beauharnois, Les Cèdres et Rivière-des-Prairies. Environnement Canada Région du Québec, Conservation de l'environnement, Centre Saint-Laurent. Rapport scientifique et technique St-14, Ottawa, Canada.

Falkowski, P.G. 2000. Rationalizing elemental ratios in unicellular algae. J. Phycol. **36**: 3–6.

Findlay, S., Pace, M.L., and Fischer, D.T. 1998. Response of heterotrophic planktonic bacteria to the zebra mussel invasion of the tidal freshwater Hudson River. Microb. Ecol. **36**: 131–140.

Fraleigh, P.C., Klerks, P.L., Gubanich, G., Matisoff, G., and Stevenson, R.C. 1993. Seasonal reproductive cycles and settlement patterns of *D. polymorpha* in western Lake Erie. *In* Zebra mussels: biology, impacts and control. *Edited by* T.F. Nalepa and D.W. Schloesser. Lewis Publishers, Boca Raton, Fla. pp. 129–143.

Frenette, J.-J., Vincent, W.F., Dodson, J.J., and Lovejoy, C. 1995. Size-dependent variations in phytoplankton and protozoan com-

© 2003 NRC Canada

munity structure across the St. Lawrence River transition region. Mar. Ecol. Prog. Ser. **120**: 99–110.

Garton, D.W., and Haag, W.R. 1993. Seasonal reproductive cycles and settlement patterns of *D. polymorpha* in western Lake Erie. *In* Zebra mussels: biology, impacts and control. *Edited by* T.F. Nalepa and D.W. Schloesser. Lewis Publishers, Boca Raton, Fla. pp. 111–128.

Healey, F., and Hendzel, L. 1980. Physiological indicators of nutrient deficiency in lake phytoplankton. Can. J. Fish. Aquat. Sci. **37**: 442–453.

Hebert, P.D.N., Muncaster, B.W., and Mackie, G.L. 1989. Ecological and genetic studies on *Dreissena polymorpha* (Pallas): a new mollusc in the Great Lakes. Can. J. Fish. Aquat. Sci. **46**: 1587–1591.

Hecky, R.E., Campbell, P., and Hendzel, L.L. 1993. The stoichiometry of carbon, nitrogen, and phosphorus in particulate matter of lakes and oceans. Limnol. Oceanogr. **38**: 709–724.

Horvath, T.G., and Lamberti, G.A. 1999. Mortality of zebra mussel, *Dreissena polymorpha*, veligers during downstream transport. Freshw. Biol. **42**: 69–76.

Järvinen, M., Salonen, J., Sarvala, J., Vuorio, K., and Virtanen, A. 1999. The stoichiometry of particulate nutrients in Lake Tanganyika — implications for nutrient limitation of phytoplankton. Hydrobiologia, **407**: 81–88.

Johnson, L.E. 1995. Enhanced early detection and enumeration of zebra mussel (*Dreissena* sp.) veligers using cross-polarised light microscopy. Hydrobiologia, **312**: 139–146.

Kern, R., Borcherding, J., and Neumann, D. 1994. Recruitment of a freshwater mussel with a planktonic life-stage in running waters: studies on *Dreissena polymorpha* in the Rhine River. Arch. Hydrobiol. **131**: 385–400.

Kilgour, B., Mackie, G., Baker, M., and Keppel, R. 1994. Effects of salinity on the condition and survival of zebra mussels (*Dreissena polymorpha*). Estuaries, **17**: 385–393.

Kranck, K. 1979. Dynamics and distribution of suspended particulate matter in the St. Lawrence estuary. Nat. Can. **106**: 163–173.

Legendre, P. 1993. Spatial autocorrelation: trouble or new paradigm? Ecology, **74**: 1659–1673.

Legendre, P., and Fortin, M.-J. 1989. Spatial pattern and ecological analysis. Vegetatio, **80**: 107–138.

Lovejoy, C., Vincent, W.F., Frenette, J.-J., and Dodson, J.J. 1993. Microbial gradients in a turbid estuary: applications of a new method for protozoan community analysis. Limnol. Oceanogr. **38**: 1295–1303.

Lucotte, M., and d'Anglejan, B. 1986. Seasonal control of the Saint-Lawrence maximum turbidity zone by tidal-flat sedimentation. Estuaries, **9**: 84–94.

Mellina, E., and Rasmussen, J.B. 1994. Occurrence of zebra mussel (*Dreissena polymorpha*) in the inter-tidal region of the St. Lawrence estuary. J. Freshw. Ecol. **9**: 81–84.

Mills, E.L., O'Gorman, R., Roseman, E.F., Adams, C., and Owens, R.W. 1995. Planktivory by alewife (*Alosa pseudoharengus*) and rainbow smelt (*Osmerus mordax*) on microcrustacean zooplankton and dreissinid (Bivalvia: Dreissenidae) veligers in southern Lake Ontario. Can. J. Fish. Aquat. Sci. **52**: 925–935.

Moon, C., and Dunstan, W.M. 1990. Hydrodynamic trapping in the formation of the chlorophyll *a* peak in turbid, very low salinity waters of estuaries. J. Plankton Res. **12**: 323–336.

National Laboratory for Environmental Testing. 1994. Manual of analytical methods. Vol. 1. Major ions and nutrients. National Laboratory for Environmental Testing, Environment Canada, Burlington, Ont.

Pace, M., Findlay, S., and Fischer, D. 1998. Effects of an invasive bivalve on the zooplankton community of the Hudson River. Freshw. Biol. **39**: 103–116.

Ricciardi, A., Neves, R.J., and Rasmussen, J.B. 1998. Impending extinctions of North American freshwater mussels (Unionidae) following the zebra mussel (*Dreissena polymorpha*) invasion. J. Anim. Ecol. **67**: 613–619.

Sprung, M. 1993. The other life: an account of present knowledge of the larval phase of *Dreissena polymorpha*. *In* Zebra mussels: biology, impacts and control. *Edited by* T.F. Nalepa and D.W. Schloesser. Lewis Publishers, Boca Raton. Fla. pp. 39–53.

Sterner, R.W. 1997. Modelling interactions of food quality and quantity in homeostatic consumers. Freshw. Biol. **38**: 473–481.

Sterner, R.W., and Hessen, D.O. 1994. Algal nutrient limitation and the nutrition of aquatic herbivores. Annu. Rev. Ecol. Syst. **25**: 1–29.

Stoeckel, J.A., Schneider, D.W., Soeken, L.A., Blodgett, K.D., and Sparks, R.E. 1997. Larval dynamics of a riverine metapopulation: implications for zebra mussel recruitment, dispersal, and control in a large-river system. J. N. Am. Benthol. Soc. **16**: 586–601.

Strayer, D.L., and Smith, L.C. 1993. Distribution of the zebra mussel (*D. polymorpha*) in estuaries and brackish waters. *In* Zebra mussels: biology, impacts and control. *Edited by* T.F. Nalepa and D.W. Schloesser. Lewis Publishers, Boca Raton. Fla. pp. 715–725.

ter Braak, C.J.F. 1998. CANOCO, a FORTRAN program for Canonical Community Ordination by [partial][detrended][canonical] correspondence analysis, principal components analysis and redundancy analysis (version 4.0). DLO-Agricultural Mathematics Group, Wageningen, The Netherlands.

Vanderploeg, H.A., Liebig, J.R., and Gluck, A.A. 1996. Evaluation of different phytoplankton for supporting development of zebra mussel larvae (*Dreissena polymorpha*): the importance of size and polyunsaturated fatty acid content. J. Great Lakes Res. **22**: 36–45.

Vincent, W.F., and Dodson, J.J. 1999. The St. Lawrence River, Canada–USA: the need for an ecosystem-level understanding of large rivers. Jpn. J. Limnol. **60**: 29–50.

Vincent, W.F., Bertrand, N., and Frenette, J.-J. 1994. Photoadaptation to intermittent light across the St. Lawrence estuary freshwater–saltwater transition zone. Mar. Ecol. Prog. Ser. **110**: 283–292.

Wacker, A., Becher, P., and Elert, E.V. 2002. Food quality effects of unsaturated fatty acids on larvae of the zebra mussel *Dreissena polymorpha*. Limnol. Oceanogr. **47**: 1242–1248.

Winkler, G., Dodson, J.J., Bertrand, N., Thivierge, D., and Vincent, W.F. 2003. Trophic coupling across the St. Lawrence River estuarine transition zone. Mar. Ecol. Prog. Ser. **251**: 59–73.

Wright, D.A., Setzler-Hamilton, E.M., Magee, J.A., Kennedy, V.S., and McInnch, S.P. 1996. Effect of salinity and temperature on survival and development of young zebra (*Dreissena polymorpha*) and quagga (*D. bugensis*) mussels. Estuaries, **19**(3): 61

© 2003 NRC Canada

Role of disease in abundance of a Pacific herring (*Clupea pallasi*) population

Gary D. Marty, Terrance J. Quinn II, Greg Carpenter, Theodore R. Meyers, and Neil H. Willits

Abstract: Disease significantly affects population abundance of Pacific herring (*Clupea pallasi*). Comprehensive epidemiological study of the Pacific herring population of Prince William Sound, Alaska, U.S.A., from 1994 to 2000 included complete necropsy examination of 230–500 fish each spring and 40–160 fish each fall (total n = 2983 fish). Mortality is best estimated, through modifications of an age-structured assessment model, using a disease index that combines the prevalence of viral hemorrhagic septicemia virus (VHSV) with the prevalence of ulcers. Risk factors for an epidemic include poor body condition and abundant recruitment before spawning in the spring. Prevalence of the pathogen *Ichthyophonus hoferi* increased as fish aged, but changes in *I. hoferi* prevalence were not related to changes in population abundance. Disease that caused an epidemic in 1998 (VHSV and ulcers) nearly disappeared from the population when changes in abundance were detected by traditional stock assessment methods in 1999. Disease significantly affects recruitment — the two lowest recruitment estimates on record, in 1994 and 1999, followed increased natural mortality of adults in 1993 and 1998.

Résumé : La maladie affecte de façon significative l'abondance des populations de harengs du Pacifique (*Clupea pallasi*). Notre étude épidémiologique détaillée de la population des harengs du Pacifique du détroit du Prince William, Alaska, États-Unis, de 1994 à 2000, comprenait l'examen complet par nécropsie de 230–500 poissons chaque printemps et de 40–160 poissons chaque automne, pour un total de 2983. La mortalité s'estime le plus précisément par un modèle d'évaluation structuré d'après l'âge qui utilise un indice de morbidité combinant la prévalence du virus de la septicémie hémorragique virale (VHSV) à celle des ulcères. Les facteurs de risque d'une épidémie incluent une mauvaise condition physique et un recrutement important avant la fraye au printemps. La prévalence de l'agent pathogène *Ichthyophonus hoferi* augmente avec l'âge des poissons, mais les changements dans la prévalence du pathogène ne sont pas reliés aux changements d'abondance de la population. La maladie (VHSV et ulcères) qui a causé une épidémie en 1998 avait presque disparu de la population lorsque des changements d'abondance de la population ont été détectés par des méthode classiques d'évaluation des stocks en 1999. La maladie affecte de façon significative le recrutement; en effet, les estimations de recrutement les plus faibles enregistrées l'ont été en 1994 et 1999 suivant une augmentation de la mortalité naturelle des adultes en 1993 et en 1998.

[Traduit par la Rédaction]

Introduction

Marine epidemics have increased in number and frequency during the last 30 years (Harvell et al. 1999; Sherman 2000), but we are only beginning to unravel the complex interactions of disease with predation, recruitment, and environmental change (Harvell et al. 1999, 2002). Among marine fish, studies have documented long-term population cycles (e.g., Lluch-Belda et al. 1992), and population decline has been associated with disease epidemics worldwide. Most epidemics in marine fish have been associated with *Ichthyophonus hoferi* (Daniel 1933; Sindermann 1958; Mellergaard and Spanggaard 1997), but other epidemics are more consistent with a viral outbreak (Tester 1942; Whittington et al. 1997). The association of a single pathogen in a marine fish population has been followed for up to 4 years (Patterson 1996), but longer-term effects of disease on marine fish populations have never been examined.

Members of the Order Clupeiformes (herring, sardine, anchovy, menhaden, and shad) are among the most abundant

Received 3 September 2002. Accepted 31 August 2003. Published on the NRC Research Press Web site at http://cjfas.nrc.ca on 7 November 2003.
J17074

G.D. Marty.[1] Department of Anatomy, Physiology, and Cell Biology, School of Veterinary Medicine, University of California, 1 Shields Ave., Davis, CA 95616-8732, U.S.A.
T.J. Quinn II. Juneau Center, School of Fisheries and Ocean Sciences, University of Alaska Fairbanks, 11120 Glacier Hwy., Juneau, AK 99801-8677, U.S.A.
G. Carpenter. Alaska Department of Fish and Game, P.O. Box 5267, Fort Richardson, AK 99505, U.S.A.
T.R. Meyers. Alaska Department of Fish and Game, Juneau Fish Pathology Laboratory, P.O. Box 25526, Juneau, AK 99802, U.S.A.
N.H. Willits. Statistics Laboratory, Department of Statistics, 1 Shields Avenue, University of California, Davis, CA 95616-8732, U.S.A.

[1]Corresponding author (e-mail: gdmarty@ucdavis.edu).

 doi: 10.1139/F03-109 © 2003 NRC Canada

fish species worldwide. The Pacific herring (*Clupea pallasi*) population of Prince William Sound, Alaska, provides an excellent model for studying the role of disease in population dynamics of this group of fish. Pacific herring are schooling fish that historically ranged throughout coastal regions of the North Pacific. They are an important component of the ecosystem as secondary consumers, and they also serve as high- quality prey for many marine birds and mammals (e.g., Thomas and Thorne 2001). In Prince William Sound, Pacific herring first spawn when 3–5 years old, live up to 15 years, and weigh up to 300 g. Mature fish spawn every year, but the adult population rarely has an abundant year-class more often than every 4 years. The most accurate biomass estimates are made in early April, when fish aggregate in shallow water to spawn. After spawning, fish disperse and do not reaggregate near spawning areas until late fall. Feeding is minimal during the winter (Foy and Norcross 2001).

The Prince William Sound Pacific herring population has been affected by three major events in the past 40 years. First, the 1964 Anchorage earthquake shifted the elevation of some spawning areas more than 5 m. Second, the *Exxon Valdez* oil spill in Prince William Sound occurred in March 1989, just before spawning. Third, a severe epidemic killed about 75% of the population over the winter of 1992–1993 (Fig. 1). Fish surviving the 1993 epidemic were lethargic, and many had external hemorrhages. The first-ever Pacific herring isolates of the North American strain of viral hemorrhagic septicemia virus (VHSV) were cultured from pooled samples from these fish (Meyers et al. 1994). Subsequent laboratory study confirmed that VHSV can kill juvenile fish (Kocan et al. 1997), but the relation of VHSV to population decline of adult fish in Prince William Sound in 1994 could not be determined. Disease involves poorly understood interactions between three major variables: the host, the pathogen, and the environment (Hedrick 1998); the mere presence of a pathogen is not equivalent to disease. A comprehensive disease study was initiated in 1994 to determine the cause of ongoing population decline, and when the population failed to recover, the study was continued through 2000. Explanations of the decline in 1993 remain controversial, but no scientific evidence directly links the oil spill to population decline (Elston et al. 1997; Marty et al. 1998). Instead, the most plausible hypothesis is that poor growth during the summer of 1992 led to poor body condition in the spring of 1993, increasing the risk for an epidemic (Pearson et al. 1999; Carls et al. 2002).

In late 1998, an age-structured mathematical model was used to predict the biomass that would return to spawn in the spring of 1999, but only about half of the expected biomass actually appeared (Fig. 1). Based on complete necropsy of 300 randomly sampled fish in April 1999, the prevalence of *I. hoferi* was 24%, the North American strain of VHSV, 1%, and ulcers, 0.6%. *Ichthyophonus hoferi* has been associated with population decline in Atlantic herring (Daniel 1933; Sindermann 1958; Mellergaard and Spanggaard 1997), and VHSV has been isolated from several stable populations of Pacific herring (Meyers and Winton 1995). Based on 1999 data alone, it would have been logical to conclude that *I. hoferi* was the most important pathogen in population decline. This conclusion is wrong. We provide evidence from 7 years of study that *I. hoferi* is a significant pathogen, but population change correlates more with an index of VHSV and ulcer prevalence than with *I. hoferi*. We show that a disease-based, age-structured model with a relationship between herring natural mortality and disease prevalence is significantly better than a traditional model with constant natural mortality.

Fig. 1. Biomass estimates of mature Pacific herring (*Clupea pallasi*) in Prince William Sound, Alaska. Unexploited spawning biomass projected in the year before spawning (○; source, Alaska Department of Fish and Game, Cordova, Alaska) and calculated after spawning (best estimate, ●) using an age-structured assessment model modified by a disease index after 1993. The *Exxon Valdez* oil spill occurred in Prince William Sound in 1989.

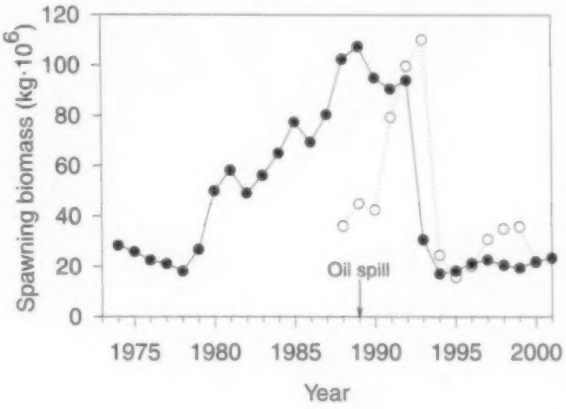

Methods

Major diseases

Adult Pacific herring from Prince William Sound, Alaska, were sampled at random and subjected to complete necropsy during two seasons: (1) spring of 1994 through 2000, sample size varied from 233 to 300 fish per year; and (2) fall of 1995 through 2000, sample size varied from 40 to 160 fish per year. Fish in Prince William Sound were all sampled from bays on the north end of Montague Island (e.g., Stockdale Harbor, Rocky Bay, and Zaikof Bay). Pacific herring were also sampled from a reference site, Sitka Sound, in the spring of 1995 and 1996 (240 fish per year). Sitka Sound had no history of a large oil spill. Pacific herring were abundant there throughout the 1990s, and population dynamics before the 1990s were very similar to those of Prince William Sound (Williams and Quinn 2000*a*). In all, 2983 Pacific herring were subjected to complete necropsy using standard methods established during the first 2 years of study (Marty et al. 1998; Davis et al. 1999). Analysis for each fish included gross examination, white blood cell differential counts, histopathology of 10 organs, a panel of plasma chemistries including plasma immunoglobulin (IgM) concentration, and culture of head kidney and spleen for virus isolation. Gross and microscopic lesions were scored as none (0), mild (1), moderate (2), or severe (3). Body weight, length, and age (from scales) determined from each fish linked our data with the historical database compiled by the

© 2003 NRC Canada

Alaska Department of Fish and Game on this population since the early 1970s. For all fish with severe external lesions, kidney was cultured for bacteria (all were negative). At Sitka Sound in March 1997, 250 Pacific herring were sampled but analysis was limited to gross necropsy, virology, and bacteriology.

Three general criteria were used to determine if changes in prevalence of an organism or lesion were significant on an individual and population scale: (1) the severity of the lesion or associated lesions (i.e., severe lesions were considered more significant than mild lesions); (2) association with changes in plasma chemistries; and (3) association of changes in prevalence with changes in population biomass. Cutaneous ulcers, VHSV, and *I. hoferi* met most of these criteria. For VHSV and *I. hoferi*, multiple stepwise regression was used to identify a subset of variables that were predictive for severity of infection or infestation by each organism. For VHSV only, combining data from 1997 and 1998 (blocked on year), adjusted odds ratios were calculated for a logistic regression that compared the frequency of VHSV + 3-year-old fish versus VHSV + older fish.

Fig. 2. Prevalence of lesions and pathogens in spring samples: (*a*) external lesion focal skin reddening (moderate, light bars; severe, darker bars); (*b*) viral hemorrhagic septicemia virus (VHSV); and (*c*) *Ichthyophonus hoferi* prevalence (bars) and mean age (●) of fish in the samples. SE, standard error.

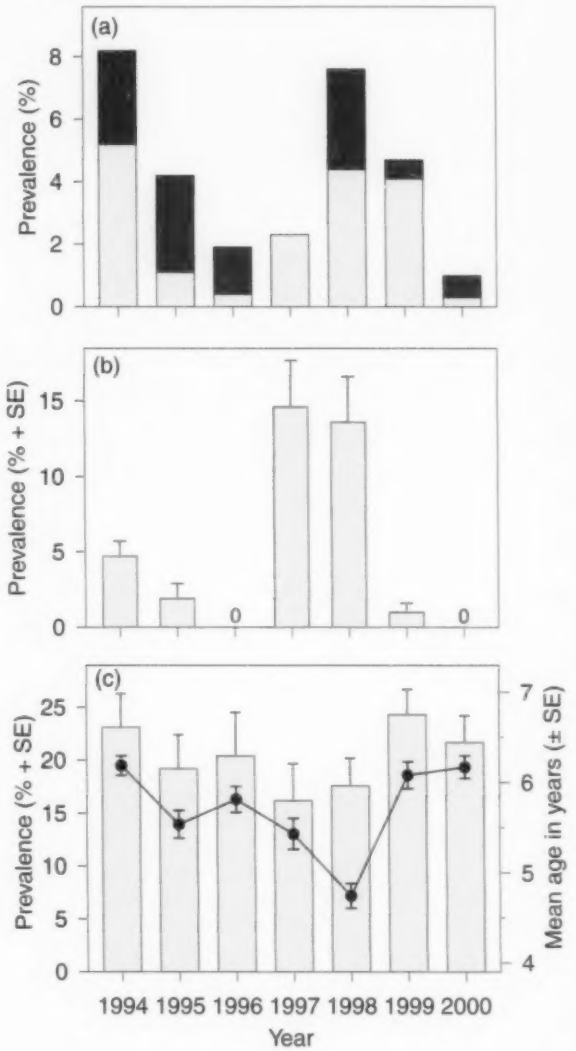

Population modeling of disease

A standard version of an age-structured assessment model (Quinn and Deriso 1999, section 8.2.5) is modified to evaluate the impact of disease on population abundance. The basic model provides an estimation framework to integrate the various sources of information about Pacific herring in Prince William Sound from 1980 to 2000, including age compositions from the purse-seine fishery and spawning surveys, egg production estimates, and mile-days of milt from aerial surveys (Quinn et al. 2001). These observations are compared with comparable model quantities in a least squares setting to obtain parameter estimates of recruitment, abundance, and biomass.

We assume that disease increases the natural mortality M for all adult ages (ages 3 and older), or equivalently, that disease lowers the corresponding natural survival S. For simplicity, S_t in year t is assumed to decrease linearly as a function of disease prevalence variables $\{x_{it}\}$, where natural survival S_0 from sources other than disease is constant. Expressed mathematically,

$$(1) \qquad S = S_0\left(1 - \sum_i \beta_i x_{it}\right)$$

where x_{it} is the sampled prevalence for pathogen i in year t and β_i represents the proportion of the infected population that dies from the particular pathogen. This is a slight generalization of the disease model in Quinn et al. (2001) in which only a single pathogen was examined at a time. Equation 1 may be expressed in terms of natural mortality using $M = -\ln(S)$. If $x_t = 1$ and $\beta = 1$ (all fish are infected and die from a single pathogen), then $S = 0$ and $M = \infty$. Parameter β can be greater than 1 if the prevalence variable underestimates the mortality resulting from the disease.

The age-structured assessment model contains information about the Pacific herring fisheries in Prince William Sound, Alaska, which include purse-seine, gillnet, and pound fisheries in the spring (mainly for roe) and a food and bait fishery in the summer and fall. Recruitment occurs at age 3 and there are parameters for recruit abundance, $\{N_{3,t}\}$, for all years (and for all abundances in the first year, 1980). From these parameters and the survival model (eq. 1), abundance at each subsequent age $a + 1$ and year $t + 1$ is estimated from

$$(2) \qquad N_{a+1,t+1} = [(N_{a,t} - C_{\text{seine}} - C_{\text{gill}} - C_{\text{pound}})S_t^{1/2} - C_{\text{food}}]S_{t+1}^{1/2}$$

in which N is abundance, C is annual catch-at-age, and $S^{1/2}$ is half-year survival, calculated as the square root of eq. 1. In eq. 2, we assume that the disease variable measured in year $t + 1$ at the time of spawning affects the population in

© 2003 NRC Canada

Fig. 3. Prevalence of viral hemorrhagic septicemia virus (light bars) and *Ichthyophonus hoferi* (darker bars) in spring samples from (*a*) 1997 and (*b*) 1998. Number examined for each year-class (*n*) varied between years.

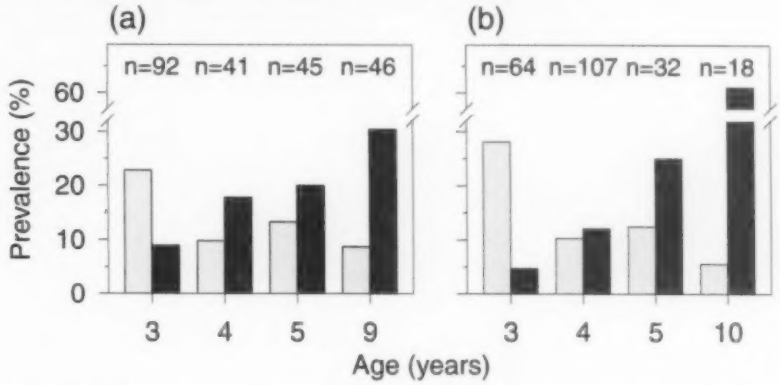

the last half-year of year t (before recruitment, spawning, and spring fisheries) and the first half-year of year $t + 1$. Another assumption is that total catch for the seine fishery and catch-at-age for the other fisheries are assumed measured without error in the model. The estimated number of spawners is the mature abundance after the spring fisheries, or

$$\text{Spawners}_t = \sum_a \text{mat}_a(N_{a,t} - C_{\text{seine}} - C_{\text{gill}} - C_{\text{pound}}) \quad (3)$$

in which mat is the proportion mature. Spawning biomass is similar to eq. 3 but also multiplies by weight-at-age.

The other parameters in the model are logistic selectivity parameters for the spawning survey (equivalent to the values of maturity) and for the purse-seine fishery, natural mortality for the plus group (aged 9+) relative to other ages, a calibration coefficient that converts the milt index into total egg production, and a parameter for estimated disease prevalence in 1992–1993 (because there is only very limited information from this period; Quinn et al. 2001). Natural mortality M_0 from all other sources was assumed to be 0.25 in accord with usual Pacific herring assessments in Alaska.

The objective function includes least squares (or negative likelihood) components for the purse-seine age composition (in years when the fishery was open: 1980–1988, 1990–1992, 1997–1998), spawning age composition (since 1982), egg survey estimates on a logarithmic scale (from 10 years between 1984 and 1997), and the egg milt index on a logarithmic scale (all years 1980–2000). Spawning age composition is weighted by the factor 10, and the egg milt index is weighted by 0.5 to avoid unwelcome patterns in the residuals. The model is contained in a spreadsheet and available from the author (Quinn).

Prevalence of cutaneous ulcers, VHSV, and *I. hoferi* is used to modify the estimate of natural mortality M in several iterations of the model (Quinn et al. 2001). We compare these models by examining their residual sums of squares and parameter estimates and by performing F tests. Such comparisons show how much additional variability is explained by the disease data, whether the reduction in variability is statistically significant, and if the parameter estimates are credible.

A bootstrap procedure (Quinn et al. 2001) is used to quantify the uncertainty in estimated β and M. The effective degrees of freedom for age composition data is calculated from the deviations between the observed and estimated age compositions, following the procedure of Williams and Quinn (1998). Bootstrap replications are generated from the multinomial distribution with the effective degrees of freedom. For the abundance indices, residuals (on a logarithmic scale) are resampled with replacement and added to estimated values from the original model, following the procedure of Efron and Tibshirani (1993). The number of replications is 1000, the recommended level for calculating confidence intervals. Because it is not possible to estimate mortality M_0 from other sources, the resulting variance estimates are conditional on the fixed value of 0.25 used and, therefore, are underestimates of the total uncertainty.

Results

Major diseases

Population health of Pacific herring in Prince William Sound followed two distinct patterns from 1994 to 2000. Decreased prevalence of severe focal skin reddening (ulcers) and VHSV in spring samples from 1994 through 1996 was consistent with recovery from the major population crash of 1993 (Figs. 2*a*, 2*b*). From 1997 to 2000, another disease outbreak cycled through the population: VHSV prevalence was high in 1997 and 1998 but returned to zero in 2000. During this outbreak, the traditional age-structured assessment model predicted greater population biomass for 1998 and 1999 than did the resultant best estimates (Fig. 1). VHSV was never isolated from samples collected in the fall. Prevalence of *I. hoferi* was relatively high in all 7 years of the study, but prevalence was related more to fish age than to differences in biomass estimates (Fig. 2*c*).

Ulcer prevalence was the best external marker of fish health during the necropsy. Filamentous bacteria consistently covered ulcers. When ulcer prevalence was high, fish behavior was abnormal. For example, in 1998, we were able to catch nonspawning fish using a cast net deployed in shallow water near shore. Prevalence of moderate to severe focal skin reddening coincided with the prevalence of VHSV in all years but 1997 (Figs. 2*a*, 2*b*). Prevalence of ciliated protozoan parasites on the gills also coincided with unexpected changes in population biomass; however, none of the gill sections had more than 1 organism per filament, and all

© 2003 NRC Canada

Fig. 4. Prevalence of *Ichthyophonus hoferi* in spring samples within large year-classes: (*a*) 1988, (*b*) 1992, (*c*) 1993, and (*d*) 1994. Number above each bar indicates number of fish examined. Arbitrary reference lines are at 20% prevalence for each year-class graph. ND, no data.

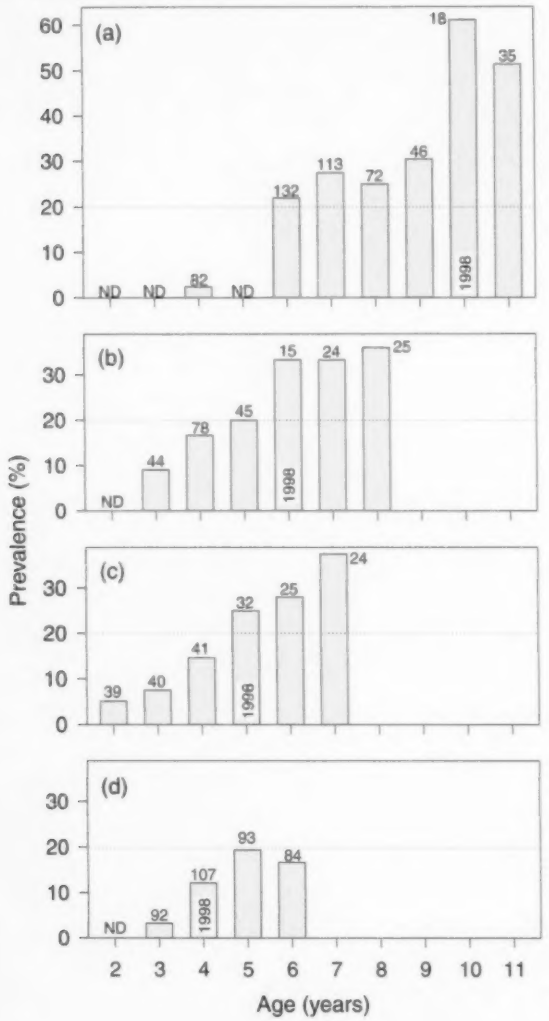

Fig. 5. Fat stores and recruitment over time: (*a*) frequency of fish with complete atrophy of pancreatic adipose tissue (score = 0); (*b*) frequency of 3-year-old fish in spring samples. ND, no data; light bars, spring samples; darker bars, fall samples.

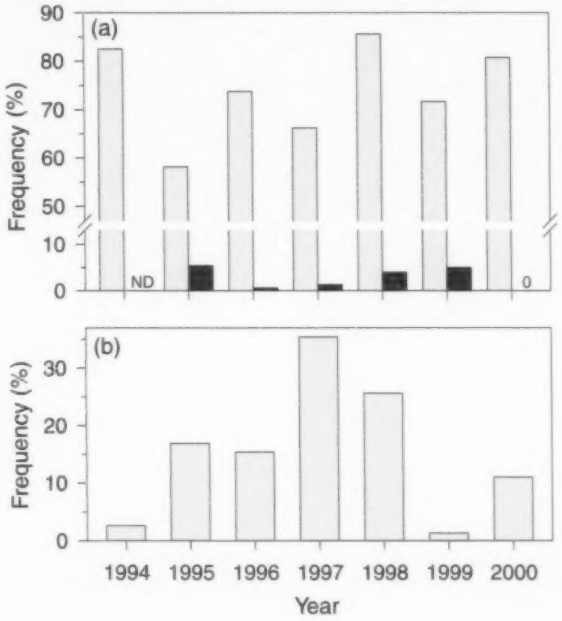

infestations were scored as mild. Because gill parasites did not meet the severity criterion, they were not considered significant causes of population change. Prevalence of ulcers and VHSV was greater in fish from Prince William Sound than in fish from the reference site (Sitka Sound). For example, only two of 730 fish sampled from Sitka Sound were VHSV positive, and both positive fish were sampled in 1997. Prevalence of *I. hoferi* was not significantly different at the two sites.

Both VHSV and *I. hoferi* were associated with significant lesions. Severe VHSV infection (titer ≥1000 plaque-forming units·mL^{-1}) was associated with decreased packed cell volume ($P = 0.007$), decreased plasma IgM ($P = 0.015$), decreased plasma glucose ($P = 0.005$), and increased total plasma protein concentration ($P = 0.001$). Fish with high VHSV titers were more likely to be infected with the gall bladder myxosporean *Ceratomyxa auerbachi* ($P = 0.007$). In 1997 and 1998, 3-year-old fish were 3.3 times more likely to be VHSV positive than were all other age groups combined ($P < 0.0001$, 95% confidence interval = 1.95, 5.45; Fig. 3); blocking for year was not significant. Fish with *I. hoferi* often had granulomatous inflammation in several organs, especially the heart, kidney, spleen, and skeletal muscle. Increasing severity scores for *I. hoferi* were associated with increased plasma aspartate aminotransferase (AST; $P < 0.0001$), IgM ($P < 0.0001$), total protein ($P < 0.0001$), and percent neutrophils ($P = 0.039$). Increasing severity scores for *I. hoferi* were associated with decreased packed cell volume ($P < 0.0001$) and decreased plasma osmolality ($P < 0.024$). *Ichthyophonus hoferi* infection severity was greater in females ($P = 0.001$), and prevalence increased with fish age ($P < 0.0001$; Fig. 3), but prevalence was not influenced by season. The increase in *I. hoferi* prevalence with age was significant for several year-classes: prevalence increased rapidly during the first 5–6 years of life, and in the 1988 year-class, it remained stable during middle age and then increased again as the fish reached old age (Fig. 4).

Potential risk factors for an outbreak of VHSV included poor body condition and a high frequency of 3-year-old fish in the population. The severity of poor body condition was estimated from pancreatic fat stores; fat stores were consistently low among fish sampled in the spring, and the highest prevalence of fish with no pancreatic fat stores occurred in the spring of 1998 (Fig. 5*a*). By comparison, few to none of the fish sampled in the fall had complete atrophy of pancre-

© 2003 NRC Canada

Fig. 6. Mean prespawning body weight of Pacific herring, *Clupea pallasi* (source: Steve Moffitt, Alaska Department of Fish and Game, P.O. Box 669 Cordova, AK 99574, U.S.A.); arbitrary reference lines highlight increasing weight at age from 1994 to 1997; age = 3 (●), age = 4 (○), age = 5 (▼).

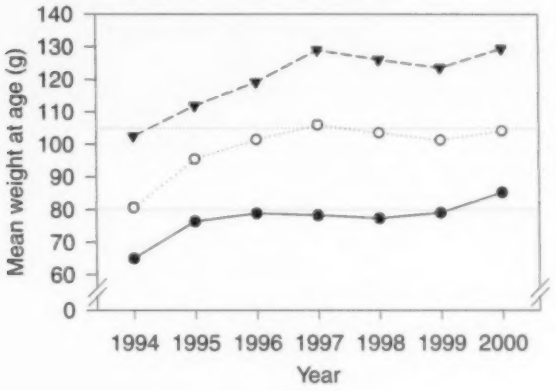

atic fat (Fig. 5*a*). The highest frequency of 3-year-old fish in the sampled population occurred in the spring of 1997 and 1998 (Fig. 5*b*), coinciding with the greatest VHSV prevalence of the study (Fig. 2*b*).

Weight-at-age provides evidence that food availability limited growth in the early 1990s but not in the late 1990s. For example, 5-year-old fish in 1994 weighed about the same as 4-year-old fish in 1996 (Fig. 6). Weight-at-age remained relatively high and constant during the 1998 disease outbreak (Fig. 6)

Population modeling of disease

Compared with the traditional model that used constant natural mortality after 1993, the disease model that included VHSV and ulcer prevalence better fitted the available population data (F test, $P = 0.04$). The best explanatory variable was an index calculated by multiplying the relative frequency of VHSV-positive fish with the relative frequency of fish with ulcers. Because some VHSV-positive fish without ulcers had evidence of disease, the prevalence of ulcers used to calculate the disease index was limited by a lower bound of 0.5%. The estimate of disease parameter β was 70, which is the multiplier of the proportion of ulcer-bearing fish that are VHSV-positive in fish collected during the spring. The bootstrap 95% confidence interval for the disease parameter β is (13, 119), indicating a significant relationship between natural mortality and disease. Although significant, the large width of the interval shows the uncertainty in the population data and the difficulty in detecting disease relationships in natural populations. Corresponding confidence intervals for natural mortality over time from the best model are narrow except for 1992–1993 and 1998 (Fig. 7*a*) when disease is operating most strongly; these intervals are conditioned on the base level $M_0 = 0.25$. Lower bounds for M are above 0.30 in 1992–1993 and 1998, the years with high disease. When *I. hoferi* prevalence was added to the population model, the estimate of the *I. hoferi* disease parameter β was zero: evidence that *I. hoferi* had no effect on changes in adult herring survival during 1994–2000.

Fig. 7. Effect of including disease information in models that estimate population size. (*a*) Conditional 95% confidence intervals for natural instantaneous mortality (±95% confidence interval) from a bootstrap procedure with 1000 replications (Quinn et al. 2001). Intervals are conditioned upon assuming that natural mortality is constant and equal to 0.25 when disease is at baseline levels. (*b*) Relative differences in traditional model estimates of prespawning biomass that used constant mortality from 1994 to 2000 (e.g., without disease information in the model, the 1999 biomass estimate was greater by about 21%). (*c*) Biomass model estimates with constant (light bars) or variable (darker bars) mortality M from 1994 to 2000. Reference line highlights biomass threshold below which commercial fisheries are closed.

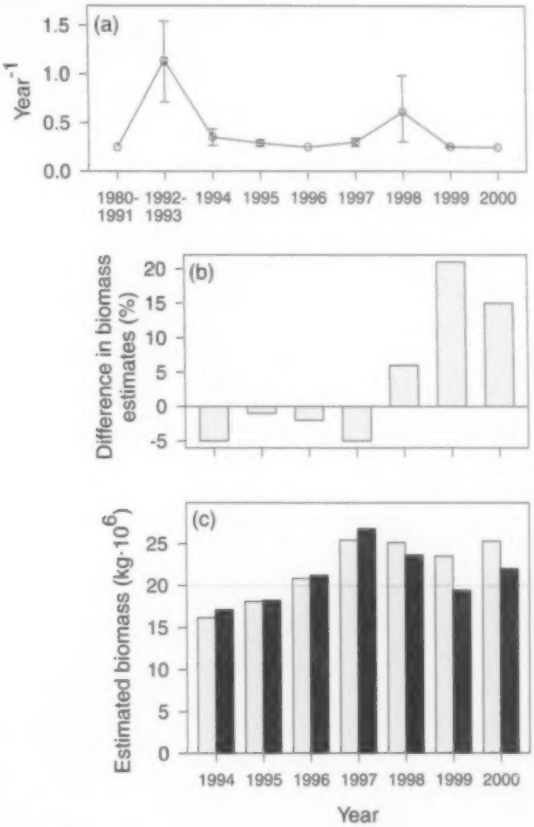

Because population models provide the basis for establishing commercial harvest quotas, errors in model estimates can put a diseased population at risk of overharvest. In Prince William Sound, differences in biomass estimates between the traditional and disease models were most distinct in 1999 (Fig. 7*b*), when the traditional model estimated a biomass above the harvest threshold (Fig. 7*c*). However, with disease information added to the model, the new model more accurately estimated biomass below the harvest threshold. Commercial fisheries were closed in 1999, and the population was protected from overfishing.

The best population model provides evidence that disease impairs recruitment. The two lowest recruitment estimates on record, in 1994 and 1999 (Fig. 5*b*), followed increased

© 2003 NRC Canada

natural mortality of adults in 1992–1993 and 1997–1998. Correspondingly, the logarithm of recruitment from the best model was negatively correlated with the disease index in the previous year (–0.92 using 1994–2000 estimates, $P < 0.01$).

Discussion

From an ecosystem perspective, disease information is crucial for understanding population dynamics. The major factors known to influence biomass of fish populations are variability in recruitment, related to environmental conditions and previous spawning biomass (Williams and Quinn 2000*b*), and fishing. This study has enlarged the perspective to show that both recruitment and adult population abundance can be strongly affected by disease. Disease reduces the lifespan of adult fish and causes mortality of juvenile fish before they mature, but until now, it has only rarely been possible to link these effects to their cause.

On a population scale, VHSV contributes more to mortality of Pacific herring when the population is young, whereas *I. hoferi* contributes more to mortality when fish are old. The age-related increase in *I. hoferi* prevalence has been previously documented among Pacific herring sampled in a single year (Marty et al. 1998; Hershberger et al. 2002), but we have shown that prevalence of *I. hoferi* increases within a year-class during most of its lifespan. Because recruitment of young fish is usually more variable than mortality rates of mature fish, VHSV has more of an effect on unexpected population change. Energy stores for overwinter survival are less in young herring than in older herring (Paul et al. 1998), and low energy stores are a risk factor for higher disease prevalence and mortality among recruiting fish. Also, younger fish have less immunity to VHSV than older fish. Laboratory studies provide evidence that Pacific herring infected with VHSV will either die or recover with immunity within about 30 days of infection, and older fish have greater innate immunity that younger fish (Kocan et al. 1997, 2001). Abundant energy stores (i.e., good body condition) and developing immunity during the summer probably both contribute to the lack of VHSV in fall samples.

The unifying feature between two distinct epidemics in Pacific herring is that poor body condition in early spring may be the most significant risk factor, regardless of the underlying mechanisms of poor condition. In the first epidemic (early 1990s), population biomass was high, summer growth was poor, and fish entered the winter of 1992–1993 with inadequate energy stores (Pearson et al. 1999). By the time that the second epidemic occurred (late 1990s), the population was low, summer growth was excellent, and fish entered the winter of 1997–1998 in good condition. However, water temperatures in Prince William Sound during the El Niño winter of 1997–1998 averaged 2 °C greater than in the winter of 1996–1997 (Foy and Norcross 2001). Warmer water temperatures increased basal metabolism, food resources were no greater than normal during the winter of 1997–1998 (Foy and Norcross 2001), and fish were in poor condition by the spring of 1998. Poor body condition in the spring of 1994 and 1998 was associated with high prevalence of VHSV and ulcers. Food availability was good after the major winter–spring disease outbreaks of 1994 and 1998, and disease prevalence in 1995 and 1999 was again low. Impacts of global warming are difficult to predict, but this study provides evidence that warmer winters increase the risk of disease outbreaks among fish populations in northern latitudes.

Acknowledgments

We thank S.D. Moffitt, N.J. Speer, C.T. Stack, F.C. Teh, W. Widmann, and T. Harrington for technical assistance. Some necropsies were performed by C.R. Davis, K.A. Burek-Huntington, K. Mero, E.F. Freiberg, S.J. Teh, and J. (Mukai) Odani. Plasma and blood analysis was under the direction of C.J. Kennedy, E.A. Thomson, and C. Ruhe. The work was supported jointly by U.S. National Science Foundation grants 9871982 and 9901351 and by the Exxon Valdez Oil Spill Trustee Council through a contract with the Alaska Department of Fish and Game.

References

Carls, M.G., Marty, G.D., and Hose, J.E. 2002. Synthesis of the toxicological impacts of the *Exxon Valdez* oil spill on Pacific herring (*Clupea pallasi*) in Prince William Sound, Alaska, U.S.A. Can. J. Fish. Aquat. Sci. **59**: 153–172.

Daniel, G.E. 1933. Studies on *Ichthyophonus hoferi*, a parasitic fungus of the herring, *Clupea harengus*. I. The parasite as it is found in the herring. Am. J. Hyg. Baltimore, **17**: 262–276.

Davis, C.R., Marty, G.D., Adkison, M.A., Freiberg, E.F., and Hedrick, R.P. 1999. Association of plasma IgM with body size, histopathologic changes, and plasma chemistries in adult Pacific herring *Clupea pallasi*. Dis. Aquat. Org. **38**: 125–133.

Efron, B., and Tibshirani, R.J. 1993. An introduction to the bootstrap. Chapman and Hall, New York.

Elston, R.A., Drum, A.S., Pearson, W.H., and Parker, K. 1997. Health and condition of Pacific herring *Clupea pallasi* from Prince William Sound, Alaska, 1994. Dis. Aquat. Org. **31**: 109–126.

Foy, R.J., and Norcross, B.L. 2001. Temperature effects on zooplankton assemblages and juvenile herring feeding in Prince William Sound, Alaska. *In* Herring: expectations for a new millennium. *Edited by* F. Funk, J. Blackburn, D. Hay, A.J. Paul, R. Stephensen, R. Toreson, and D. Witherell. University of Alaska Sea Grant AK-SG-01-04, Fairbanks. pp. 21–35.

Harvell, C.D., Kim, K., Burkholder, J.M., Colwell, R.R., Epstein, P.R., Grimes, D.J., Hofmann, E.E., Lipp, E.K., Osterhaus, A.D.M.E., Overstreet, R.M., Porter, J.W., Smith, G.W., and Vasta, G.R. 1999. Emerging marine diseases — climate links and anthropogenic factors. Science (Wash., D.C.), **285**: 1505–1510.

Harvell, C.D., Mitchell, C.E., Ward, J.R., Altizer, S., Dobson, A.P., Ostfeld, R.S., and Samuel, M.D. 2002. Ecology — climate warming and disease risks for terrestrial and marine biota. Science (Wash., D.C.), **296**: 2158–2162.

Hedrick, R.P. 1998. Relationships of the host, pathogen, and environment: implications for diseases of cultured and wild fish populations. J. Aquat. Anim. Health, **10**: 107–111.

Hershberger, P.K., Stick, K., Bui, B., Carroll, C., Fall, B., Mork, C., Perry, J.A., Sweeney, E., Wittouck, J., and Kocan, R.M. 2002. Incidence of *Ichthyophonus hoferi* in Puget Sound fishes and its increase with age of adult Pacific herring. J. Aquat. Anim. Health, **14**: 50–56.

Kocan, R., Bradley, M., Elder, N., Meyers, T., Batts, W., and Winton, J. 1997. The North American strain of viral hemorrhagic septice-

© 2003 NRC Canada

mia virus is highly pathogenic for laboratory reared Pacific herring. J. Aquat. Anim. Health, **9**: 279–290.

Kocan, R.M., Hershberger, P.K., Elder, N.E., and Winton, J.R. 2001. Epidemiology of viral hemorrhagic septicemia among juvenile Pacific herring and Pacific sand lance in Puget Sound, Washington. J. Aquat. Anim. Health, **13**: 77–85.

Lluch-Belda, D., Schwartzlose, R.A., Serra, R., Parrish, R., Kawasaki, T., Hedgecock, D., and Crawford, R.J.M. 1992. Sardine and anchovy regime fluctuations of abundance in four regions of the world oceans: a workshop report. Fish. Oceanogr. **1**: 339–347.

Marty, G.D., Freiberg, E.F., Meyers, T.R., Wilcock, J., Farver, T.B., and Hinton, D.E. 1998. Viral hemorrhagic septicemia virus, *Ichthyophonus hoferi*, and other causes of morbidity in Pacific herring *Clupea pallasi* spawning in Prince William Sound, Alaska, U.S.A. Dis. Aquat. Org. **32**: 15–40.

Mellergaard, S., and Spanggaard, B. 1997. An *Ichthyophonus hoferi* epizootic in herring in the North Sea, the Skagerrak, the Kattegat and the Baltic Sea. Dis. Aquat. Org. **28**: 191–199.

Meyers, T.R., and Winton, J.R. 1995. Viral hemorrhagic septicemia virus in North America. Ann. Rev. Fish Dis. **5**: 3–24.

Meyers, T.R., Short, S., Lipson, K., Batts, W.N., Winton, J.R., Wilcock, J., and Brown, E. 1994. Association of viral hemorrhagic septicemia virus with epizootic hemorrhages of the skin in Pacific herring *Clupea harengus pallasi* from Prince William Sound and Kodiak Island, Alaska, U.S.A. Dis. Aquat. Org. **19**: 27–37.

Patterson, K.R. 1996. Modelling the impact of disease-induced mortality in an exploited population: the outbreak of the fungal parasite *Ichthyophonus hoferi* in the North Sea herring (*Clupea harengus*). Can. J. Fish. Aquat. Sci. **53**: 2870–2887.

Paul, A.J., Paul, J.M., and Brown, E.D. 1998. Fall and spring somatic energy content for Alaskan Pacific herring (*Clupea pallasi* Valenciennes 1847) relative to age, size and sex. J. Exp. Mar. Biol. Ecol. **223**: 133–142.

Pearson, W.R., Elston, R.A., Bienert, R.W., Drum, A.S., and Antrim, L.D. 1999. Why did the Prince William Sound, Alaska, Pacific herring (*Clupea pallasi*) fisheries collapse in 1993 and 1994? Review of the hypotheses. Can. J. Fish. Aquat. Sci. **56**: 711–737.

Quinn, T.J., II, and Deriso, R.B. 1999. Quantitative fish dynamics. Oxford University Press, New York.

Quinn, T.J., II, Marty, G.D., Wilcock, J., and Willette, M. 2001. Disease and population assessment of Pacific herring in Prince William Sound, Alaska. *In* Herring: expectations for a new millennium. *Edited by* F. Funk, J. Blackburn, D. Hay, A.J. Paul, R. Stephensen, R. Toreson, and D. Witherell. University of Alaska Sea Grant AK-SG-01-04, Fairbanks. pp. 363–379.

Sherman, B.H. 2000. Marine ecosystem health as an expression of morbidity, mortality and disease events. Mar. Pollut. Bull. **41**: 232–254.

Sindermann, C.J. 1958. An epizootic in Gulf of St. Lawrence fishes. Trans. N. Am. Wildl. Conf. **23**: 349–360.

Tester, A.L. 1942. Herring mortality along the south-east coast of Vancouver Island. Fish. Res. Board Can. Prog. Rep. Pac. Coast Stn. No. 52. pp. 11–15.

Thomas, G.L., and Thorne, R.E. 2001. Night-time predation by Stellar sea lions. Nature (Lond.), **411**: 1013.

Whittington, R.J., Jones, J.B., Hine, P.M., and Hyatt, A.D. 1997. Epizootic mortality in the pilchard *Sardinops sagax neopilchardus* in Australia and New Zealand in 1995. I. Pathology and epizootiology. Dis. Aquat. Org. **28**: 1–16.

Williams, E.H., and Quinn, T.J., II. 1998. A parametric bootstrap of catch-age compositions using the Dirichlet distribution. *In* Fishery stock assessment models. *Edited by* F. Funk, T.J. Quinn II, J. Heifetz, J.N. Lanelli, J.E. Powers, J.F. Schweigert, P.J. Sullivan, and C.-I. Zhang. University of Alaska Sea Grant AK-SG-98-01, Fairbanks. pp. 371–384.

Williams, E.H., and Quinn, T.J., II. 2000*a*. Pacific herring, *Clupea pallasi*, recruitment in the Bering Sea and Northeast Pacific Ocean. I. Relationships among different populations. Fish. Oceanogr. **9**: 285–299.

Williams, E.H., and Quinn, T.J., II. 2000*b*. Pacific herring, *Clupea pallasi*, recruitment in the Bering Sea and Northeast Pacific Ocean. II. Relationships to environmental variables and implications for forecasting. Fish. Oceanogr. **9**: 300–315.

© 2003 NRC Canada

Thermal heterogeneity, stream channel morphology, and salmonid abundance in northeastern Oregon streams

Joseph L. Ebersole, William J. Liss, and Christopher A. Frissell

Abstract: Heterogeneity in stream water temperatures created by local influx of cooler subsurface waters into geomorphically complex stream channels was associated with increased abundance of rainbow trout (*Oncorhynchus mykiss*) and chinook salmon (*Oncorhynchus tshawytscha*) in northeastern Oregon. The addition of cold water patch frequency and area as explanatory variables in salmonid habitat models indicated that doubling of cold water patch frequency was associated with increases in rainbow trout and chinook salmon abundances of 31% and 59%, respectively. Doubling of cold water patch area was associated with changes of 10% in rainbow trout abundance but was not associated with chinook abundance after accounting for other habitat factors. The physiognomy, distribution, and connectivity of cold water patches, important attributes determining the effectiveness of these habitats as thermal refuges for stream fishes, were associated with channel bedform and riparian features. Monitoring of thermal heterogeneity and salmonid populations in response to ongoing habitat restoration efforts will provide additional insights into causal relationships among these factors.

Résumé : L'hétérogénéité des températures de l'eau dans les cours d'eau causée par les influx locaux d'eau souterraine plus fraîche dans des chenaux à géomorphologie complexe s'accompagne d'une abondance accrue de truites arc-en-ciel (*Oncorhynchus mykiss*) et de saumons quinnat (*Oncorhynchus tshawytscha*) dans le nord-est de l'Oregon. L'addition de la fréquence et de la surface des taches d'eau froide comme variables explicatives dans les modèles d'habitat des salmonidés montre qu'un dédoublement de la fréquence des taches d'eau froide entraîne des augmentations d'abondance chez la truite arc-en-ciel et le saumon quinnat, respectivement de 31 % et de 59 %. Un dédoublement de la surface des taches d'eau froide est associé à un accroissement de l'abondance de 10 % chez la truite arc-en-ciel, mais il n'est pas relié à l'abondance des saumons quinnat, lorsque les autres facteurs de l'habitat sont pris en compte. La physionomie, la répartition et la connectivité des taches d'eau froide, caractéristiques importantes qui déterminent l'efficacité de ces habitats comme refuges thermiques pour les poissons d'eau courante, sont associées à la forme du lit du chenal et aux caractéristiques de la berge. La surveillance de l'hétérogénéité thermique et des populations de salmonidés en réponse aux efforts de restauration permettra de mieux comprendre les relations causales entre ces facteurs.

[Traduit par la Rédaction]

Introduction

The diversity of habitats and thermal gradients may directly or indirectly influence the structure and stability of biotic communities in aquatic ecosystems, as well as the persistence of individual populations and species (Frissell et al. 1986; Townsend et al. 1997*a*; Dent et al. 2000). Development and life history events (e.g., emergence, mating, migration) of locally adapted populations of aquatic insects (Ward and Stanford 1982) and fishes (Holtby et al. 1989) are closely timed to prevailing thermal regimes. The availability of a diverse array of thermal habitats in many aquatic ecosystems provides ectothermic organisms the opportunity to behaviorally thermoregulate, optimizing their energy intake relative to physiological costs and thus affecting growth and survival (Ward and Stanford 1982; Crowder and Magnuson 1983; Berman and Quinn 1991). Thermally distinct habitats may also serve as refuges, providing critical thermal resources during periods of temperature stress (Magnuson et al. 1979). Numerous researchers have documented cold water dependent fish species persisting in warm rivers during summer months by seeking groundwater-cooled thermal refuges (Gibson 1966; Berman and Quinn 1991; Nielsen et al. 1994).

Cold water refuges for fishes within warm streams can form where subsurface and surface waters mix and are colder than ambient surface waters (Bilby 1984; Ozaki 1988). The degree and extent of hyporheic–surface water interaction, and subsequent influences on surface water temperature patterns,

Received 19 December 2002. Accepted 31 August 2003. Published on the NRC Research Press Web site at http://cjfas.nrc.ca on 7 November 2003.
J17248

J.L. Ebersole[1,2] **and W.J. Liss.** Department of Fisheries and Wildlife, Oregon State University, Corvallis, OR 97331, U.S.A.
C.A. Frissell. Pacific Rivers Council, PMB 219, 1 2nd Avenue East, Suite C, Polson, MT 59860, U.S.A.

[1]Corresponding author (e-mail: ebersole.joe@epa.gov).
[2]Present address: U.S. Environmental Protection Agency, Western Ecology Division, 200 S.W. 35th Street, Corvallis, OR 97333, U.S.A.

 doi: 10.1139/F03-107 © 2003 NRC Canada

is hypothesized to be a function of channel morphology (Poole and Berman 2001). Development and extent of hyporheic exchange with surface waters may be highly spatially variable and reflect a variety of landscape characteristics including geology, basin topography, and basin hydrology (Valett et al. 1996). Within alluvial channels, degree of hyporheic exchange is thought to be driven by channel sinuosity (Poole and Berman 2001), bed topographic complexity (Harvey and Bencala 1993), and existence of complex floodplain flowpaths (Stanford and Ward 1993). These channel structural features are also recognized as important factors contributing to the buffering or insulating characteristics of surface waters (Poole and Berman 2001) and aid the development of thermal heterogeneity within alluvial river reaches (Arscott et al. 2000).

Refuges can confer resilience to stream organisms under fluctuating or marginal abiotic conditions, but the effectiveness of refuges at sustaining populations will be dependent on the attributes of the refuge patch (Townsend et al. 1997*b*). Attributes likely to be important in determining refuge effectiveness include the spatial arrangement, frequency, and connectivity of refuge patches (Dunning et al. 1992), as well as conditions within the refuge itself. The spatial distribution and characteristics of thermal refuges within stream and river systems is therefore of interest to conservation and management of fish species in thermally marginal stream habitats.

Human disturbances in the drainage basin and floodplain that decrease the complexity and stability of riverine habitats may also reduce connectivity of surface and subsurface waters and deplete the availability of potential refuges, including cold water patches (Sedell et al. 1990; Pringle and Triska 2000; Poole and Berman 2001). However, specific linkages and associations between stream channel thermal diversity at the reach scale and the physical characteristics of floodplains and channels seldom have been explored (but see Frissell et al. 1996).

Several authors have called for the identification of the spatial distribution and characteristics of lotic habitats potentially serving as refuges (Hynes 1983; Sedell et al. 1990; Cunjak 1996). Information on the stream channel structural characteristics associated with refuge formation can help guide and refine hypotheses regarding stream management practices best suited to maintaining surface–subsurface interaction and cold water refuges in streams where ambient temperatures may exceed lethal levels for fish. Assessment of spatial heterogeneity in water temperature may be particularly relevant given that alteration of thermal heterogeneity may occur well before changes to "average" main channel temperatures are detected (Pringle and Triska 2000; Poole and Berman 2001). Because maintenance of thermal complexity may be critical for the persistence of species cued to use of thermally buffered patches (refuges), identification and monitoring of such critical habitats is needed. With the exception of Frissell et al. (1996), we are aware of no systematic efforts relating the distribution or frequency of these cold water habitats to landscape features within different portions of a drainage basin. Given the possible importance of these habitats to native cold-water fishes, including endangered species such as Snake River spring–summer chinook salmon (*Oncorhynchus tshawytscha*) and steelhead (*Oncorhynchus mykiss*), the identification of potential refuge habitats and the geomorphic conditions and land uses influencing their distribution and quality is needed. The purpose of this paper is to identify associations between thermal diversity, salmonid abundance, and channel complexity in alluvial river reaches of a semi-arid river basin. Our objectives were to characterize the distribution (e.g., frequency, relative area) of cold water patches potentially serving as thermal refuges, identify associations between cold water patch occurrence and measures of riparian condition and channel morphology, and relate salmonid abundance to cold water patch availability.

Materials and methods

Study area

The Grande Ronde River is located in the Blue Mountains of northeastern Oregon, flowing northeast to join the Snake River in southeastern Washington (Fig. 1). The region is underlain by the Grande Ronde basalts, a member of the Columbia River basalt group. Stream courses generally follow alluviated troughs; in areas of recent uplift, channels sharply dissect the basalt terrain into a mosaic of finger ridges and steep canyons (Orr et al. 1992). High topographic relief within the basin, which ranges from 300 m to over 2300 m in elevation, is associated with substantial variation in local climatic conditions and vegetation zones (Bryce and Clarke 1996). Mean annual precipitation ranges from 30 cm to over 100 cm, increasing with elevation. Vegetation in the subalpine headwater regions of the basin is characterized by grand fir (*Abies grandis*), Douglas fir (*Pseudotsuga menziesii*), and Engelman spruce (*Picea engelmanii*) forests, shifting to ponderosa pine (*Pinus ponderosa*) – Douglas fir forests with some open parklands and savannah at lower elevations (Franklin and Dyrness 1973). At all elevations, vegetative patterns have been extensively altered through logging, fire suppression, and livestock grazing. These land uses, in addition to stream channelization and removal of instream wood, have caused extensive stream and riparian habitat simplification, including loss of pools, loss of large riparian conifers, and straightening of river channels (McIntosh et al. 1994; Wissmar et al. 1994). High summertime water temperatures in the mainstem Grande Ronde and the lower portions of its tributaries create thermal barriers, restricting movements of adult salmonids and limiting the quantity and quality of available rearing habitat for juveniles (Ebersole et al. 2001). Fish species of concern include summer steelhead (*Oncorhynchus mykiss*), bull trout (*Salvelinus confluentus*), and endangered populations of Snake River spring–summer and fall chinook salmon. Land-use patterns, fish habitat, and water quality concerns make the Grande Ronde basin typical of many mixed-ownership watersheds in the western United States in which the cumulative impacts of a wide range of land uses have induced depletions and extinctions of aquatic fauna through habitat simplification and loss (Miller et al. 1989; McIntosh et al. 1994).

Study site selection

As a preliminary assessment of valley corridor geomorphology within the study area, we identified alluvial river segments (valley width more than twice the active channel width, valley gradient <4%; Ebersole 1994) within third-

© 2003 NRC Canada

Fig. 1. Sampling locations in the Upper Grande Ronde, Wenaha – Lower Grande Ronde, Catherine Creek, and Lostine River subbasins, Oregon.

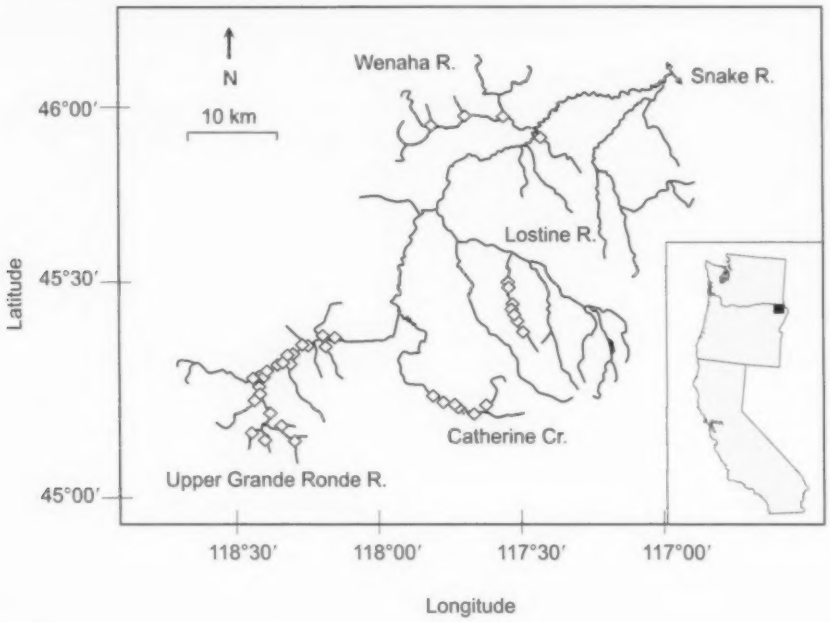

order and larger stream valleys in the Wenaha River – Lower Grande Ronde (LGR), Lostine River, Catherine Creek, and Upper Grande Ronde (UGR, above river kilometre 266) subbasins. Data on valley width and valley gradient were obtained from 7.5 min United States Geological Survey topographic maps and low-level air photos. Valley and channel type can strongly influence in-stream and riparian characteristics and provide a broad context for both physical processes and aquatic communities (Frissell et al. 1986; Montgomery 1999). Alluvial valleys were selected for this study based on the prediction that channels in alluvial valleys can be characterized by complex off-channel habitats and extensive hyporheic connectivity (Brunke and Gonser 1997; Montgomery 1999; Arscott et al. 2000). In addition, alluvial valleys have provided historically productive habitats for native fishes and possess high restoration potential (McIntosh et al. 1994). To verify segment classification, we measured valley widths, active channel widths, valley fill, and floodplain landforms during site visits.

A sampling frame listing all alluvial segments (n = 182) in the upper Grande Ronde River, Catherine Creek, Lostine, and Wenaha–LGR river subbasins was constructed. We randomly selected a representative sample of study reaches proportional to alluvial segment abundance within each subbasin from this sampling frame. We selected reaches by ordering the sampling frame first by subbasin and secondly by channel sinuosity as estimated from 7.5 min topographic maps. We then selected every fifth segment from this ordered list to obtain a desired sample size of 37. This sample size was estimated to reflect our maximum feasible workload. By ordering the sampling frame by sinuosity, we intended to increase the chances of obtaining a sample of reaches that encompasses a wider array of channel conditions than would be obtained by an unordered random sample. Maximizing variation in reach physical characteristics should optimize regression-based approaches (Neter et al. 1989). Sinuosity was chosen as the ordering criterion because it is the only measure of reach morphometric complexity (Schumm 1977) that can be determined from maps before visiting the reaches. In addition, highly sinuous channels with braiding should have highest rates of surface water – groundwater exchange through the channel bed and banks (Brunke and Gonser 1997) and thus may serve as a proxy for estimating capacity for development of groundwater-fed thermal complexity (Poole and Berman 2001).

Access to 10 reaches on private lands was denied. These reaches were replaced with reaches selected from our sampling frame based on geographic proximity and similarity of geomorphic, vegetative, and land-use characteristics. An additional four reaches in the Wenaha River mainstem could not be sampled because of higher stream flows (>6 $m^3 \cdot s^{-1}$) that would have compromised divers' abilities to effectively search all portions of the habitat for fish presence in a manner comparable with other sites. These mainstem reaches were replaced with nearby tributary reaches. Failure to incorporate all randomly selected reaches weakens the inferential power of our sample, particularly because the probability of being denied access because of landowner concerns may be related to our variables of interest (Thompson 1992; e.g., streams on properties where landowners denied access may differ from streams where permission was granted).

Field methods

Each of the 37 reaches selected was sampled once during the period of summer baseflow and maximum annual stream temperatures between 1 July and 1 September 1997. For

© 2003 NRC Canada

each reach, we measured channel and riparian characteristics that together provide an approximate measure of channel complexity, as well as factors that could influence cold water patch frequency or detectability. We used physical assessment procedures developed for the United States Environmental Protection Agency's Environmental Monitoring and Assessment Program (EMAP; Kaufmann 2002). This procedure was structured to provide rapid but quantifiable information on stream geometry and bank and riparian conditions gathered via longitudinal thalweg profiles and systematically spaced channel transects. The total stream length surveyed at each sample reach was a function of stream size and approximated 40 times the wetted channel width. Eleven equally spaced transects were established in each sampling reach, beginning at a randomly selected starting point within each reach selected from our sampling frame. At each transect, we measured active-channel cross-section dimensions (width and mean depth) with tapes and a surveying rod. Substrate mean diameter was estimated by eye at five equally spaced points along each transect and was categorized by substrate size class (Bain et al. 1985). Embeddedness, a measure of the proportion of a particle's surface surrounded by fine sand or silt substrates, was estimated visually for each substrate particle >10 cm in diameter (Kaufmann 2002). Riparian canopy cover for each transect location was estimated from an average of six spherical densiometer readings (Strichler 1959) recorded 1 m above the water surface from a midchannel location facing in four directions (upstream, downstream, left, and right) and from a position facing each bank at the channel margin. Presence of riparian vegetation from each of three vertical layers classified by height (canopy, >5 m; midstory, 0.5–5 m; ground cover, <0.5 m) was estimated from 10 m × 10 m plots centered on each bank at each transect location. Areal cover provided by in-stream and riparian objects including algae, aquatic macrophytes, large wood (>10 cm diameter and >1 m length), fine wood (any wood smaller than large wood), overhanging vegetation within 0.5 m of the water surface, overhanging banks, or boulders was estimated for that portion of stream channel within 5 m upstream and downstream of each transect.

Between transects, channel water surface gradient was estimated with a clinometer with measurements recorded to the nearest 0.5% (Platts et al. 1987). Bearing (degrees) between transects was recorded and subsequently used to calculate channel sinuosity, an index of the ratio of the channel length within the reach divided by the straight-line distance between the two reach ends (Kaufmann 2002). An additional wetted-width measurement was taken between each pair of transects. Between transects, thalweg profiles (maximum depth) were measured at 10 equally spaced intervals. Large wood pieces >10 cm diameter and >1 m in length that were partially or completely within the active channel were counted and summed for the entire reach. Mean lengths and widths of pool mesohabitat types (Bisson et al. 1982) were estimated from at least three measurements along each dimension, and total pool area was calculated for the entire reach as the proportion of total reach area.

We surveyed each reach for the presence of discrete areas of colder water more than 3 °C colder than the adjacent ambient stream flow (Ozaki 1988), henceforth "cold water patches". These thermal habitat patches are formed by upwelling or seepage of colder subsurface waters into surface channels. Sources of cold water to cold water patches may include "true" deep aquifer groundwater, shallow groundwater, hyporheic flow, hillslope groundwater, or through-gravel flow (Ozaki 1988). Similar features have been identified in previous studies as "cold pools" (Ozaki 1988; Keller et al. 1990), "cool water areas" (Bilby 1984), and "stratified pools" (Nielsen et al. 1994). Cold water patches used by fish, presumably to avoid stressful thermal conditions, have also been termed "cold water refuges" (Kaya et al. 1977). Cold water patches are also created by surface tributary inflow and provide important thermal habitats for aquatic vertebrates, but we did not include these areas because they are readily identifiable in the field or from maps. Our objective was to focus on the much more cryptic and poorly understood groundwater-fed habitats.

We used handheld digital thermometers (model 39658-K, accuracy ±0.1 °C, response rate < 0.5 s; Cooper-Atkins Corp., Middlefield, Conn.) attached to probes 5 m in length to locate cold water patches in the selected study reaches (Ebersole et al. 2001). Thermal surveys consisted of methodically sweeping the thermometer probe back and forth within 5 cm of the stream channel bottom while wading upstream. A minimum sweep frequency of one sweep per linear metre of stream channel was maintained along the channel margins to maximize the probability of detection of small cold water patches. In the channel thalweg, we swept the probe along the channel bottom once every 5 m. This distribution of effort is based on prior research in which we found 86% (162/188) of the observed cold water patches within 1/4 channel width of the channel margin (Ebersole 1994). In previous studies, we observed that cold water patches >1/4 channel width from the stream margin were mostly large stratified pools that should be readily detected by a 5-m sweep frequency (Ebersole 1994). When temperatures more than 3 °C cooler than the ambient stream flow were encountered, we delineated the spatial bounds (region more than 3 °C cooler than ambient) of the cold water patch with intensive probing. Because temperatures in cold water patches reflect not only the input of subsurface flow but may also be influenced by mixing with ambient stream water, temperatures (and thus the spatial boundaries of the cold water patch) are constantly shifting as the ambient stream flow heats and cools through the day. Changes in stream flow, as well as in the quantity and temperature of groundwater seeping into the cold water patch, are likely to change daily and over the course of the summer. This variation represents a potential source of measurement error. To minimize this, we restricted sampling of cold water patches to afternoon periods (1200–1800) when ambient stream temperatures approached daily maxima and cold water patch volumes were minimized. This ensured that our estimate of total cold water patch volume was most accurate with respect to the period of maximum potential biological risk due to high ambient stream temperatures (e.g., when ambient temperatures were highest and cold water patch volumes were smallest because of diel warming). However, restricting sampling to periods of minimal cold water patch volume and maintaining a scanning frequency of one sweep per meter increased our likelihood of overlooking small cold water patches (<0.5 m in any dimen-

© 2003 NRC Canada

sion). Thus our cold water patch frequency estimates are likely underestimates.

In each cold water patch, we measured maximum width, length, and depth and estimated mean values for each dimension from a minimum of three measurements. To assess degree of spatial isolation of the cold water patch from the main channel, we measured the distance of the cold water patch from the main channel (cold water patch distance) and the minimum depth of the corridor between the cold water patch and the main channel (crest depth; Ebersole et al. 2003). Where cold water patches were immediately adjacent, within, or extended to the main channel, distance was recorded as zero. Longitudinal variation in temperature within cold water patches was assessed by measuring the maximum range in temperature along the longest horizontal axis of the cold water patch (spatial temperature range). Each cold water patch was sketched to illustrate its position with respect to the stream channel and location of measurement points.

Temperature loggers (Optic StowAway, accuracy ±0.2 °C; Onset Computer Corp., Pocasset, Mass.) were placed in the coldest portion of each cold water patch for at least 24 h to record diel temperature patterns. StowAway temperature loggers also were placed in a well-mixed portion of the adjacent ambient stream flow to measure ambient stream temperatures. Temperature loggers were programmed to record at 30-min intervals. Temperatures within 27 cold water patches and 37 main-channel locations were monitored for the period of 1 July to 1 September 1997 to assess temporal trends and seasonal maxima. Temperatures for cold water patches and adjacent main channel sites were summarized using a weekly average daily maximum statistic, computed as the average of the maximum daily water temperatures for the warmest, consecutive 7-day period during the year (hereafter, maximum temperature). This statistic is frequently used in regional water quality standards (Debra Sturdevant, Oregon DEQ, 811 SW Sixth Avenue, Portland, Oreg., personal communication). As an index of daily temporal variability in water temperature, mean diel flux was estimated for the period of 1 July to 1 September, calculated as the average difference between the daily maximum and minimum temperatures recorded at a site. To compare cold water patch temperatures and adjacent mainstem temperatures, we calculated the mean difference between the daily maximum temperatures of the cold water patch and the daily maximum temperatures of the adjacent main channel site (ΔT) for the period of 1 July to 1 September.

Each of the 37 sample reaches was visited by a team of two to three snorkelers to identify and count fish species. Concerns of possible disturbance or injury to endangered Snake River spring–summer chinook salmon associated with handling necessitated reliance on uncalibrated, visual estimates of abundance. Snorkelers used the underwater methods of Thurow (1994), moving slowly upstream through the reach and counting all fish observed. Fish were identified to species and classified into 5-cm length categories. Counts were standardized by sampling area and reported as total reach densities (number·100 m^{-2}).

Snorkel surveys were conducted during afternoon periods for all reaches (generally 1400–1800) to minimize effects of time of day on snorkel counts. Mark–recapture estimates of efficiency of snorkeling efforts using methods similar to ours at temperatures of 14 °C to 18 °C range from 40% to 90% (Hillman et al. 1992). Thus our counts are almost certainly underestimates of abundance. We assume equal sampling efficiency among sites using our methods. Although this assumption is untested and may be invalid (Bayley and Dowling 1993), we attempted to minimize variation in sampling efficiency by restricting sampling to periods when visibility exceeded distance between divers and used handheld lights and searched substrate crevices and undercut banks for concealed fish in complex habitats.

Data management and analysis

Before all statistical tests and model building, data were screened for multivariate outliers (>2 standard deviations above mean average Sorensen's distance measure between all sites; Tabachnick and Fidell 1996). Only one reach was identified as a potential multivariate outlier. In this reach (Jordan Creek), surface stream flow ceased in midsummer, creating a series of pools connected only by subsurface flow. The ephemeral flow conditions at this site were deemed atypical and data for this reach were subsequently removed as outliers.

Univariate data were screened for normality by plotting frequency histograms of all variables and examining skewness and kurtosis scores. Variables were transformed where necessary using log, arcsine, and square-root transformations to approach normal distributions (Table 1). When reasonable normality could not be achieved through these transformations, data were converted to dichotomous or quartile values. Variable biplots were examined for apparent departures from linearity that might suggest need for polynomial factors in regression equations. Residuals from regression analysis were also examined for constant error variance and normality using residual plots and normal probability plots.

We performed multiple regression and correlation analyses using SAS version 8.1 (SAS 1999) and Statgraphics version 5 (Manugistics Inc. 2000) to identify associations between reach characteristics, cold water patch availability, and salmonid abundance. We conducted three separate analyses to test these associations. To identify factors associated with the frequency and area of cold water patches in stream reaches, we developed models using cold water patch frequency and cold water patch relative area as response variables and habitat characteristics of stream reaches as explanatory variables. We restricted the set of potential explanatory variables to a subset of reach-level metrics that were relatively uncorrelated (Pearson's $r < 0.40$, $P > 0.10$) and were believed to be relatively robust estimators of stream ecological condition (Kaufmann 2002; Table 1). Correlation analysis (Pearson's r) was used to identify relationships between cold water patch characteristics (including distance from main channel, crest depth, maximum depth, cold water patch riparian density, cold water patch temperature range, and cold water patch maximum temperature) and reach characteristics included in best-subsets regression models. The significance level for individual correlations was adjusted to maintain an experimentwise $\alpha = 0.10$ by using the Bonferroni adjustment in which the adjusted significance level was equal to 0.10 divided by the total number of tests performed (Zar 1984).

To evaluate the relationship between cold water patch availability and salmonid abundance, we used a model-averaging

© 2003 NRC Canada

Table 1. Mean, minimum, and maximum values and coefficients of variation (CV) of environmental characteristics from 37 alluvial river reaches in the Grande Ronde basin.

Metric	Mean	Minimum	Maximum	CV (%)	Transformation
Elevation (m)*	1076	525	1513	24	—
Cold water patch total area (m^2)	94.8	0	482.19	165	—
Cold water patch proportional area ($m^2 \cdot m^{-2}$)*	0.03	0	0.30	276	Arcsine(x)
Cold water patch frequency (number·100 m^{-1})*	0.39	0	1.6	107	$\text{Log}_{10}(x + 0.01)$
Mean thalweg depth (m)	0.41	0.035	1.16	63	$\text{Log}_{10}(x)$
Mean channel wetted width (m)	10.56	0.28	34.58	87	$\text{Log}_{10}(x)$
Mean channel wetted width–depth ratio*	26.44	12.17	55.25	49	$\text{Log}_{10}(x)$
Proportion of channel as pool*	0.18	0	0.55	83	Arcsine(x)
Maximum daily temperature (°C)	21.04	11	30.00	24	—
Maximum 7-day mean daily maximum temperature (°C)*	20.23	10.59	27.60	23	—
In-channel large wood (pieces·100 m^{-1})*	25.24	0	125.16	145	$\text{Log}_{10}(x + 0.1)$
Reach riparian density*	0.15	0.02	0.66	113	Arcsine(x)
Substrate embeddedness (%)*	32.40	15.2	52.73	25	—
Channel slope (%)*	1.67	0.71	2.90	35	—
Sinuosity*	1.18	1.02	1.54	14	$\text{Log}_{10}(x)$
Proportion of reach with three-layer riparian cover	0.63	0	1.00	36	Arcsine (x)

Note: Asterisks indicate metrics used in multiple regression analysis after applying appropriate transformation.

approach in which we calculated a weighted average coefficient estimate and associated P value of cold water patch availability on salmonid abundance across several likely candidate salmonid-habitat models. This approach helps minimize model selection uncertainty associated with approaches that evaluate one "best" model, as well as reducing uncertainty associated with individual parameter estimation (Ramsey and Schafer 1997). Candidate models were derived using best-subsets regression with rainbow trout or chinook salmon density as the response variables and reach habitat characteristics (Table 1) as potential explanatory variables. Models were assessed and ranked according to Schwarz's Bayesian information criterion (BIC) scores. The BIC is based on probability theory and also provides a means to rank models based on model variance and number of parameters. Models with smaller values of BIC are preferred (Ramsey and Schafer 1997). We did not include cold water patch frequency and cold water patch area as potential explanatory models in this first set of models. Instead, to estimate the influence of cold water patch frequency and cold water patch area on salmonid densities after accounting for the effect of other habitat factors, cold water patch frequency and cold water patch area were subsequently added as explanatory variables to the 10 best-subset models for rainbow trout and chinook density. To examine the reliability of individual cold water patch frequency and cold water patch area parameter estimates for the best 10 habitat models for chinook salmon and rainbow trout, we calculated Bayesian posterior probability estimates, $\Pr\{M_i|D\}$, given the data (D) for each model i (M_i):

$$\Pr\{M_i|D\} = \Pr\{M_i\} \exp\{-\text{BIC}_i\} / \sum_{i=1}^{10} \Pr\{M_i\} \exp\{-\text{BIC}_i\}$$

Prior probabilities, $\Pr\{M_i\}$, were assumed equal among candidate models. Posterior probability estimates then were used to weight cold water patch parameter estimates and P values for each model. Weighted cold water patch parameter estimates and P values, $f(\delta)$, were calculated as follows:

$$f(\delta) = \sum_{i=1}^{10} f(\delta|m_i) \Pr\{M_i|D\}$$

Thus the Bayesian posterior probability estimates account for model selection uncertainty when assigning a probability that the effect of cold water patch frequency or cold water patch area is greater than zero (Ramsey and Schafer 1997).

Effects of cold water patch frequency on chinook salmon and rainbow trout densities were estimated using the most likely model for each species. Estimates were plotted to illustrate projected effects of cold water patch availability under typical habitat conditions. Stream habitat parameters included in the most likely models were held constant, using median values derived from the study sites, while allowing cold water patch frequency to vary across the range observed among the study sites.

Polynomial terms were included as potential variables when suggested by nonlinear scatterplots of the response variable on individual factors. Interaction terms were not considered with the exception of the interaction of maximum temperature and cold water patch frequency. This interaction was included because of our explicit a priori assumption that the influence of cold water refuges should increase as water temperatures increase (Ebersole et al. 2001). To account for potential effects of subbasin location on response variables (Dunham and Vinyard 1997), we included catchment location (Upper Grande Ronde, Lostine, Catherine Creek, or Wenaha–LGR subbasin) as an indicator variable in all final regression models. We used the variance inflation factor (VIF) as a diagnostic of multicollinearity in multiple regression models. VIF values greater than 10 indicate substantial problems with multicollinarity (Neter et al. 1989).

Results

Maximum stream temperatures exceeded 26 °C, the approximate upper incipient lethal temperature for salmonids such as rainbow trout and chinook salmon under laboratory conditions (McCullough 1999), at some point during the

© 2003 NRC Canada

summer sampling period in five of 37 reaches. Summertime daily maxima ranged from 11 °C to 30 °C (mean = 21 °C) and peaked in late July for all sites except those in the Lostine River subbasin, which attained summer maxima in mid-August. Salmonids used cold water patches frequently during warm periods as has been documented elsewhere within the region (Ebersole et al. 2001). For a subset of cold water patches monitored throughout the summer in a companion study, the proportion of salmonids within a reach observed within cold water patches varied with ambient stream temperature, averaging 2% at ambient temperatures of 9 °C to 16 °C and averaging 54% at ambient temperatures of 22 °C to 24 °C (J.L. Ebersole, unpublished data).

Cold water patch frequency and relative area: associations with reach level metrics

Within the 16 km of stream channel surveyed, we observed a total of 57 cold water patches, for a mean frequency of 0.39 cold water patches/100 m of stream channel length. Among sites where cold water patches occurred, cold water patch frequency was negatively associated with mean reach wetted channel width–depth ratio ($F = 7.89$, $P = 0.009$, $R^2 = 0.22$). No other reach level characteristics, including channel sinuosity, proportional pool area, substrate embeddedness, or canopy density, were significantly associated with reach cold water patch frequency when considered singly or together in a best-subsets multiple regression model analysis (two-sided t test; $P > 0.05$ for all factors).

The proportion of total reach area comprised of cold water patches ranged from 0% to 30% but was highly variable among sites relative to channel and riparian characteristics. None of the reach characteristics was significantly correlated (Pearson's r, $P > 0.10$) with cold water patch area, and subsequently, no significant multiple regression models relating relative cold water patch area to reach characteristics were obtained.

Characteristics of cold water refuges were associated with reach characteristics. Distance of the cold water patch from the main channel, a measure of degree of potential isolation for fishes moving between mainstem and stream margin habitats, was positively correlated with channel width–depth ratio (Pearson's $r = 0.65$, $P < 0.003$) and inversely related to channel sinuosity (Pearson's $r = -0.64$, $P < 0.003$). Maximum temperatures within cold water patches were inversely related to the frequency of large wood and proportion of pools within reaches ($r = -0.64$, $P = 0.003$; $r = -0.63$, $P < 0.003$, respectively; Table 2).

Salmonid abundance: associations with reach level metrics and cold water patch availability

Abundance of rainbow trout and chinook salmon was related to several reach characteristics. The best habitat models, as ranked by the BIC, explained between 69% and 76% of the variation in chinook salmon abundance among sites (Table 3). The BIC assigned highest posterior probabilities to two models: Ch1 and Ch2. Both models include channel width–depth ratio and proportional pool area. These parameters also are included in all of the other 10 best models, and parameter estimates for channel width–depth ratio and proportional pool area are relatively consistent across models, suggesting that chinook abundance was negatively associated with increasing width–depth ratio (i.e., decreasing depth and increasing width) of channels and positively associated with the proportional pool area available (Table 3). An indicator variable for locations within the Catherine Creek subbasin was also included in Ch1 and Ch2, indicating higher densities of chinook salmon within Catherine Creek sites relative to other subbasins after accounting for variation in other habitat parameters in the models. Ch2 included a parameter estimate for channel sinuosity. The addition of sinuosity to Ch1 increased the total variance explained by 4%. The parameter estimate for sinuosity is consistently negative among seven of the top 10 models, suggesting that chinook salmon density declined with increasing channel sinuosity among our sites. Other factors included in the less likely models (i.e., Bayesian posterior probability <0.06) were wood frequency and indicator variables for Lostine and Wenaha subbasin locations, substrate embeddedness, and maximum temperature (Table 3).

Rainbow trout density was associated consistently with several factors that were included in the two most likely models (Rb1 and Rb2), as well as most of the best models. These factors included riparian canopy density, which was positively associated with rainbow trout abundance, and maximum temperature, which was negatively associated with rainbow trout density. Densities of rainbow trout were lower within sites in the Lostine and Wenaha subbasins, after accounting for maximum temperature and canopy density. Rainbow trout densities increased with decreased substrate embeddedness among sites (Table 4). Proportional pool area and channel sinuosity were positively associated with rainbow trout abundance in a few of the models (Table 4).

Addition of cold water patch frequency and proportional cold water patch area to the best habitat models for chinook salmon indicated that cold water patch frequency was associated with chinook density after accounting for other habitat factors (Bayesian posterior means coefficient estimate for CpF = 0.60, Bayesian posterior probability = 0.06; Table 5). This effect level is equivalent to an increase in chinook density of 52% (95% confidence interval = 0–128%) for each doubling of cold water patch frequency (Fig. 2). Proportional cold water patch area was not associated with chinook density after accounting for other habitat factors (Bayesian posterior means coefficient estimate = 0.12, Bayesian posterior probability = 0.18; Table 5).

Addition of cold water patch frequency and proportional cold water patch area to models for rainbow trout indicate that increases in cold water patch frequency were associated with increased abundance of rainbow trout after accounting for other habitat factors (Bayesian posterior means estimate = 0.39, Bayesian posterior probability = 0.04; Table 6). This effect level is equivalent to an increase in rainbow trout density of 31% (95% confidence interval = 3–65%) for each doubling of cold water patch frequency (Fig. 2). Proportional cold water patch area was also positively associated with increased rainbow trout abundance (Bayesian posterior means estimate for CpA = 0.14, Bayesian posterior probability = 0.04; Table 6). Among our sites, rainbow trout abundance increased 10% (95% confidence interval = 1–20%) with each doubling of cold water patch area.

© 2003 NRC Canada

Table 2. Correlation matrix of reach-level and cold water patch characteristics.

Variable	IsolatD	CpCrest D	CpMaxD	CpCanD	CpTempRange	CpMaxT	EM	WD	PP	WdF	CAN
CpCrestD	–0.49	—									
CpMaxD	–0.01	0.62	—								
CpCanD	–0.20	–0.00	0.01	—							
CpTempRange	0.42	–0.44	–0.14	–0.22	—						
CpMaxT	0.31	–0.44	–0.62	–0.35	0.21	—					
EM	0.42	–0.34	–0.10	0.19	0.26	0.11	—				
WD	0.65*	–0.34	–0.04	–0.50	0.60	0.53	0.18	—			
PP	–0.47	0.44	0.36	0.30	–0.37	–0.64*	–0.21	–0.64*	—		
WdF	0.06	0.13	0.48	0.24	–0.05	–0.63*	0.27	–0.08	0.23	—	
CAN	–0.34	–0.12	–0.13	0.47	–0.04	–0.06	–0.23	–0.47	0.12	–0.05	—
SIN	–0.64*	0.51	0.06	0.14	–0.36	–0.12	–0.17	–0.47	0.53	–0.24	–0.11

Note: Pearson's r values are shown. Significant correlations ($P < 0.10$ after Bonferroni adjustment) denoted with asterisks. IsolatD, $\log_{10}$ cold water patch distance from main channel (m); CpCrestD, minimum depth of corridor between cold water patch and main channel (m); CpMaxD, $\log_{10}$ cold water patch maximum depth (m); CpCanD, arcsine cold water patch riparian canopy density; CpTempRange, difference between cold water patch spatial maximum and spatial minimum (°C); CpMaxT, maximum spatial temperature of cold water patch (°C); EM, mean reach substrate embeddedness; WD, $\log_{10}$ mean reach channel width–depth ratio; PP, arcsine proportional reach pool area; WdF, $\log_{10}$ reach in-channel large wood frequency (number pieces·100 m^{-1}); CAN, arcsine mean reach riparian canopy density; SIN, $\log_{10}$ channel sinuosity.

Discussion

The interaction of surface and hyporheic water and deep groundwater flow sources along the riverbed creates complex flow paths at spatial scales ranging from catchment ($1–10^2$ km) to reach ($10^2–10^3$ m; Wondzell and Swanson 1996) and channel unit (1–10 m; Brunke and Gonser 1997; Boulton et al. 1998; Poole and Berman 2001). Differential mixing and heating of these flow sources can create spatially diverse patterns of temperature over distances of many kilometres via downstream warming or cooling of the main water column at the catchment scale (Beschta et al. 1986; Torgersen et al. 1999; Poole and Berman 2001), localized cool or warm habitat patches in pools or side channels at the reach scale (Bilby 1984; Ozaki 1988; Arscott et al. 2000), or vertically and laterally within the channel and substrate at the channel-unit and microhabitat scales (Shepherd et al. 1986; Hendricks and White 1991; Fig. 3). The cold water patches that we describe in this paper are one example of thermal diversity at the reach and channel-unit scales providing opportunities for fish thermoregulation in warm streams.

The associations that we observed are suggestive of potential linkages between the characteristics and occurrence of cold water patches in streams and channel and riparian structure. Channel configuration and structural complexity can influence the degree to which cold water inflow is intercepted and stored. Numerous authors have suggested that floodplain isolation and channel simplification associated with channelization, logging, and other land uses in general disconnect desirable stream–land interactions, including groundwater – stream water interchange (Bilby 1984; Pringle and Triska 2000; Fernald et al. 2001). As channels became wider and shallower among our study sites (width–depth ratio increased), distances of cold water patches from the main channel increased. As channel width–depth ratio increased, frequency of cold water patches declined, though much of the variation in cold water patch frequency remained unexplained in our simple model ($R^2 = 0.22$).

Variation in detected cold water patch frequencies between reaches likely reflects an array of processes, many of which were not considered in this study. Whitehead (1992) suggested that groundwater movements in basalt, which comprises most of our study area, may be locally heterogeneous because of bedrock fractures and faulting that may not be directly associated with the morphology of alluvial channels. Intrusions of deep groundwater may therefore overwhelm and obscure patterns of stream water – subsurface water interchange at the reach and channel-unit scale. Land uses may also influence groundwater – stream water interchange rates and temperatures. Logging or other vegetation removal can lead to increases in shallow groundwater temperature (Hewlett and Fortson 1982; Holtby 1988). Changes in timing and magnitude of peak flows associated with logging or river regulation may alter floodplain recharge and the subsequent release into stream channels (Shepherd et al. 1986). Coarse sediments from roads, grazing, or logging may induce channel aggradation, widening, and structural simplification, thereby increasing surface-water exposure to solar radiation (Beschta et al. 1986). Our observation that maximum temperatures within cold water patches were higher in reaches with lower frequencies of large wood and fewer pools is consistent with hypotheses linking channel simplification, straightening, and widening to increased fragmentation of cold water refuges (Poole and Berman 2001).

Channel width–depth ratio, a dimensionless index of channel shape, may serve as a useful indicator of a suite of processes (e.g., bed load dynamics, stream-bank and riparian vegetation condition) influencing aquatic habitats within alluvial channels. Channel width–depth ratio may be sensitive to riparian and watershed management, responding directly (widening and shallowing) in response to increases in sediment supply or loss of bank stability, or inversely (narrowing and deepening) in response to increases in stream transport power or increased bank resistance (Leopold et al. 1964). Channel width–depth ratio is also frequently correlated with pool frequency in alluvial channels, as was observed in this study, and has been used as an index of channel recovery following human changes to streams and watersheds because of its sensitivity both to on-site influences such as riparian vegetation and bank condition associated with livestock

© 2003 NRC Canada

Table 3. Habitat models relating chinook (Ch) density to channel wetted width–depth ratio (WD), proportional pool area (PP), channel sinuosity (SIN), mean substrate embeddedness (EM), large wood frequency (number·100 m^{-1}), maximum 7-day mean maximum daily temperature (MaxT), and subbasin location (LOS, Lostine; WEN, Wenaha; CAT, Catherine).

					Model parameter estimates									
Model	BIC	BPP	R^2	R^2_{adj}	Intercept	WD	PP	SIN	EM	WdF	MaxT	CAT	LOS	WEN
Ch1	–7.64	0.37	0.70	0.67	7.02	–4.63**	2.44**					0.69*		
Ch2	–7.50	0.32	0.74	0.69	7.67	–4.91**	2.84**	–6.42*				0.72*		
Ch3	–6.48	0.12	0.69	0.65	9.32	–5.98**	2.10**	–6.03**						
Ch4	–5.84	0.06	0.71	0.66	7.27	–4.61**	2.52**		–0.01*			0.70*		
Ch5	–5.34	0.04	0.70	0.65	9.49	–5.81**	3.00**	–9.06**					–0.53*	
Ch6	–5.18	0.03	0.74	0.68	7.64	–4.81**	2.92**	–9.58**				0.86**		0.89*
Ch7	–5.10	0.03	0.74	0.68	7.82	–5.48**	3.01**	–8.13**		0.64*			–1.04**	
Ch8	–5.09	0.03	0.70	0.65	4.83	–5.11**	2.08*			0.72**			–0.76*	
Ch9	–3.35	0.01	0.76	0.69	9.44	–5.46**	4.00**	–11.56**	–0.05*	0.83**			–1.42**	
Ch10	–2.88	<0.01	0.75	0.67	9.63	–4.27**	2.54**	–8.82**		0.42*	–0.12*		–1.80**	

Note: BPP, Bayesian posterior probability; BIC, Bayesian information criterion. Model parameter estimates significantly different from zero (two-sided t test) are denoted with ** ($P < 0.05$) or * ($P < 0.10$).

Table 4. Habitat models relating rainbow trout density to channel wetted width–depth ratio (WD), proportional pool area (PP), channel sinuosity (SIN), mean substrate embeddedness (EM), large wood frequency (number·100 m^{-1}), maximum 7-day mean maximum daily temperature (MaxT), riparian canopy density, and subbasin location (LOS, Lostine; WEN, Wenaha).

					Model parameter estimates									
Model	BIC	BPP	R^2	R^2_{adj}	Intercept	WD	PP	SIN	EM	WdF	MaxT	CAN	LOS	WEN
Rb1	–15.91	0.49	0.67	0.60	6.04**		1.21*		–0.03*		–0.14**	1.79**	–2.34**	–0.64**
Rb2	–15.00	0.20	0.66	0.59	5.54**			6.89*	–0.03**		–0.14**	2.07**	–2.47**	–0.64**
Rb3	–14.53	0.12	0.62	0.56	6.86**				–0.03**		–0.16**	1.76**	–2.41**	–0.57**
Rb4	–13.47	0.04	0.68	0.60	5.44**		0.53*	5.54*	–0.03**		–0.13**	2.01**	–2.12**	–0.66**
Rb5	–13.40	0.04	0.68	0.60	4.48**			7.50**	–0.03**	0.39*	–0.12**	2.15**	–2.25**	–0.65**
Rb6	–13.25	0.03	0.61	0.55	4.81**		1.13*		–0.02**		–0.11**	1.93**	–2.12**	
Rb7	–13.04	0.03	0.57	0.51	2.72**				–0.02**		–0.13**	1.89**	–2.18**	
Rb8	–12.95	0.03	0.68	0.60	5.72**	–1.00*	0.94*		–0.02**		–0.08**	1.73**	–1.89**	–0.79**
Rb9	–12.37	0.01	0.64	0.56	4.77**	–0.32*			–0.03**		–0.11**	2.08*	–2.17**	–0.60*
Rb10	–12.29	0.01	0.60	0.53	7.92**			5.35*	–0.04**		–0.17**		–2.50**	–0.82**

Note: BPP, Bayesian posterior probability; BIC, Bayesian information criterion. Model parameter estimates significantly different from zero (two-sided t test) are denoted with ** ($P < 0.05$) or * ($P < 0.10$).

© 2003 NRC Canada

Table 5. Estimated effect of cold water patch frequency (CpF; cold water patches·100 m^{-1}) and proportional relative cold water patch area (CpA; $m^2 \cdot m^{-2}$) on chinook salmon densities (log_{10} number·100 m^{-2}) after addition to 10 best habitat models.

			Addition of CpF			Addition of CpA		
Habitat model	Parameters	BIC	Coefficient estimate	SE	*P*	Coefficient estimate	SE	*P*
Ch1	WD, PP, CAT	–7.64	0.63	0.35	0.05	0.12	0.15	0.17
Ch2	WD, PP, SIN, CAT	–7.50	0.59	0.34	0.05	0.14	0.12	0.12
Ch3	WD, PP, SIN	–6.48	0.62	0.36	0.05	0.08	0.12	0.25
Ch4	WD, PP, CAT, EM	–5.84	0.57	0.42	0.09	0.12	0.13	0.18
Ch5	WD, PP, SIN, LOS	–5.34	0.53	0.37	0.08	0.10	0.13	0.23
Ch6	WD, PP, SIN, CAT, WEN	–5.18	0.55	0.34	0.06	0.17	0.13	0.09
Ch7	WD, PP, SIN, LOS, WdF	–5.10	0.42	0.36	0.12	0.04	0.13	0.37
Ch8	WD, PP, LOS, WdF	–5.09	0.51	0.37	0.09	0.13	0.13	0.46
Ch9	WD, PP, SIN, LOS, WdF, EM	–3.35	0.74	0.49	0.07	0.03	0.13	0.39
Ch10	WD, PP, SIN, LOS, WdF, MaxT	–2.88	0.38	0.34	0.14	0.09	0.13	0.25

Note: BIC, Bayesian information criterion. Parameter coefficient estimate, standard error (SE), and one-sided *P* value are shown. Habitat model parameter codes and parameter estimates are provided in Table 3.

Fig. 2. Estimated effect of cold water patch frequency on rainbow trout (solid circles) and chinook salmon (open circles) densities.

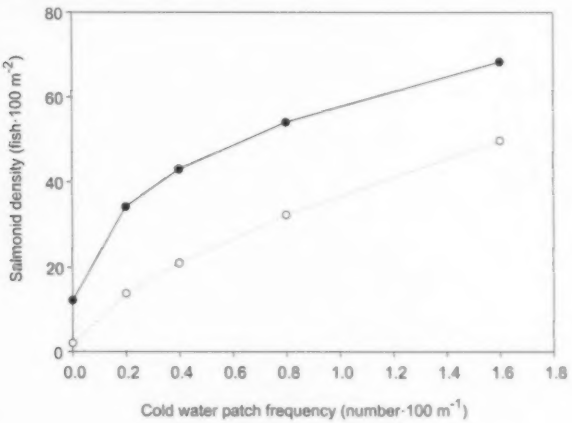

grazing (Platts 1991) and catchment-scale processes including sediment supply and basin hydrology.

The relationships of salmonid abundance to habitat characteristics identified in the habitat models are plausible, given relationships identified from the expansive literature on salmonid habitat relationships in streams (e.g., reviewed by Fausch et al. 1988). Juvenile chinook salmon and rainbow trout differed with respect to stream habitat characteristics that were important in our multiple regression models for abundance. Proportional pool area was positively associated with abundance of chinook salmon in this study. Proportional pool area was not significantly associated with rainbow trout abundance in our best-subsets models, although parameter estimates for proportional pool area approached significance ($P < 0.10$). Proportional pool area is an index of habitat unit composition and hydraulic conditions within a stream reach. Pools, particularly those providing complex cover and flow refuges, can provide critical overwintering habitats for salmonids (Solazzi et al. 2000). Similarly, in streams with low summertime base flows, pools can provide depth cover for stream fishes and may serve as refuges from drought or predation (Harvey and Stewart 1991; Lonzarich and Quinn 1995). Chinook salmon generally use pool habitats to a greater extent than rainbow trout, which may be better suited morphologically for foraging in faster-water habitats (Bisson et al. 1988).

Riparian canopy density was positively associated with abundance of rainbow trout but not chinook salmon in our habitat models. Riparian canopy density provides an index of riparian vegetation height and structure. Riparian vegetation is associated with important sources of invertebrate prey for stream fishes (Nakano et al. 1999) and has been identified as being an important predictor of salmonid biomass in streams similar to the ones that we studied (Li et al. 1994). The riparian canopy also can buffer the stream and near-stream environment from atmospheric influences on water temperature (Poole and Berman 2001) that, in turn, is a strong factor regulating salmonid distribution and abundance in streams (reviewed by McCullough 1999). However, reach riparian canopy density and maximum summer stream temperatures were not correlated among our sites (Pearson's $r = -0.16$, $P = 0.39$), likely because of the multiple factors influencing stream temperatures across a wide array of elevations and stream channel morphologies (Poole and Berman 2001). Riparian canopy cover manipulations strongly influenced temperatures of cold water refuges in a companion study (Ebersole et al. 2003).

Maximum stream temperature was negatively associated with rainbow trout abundance in our habitat models, consistent with the findings of other studies in the region (Li et al. 1994; Ebersole et al. 2001). Although chinook salmon abundance was negatively associated with maximum stream temperature (Pearson's $r = -0.59$, $P = 0.01$), this effect did not significantly contribute to our models after accounting for channel width–depth ratio, proportional pool area, and basin location.

Substrate embeddedness was negatively associated with rainbow trout abundance across all models examined. Substrate embeddedness is a measure of substrate composition; high lev-

© 2003 NRC Canada

Table 6. Estimated effect of cold water patch frequency (CpF; $\log_{10}$ cold water patches·100 m^{-1}) and arcsine proportional relative cold water patch area (CpA; $m^2 \cdot m^{-2}$) on rainbow trout densities ($\log_{10}$ number·100 m^{-2}) after addition to 10 best habitat models.

			Addition of CpF			Addition of CpA		
Habitat model	Parameters	BIC	Coefficient estimate	SE	*P*	Coefficient estimate	SE	*P*
Rb1	LOS, WEN, PP, EM, MaxT, CAN, SIN, WD, WdF	−15.91	0.34	0.20	0.05	0.13	0.20	0.05
Rb2	LOS, WEN, PP, EM, MaxT, CAN	−15.00	0.49	0.19	0.01	0.15	0.19	0.01
Rb3	LOS, WEN, EM, MaxT, CAN, SIN	−14.53	0.38	0.21	0.04	0.13	0.21	0.04
Rb4	LOS, WEN, EM, MaxT, CAN	−13.47	0.46	0.20	0.01	0.15	0.20	0.01
Rb5	LOS, WEN, PP, EM, MaxT, CAN, SIN	−13.40	0.50	0.19	0.01	0.14	0.19	0.01
Rb6	LOS, WEN, EM, MaxT, CAN, SIN, WdF	−13.25	0.36	0.20	0.04	0.16	0.20	0.04
Rb7	LOS, PP, EM, MaxT, CAN	−13.04	0.49	0.19	0.01	0.16	0.19	0.01
Rb8	LOS, EM, MaxT, CAN	−12.95	0.38	0.20	0.04	0.17	0.20	0.04
Rb9	LOS, WEN, PP, EM, MaxT, CAN, WD	−12.37	0.51	0.21	0.01	0.15	0.08	0.03
Rb10	LOS, WEN, EM, MaxT, CAN, WD	−12.29	0.33	0.22	0.07	0.13	0.22	0.07

Note: BIC, Bayesian information criterion. Parameter coefficient estimate, standard error (SE), and one-sided *P* value are shown. Habitat model parameter codes and parameter estimates are provided in Table 4.

els of embeddedness (>40%) can severely impact egg–fry survival in stream salmonids and can reduce interstitial spaces used by benthic invertebrates that serve as potential prey items for salmonids (Minshall 1984). Substrate embeddedness was less important in models of chinook abundance, being included in only two of the best 10 models examined.

Chinook salmon and rainbow trout also differed with respect to the sensitivity of their response to cold water patch availability. The addition of cold water patch frequency and relative area to habitat models indicated that cold water patch availability was associated with higher abundances of rainbow trout after accounting for other habitat factors. Chinook salmon abundance responded positively to increases in cold water patch frequency but was not associated with cold water patch relative area among the sites examined.

Differences in modeled fish-habitat relationships for chinook salmon and rainbow trout could have several sources. Successful modeling of fish-habitat relationships is dependent on collection of accurate and precise metrics (Platts and Nelson 1988) and requires critical assumptions regarding the relationship of fish abundances to habitat characteristics (Terrell et al. 1996).

Among our sites, located in headwater drainages of the Snake River, abundances of juvenile migratory salmonids may be influenced by abundances and distributions of spawners (e.g., Beard and Carline 1991) which in turn are limited by mortality associated with a variety of factors ranging from passage through hydroelectric dams and reservoirs to predation in the ocean environment. Within the Upper Grande Ronde, spring chinook salmon are more spatially restricted in geographic distribution, and overall population sizes are lower and at higher risk of extinction (Matthews and Waples 1991). Thus, strong relationships between abundance of chinook salmon and habitat may not be expected, and inferences drawn from individual model parameter estimates for chinook salmon should be done with caution (Fausch et al. 1988). By using a model-averaging approach, we improved the reliability of individual parameter estimates by incorporating model selection uncertainty, in essence deriving estimates drawing on several models with highest likelihood of approximating the data well (Ramsey and Schafer 1997). Parameter estimates could have been further improved by inclusion of spatially explicit densities of spawners, and subsequent dispersal of juveniles of migratory salmonids, into regression modeling approaches. We lacked the necessary empirical data to attempt this.

Temporal bias due to single point-in-time measurements over a period of environmental change could potentially influence model results. Discharge declined across all sites over the study period, and subbasins exhibited different runoff characteristics (e.g., Wallowa Mountain snowmelt delayed summer baseflow conditions in the Lostine and Catherine Creek subbasins) that could have introduced systematic bias in measurements of habitat or cold water patch availability across subbasins and over the course of the study period. We attempted to account for systematic bias by including a subbasin factor in our modeling approach. However, seasonal (and annual) changes in cold water patch area and frequency are a reality that we were unable to address adequately in this study. The influence of temporal variance in environmental factors (like cold water patch availability) on temporal variation in fish abundance remains a daunting challenge for fish-habitat modeling. We restrict our inference to the specific times and places included in our sample and assume that although these results represent these data well, results elsewhere may differ. Validation of this model in other locations at other times will help clarify its utility.

Differences in salmonid-habitat models between species could also reflect fundamental differences in habitat preference or patterns of habitat use. Chinook salmon and rainbow trout differ with respect to time of emergence and subsequent size during the summer rearing season and consequently have differing preferences for depth and velocity positions within streams (Everest and Chapman 1972). The two species may also differ with respect to degree of habitat specialization and intra- and inter-specific habitat segregation. Rainbow trout are more general in their habitat associations within streams, being found within a wider variety of depth and velocity positions. Rainbow trout are more likely to occur as single individuals and to compete for individual

© 2003 NRC Canada

Fig. 3. Levels of spatial thermal diversity in a third-order stream system.

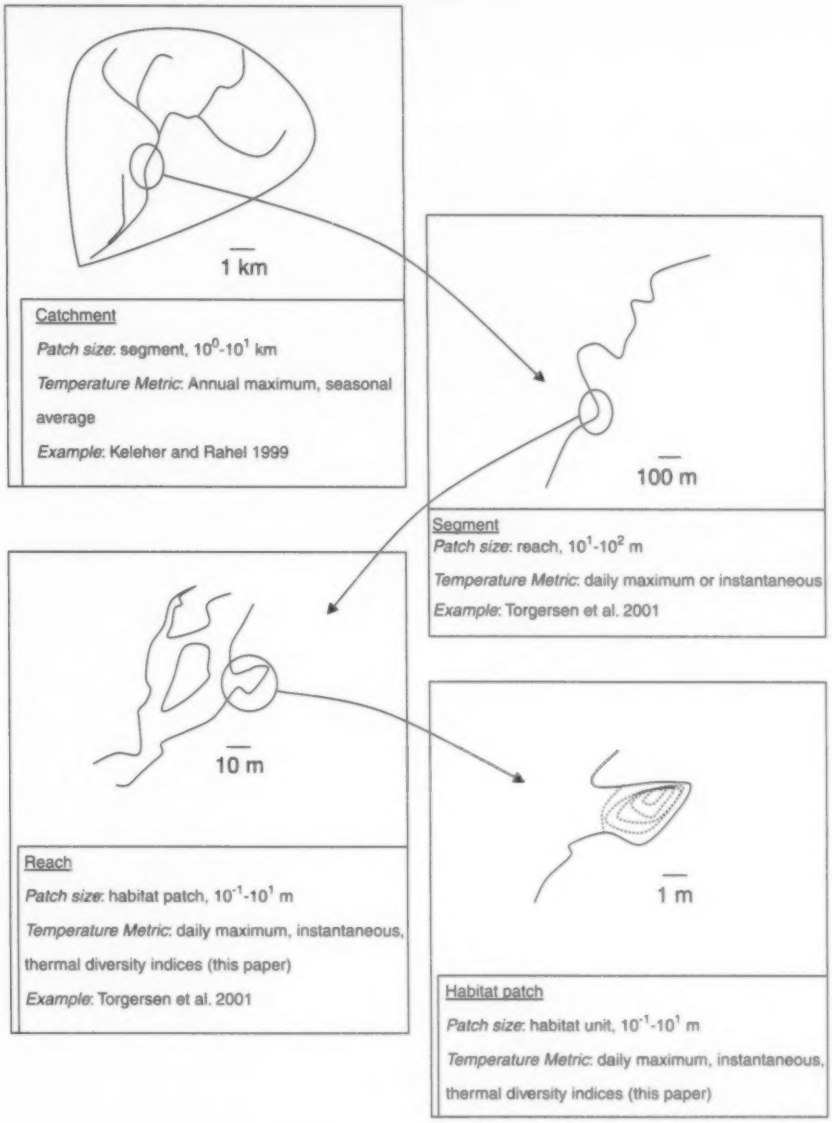
1 km
Catchment
Patch size: segment, 10^0-10^1 km
Temperature Metric: Annual maximum, seasonal average
Example: Keleher and Rahel 1999
100 m
Segment
Patch size: reach, 10^1-10^2 m
Temperature Metric: daily maximum or instantaneous
Example: Torgersen et al. 2001
10 m
Reach
Patch size: habitat patch, 10^{-1}-10^1 m
Temperature Metric: daily maximum, instantaneous, thermal diversity indices (this paper)
Example: Torgersen et al. 2001
1 m
Habitat patch
Patch size: habitat unit, 10^{-1}-10^1 m
Temperature Metric: daily maximum, instantaneous, thermal diversity indices (this paper)

foraging locations than chinook salmon, which tend to shoal within pool habitats (Everest and Chapman 1972). Willingness to use shallow stream-margin cold water patches may also differ between chinook salmon and rainbow trout. In a parallel study, we have found that cold water patch depth was an important factor in predicting cold water patch use by chinook salmon, but not for rainbow trout (J.L. Ebersole, unpublished data). If cold water patches are too shallow for chinook salmon to use, their availability may have little influence of reach-level abundances measured in this study.

Ebersole et al. (2001) found that cold water patch frequency did not explain variation in rainbow trout abundance in northeastern Oregon streams after accounting for the influence of ambient water temperatures. They proposed that the overwhelming influence of high ambient stream temperatures in the warm streams examined, combined with relatively limited refuge space, prohibited a substantial cold water refuge effect. Power to detect a significant refuge effect was very low for their study because of a small sample of sites ($n = 12$); sample sizes necessary to detect a cold water patch influence on salmonid abundance given observed variation in the data would have exceeded 50 sites. By increasing sample sizes and stratifying across geomorphically similar reaches, we were able to detect a small but significant effect of cold water patch availability on salmonid abundance in this study.

Ambitious restoration efforts of stream habitat in the western United States are underway and provide the opportunity

© 2003 NRC Canada

to test potential causal mechanisms for patterns observed and proposed by this research. Monitoring changes in channel morphology, riparian vegetation, thermal diversity, and salmonid populations can help refine estimates of whether increased availability of cold water refuges is provided by riparian and upland restoration and in turn enables improved persistence of salmonids in thermally marginal stream reaches.

Acknowledgments

We thank Byung Park and Virginia Lesser for generous assistance with statistical methods. John Bartholow, Bob Beschta, Hiram Li, John Van Sickle, and Al Zale provided helpful comments on earlier drafts of this paper. We are grateful to Troy Guy, Erik Hedburg, and Lauren Penner for assistance in the field. Financial support for this research was provided by the Oregon Department of Fish and Wildlife, the United States Environmental Protection Agency, and the National Science Foundation.

References

Arscott, D.B., Tockner, K., and Ward, J.V. 2000. Aquatic habitat diversity along the corridor of an alpine floodplain river (Fiume Tagliamento, Italy). Arch. Hydrobiol. **149**: 679–704.

Bain, M.B., Finn, J.T., and Booke, H.E. 1985. Quantifying stream substrate for habitat analysis studies. N. Am. J. Fish. Manag. **4**: 499–506.

Bayley, P.B., and Dowling, D.C. 1993. The effect of habitat in biasing fish abundance and species richness estimates when using various sampling methods in streams. Pol. Arch. Hydrobiol. **40**: 5–14.

Beard, T.D., Jr., and Carline, R.F. 1991. Influence of spawning and other stream habitat features on spatial variability of wild brown trout. Trans. Am. Fish. Soc. **120**: 711–722.

Berman, C.H., and Quinn, T.P. 1991. Behavioural thermoregulation and homing by spring chinook salmon, *Oncorhynchus tshawytscha* (Walbaum), in the Yakima River. J. Fish Biol. **39**: 301–312.

Beschta, R.L., Bilby, R.E., Brown, G.W., Holtby, L.B., and Hofstra, T.D. 1986. Stream temperature and aquatic habitat: fisheries and forestry interactions. *In* Streamside management: forest and fishery interactions. *Edited by* E.O. Salo and T.W. Cundy. University of Washington, Seattle. pp. 191–232.

Bilby, R.E. 1984. Characteristics and frequency of cool-water areas in a western Washington stream. J. Freshw. Ecol. **2**: 593–602.

Bisson, P.A., Nielsen, J.L., Palmason, R.A., and Grove, L.E. 1982. A system of naming habitat types in small streams, with examples of habitat utilization by salmonids during low stream flow. *In* Acquisition and utilization of aquatic habitat inventory information. Proceedings of a symposium held 28–30 October 1981, Portland, Oreg. *Edited by* N.B. Armantrout. Western Division, American Fisheries Society, Bethesda, Md. pp. 62–73.

Bisson, P.A., Sullivan, K., and Nielsen, J.L. 1988. Channel hydraulics, habitat use, and body form of juvenile coho salmon, steelhead, and cutthroat trout in streams. Trans. Am. Fish. Soc. **117**: 262–273.

Boulton, A.J., Findlay, S., Marmonier, P., Stanley, E.H., and Valett, H.M. 1998. The functional significance of the hyporheic zone in streams and rivers. Annu. Rev. Ecol. Syst. **29**: 59–81.

Brunke, M., and Gonser, T. 1997. The ecological significance of exchange processes between rivers and groundwater. Freshw. Biol. **37**: 1–33.

Bryce, S.A., and Clarke, S.E. 1996. Landscape-level ecological regions: linking state-level ecoregion frameworks with stream habitat classifications. Environ. Manag. **20**: 297–311.

Crowder, L.B., and Magnuson, J.J. 1983. Cost-benefit analysis of temperature and food resource use: a synthesis with examples from the fishes. *In* Behavioral energetics: the cost of survival in vertebrates. *Edited by* W.P. Aspey and S.I. Lustick. Ohio State University Press, Columbus. pp. 189–221.

Cunjak, R.A. 1996. Winter habitat of selected stream fishes and potential impacts from land-use activity. Can. J. Fish. Aquat. Sci. **53**(Suppl. 1): 267–282.

Dent, C.L., Schade, J.D., Grimm, N.B., and Fisher, S.G. 2000. Subsurface influences on surface biology. *In* Streams and ground waters. *Edited by* J.B. Jones and P.J. Mulholland. Academic Press, San Diego, Calif. pp. 381–402.

Dunham, J.B., and Vinyard, G.L. 1997. Incorporating stream level variability into analyses of site level fish habitat relationships: some cautionary examples. Trans. Am. Fish. Soc. **126**: 323–329.

Dunning, J.B., Danielson, B.J., and Pulliam, H.R. 1992. Ecological processes that affect populations in complex landscapes. Oikos, **65**: 169–175.

Ebersole, J.L. 1994. Stream habitat classification and restoration in the Blue Mountains of northeast Oregon. M.Sc. thesis, Oregon State University, Corvallis, Oreg.

Ebersole, J.L., Liss, W.J., and Frissell, C.A. 2001. Relationship between stream temperature, thermal refugia and rainbow trout *Oncorhynchus mykiss* abundance in arid-land streams in the northwestern United States. Ecol. Freshw. Fish, **10**: 1–10.

Ebersole, J.L., Liss, W.J., and Frissell, C.A. 2003. Cold water patches in warm streams: physiochemical characteristics and the influence of shading. J. Am. Water Resour. Assoc. **39**: 355–368.

Everest, F.H., and Chapman, D.W. 1972. Habitat selection and spatial interaction by juvenile chinook salmon and steelhead trout in two Idaho streams. J. Fish. Res. Board Can. **29**: 91–100.

Fausch, K.D., Hawkes, C.L., and Parsons, M.G. 1988. Models that predict standing crop of stream fish from habitat variables: 1950–85. U.S. Dep. Agric. For. Serv. Gen. Tech. Rep. No. PNW-213.

Fernald, A.G., Wigington, P.J., and Landers, D.H. 2001. Transient storage and hyporheic flow along the Willamette River, Oregon: field measurements and model estimates. Water Resour. Res. **37**: 1681–1694.

Franklin, J.F., and Dyrness, C.T. 1973. Natural vegetation of Oregon and Washington. U.S. Dep. Agric. For. Serv. Gen. Tech. Rep. No. GTR-PNW-8.

Frissell, C.A., Liss, W.J., Warren, C.E., and Hurley, M.D. 1986. A hierarchical framework for stream habitat classification: viewing streams in a watershed context. Environ. Manag. **10**: 199–214.

Frissell, C.A., Ebersole, J.L., Liss, W.J., Cavallo, B.J., Poole, G.C., and Stanford, J.A. 1996. Potential effects of climate change on thermal complexity and biotic integrity of streams: seasonal intrusion of non-native fishes. U.S. Environmental Protection Agency Final Rep. No. CR-822019-01-0.

Gibson, R.J. 1966. Some factors influencing the distributions of brook trout and young Atlantic salmon. J. Fish. Res. Board Can. **23**: 1977–1979.

Harvey, B.C., and Stewart, A.J. 1991. Fish size and habitat depth relationships in headwater streams. Oecologia, **87**: 336–342.

Harvey, J.W., and Bencala, K.E. 1993. The effect of streambed topography on surface–subsurface water exchange in mountain catchments. Water Resour. Res. **29**: 89–98.

Hendricks, S.P., and White, D.S. 1991. Physicochemical patterns within a hyporheic zone of a northern Michigan river, with comments on surface water patterns. Can. J. Fish. Aquat. Sci. **48**: 1645–1654.

© 2003 NRC Canada

Hewlett, J.D., and Fortson, J.C. 1982. Stream temperature under an inadequate buffer strip in the Southeast Piedmont. Water Resour. Bull. **18**: 983–988.

Hillman, T.W., Mullan, J.W., and Griffith, J.S. 1992. Accuracy of underwater counts of juvenile chinook salmon, coho salmon, and steelhead. N. Am. J. Fish. Manag. **12**: 598–603.

Holtby, L.B. 1988. Effects of logging on stream temperatures in Carnation Creek, British Columbia, and associated impacts on the coho salmon (*Oncorhynchus kisutch*). Can. J. Fish. Aquat. Sci. **45**: 502–515.

Holtby, L.B., MaMahon, T.E., and Scrivener, J.C. 1989. Stream temperatures and interannual variability in the emigration timing of coho salmon (*Oncorhynchus kisutch*) smolts and fry and chum salmon (*O. keta*) fry from Carnation Creek, British Columbia. Can. J. Fish. Aquat. Sci. **46**: 1396–1405.

Hynes, H.B.N. 1983. Groundwater and stream ecology. Hydrobiologia, **100**: 93–99.

Kaufmann, P.R. 2002. Physical habitat characterization. *In* Environmental monitoring and assessment program — surface waters: western pilot study field operations manual for wadeable streams. *Edited by* D.V. Peck, J.M. Lazorchak, and D.J. Klemm. U.S. Environmental Protection Agency, Office of Research and Development, Washington, D.C. pp. 103–160.

Kaya, C.M., Keading, L.R., and Burkhalter, D.E. 1977. Use of a cold water refuge by rainbow and brown trout in a geothermally heated stream. Prog. Fish. Cult. **39**: 37–39.

Keleher, C.J., and Rahel, F.J. 1996. Thermal limits to salmonid distributions in the Rocky Mountain region and potential habitat loss due to global warming: a geographic information system (GIS) approach. Trans. Am. Fish. Soc. **125**: 1–13.

Keller, E.A., Kondolf, G.M., and Hagerty, D.J. 1990. Groundwater and fluvial processes: selected observations. *In* Groundwater geomorphology: the role of subsurface water in Earth-surface processes and landforms. *Edited by* C.G. Higgins and D.R. Cotes. Geological Society of America Special Paper, Boulder, Co. pp. 319–340.

Leopold, L.B., Wolman, M.G., and Miller, J.P. 1964. Fluvial processes in geomorphology. W.H. Freeman, San Francisco, Calif.

Li, H.W., Lamberti, G.A., Pearsons, T.N., Tait, C.K., Li, J.L., and Buckhouse, J.C. 1994. Cumulative effects of riparian disturbances along high desert trout streams of the John Day Basin, Oregon. Trans. Am. Fish. Soc. **123**: 627–640.

Lonzarich, D.G., and Quinn, T.P. 1995. Experimental evidence for the effect of depth and structure on the distribution, growth, and survival of stream fishes. Can. J. Zool. **73**: 2223–2230.

Magnuson, J.J., Crowder, L.B., and Medvick, P.A. 1979. Temperature as an ecological resource. Am. Zool. **19**: 331–343.

Manugistics, Inc. 2000. Statgraphics 5.0 user's manual. Manugistics, Inc., Rockville, Md.

Matthews, G.M., and Waples, R.S. 1991. Status review for Snake River spring and summer chinook salmon. National Marine Fisheries Service NOAA Tech. Memo No. NMFS F/NWC-200.

McCullough, D.A. 1999. A review and synthesis of effects of alterations to the water temperature regime on freshwater life stages of salmonids, with special reference to chinook salmon. U.S. Environmental Protection Agency, Region 10, No. 910-R-010.

McIntosh, B.A., Sedell, J.R., Smith, J.E., Wissmar, R.C., Clarke, S.E., Reeves, G.H., and Brown, L.A. 1994. Historical changes in fish habitat for select river basins of eastern Oregon and Washington. Northw. Sci. **68**: 36–53.

Miller, R.R., Williams, J.D., and Williams, J.E. 1989. Extinctions of North American fishes during the past century. Fisheries, **14**: 22–38.

Minshall, G.W. 1984. Aquatic insect–substratum relationships. *In* The ecology of aquatic insects. *Edited by* V.H. Resh and D.M. Rosenberg. Praeger, New York. pp. 358–400.

Montgomery, D.R. 1999. Process domains and the river continuum. J. Am. Water Resour. Assoc. **35**: 397–410.

Nakano, S., Kawaguchi, Y., Taniguchi, Y., Miyasaka, H., Shibata, Y., Urabe, H., and Kuhara, N. 1999. Selective foraging on terrestrial invertebrates by rainbow trout in a forested headwater stream in northern Japan. Ecol. Res. **14**: 351–360.

Neter, J., Wasserman, W., and Kutner, M.H. 1989. Applied linear regression models. Richard D. Irwing, Inc., Homewood, Ill.

Nielsen, J.L., Lisle, T.E., and Ozaki, V. 1994. Thermally stratified pools and their use by steelhead in northern California streams. Trans. Am. Fish. Soc. **123**: 613–626.

Orr, E.L., Orr, W.N., and Baldwin, E.M. 1992. The geology of Oregon. Kendall/Hunt, New York.

Ozaki, V. 1988. Geomorphic and hydrologic conditions for cold pool formation on Redwood Creek, California. Redwood National Park Tech. Rep. No. 24.

Platts, W.J. 1991. Livestock grazing. *In* Influences of forest and rangeland management on salmonid fishes and their habitats. *Edited by* W.R. Meehan. American Fisheries Society, Bethesda, Md. pp. 389–423.

Platts, W.S., and Nelson, R.L. 1988. Fluctuations in trout populations and their implications for land-use evaluation. N. Am. J. Fish. Manag. **8**: 333–345.

Platts, W.S., Lienkaemper, G.W., Amour, C., Minshall, G.W., Booth, G.D., Monsen, S.B., Bryant, M., Nelson, R.L., Bufford, J.L., Sedell, J.R., Cuplin, P., Tuhy, J.S., and Jensen, S. 1987. Methods for evaluating riparian habitats with applications to management. U.S. Dep. Agric. For. Serv. Gen. Tech. Rep. No. INT-221.

Poole, G.C., and Berman, C.H. 2001. An ecological perspective on in-stream temperature: natural heat dynamics and mechanisms of human-caused thermal degradation. Environ. Manag. **27**: 787–802.

Pringle, C.M., and Triska, F.J. 2000. Emergent biological patterns and surface–subsurface interactions at landscape scales. *In* Streams and ground waters. *Edited by* J.B. Jones and P.J. Mulholland. Academic Press, San Diego, Calif. pp. 167–193.

Ramsey, F.L., and Schafer, D.W. 1997. The statistical sleuth: a course in methods of data analysis. Duxbury Press, Belmont, Calif.

SAS. 1999. SAS OnlineDoc®. Version 8. SAS Inc., Cary, N.C.

Schumm, S.A. 1977. The fluvial system. John Wiley and Sons, New York.

Sedell, J.R., Reeves, G.H., Hauer, F.R., Stanford, J.A., and Hawkins, C.P. 1990. Role of refugia in recovery from disturbances: modern fragmented and disconnected river systems. Environ. Manag. **14**: 711–724.

Shepherd, B.G., Hartman, G.F., and Wilson, W.J. 1986. Relationships between stream and intragravel temperatures in coastal drainages, and some implications for fisheries workers. Can. J. Fish. Aquat. Sci. **43**: 1818–1822.

Solazzi, M.F., Nickelson, T.E., Johnson, S.L., and Rodgers, J.D. 2000. Effects of increasing winter rearing habitat on abundance of salmonids in two coastal Oregon streams. Can. J. Fish. Aquat. Sci. **57**: 906–914.

Stanford, J.A., and Ward, J.V. 1993. An ecosystem perspective of alluvial rivers: connectivity and the hyporheic corridor. J. N. Am. Benthol. Soc. **12**: 48–60.

Strichler, G.S. 1959. Use of the densiometer to estimate density of forest canopy on permanent sample plots. U.S. Department of Agriculture, Pacific Northwest Forest and Range Experiment Station Res. Note No. INT-180.

© 2003 NRC Canada

Tabachnick, B.G., and Fidell, L.S. 1996. Using multivariate statistics. Harper Collins, New York.

Terrell, J.W., Cade, B.S., Carpenter, J., and Thompson, J.M. 1996. Modeling stream fish habitat limitations from wedge-shaped patterns of variation in standing stock. Trans. Am. Fish. Soc. **125**: 104–117.

Thompson, S.K. 1992. Sampling. John Wiley and Sons, Inc., New York.

Thurow, R.F. 1994. Underwater methods for study of salmonids in the Intermountain West. U.S. Dep. Agric. For. Serv., Intermountain Station Gen. Tech. Rep. No. INT-GTR-307.

Torgersen, C.E., Price, D.M., Li, H.W., and McIntosh, B.A. 1999. Multiscale thermal refugia and stream habitat associations of chinook salmon in northeastern Oregon. Ecol. Appl. **9**: 301–319.

Townsend, C.R., Doledec, S., and Scarsbrook, M.R. 1997*a*. Species traits in relation to temporal and spatial heterogeneity in streams: a test of habitat templet theory. Freshw. Biol. **37**: 367–387.

Townsend, C.R., Scarsbrook, M.R., and Doledec, S. 1997*b*. The intermediate disturbance hypothesis, refugia, and biodiversity in streams. Limnol. Oceanogr. **42**: 938–949.

Valett, H.M., Morrice, J.A., Dahm, C.N., and Campana, M.E. 1996. Parent lithology, surface–groundwater exchange, and nitrate retention in headwater streams. Limnol. Oceanogr. **41**: 333–345.

Ward, J.V., and Stanford, J.A. 1982. Thermal responses in the evolutionary ecology of aquatic insects. Annu. Rev. Entomol. **1982**: 97–117.

Whitehead, R.L. 1992. Geohydrologic framework of the Snake River plain regional aquifer system, Idaho and eastern Oregon. U.S. Geol. Surv. Professional Pap. No. 1408-B.

Wissmar, R.C., Smith, J.E., McIntosh, B.A., Li, H.W., Reeves, G.H., and Sedell, J.R. 1994. A history of resource use and disturbance in riverine basins of eastern Oregon and Washington (early 1800s–1990s). Northw. Sci. **68**: 1–35.

Wondzell, S.M., and Swanson, F.J. 1996. Seasonal and storm dynamics of the hyporheic zone of a 4th-order mountain stream. I. Hydrologic processes. J. N. Am. Benthol. Soc. **15**: 3–19.

Zar, J. 1984. Biostatistical analysis. Prentice-Hall, Inc., Englewood Cliffs, N.J.

© 2003 NRC Canada

Fatty acid metabolism in rainbow trout (*Oncorhynchus mykiss*) tissues: differential incorporation of palmitate and oleate

Jean-Michel Weber, Gérard Brichon, and Georges Zwingelstein

Abstract: Total fatty acid (FA) fluxes of teleost have been well characterized, but the tissues incorporating FA from the circulation and the metabolic fate of these FA remain unclear. Our goals were to determine (*i*) the relative roles of different tissues in incorporating FA, (*ii*) the lipid pools that include FA (phospholipids (PL) or neutral lipids (NL)), and (*iii*) whether saturated and monounsaturated FA behave differently. Fatty acid incorporation was measured after administration of 1-^{14}C-palmitate and 9,10-^{3}H-oleate in rainbow trout (*Oncorhynchus mykiss*). Results show that FA incorporation varies tremendously among tissues and that the dominant physiological roles of palmitate and oleate are different. For all tissues, oleate is incorporated more rapidly than palmitate into NL (ratio oleate–palmitate 2.8 ± 0.3), showing that oleate plays a prominent role in energy metabolism. However, the two FA enter tissue PL to the same extent (incorporation ratio 1.0 ± 0.2), suggesting equal contributions to membrane turnover. This study reveals a novel aspect of the dominant role played by monounsaturates in energy metabolism: their preferential incorporation in triacylglycerol reserves.

Résumé : Les flux globaux d'acides gras (FA) sont bien caractérisés chez les téléostéens, mais les tissus où ces acides gras s'incorporent à partir de la circulation et le destin métabolique des acides gras restent encore mal connus. Nos objectifs sont (*i*) de déterminer les rôles relatifs des divers tissus dans l'incorporation des acides gras, (*ii*) d'identifier les réservoirs lipidiques dans lesquels les acides gras sont inclus, soit les phospholipides (PL) ou les lipides neutres (NL) et (*iii*) de voir si les acides gras saturés et monoinsaturés se comportent de façon différente. L'administration de 1-^{14}C-palmitate et de 9,10-^{3}H-oléate à des truites arc-en-ciel (*Oncorhynchus mykiss*) a permis de mesurer l'incorporation des acides gras. Cette incorporation varie considérablement d'un tissu à l'autre et les rôles physiologiques principaux du palmitate et de l'oléate sont différents. Dans tous les tissus, l'oléate est incorporé plus rapidement dans les lipides neutres que le palmitate (rapport oléate–palmitate 2,8 ± 0,3), ce qui indique que l'oléate joue un rôle primordial dans le métabolisme énergétique. Cependant, les deux acides gras s'incorporent aux phospholipides des tissus au même rythme (rapport des incorporations 1,0 ± 0,2), ce qui indique une contribution égale des deux acides au renouvellement des membranes. Notre étude met en lumière un aspect nouveau du rôle joué par les acides monoinsaturés dans le métabolisme énergétique, soit leur incorporation préférentielle dans les réserves de triacylglycérol.

[Traduit par la Rédaction]

Introduction

Fatty acids (FA) and their associated metabolites play fundamental roles in energy metabolism, in signal transduction pathways, and, more importantly for ectotherms, in stabilizing membranes when body temperature fluctuates (Greene and Selivonchick 1987). In rainbow trout (*Oncorhynchus mykiss*), changes in the turnover rate of plasma fatty acids have been investigated in vivo under a variety of environmental and physiological conditions. Rates of appearance and disappearance of circulating palmitate have been quantified at rest (Weber et al. 2002), during prolonged swimming (Bernard et al. 1999), and when the fish were acutely exposed to hypoxia or low water temperature (Haman et al. 1997*b*). Even though total flux out of the circulation has been well characterized at the whole-organism level, the main tissues that incorporate fatty acids from the blood compartment and the metabolic fate of fatty acids remains unclear. Here, our goals were to determine (*i*) the relative roles of different tissues in incorporating circulatory fatty acids, (*ii*) the specific lipid pools in which they are included within each tissue (phospholipids (PL) or neutral lipids (NL)), and (*iii*) whether important differences are found between specific fatty acids of different degrees of saturation with respect to *i* and *ii*. To address these questions, we compared the most common saturated fatty acid (palmitate, 16:0) with its monounsaturated counterpart (oleate, 18:1). The experiments were divided into two parts. In the first part (pub-

Received 17 January 2003. Accepted 31 August 2003. Published on the NRC Research Press Web site at http://cjfas.nrc.ca on 12 November 2003.
J17290

J.-M. Weber.[1] Biology Department, University of Ottawa, 30 Marie Curie, Ottawa, ON K1N 6N5, Canada.
G. Brichon and G. Zwingelstein. Institut Michel Pacha, Université Claude Bernard Lyon 1, 83500 La Seyne sur Mer, France.

[1]Corresponding author (e-mail: jmweber@science.uottawa.ca).

 doi: 10.1139/F03-110 © 2003 NRC Canada

lished previously (Weber et al. 2002)), the kinetics of palmitate and oleate were quantified, and the rates of incorporation of these two fatty acids into plasma lipids were monitored. We found that palmitate and oleate can both be used as tracers to measure total fatty acid kinetics and showed that palmitate is preferentially incorporated into plasma phospholipids, suggesting that it is mainly involved in membrane metabolism. In contrast, oleate is incorporated preferentially into plasma neutral lipids, suggesting a more prominent role in energy metabolism for this acid (Weber et al. 2002). Here, we report the second part of the study that deals with the incorporation and metabolism of palmitate and oleate in tissue lipids. Several studies show that monounsaturates play a dominant role in the energy metabolism of vertebrates in general, but even more so in situations in which energy reserves are particularly limiting. These studies demonstrate that hibernating mammals (Florant et al. 1990), migrating birds (Blem 1990), and Antarctic fish (Sidell 1991; Lund and Sidell 1992) store monounsaturates preferentially over other fatty acids. Additional studies in fish and mammals also reveal that monounsaturates are usually mobilized (Jezierska et al. 1982; Raclot and Groscolas 1993, 1995), as well as oxidized (Leyton et al. 1987; Sidell 1991; Sidell et al. 1995), more readily than saturated fatty acids. Consequently, we hypothesized that oleate would be incorporated preferentially into tissue neutral lipids used for energy storage. Results show that the dominant physiological roles of palmitate and oleate are different. Oleate plays a prominent role in energy metabolism, whereas both FA appear to contribute equally to membrane turnover of all tissues.

Materials and methods

Animals

Rainbow trout, *Oncorhynchus mykiss* (Walbaum), of both sexes (565 ± 31 g, $N = 5$) were purchased from Linwood Acres Trout Farm (Campbellcroft, Ontario, Canada) and held at 12 °C in a 1300-L flow-through tank. They were kept in dechlorinated, well-oxygenated water under a 12 h light – 12 h dark photoperiod and fed floating trout pellets every second day (11% lipids, 42% proteins, 20% carbohydrates) until satiation (see Weber et al. (2002) for the fatty acid composition of the food). This diet provided all of the necessary minerals, vitamins, and oligoelements. It contained 35.6 µmol palmitate and 42.9 µmol oleate per gram. The animals were acclimated to these conditions for at least 6 weeks before experiments.

Administration of labeled fatty acids in vivo

Food was withdrawn for 18 h before dorsal aorta catheters were surgically implanted under MS-222 anesthesia (0.1 $g \cdot L^{-1}$ ethyl-*N*-aminobenzoate sulphonic acid buffered with 0.2 $g \cdot L^{-1}$ sodium bicarbonate). Continuous infusions of 1-^{14}C-palmitate and 9,10-^{3}H-oleate (Amersham, Oakville, Ontario, Canada) were then carried out. Detailed procedures for catheterizations and isotope infusions were published elsewhere (Haman and Weber 1996; Haman et al. 1997*a*; Weber et al. 2002). Briefly, radiolabeled metabolites were infused in resting animals kept in opaque Plexiglas chambers (60 cm × 18 cm × 16 cm). For each experiment, the infusate was prepared immediately before starting the infusion by mixing ~10 µCi 1-^{14}C-palmitate and ~10 µCi 9,10-^{3}H-oleate (Amersham) with 0.3 mL of trout plasma from donor animals of the same batch and then diluting in fish saline. All scintillation counting was performed on a Tri-Carb 2500 (Packard, Mississauga, Canada) with external quench correction. Each infusate was counted before and after infusion to determine its activity. The infusate was administered with a calibrated syringe pump (Harvard Apparatus, South Natick, Mass.) at a rate of 1 $mL \cdot h^{-1}$ for 1 h. After infusing the tracers, the animals were left undisturbed for 24 h in the same Plexiglas chambers supplied with the same water as their holding tanks at a rate of 5 $L \cdot min^{-1}$. During the continuous infusions, total doses of radioactivity administered were 28 069 ± 2166 disintegrations per minute (DPM) per gram (1 DPM = 1/60 Bq) for 1-^{14}C-palmitate and 28 899 ± 2166 $DPM \cdot g^{-1}$ for 9,10-^{3}H-oleate ($N = 5$).

Tissue sampling

Twenty-four hours after administration of the isotopes, the animals were killed by intravascular injection of 2 $mL \cdot kg^{-1}$ Somnotol (MTC Pharmaceuticals, Cambridge, Ont.) through one of the catheters, and tissue samples were harvested immediately. Between 1 and 2 g of each tissue were collected. Pieces of white muscle, lateral red muscle, heart, liver, gill, intestine, and adipose tissue were dissected and weighed. All tissues were sampled within 3 min after death. Tissue lipids were extracted and purified immediately by placing ~1 g of each sample in 30 mL chloroform–methanol (2:1, v/v) (Folch et al. 1957) and homogenizing for 3 × 10 s (Polytron, Luzern, Switzerland). For each fish, the extraction of all tissue lipids was completed within 30 min after killing the animal.

Fatty acid composition of total lipids, neutral lipids, and phospholipids

The neutral lipid fraction (mostly triacylglycerol) and the phospholipid fraction were separated from total lipids by preparative thin-layer chromatography (TLC) using precoated silica gel 60 plates (Merck, Darmstadt, Germany) and isopropyl ether as migration solvent. Silica gel bands corresponding to neutral lipids and phospholipids were scraped into screw-capped tubes. Heptadecanoic acid (17:0) was used as an internal standard and the mixture was transmethylated by heating (90 °C for 90 min) after the addition of acetyl chloride (1.5 $mol \cdot L^{-1}$ in methanol) (Zwingelstein et al. 1978). The methyl esters were extracted with hexane after adding water. An aliquot of the tissue lipids taken before TLC separation was also transmethylated after adding heptadecanoic acid to determine the fatty acid composition of total lipids independently. All fatty acid methyl esters were analyzed by gas chromatography (Chrompack CP 900 (Chrompack, Les Ulis, France) equipped with a Omegawax 320 glass capillary column, 30 mm × 0.32 mm inside diameter (ID), 0.25-µm film thickness) using nitrogen as carrier gas. The following temperature conditions were used for gas chromatography: 200 °C (oven), 220 °C (injector), and 260 °C (detector) (Zwingelstein et al. 1978). Each methyl ester was identified specifically by determining exact retention times with authentic standards (Sigma-Aldrich, St. Louis,

© 2003 NRC Canada

Mo.). Only the fatty acids representing more than 1% of total fatty acids within each tissue or lipid fraction are reported.

^{3}H and ^{14}C activity in tissue fatty acids

To determine to what extent elongation or desaturation of fatty acids were taking place, total tissue lipids, NL, and PL were saponified with 90% methanolic KOH (0.3 mol·L^{-1}) for 1 h at 80 °C. Unsaponifiable compounds were extracted with ethyl ether. The alcoholic phase was acidified with 3 mol·L^{-1} HCl, and the fatty acids were extracted with hexane. Fatty acid methyl esters were prepared by adding dimethoxypropane and concentrated HCl. Samples were left for 30 min at room temperature and dried under N_2. After evaporation, radioactive fatty acid methyl esters were separated by TLC on 10% $AgNO_3$ – silica gel according to their degree of unsaturation (Dudley and Anderson 1975). All fatty acid ester spots were scraped into scintillation vials and their activities were counted after adding 3 mL ethanol–water (1:1, v/v) and 8 mL scintillation fluid (Picofluor, Packard). Ninety-three percent of the ^{3}H activity was recovered in the monoene species, and 95% of the ^{14}C activity was found in the saturate species. The saturate and monoene spots from another chromatogram were recovered and the fatty acid esters were eluted with chloroform–methanol (1:1, v/v). Each eluted fraction was separated according to chain length, using reverse-phase TLC on KC18F C_{18} – silica gel plates (Whatman, Clifton, N.J.) in acetonitrile – acetic acid – water (70:10:25, v/v/v). Most of the activity (93–97%) was found in the octadecanoic spot (C18) from the monoene species for ^{3}H and in the hexadecanoic spot (C16) from the saturate species for ^{14}C.

Composition of tissue phospholipids

Total phospholipid concentration was measured by drying an aliquot of total lipid extracts under nitrogen. Concentrated H_2SO_4, concentrated $HClO_4$, and 0.1% V_2O_4 were added and the mixture was heated to 180 °C until clear (Portoukalian et al. 1978). After cooling, the digests were diluted with 9 mL distilled water, and phosphorus was measured with the Fiske-Subbarow reagent (Bartlett 1959). Phospholipid composition was measured by spotting aliquots of the lipids on 10 × 10 cm silica gel 60 precoated plates, and separation of the different phospholipids was carried out using two-dimensional chromatography (Portoukalian et al. 1978). The spots were identified with the Dittmer and Lester reagent (Dittmer and Lester 1964) and transferred to test tubes for phosphorus determination.

Calculations and statistics

To allow meaningful comparisons, all activities were corrected for a standard dose of radioactivity administered of 10^7 DPM (166 667 Bq) and standard body mass of 500 g. Results were analyzed by one- or two-way analysis of variance with replication (ANOVA). When the assumptions of normality or homoscedasticity were not met, a nonparametric ANOVA on ranks was carried out. The Student–Newman–Keul procedure was used as a post hoc test to determine which means were significantly different from each other. Percentages were transformed to the arcsine of their square root before statistical analysis. All values given are means ± standard error of the mean (SEM).

Results

Tissue contents in total lipids, neutral lipids, and phospholipids

We present weight percentages (% wet weight) for total lipids, neutral lipids, and phospholipids of rainbow trout tissues (Table 1). Only total lipids are reported for adipose tissue because its large NL content prevented accurate measurement of PL. The fatty acid composition (% total fatty acids within each lipid class) of tissue NL and PL is given (Fig. 1). Overall, monounsaturated fatty acids were more abundant in NL than in PL, whereas the opposite was true for saturated fatty acids ($p < 0.01$). Tissue PL contained particularly large amounts of the polyunsaturated, docosahexaenoic acid (22:6), ranging between 29% in gills and 47% in liver. Arachidonic acid (20:4) was more abundant in the intestine (4.9%) and in the gills (4.6%) than in other tissues (1.2–2.8%).

Composition of tissue phospholipids

Analysis of phosphate distribution allowed us to quantify the composition of tissue phospholipids. The percent contribution of the different classes of phospholipids to total lipid phosphorus is presented (Table 2). Phosphatidylcholine content dominated in all tissues, accounting for 47–65% of total PL. Diphosphatidylglycerol content was much higher in red muscle and heart (12–13%) than in all other tissues (2–3%).

Standardized specific activities of palmitate and oleate

Tissue specific activities of palmitate (^{14}C) and oleate (^{3}H) measured 24 h after tracer administration are presented for NL and PL (Figs. 2*a*, 2*b*). No differences were found between palmitate and oleate, although a trend towards higher activities in palmitate than in oleate was apparent in PL ($p = 0.08$). Specific activities were widely different between tissues for both NL and PL ($p < 0.001$). In NL (Fig. 2*a*), the following hierarchy was observed: liver > heart > red muscle = white muscle = gill > intestine = adipose. In PL (Fig. 2*b*), liver and heart had the highest specific activities (as in NL), but a different ranking than in NL was found for the other tissues: liver > heart > gill > intestine > white muscle > red muscle.

We give the ratios of specific activities (oleate to palmitate) for NL and PL (Fig. 3). These ratios were very different between tissues ($p < 0.001$) but were the same for NL and PL within the same tissue ($p = 0.24$). Specific activity ratios showed the following hierarchy between tissues: white muscle > red muscle = intestine = liver = heart = gill > adipose.

Incorporation of palmitate and oleate after 24 h

We present the incorporation of fatty acids into tissue lipids (Figs. 4 and 5). Incorporation of palmitate and oleate into total lipids (in nanomoles of fatty acid per gram tissue) showed large differences between tissues ($p < 0.001$): liver > heart = red muscle > gill > intestine > white muscle. However, the two fatty acids were incorporated into total lipids at

© 2003 NRC Canada

Table 1. Percentages (% wet weight) of total lipids, neutral lipids, and phospholipids in the tissues of adult rainbow trout (*Oncorhynchus mykiss*).

Tissue	Percent total lipids per gram tissue	Percent neutral lipids per gram tissue	Percent phospholipids per gram tissue
White muscle	1.57±0.12	0.93±0.14	0.72±0.03
Red muscle	22.09±1.53	20.98±0.38	1.18±0.12
Heart	2.35±0.06	0.65±0.14	1.91±0.13
Liver	3.34±0.06	0.58±0.13	2.76±0.14
Gills	1.49±0.04	0.55±0.11	1.02±0.04
Intestine	2.58±0.20	1.35±0.33	1.14±0.12
Adipose	67.5±2.50	ND	ND

Note: Values are means ± standard error of the mean (N = 5). ND, not determined.

Fig. 1. Fatty acid composition of the neutral lipids (solid bars) and phospholipids (open bars) in (*a*) white muscle, (*b*) red muscle, (*c*) heart, (*d*) liver, (*e*) gills, and (*f*) intestine of adult rainbow trout (*Oncorynchus mykiss*). Values are percentages of total fatty acids in each lipid class. They are presented as means ± standard error of the mean (N = 5).

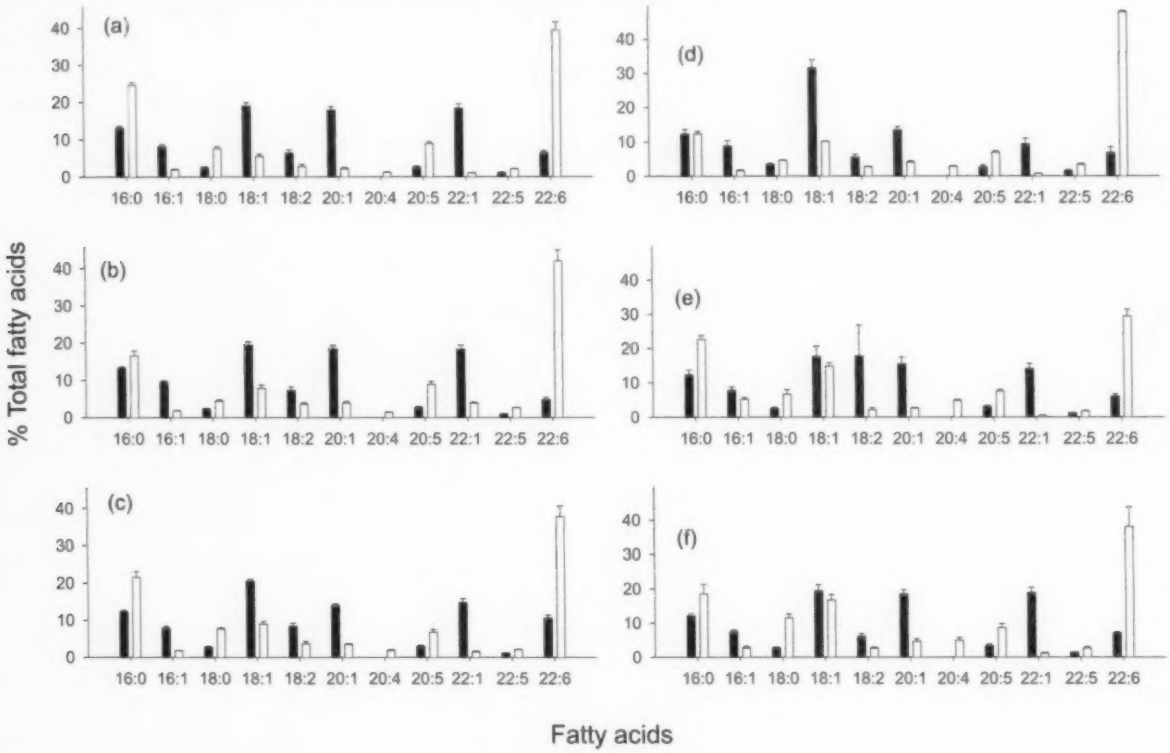

the same rate within each tissue ($p > 0.05$). Incorporation of fatty acids into specific lipid classes are presented for PL and NL (Figs. 5*a*, 5*b*). Incorporation of fatty acids were very different between tissues for both PL and NL ($p < 0.001$). For PL, liver > heart > gill > intestine > red muscle > white muscle. For NL, liver = red muscle = heart > gill = white muscle = intestine.

Incorporation into PL was the same for oleate and palmitate ($p = 0.83$), but oleate was incorporated much more rapidly than palmitate into NL ($p = 0.01$). The difference was particularly large for red muscle where oleate was incorporated 3.3 times more rapidly than palmitate ($p < 0.01$). The ratios of incorporation (oleate to palmitate) are presented for PL and NL (Fig. 6). No differences were found between tissues ($p = 0.4$), but these ratios were significantly higher for NL (2.79 ± 0.30, N = 6) than for PL (1.00 ± 0.14, N = 6) ($p < 0.001$). On average, therefore, oleate was incorporated into NL 2.8 times more rapidly than palmitate, whereas both fatty acids were incorporated at the same rate into PL.

Discussion

This study shows that fatty acid incorporation varies tremendously between tissues and that the dominant physiolog-

© 2003 NRC Canada

Table 2. Composition of tissue phospholipids expressed as percentages of total lipid phosphate in adult rainbow trout (*Oncorhynchus mykiss*).

Tissue	LPC	SPH	PC	PS	PI	PE	DPG	PA
White muscle	ND	3.0±0.6	64.8±1.4	3.5±0.7	4.0±0.4	21.7±0.7	2.3±0.7	0.7±0.3
Red muscle	ND	3.2±0.8	56.1±1.2	2.5±0.4	4.9±0.5	21.1±1.8	12.4±0.7	ND
Heart	ND	7.4±1.4	47.2±4.4	3.5±0.6	5.5±0.5	23.3±2.9	13.2±1.4	ND
Liver	0.6±0.2	7.7±0.9	55.0±0.7	5.9±0.7	4.0±0.7	23.7±0.8	2.9±0.5	0.3±0.1
Gills	1.8±0.6	5.8±0.9	57.8±1.9	4.5±0.9	3.8±0.6	22.9±1.0	3.0±0.4	0.4±0.2
Intestine	2.2±0.5	9.0±0.4	53.2±1.3	5.6±0.8	5.7±0.6	21.3±1.0	2.4±0.5	0.5±0.2

Note: Values are means ± standard error of the mean (N = 5 animals). LPC, lysophosphatidylcholine; SPH, sphingomyelin; PC, phosphatidylcholine; PS, phosphatidylserine; PI, phosphatidylinositol; PE, phosphatidylethanolamine; DPG, diphosphatidylglycerol; PA, phosphatidic acid; ND, not detected.

Fig. 2. Measured specific activities of oleate (solid bars) and palmitate (open bars) in (*a*) the neutral lipids and (*b*) the phospholipids of rainbow trout tissues (*Oncorynchus mykiss*) 24 h after administration of 1-^{14}C-palmitate and 9,10-^{3}H-oleate. Values shown were corrected for a standard dose of radioactivity administered (10^7 disintegrations per min or 166 667 Bq) and for a standard body mass of 500 g. They are means ± standard error of the mean (N = 5).

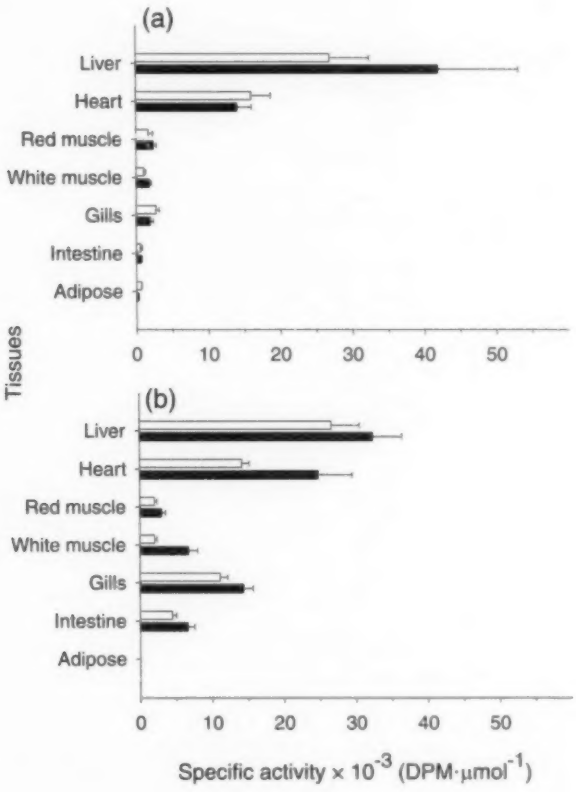

Fig. 3. Ratios of oleate specific activity over palmitate specific activity in the neutral lipids (solid bars) and phospholipids (open bars) of rainbow trout tissues (*Oncorynchus mykiss*) 24 h after administration of 1-^{14}C-palmitate and 9,10-^{3}H-oleate. Values are means ± standard error of the mean (N = 5).

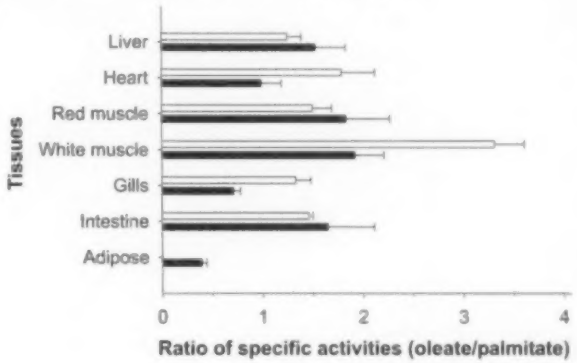

Fig. 4. Oleate (open bars) and palmitate incorporation (solid bars) in total lipids of resting rainbow trout tissues (*Oncorynchus mykiss*). Values are means ± standard error of the mean (N = 5).

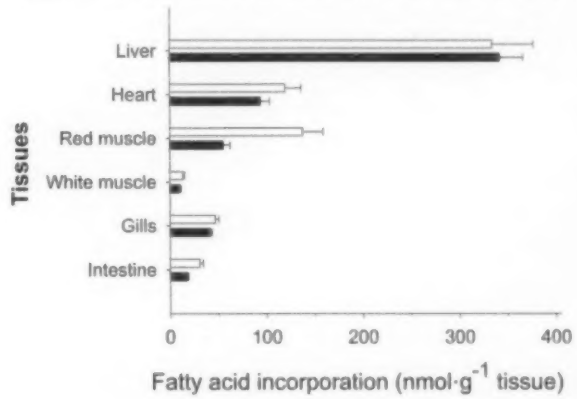

ical roles of palmitate and oleate are different. The highest rates of fatty acid fixation were found in liver, where oleate was incorporated 25 times faster and palmitate 35 times faster than in white muscle. When examining more specifically in which lipid classes these circulating fatty acids were included, we found that their incorporation was higher in PL than in NL for most tissues. Therefore, the most striking difference between tissues was observed for fatty acid incorporation into PL, which was 43 times higher in liver than in white muscle. More importantly, our results show that oleate is incorporated much more rapidly than palmitate into the storage lipids of all tissues (NL), showing that oleate plays a

© 2003 NRC Canada

Fig. 5. Oleate (open bars) and palmitate incorporation (solid bars) in (*a*) the phospholipids and (*b*) the neutral lipids of resting rainbow trout tissues (*Oncorynchus mykiss*). Values are means ± standard error of the mean (N = 5).

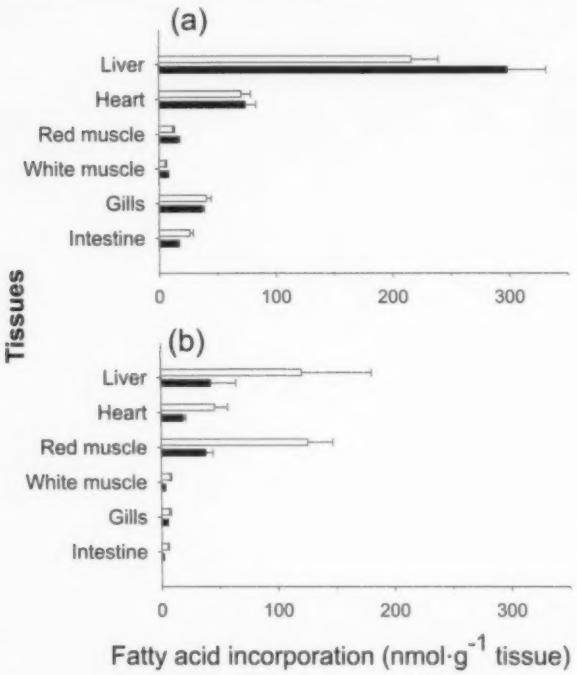

Fig. 6. Ratios of oleate incorporation over palmitate incorporation in the phospholipids (open bars) and neutral lipids (solid bars) of resting rainbow trout tissues (*Oncorynchus mykiss*). Values are means ± standard error of the mean (N = 5).

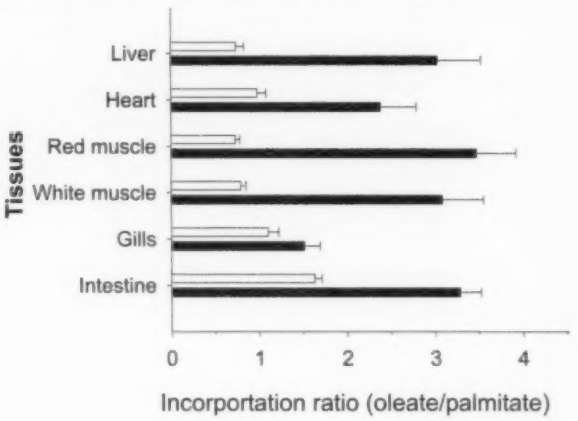

prominent role in energy metabolism (mean ratio oleate to palmitate for rate of incorporation into NL = 2.8 ± 0.3). In contrast, both fatty acids are incorporated equally into tissue PL (mean ratio for incorporation into PL = 1.0 ± 0.2), suggesting that oleate and palmitate contribute equally to membrane turnover.

Intertissue differences in tissue uptake

How can such large intertissue differences in fatty acid incorporation be explained? The rate of long-chain fatty acid entry into mammalian cells depends on the density of several membrane-bound fatty acid transport proteins (fatty acid translocase, FAT/CD36; fatty acid transport protein, FATP; membrane fatty acid binding protein, FABPm) (Abumrad et al. 1999), as well as on the concentration of cytosolic fatty acid binding proteins, FABPc (Storch and Thumser 2000). For example, the higher rate of fatty acid incorporation for red vs. white muscle in the rat is associated with a fivefold difference in FABPc concentration between these two tissues (Bonen et al. 1998). In fish, the membrane-bound fatty acid transporters have not been characterized, and limited information is available for FABPc (Londraville and Sidell 1995; Stewart and Driedzic 1988). Important intertissue differences in the concentrations of FAT/CD36, FATP, FABPm, and FABPc (or their fish equivalents) may be responsible for the large differences in incorporation rates observed here. Measuring the density and the kinetics of these proteins in fish tissues will provide a new dimension to the understanding of fatty acid metabolism in this group of vertebrates. For example, interesting cycles in the abundance of the translocase (FAT/CD36) or the transport protein (FATP) would be expected to occur in synchrony with seasonal changes in fatty acid utilization.

The fatty acid incorporation measured here represents tissue uptake minus oxidation. Estimating rates of tissue uptake from our results is not possible because prevailing oxidation rates were not measured in our experiments. Measurements of palmitate metabolism in isolated rainbow trout hearts show that the ratio between oxidation rate and incorporation rate can vary between about 0.1 at low temperature and 1 at high temperature (Bailey and Driedzic 1993). Therefore, using measured rates of incorporation as indices of tissue uptake would lead to ~50% error for heart tissue at high temperature. Alternately, it could be argued that oxidation rates are minimal compared with incorporation rates because only a small fraction of total tissue fatty acids is oxidized in 24 h (the time used here to measure incorporation rate). Using published rates of fatty acid oxidation in isolated fish mitochondria (Bilinski and Jonas 1970; Henderson and Sargent 1985) and in perfused tissues (Sidell et al. 1995), we can calculate that a maximum of 1.5% of total stored fatty acids is oxidized per day. This maximal value of 1.5% was calculated for the heart, whereas tissues such as liver (1.3%), red muscle (0.4%), and white muscle (0.08%) have lower values. Using the different lines of reasoning discussed above, we can conclude that oxidation rate can go from less than 1% to close to 50% of uptake rate depending on tissue type and temperature.

Preferential role of monounsaturates in energy metabolism

Previous studies report preferential mobilization of oleate from triacylglycerol reserves (Jezierska et al. 1982; Raclot and Groscolas 1993, 1995) and preferential oxidation of oleate over saturated fatty acids (Leyton et al. 1987; Sidell 1991; Sidell et al. 1995). Here, we show that oleate is incor-

© 2003 NRC Canada

porated into storage lipids 2.8 times more rapidly than the saturated fatty acid palmitate. This may be a general feature of vertebrates because oleate is also often the most abundant fatty acid present in the lipid reserves of fish, birds, and mammals (Blem 1990; Florant et al. 1990; Lund and Sidell 1992). Further research is needed to address the mechanistic reasons for more rapid oleate incorporation, but our data suggest selectivity for oleate in several proteins involved in the pathway for fatty acid storage. They include fatty acid binding proteins, transmembrane translocases, and the enzymes responsible for triacylglycerol synthesis (glycerol phosphate acyltransferase and the triacylglycerol synthetase complex).

It is clear that the regulation of fatty acid metabolism can take place at many different levels: storage, mobilization, transport, and oxidation. To our knowledge, selectivity for oleate in the mobilization step or lipolysis (i.e., selectivity by hormone-sensitive lipase or lipoprotein lipase shown through substrate competition experiments) and in the various transport steps (fatty acid binding proteins and translocases) has not been demonstrated in fish. Our results show that the storage of oleate is favored, and they are consistent with several studies demonstrating that monounsaturates are oxidized preferentially in fish. In vitro, isolated tissues from Antarctic fish (heart, skeletal muscle) (Sidell et al. 1995) and isolated mitochondria from rainbow trout (white muscle, red muscle, heart, and liver) (Bilinski and Jonas 1970) have been shown to oxidize oleate much more rapidly than palmitate. Another study reported preferential in vivo depletion of monounsaturates in the liver and skeletal muscle of rainbow trout during starvation (Jezierska et al. 1982). At the present time, no convincing theoretical argument has been proposed to explain why monounsaturated fatty acids are playing such a prominent role in energy metabolism. Therefore, future research should attempt to answer the more fundamental question: what advantage(s) do monounsaturates provide over saturates or polyunsaturates, if any?

Tissue lipid content and composition

Adipose tissue (68% lipids) and red muscle (22% lipids) stand out for storing particularly large amounts of fat, and these essential energy reserves are strategically located to support prolonged fasting and endurance swimming. In contrast, all other tissues only store modest amounts of lipids (1.5–3.3%). When analyzing the fatty acid composition of tissue lipids, we observed that palmitate was overall more abundant in PL (19%) than in NL (13%) or than in the food (10%) (Weber et al. 2002). This difference between PL and NL is consistent with the pattern seen in plasma lipids where PL had 24% palmitate vs. only 11% in NL (Weber et al. 2002). Therefore, these results show that palmitate is actively accumulated in membrane phospholipids. Interestingly, oleate is not actively concentrated in tissue PL, but it is in NL (21% oleate in NL, 10% in PL, and 13% in food), again matching the pattern previously observed in plasma (22% oleate in NL, but only 10% in PL) (Weber et al. 2002). It is conceivable that the organism spares palmitate for PL synthesis and, therefore, only channels minimal amounts of this FA towards energy metabolism. Finally, trout membrane PL are particularly rich in docosahexaenoic acid (22:6), representing 29–47% of total fatty acids in tissue PL, a pattern consistent with plasma PL (35% 22:6). Trout must presumably pay a significant metabolic cost to maintain such high levels of this key membrane component because it only represents 11% and 7% of total fatty acids in plasma nonesterified fatty acids and in their diet, respectively (Weber et al. 2002).

With the notable exception of diphosphatidylglycerol (DPG), the different classes of PL are represented similarly in all rainbow trout tissues. Phosphatidyl choline (47–65% total membrane PL) and phosphatidyl ethanolamine (21–24%) are always the main membrane constituents, whereas sphyngomyelin (3–9%) and phosphatidyl serine (3–6%) play a more minor role. The percentage of phosphatidyl ethanolamine measured here (21–24%) appears to be necessary for the proper functioning of fish membranes at the temperature of our experiments (12 °C). However, percent phosphatidyl ethanolamine is known to increase significantly during acclimation to lower temperatures (Hazel 1984).

Because DPG is a phospholipid found exclusively in mitochondrial membranes, its abundance varies with mitochondrial density. Therefore, highly aerobic tissues such as heart and red muscle have relatively high levels of DPG (12–13% DPG in total tissue PL), whereas all other tissues have only 2–3%. Mitochondrial density is usually quantified directly using morphometric methods (Cruz-Orive and Weibel 1990) or indirectly by measuring the activities of citrate synthase or cytochrome oxidase. To our knowledge, DPG concentration has never been used as an index of mitochondrial density and it would be interesting to determine how well it correlates with these other measurements.

In conclusion, this study reveals a novel aspect of the dominant role played by oleate in the energy metabolism of fish: its preferential incorporation in the triacylglycerol reserves of all tissues. Even though fatty acid incorporation in tissue lipids varies tremendously among tissues, oleate and palmitate enter phospholipids at similar rates within each tissue and, therefore, contribute equally to membrane turnover. Finally, we propose that diphosphatidylglycerol concentration in tissues could be used as a convenient index of their mitochondrial density.

Acknowledgements

We thank Leonardo Magnoni for helpful comments and discussions. This research was supported by a discovery grant to J.-M.W. from the Natural Sciences and Engineering Research Council of Canada (NSERC).

References

Abumrad, N., Coburn, C., and Ibrahimi, A. 1999. Membrane proteins implicated in long-chain fatty acid uptake by mammalian cells: CD36, FATP and FABPm. Biochim. Biophys. Acta, **1441**: 4–13.

Bailey, J.R., and Driedzic, W.R. 1993. Influence of low temperature acclimation on fate of metabolic fuels in rainbow trout (*Oncorhynchus mykiss*) hearts. Can. J. Zool. **71**: 2167–2173.

Bartlett, G.R. 1959. Phosphorus assay in column chromatography. J. Biol. Chem. **234**: 466–468.

© 2003 NRC Canada

Bernard, S.F., Reidy, S.P., Zwingelstein, G., and Weber, J.-M. 1999. Glycerol and fatty acid kinetics in rainbow trout: effects of endurance swimming. J. Exp. Biol. **202**: 279–288.

Bilinski, E., and Jonas, R.E.E. 1970. Effects of coenzyme A and carnitine on fatty acid oxidation by rainbow trout mitochondria. J. Fish. Res. Board Can. **27**: 857–864.

Blem, C.R. 1990. Avian energy storage. Curr. Ornithol. **7**: 59–113.

Bonen, A., Luiken, J.J.F.P., Liu, S., Dyck, D.J., Kiens, B., Kristiansen, S., Turcotte, L.P., Van der Vusse, G.J., and Glatz, J.F.C. 1998. Palmitate transport and fatty acid transporters in red and white muscles. Am. J. Physiol. **275**: E471–E478.

Cruz-Orive, L.M., and Weibel, E.R. 1990. Recent stereological methods for cell biology: a brief survey. Am. J. Physiol. **258**: L148-L156.

Dittmer, J.C., and Lester, R.L. 1964. A simple specific spray for the detection of phospholipids on thin-layer chromatograms. J. Lipid Res. **5**: 126–127.

Dudley, P.A., and Anderson, R.E. 1975. Separation of polyunsaturated fatty acids by argentation thin layer chromatography. Lipids, **10**: 113–115.

Florant, G.L., Nuttle, L.C., Mullinex, D.E., and Rintoul, D.A. 1990. Plasma and white adipose tissue lipid composition in marmots. Am. J. Physiol. **258**: R1123–R1131.

Folch, J., Lees, M., and Sloane-Stanley, G.H. 1957. A simple method for the isolation and purification of total lipids from animal tissues. J. Biol. Chem. **226**: 497–509.

Greene, D.H.S., and Selivonchick, D.P. 1987. Lipid metabolism in fish. Prog. Lipid Res. **26**: 53–85.

Haman, F., and Weber, J.-M. 1996. Continuous tracer infusion to measure in vivo metabolite turnover rates in trout. J. Exp. Biol. **199**: 1157–1162.

Haman, F., Powell, M., and Weber, J.-M. 1997*a*. Reliability of continuous tracer infusion for measuring glucose turnover rate in rainbow trout. J. Exp. Biol. **200**: 2557–2563.

Haman, F., Zwingelstein, G., and Weber, J.-M. 1997*b*. Effects of hypoxia and low temperature on substrate fluxes in fish: plasma metabolite concentrations are misleading. Am. J. Physiol. **273**: R2046–R2054.

Hazel, J.R. 1984. Effects of temperature on the structure and metabolism of cell membranes in fish. Am. J. Physiol. **246**: R460–R470.

Henderson, R.P., and Sargent, J.R. 1985. Chain length specificities of mitochondrial and peroxisomal β-oxidation of fatty acids in liver of rainbow trout (*Salmo gairdneri*). Comp. Biochem. Physiol. B, **82**: 79–85.

Jezierska, B., Hazel, J.R., and Gerking, S.D. 1982. Lipid mobilization during starvation in the rainbow trout *Salmo gairdneri* Richardson, with attention to fatty acids. J. Fish Biol. **21**: 681–692.

Leyton, J., Drury, P.J., and Crawford, M.A. 1987. Differential oxidation of saturated and unsaturated fatty acids in vivo in the rat. Br. J. Nutr. **57**: 383–393.

Londraville, R.L., and Sidell, B.D. 1995. Purification and characterization of fatty acid-binding protein from aerobic muscle of the Antarctic icefish *Chaenocephalus aceratus*. J. Exp. Zool. **273**: 190–203.

Lund, E.D., and Sidell, B.D. 1992. Neutral lipid compositions of Antarctic fish tissues may reflect use of fatty acyl substrates by catabolic systems. Mar. Biol. **112**: 377–382.

Portoukalian, J., Meister, R., and Zwingelstein, G. 1978. Improved two-dimensional solvent system for thin-layer chromatographic analysis of polar lipids on silica gel 60 precoated plates. J. Chromatogr. **152**: 569–574.

Raclot, T., and Groscolas, R. 1993. Differential mobilization of white adipose tissue fatty acids according to chain length, unsaturation, and positional isomerism. J. Lipid Res. **34**: 1515–1526.

Raclot, T., and Groscolas, R. 1995. Selective mobilization of adipose tissue fatty acids during energy depletion in the rat. J. Lipid Res. **36**: 2164–2173.

Sidell, B.D. 1991. Physiological roles of high lipid content in tissues of Antarctic fish species. *In* Biology of Antarctic fish. *Edited by* G. di Prisco, B. Maresca, and B. Tota. Springer-Verlag, New York. pp. 220–231.

Sidell, B.D., Crockett, E.L., and Driedzic, W.R. 1995. Antarctic fish tissues preferentially catabolize monoenoic fatty acids. J. Exp. Zool. **271**: 73–81.

Stewart, J.M., and Driedzic, W.R. 1988. Fatty acid binding proteins in teleost fish. Can. J. Zool. **66**: 2671–2675.

Storch, J., and Thumser, A.E. 2000. The fatty acid transport function of fatty acid-binding proteins. Biochim. Biophys. Acta, **1486**: 28–44.

Weber, J.-M., Brichon, G., Bodennec, J., and Zwingelstein, G. 2002. Palmitate and oleate metabolism of rainbow trout in vivo. Comp. Biochem. Physiol. A, **131**: 409–416.

Zwingelstein, G., Abdul-Malak, N., and Brichon, G. 1978. Effect of environmental temperature on biosynthesis of liver phosphatidylcholine in the trout (*Salmo gairdneri*). J. Therm. Biol. **3**: 229–233.

© 2003 NRC Canada

The risk of running on empty: the influence of age on starvation and gut fullness in larval Atlantic cod (*Gadus morhua*)

Adrian Jordaan and Joseph A. Brown

Abstract: Two experiments were set up to evaluate whether the response of Atlantic cod (*Gadus morhua*) larvae to no-prey conditions changes with age. The first experiment was designed to test for age-specific starvation with starvation trials at 0, 5, 15, 30, and 45 days after hatching. Mortality, length, and swimming activity data were collected. A second experiment was conducted to determine the effect of non-feeding conditions on the residency of prey in the gut at 5, 15, 30, and 45 days after hatching. The results of experiment 1 indicated that mortality occurred most rapidly at 15 and 30 days and was delayed during the yolk-sac period (day 0). Larvae in non-fed treatments showed significantly lower activity levels, except in the 45-day treatment, and the reduction in activity occurred before the onset of mortality. In experiment 2, gut residencies displayed an age-dependent response, with 5- and 45-day-old larvae having significantly shorter residency times. We conclude that beyond the yolk-sac period, cod larvae exhibit an age-dependent trade-off between growth and starvation risk. Larval age also influences patterns of gut fullness over time, with the fastest rates of gut clearance found at first-feeding and metamorphosis.

Résumé : Deux expériences ont permis de déterminer si la réaction des larves de la morue franche de l'Atlantique (*Gadus morhua*) à l'absence de proies change avec l'âge. La première expérience était destinée à vérifier la famine par des essais aux jours 0, 5, 15, 30 et 45 après l'éclosion; la mortalité, la longueur et l'activité de nage ont été notées. La seconde expérience avait pour but de vérifier l'effet de l'absence d'alimentation sur la durée de résidence des proies dans le tube digestif aux jours 5, 15, 30 et 45 après l'éclosion. Les résultats de la première expérience indiquent que la mortalité se produit plus rapidement aux jours 15 et 30 et qu'elle est retardée lorsqu'il y a encore un sac vitellin (jour 0). Sauf au jour 45, les larves non alimentées ont des niveaux d'activité significativement réduits et le déclin de l'activité se produit avant le début de la mortalité. Dans la seconde expérience, les durées de résidence des proies s'avèrent être reliées à l'âge, les larves âgées de 5 et de 45 jours affichant les temps de résidence significativement les plus courts. Nous concluons qu'après le stade du sac vitellin, les larves de morue font un compromis en fonction de l'âge entre la croissance et le danger de famine. L'âge des larves influence aussi les patterns de remplissage du tube digestif dans le temps et les taux d'évacuation du tube digestif les plus rapides se produisent lors de la première prise de nourriture et lors de la métamorphose.

[Traduit par la Rédaction]

Introduction

Hjort (1914) was the first to suggest that critical periods could contribute to the large decrease in fish abundance observed between spawning and the age at which individuals enter into a fishery. An increased risk of starvation during the transition from an endogenous to an exogenous food source has received much attention as a probable critical period (Hjort 1914), in particular through the development of the match–mismatch hypothesis (Cushing 1990). Pepin (1991), using a meta-analysis of larval studies, showed that the mortality rate of larvae decreases with increasing age. Enhanced energy storage capacity in larger larvae is presumably the cause of decreased starvation susceptibility with age reported for a number of species (Hunter 1981).

More recent research has contrasted with the longer-held idea that first-feeding larvae are at increased risk of starvation. Miller et al. (1988), also using a meta-analysis of larval studies, found no evidence that first-feeding larvae were more susceptible to starvation than feeding larvae of a similar size. Cod (*Gadus morhua*) larvae starved from hatch had significant differences in levels of RNA (potential for protein synthesis and growth) and DNA (measure of mass) compared with feeding larvae at 5 and 11 days after hatching, respectively (McNamara et al. 1999). When starvation was applied at 29 days after hatching, the number of days before significant differences were observed between starved and fed larvae was reduced to 1–3 days for RNA and 3–5 days for DNA. This suggests that older cod larvae are less capable than young yolk-sac larvae of surviving periods of star-

Received 19 December 2002. Accepted 31 August 2003. Published on the NRC Research Press Web site at http://cjfas.nrc.ca on 12 November 2003.
J17106

A. Jordaan. School of Marine Sciences, 214 Libby Hall, University of Maine, Orono, ME 04469, U.S.A.
J.A. Brown. Ocean Sciences Centre, Memorial University of Newfoundland, St. John's, NL A1B 3X9, Canada.

 doi: 10.1139/F03-108 © 2003 NRC Canada

vation. Thorisson (1994) presents evidence that starvation contributes to a period of increased, but variable, mortality of cod around metamorphosis. Cushing (1990) also discusses extending the match–mismatch hypothesis to cover a longer period of early life histories. We believe that documentation of age-mediated changes in the response to food deprivation may help improve overall understanding of energetic priorities and life-history strategies of larval cod and whether critical periods result from differences in larval ability or from oceanographic processes.

Swimming activity has been related to interspecies differences in time to irreversible starvation (Hunter 1981) and has been used to infer the priorities of energy allocation (Skiftesvik 1992). Search swimming represents the largest energy expenditure during feeding (Drost and van den Boorgaart 1986). Increased larval size has been related to increases in feeding frequency and gut fullness (e.g., McLaren et al. 1997; Puvanendran and Brown 1999; Puvanendran et al. 2002). Both physical (gape size and muscle development) and physiological (perception and capture ability) constraints of prey ingestion change rapidly during development (Williams et al. 1996; Pepin and Penney 1997). These changes, coupled with an improvement in digestive abilities (Morrison 1993; Hunt von Herbing and Boutilier 1996), could result in changing activity levels and susceptibility to starvation as larvae grow.

Growth through protein synthesis is highest after feeding because of the delivery of dietary amino acids (Houlihan et al. 1995). Information regarding age or size effects on gut processes may be useful in understanding the growth of cod larvae. Gut fullness has been suggested as a measure of fitness (Hughes 1997) and has been used to estimate feeding success in wild cod larvae (McLaren et al. 1997). Gut fullness has also been used to infer larval consumption of zooplankton (Pepin and Penney 2000) and the influence of turbulence on larval feeding (Dower et al. 1998). These applications assume, in comparing larvae of different sizes or ages, that there is an equal response of larval gut fullness to prey conditions throughout larval development. At hatch, the gut of cod is underdeveloped compared with that of adult fish (Morrison 1993). The presence of a true stomach with glands, associated low pH levels, and dependence on extracellular digestion (chitinase and pepsin) does not occur until metamorphosis (16–20 mm; Govoni et al. 1986; Petersen and Falk-Petersen 1992). A gradual increase of gut surface area through the larval period (Petersen and Falk-Petersen 1992) could also influence gut fullness. Furthermore, the number of prey contained in a larval gut increases with larval size (Gamble and Houde 1984), suggesting that the patterns of gut fullness over the larval period may not be identical.

Cod larvae 7 mm long are capable of ingesting an average of 2.4 nauplii in 0.5 h and digesting them in 2 h at 5 °C (Tilseth and Ellertsen 1984). The authors also found that by using a 3-h feeding time, a feeding incidence (number feeding/total number of larvae × 100) of 90% was reached. Kane (1984) showed that at peak feeding around sunset, cod larvae in the wild averaged more than 15 prey per gut. Large numbers of cod larvae with empty guts, poor feeding conditions, and high metabolic demands during metamorphosis compelled Thorisson (1994) to suggest a second critical period for cod larvae. An ability to understand the complex nature of cod development, patterns of gut fullness, and the consequences of these on larval ecology, in particular with regards to critical periods and growth, will depend on good information relating these variables.

The purpose of this paper is to provide information regarding the responses of larval cod (*Gadus morhua*) to food deprivation in both the long term (survival) and the short term (gut residency) by testing the null hypothesis of no effect of age. There are two experiments reported. The first will use measurements of mortality, growth, and swimming activity to determine whether susceptibility to starvation for larval cod is independent of age. The second experiment will determine whether there are any age-dependent differences in the patterns of gut fullness once larvae are exposed to conditions devoid of prey.

Materials and methods

Larval rearing

The broodstock were collected from Trinity Bay (Newfoundland; 48–00°N, 53–30°W) and placed in tanks at the Ocean Sciences Centre, Memorial University of Newfoundland, St. John's, Newfoundland. Naturally spawned eggs were collected from broodstock tanks and transferred to a rearing tank. The rearing tank had two inflows of chilled seawater that ensured good water mixing and temperatures of 7.7 ± 0.6 °C. The tank was siphoned daily to remove dead eggs and larvae and to prevent bacterial growth. At hatch, the volume of the tank was increased from 30 L to 80 L. Two air stones were placed in the tank. The water outflow was placed mid-depth to minimize affects on the buoyant newly hatched larvae.

The larvae were fed 4000 prey·L^{-1} twice per day, once in the morning and once in the afternoon (Puvanendran and Brown 1999). Rotifers (*Brachionus plicatilis*) were used for the first 15 days and a 1:1 mixture of rotifers and 2-day-old *Artemia* nauplii was used for the next 15 days. The larvae were placed on an exclusively *Artemia* diet from day 31 until the completion of the experiment. Protein selco and super selco (INVE, Belgium) were used for enriching rotifers and *Artemia*, respectively. Algae (1–4 L of *Isochrisis* spp.) was added daily to larval tanks for the first 10 days and was also used in the enrichment of rotifers. Light intensity varied across the surface of the tank from approximately 4.7 μE·m^{-2}·s^{-1} at the edge to 18.7 μE·m^{-2}·s^{-1} in the center of the tank.

Experiment 1

On 0, 5, 15, 30, and 45 days after hatching, larvae were collected from the rearing tank described above after a 3-h feeding period. All larvae were gently moved through three water changes with filtered seawater to remove any prey items that may have been transferred from the rearing tank. All seawater used in experiments was filtered through four filters (prefilter, 120 μm, 20 μm, and 3 μm) and an ultraviolet filter and was adjusted to temperature before use. Glass bowls (10 L) with depths about twice the diameter were stocked at 12 larvae·L^{-1} for a total of 120 larvae/bowl. The static bowls had slight aeration and a light intensity of 10.9 (±0.4) μE·m^{-2}·s^{-1}. Water changes were done every 2–3 days using filtered seawater, and daily siphoning maintained water quality throughout each experiment. Two treatments were

© 2003 NRC Canada

set up: no feeding (non-fed) and feeding (fed). Each treatment was replicated (n = 2). The non-fed bowls were checked and monitored to ensure that no food was present. The controlled feeding bowls had prey added to maintain prey densities of 4000 prey·L^{-1}. Each bowl was checked daily for mortalities, which were identified by sliding a white background under the bowls and scanning the entire bottom twice. Larvae become white at death; therefore, pairs of black eyes were the primary method of detection. Mortalities were tallied and removed from the tanks. Larvae were sampled at the beginning of each trial (n = 20) from the common population in the rearing tank for initial standard length (measure from the tip of the snout to the end of the notochord). Larvae were sampled (n = 10) again at the point of 50% mortality in the non-fed treatment from both the fed and non-fed treatments for standard lengths. During sampling for measurements, the condition of larvae was also noted.

A daily observation of swimming behaviour of larvae in the experimental bowls was done before morning feeding. The observations were taken from ca. 50 cm above the bowl, randomly choosing five larvae from each bowl per day and following each for 1 min. Activity was recorded by stopwatch as the amount of time that an individual larvae spent swimming. This method was practiced for 2 weeks before the initiation of experiments. When cannibalistic events occurred, they were noted. A cannibalistic event was limited to biting and chasing behaviour towards or by the observed larvae. The number of larvae within 1–2 cm of the bottom and at the surface was also noted. The water temperature was recorded at the time of the activity observations.

Experiment 2

A second experiment was conducted to determine the rate of gut clearance. The term gut clearance will be used instead of gut evacuation because evacuation implies passage of food items through the gut. This occurs in continuous feeding, but not under the conditions of this experiment. On 5, 15, 30, and 45 days after hatching, 400 larvae were removed from the rearing tank 3 h after feeding and placed in a bucket. Three hours was chosen based on published data (Tilseth and Ellertsen 1984). The larvae were gently placed through three water changes. The water was checked for prey before the experiment started. The larvae were then divided into each of two 7-L bowls containing filtered seawater. Once the transfer was completed, 10 larvae (five from each bowl) were immediately removed by pipette and placed in a beaker that was kept on ice to maintain low temperatures. The larvae were immediately observed individually by stereomicroscope. The proportion of larvae with food present was noted, as well as the number of prey and prey type and colour when possible. Larvae were sampled from the 7-L bowls every hour until two consecutive hours of larvae with no prey in the gut were observed.

Statistics

Mortality data were analyzed using the nonparametric Kaplan–Meier (K–M) or product limit estimator (Lee 1992) to generate a survivorship curve. The K–M estimate is a step function available in the survival analysis option in SYSTAT™ (version 9.0; Systat Software Inc., Richmond, Calif.). The standard error reported for the survivor functions was computed using Greenwood's formula (SYSTAT™ version 9.0). K–M analysis returns the probability of being alive at a particular time. Individual mortalities are scored as deaths ("failures" in K–M terminology) associated with the day previous to removal. Larvae that were remaining at the conclusion of the experiments were right-censored, which identifies the larvae as alive at the time of sampling, versus being considered a "failure". Larvae must be scored as either a failure or be right-censored. The 10 larvae sampled at 50% mortality and any "missing" larvae at the conclusion of the experiment were subtracted from the initial trial number. The treatment effect (fed, non-fed) was tested first in a full model by assigning it as the covariate. The effect of age was tested using Cox proportional hazards estimation with stratification on age. The model was then split into fed and non-fed models keeping the age as strata and having no covariate for either. The replicates were also tested for significant differences using Cox proportional hazards estimation with stratification on replicate and age assigned as the covariate. When age had a significant effect in the model, the daily mortality of each age was compared using two-sample Kolmogorov–Smirnov (K–S) tests in which cumulative distribution functions are compared to determine whether they originate from the same sample. Growth differences between fed and non-fed treatments at 50% mortality were compared by pooling larvae by treatment and using two-sample t tests. The activity data were also pooled and are presented with error bars representing the 95% confidence intervals to illustrate the mean larval swimming response and the associated variation. The 95% confidence intervals were calculated assuming a t distribution.

The gut residency times were evaluated using the same method described for the mortality. The transparency of larvae makes observations of fullness simple and accurate. Larvae were assigned as failures when the gut was empty or the remaining material in the gut was nondigestible. Larvae that had food remaining in the gut were right-censored, which identifies the larvae as full (or alive) at the time of sampling. The K–M analysis of the gut data will return the probability of an individual being empty at a given time.

A conservative statistical significance (α) of 0.01 was set for all statistical tests because of low replicate size. To reduce experimentwide error as a result of multiple comparisons, the α level was adjusted using Bonferroni correction ($\alpha = \alpha/k$, where k is the number of comparisons (Sokal and Rohlf 1995)). All reported p values are Bonferroni adjusted. SYSTAT™ (version 9.0) was used for all statistical analyses.

Results

Experiment 1

On 0, 5, 15, 30, and 45 days after hatching, the mean standard lengths of larvae were 3.9, 4.2, 5.0, 8.0, and 12.3 mm, respectively (Table 1). At hatch, the larvae had a large yolk sac and a nonfunctional mouth. Feeding began on day 2 and the yolk sac was largely absorbed by day 7. The periods between days 15–30 and 30–45 showed the most rapid growth (Table 1), characterized by approximately 4% daily increases in standard length.

© 2003 NRC Canada

Table 1. The mean standard length (SL) and feeding incidence (FI), determined from the first 3 h of gut-residency observations as the proportion of cod larvae with prey in the gut, at trial initiation and the mean temperature (T), 50% mortality standard lengths (50% SL), and proportional difference (PD) between 50% SL means for fed and non-fed treatments for each trial.

Age, days after hatching	Treatment	SL ± SD (mm)	FI	T (°C)	50% SL ± SD (mm)	PD
0	Fed	3.9±0.14	N/A	11.1	4.8±0.52	0.19
	Non-fed			11.1	3.9±0.32	
5	Fed	4.2±0.29	0.88	10.9	4.9±0.41	0.13
	Non-fed			10.9	4.3±0.52	
15	Fed	5.0±0.40	0.78	11.5	5.8±0.53	0.12
	Non-fed			11.6	5.1±0.53	
30	Fed	8.0±0.60	0.94	12.1	10.0±0.65	0.18
	Non-fed			12.1	8.2±0.71	
45	Fed	12.3±1.71	0.94	10.7	15.4±1.01	0.17
	Non-fed			10.7	12.7±1.15	

Note: SD, standard deviation.

At 50% mortality in the non-fed tanks, the non-fed larvae exhibited clear losses in pigmentation, changes in myotome appearance (loss of definition and increased opacity), and collapsing of the gut compared with larvae from fed treatments. At all ages, the paired *t* tests showed no significant differences between the 50% mortality standard lengths and the initial standard lengths. All ages had significant differences between fed and non-fed standard lengths at 50% mortality ($p < 0.00065$; Table 1). All non-fed groups were reduced 12% to 19% of the standard length of their respective fed groups (Table 1).

The results of the K–M analysis indicate that non-feeding had a significant effect on the probability of survival (treatment estimate = –1.801, standard error (SE) = 0.070, *t* ratio = –25.847, $p < 0.001$). Age was significant in the model for the Mantel, Breslow-Gehan, and Tarone-Ware chi-squared statistics (χ^2 = 150.7, 209.3, and 182.2, respectively, df = 4, $p < 0.001$). Once the model was divided into fed and non-fed survivorship curves (Fig. 1), the effect of age was still significant with the Tarone-Ware chi-squared statistic (χ^2 = 133.9 and 361.8 for the fed and non-fed larvae, respectively, df = 4, $p < 0.001$). The results of the K–S tests separated the ages as follows. Progressing from lowest to highest mortality rates, the fed treatments order is 0 < 5 < 30, 45 < 15 days and the non-fed treatment order is 0 < 5, 45 < 15 < 30 days ($p \leq 0.000\,026$ for all significant comparisons). In testing the replicates for significant differences, age significantly influenced survival in both the fed and non-fed models ($p \leq 0.001$), and the replicates had no significant effect ($p > 0.05$ for all calculations).

The activity levels reflected the effects of food deprivation for all ages except the 45-day trial (Fig. 2). Individual swimming activity became erratic for the 45-day non-fed larvae, reflected in values well above zero for starving larvae. Non-fed larvae in the 0-, 5-, 15-, and 30-day trials were characterized by nonactive individuals that accumulated on the bottom of the tanks, whereas at 45 days, they collected on the surface. For the 0-, 5-, 15-, and 30-day non-fed larvae, using the last day of each trial, only 7% were in the water column and the rest were on the bottom. For the 45-day non-fed larvae, 40% were on the surface and 0% accumulated on the bottom. This compared with the average percentage of fed larvae found throughout the water column (not on surface or bottom) of 90%, with no values lower than 80% at any age. The 4th day of the 30-day trial had one non-fed larvae swim the entire 60-s observation period, resulting in a high mean and large 95% confidence intervals for that day. Cannibalistic events were observed only for the 30- and 45-day non-fed larvae with 0.15 and 1.8 events per 5 min of observations, respectively.

Experiment 2

Consumed prey was held in the entire gut (fore-, mid-, and hind-gut), and freshly eaten prey was often still alive in initial samples. The color of prey ranged from green for rotifers and red for *Artemia* nauplii to a white mass of indigestible material, for both, over the course of each trial.

The results of the K–M analysis and Cox proportional hazards estimation with stratification on age indicated that age had a significant effect on the probability of being empty (Fig. 3). The Mantel, Breslow-Gehan, and Tarone-Ware chi-squared statistics were all significant (χ^2 = 224.1, 100.3, and 153.7, respectively, df = 3, $p < 0.000\,000\,01$). The K–S tests confirmed that the 5- and 45-day larvae were not different ($p = 1.0$) and had significantly shorter gut residency times than the 15- and 30-day larvae ($p < 0.000\,000\,6$). The 30- and 45-day larvae were also different from each other, with the 30-day old larvae having the longest gut residency time ($p = 0.000\,066$). The test determined that there were differences in the rate of gut clearance, from a full gut to a gut filled only with indigestible material, at different ages.

Discussion

In the present study, if the tailing-off of the survivor curves in the non-fed treatments is disregarded, the failure points (100% mortality) of the population would have occurred at about 10.5, 6, 7, 6.5, and 7.5 days for the 0-, 5-, 15-, 30-, and 45-day groups, respectively. There was no decrease in mortality for fed and non-fed larvae after the shift from endogenous to exogenous feeding, and it is evident that susceptibility to starvation did not decrease with age. This provides support for the comments of Miller et al. (1988)

© 2003 NRC Canada

Fig. 1. Kaplan–Meier generated survivorship curves for cod (*Gadus morhua*) larvae 0, 5, 15, 30, and 45 days after hatching over time (in days) for (*a*) fed and (*b*) non-fed treatments. Vertical bars depict standard error. Different letter superscripts (A, B, C, D) in legend indicate significant difference between ages from Kolmogorov–Smirnov tests ($\alpha = 0.01$).

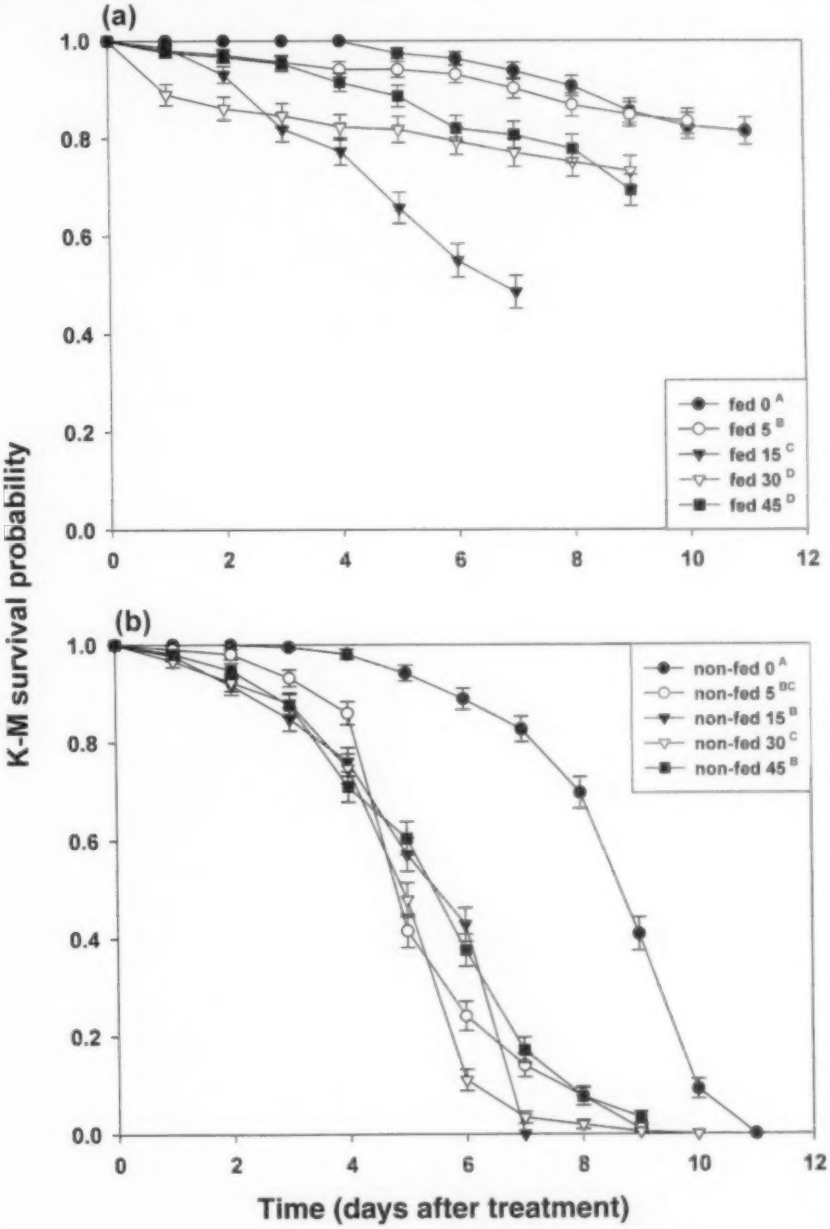

that first-feeding larvae are no more susceptible to starvation than larvae of equal size that had been feeding and then starved. Realistically, the yolk-sac period is the most flexible period, with a significant energy reserve that does not occur again until after metamorphosis.

The inability of older larvae to live longer suggests that little investment was made to energy stores in case of a loss of prey abundance. We suspect that cod larvae exercise a trade-off between growth and survival, which is evident in the response to food deprivation. Reduced protein turnover rates, which correlate with fast growth in individual fish, result in increased susceptibility to environmental stress (Houlihan et al. 1995). By maximizing growth rates, we suggest that larvae expose themselves to increased risks of starvation but are able to grow quicker than would be possible if investing in significant energy storage. Otterlei et al. (1999)

© 2003 NRC Canada

Fig. 2. Daily mean swimming activity and 95% confidence intervals of fed (●) and non-fed (■) treatments for (*a*) 0-, (*b*) 5-, (*c*) 15-, (*d*) 30-, and (*e*) 45-day-old cod (*Gadus morhua*) larvae; asterisk (*) indicates samples of only five individuals.

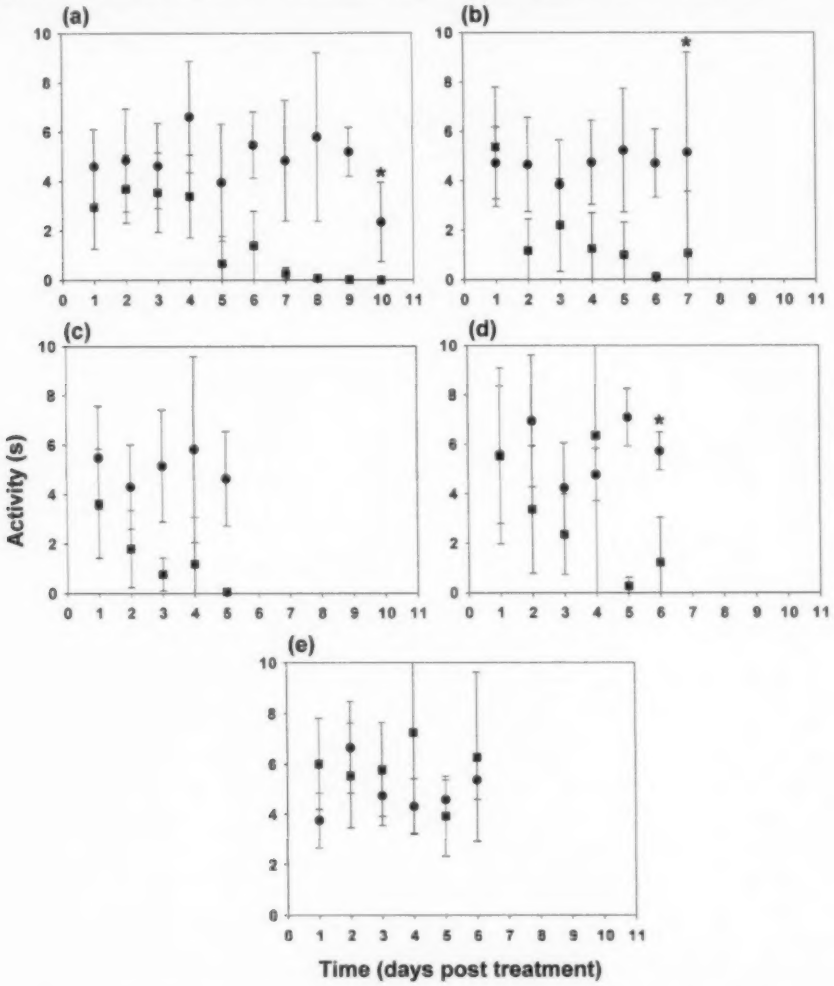

showed that the fastest growth in cod larvae occurs at about 25 days after hatching at 10–12 °C. This corresponds to the periods of highest mortality in both fed and non-fed larvae in the present study. With the high investment in growth up to metamorphosis, larvae that are not feeding will not survive, irrespective of age or size. When taken with observations by Pepin (1991) and Houde and Zastrow (1993) that growth and mortality rates are correlated, the results of this study suggest that faster growth in cod larvae incurs elevated risks of starvation and, as a consequence, preyless conditions translate more quickly to mortality during faster growth periods.

During the present study, the non-fed larvae displayed significantly reduced swimming activity compared with larvae in the fed treatments. Although increased swimming in low prey densities has been reported for cod (Puvanendran and Brown 1999; Puvanendran et al. 2002), reduced swimming under no-prey conditions was observed and is discussed by Skiftesvik (1992). Skiftesvik (1992) noted that reduced swimming might be an antipredatory response. However, if larvae are largely incapable of locating patches of prey and depend more on advection and retention in areas of optimal prey conditions (see Townsend and Pettigrew 1996) and turbulence to increase encounter rates with prey organisms (MacKenzie and Leggett 1991), then reduced swimming is likely an important, and perhaps the only, energy-saving mechanism available to larval fish.

Larvae in the 0-, 5-, 15-, and 30-day non-fed treatments were all found to exhibit low activity levels and accumulate on the bottom, whereas in the 45-day non-fed treatment, the larvae tended to float on the surface. Buoyancy and osmotic control are confounding factors, each being affected by food deprivation and each resulting in loss of hydrostatic lift and an increased sinking rate (Sclafani et al. 1997). Neilson et al. (1986) suggested that lower specific gravity of poorly fed larvae might lead to increased buoyancy and found that the larvae with the highest specific gravity, those that should be the least buoyant, were yolk-sac larvae. Both of these studies

© 2003 NRC Canada

Fig. 3. Kaplan–Meier generated gut-residency curves for 5-, 15-, 30-, and 45-day-old cod (*Gadus morhua*) larvae. Different letter superscripts (A, B, C) in legend indicate significant difference between ages from Kolmogorov–Smirnov tests ($\alpha = 0.01$).

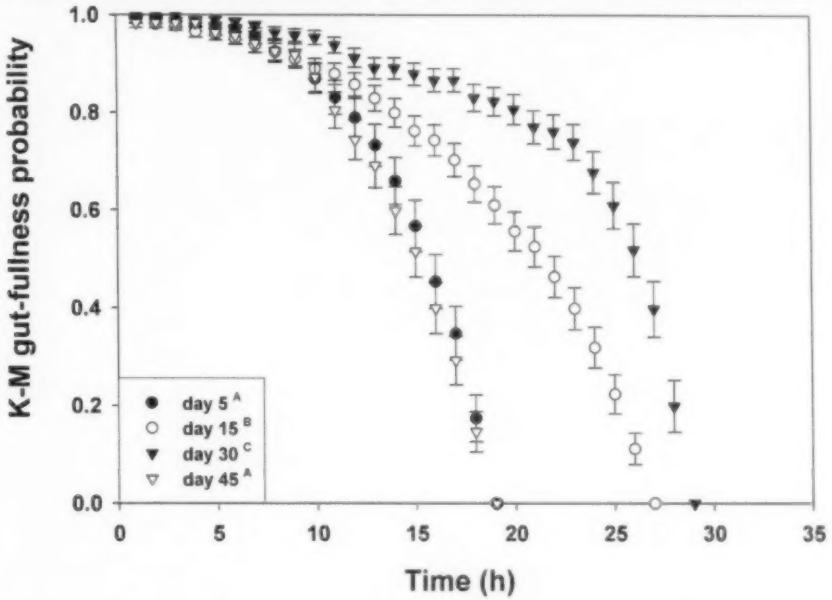

used larvae younger that those of the present study. Sclafani et al. (1997) starved larvae from hatch until 12 days after hatching, whereas Neilson et al. (1986) used four prey densities and reared the larvae until 21 days after hatching. The results of the present study concur with Sclafani et al. (1997) that starved larvae sink, but places an upper limit on this trend in that at some point between 8 mm and 12 mm starved cod larvae will float. If, as Sclafani et al. (1997) argue, buoyancy is important in controlling vertical distribution, then starved larvae may be absent from surface waters before they experience mortality over much of the larval stage.

The survival curves provide evidence of higher mortality in 15-day fed larvae, and during the first day of the 30-day fed trial where a number of moralities occurred in one replicate. The loss of feeding larvae at 15 days is not the result of starvation through inability to first-feed as this mortality was observed in the 0- and 5-day treatments. Activity levels in the 15-day fed treatment show no evidence of food deprivation. The 5-mm size (initial length of 15-day trials) corresponds to a food-independent drop in trypsin that has been equated with development in herring and cod larvae (Pedersen et al. 1990) and has also been noted in other larval fish (Ribeiro et al. 1999). In first-feeding cod, the level of total tripsinogen (protease precursor) and tripsin per larvae dropped ~80% at 5 days after hatch and subsequently remained at a low level until day 18 (5–8 °C) when an increase occurred (Hjelmeland et al. 1984). There is also a reported change in the digestive ability of cod larvae around 15–17 days at 6–8 °C (Kjorsvik et al. 1991). It is not possible to separate the observed mortality in fed treatments from factors associated with the rearing environment. Cod, unlike salmonids, have not been selected for growth under artificial conditions and broodstocks are entirely made up of adults caught from the wild. Because larvae operate on a tight energy budget (Wieser 1991), deviations from optimal rearing conditions are likely to impact survival directly. It should be recognized that as improvements are made in rearing techniques and nutrition of broodstock and larval diets, the impacts on survival may be minimized. The prey types offered to the larvae was also changed over this period, although it is not clear what role, if any, this could have played on survival. It does appear that cod are vulnerable to deviations in environmental conditions during the fast-growth period of the larval stage.

In experiment 2, the quickest gut residency times were at 4.2 mm (5 days after hatching) and 12.3 mm (45 days after hatching) standard length. Because of the release of high levels of trypsin at first feeding (Hjelmeland et al. 1984), it could be expected that the digestion times in the simple tube would be fast. The investment in ensuring successful first feeding is high and appears to result in much longer digestion times 2 weeks after hatch for larvae around 5 mm, when trypsin levels are reported to be much lower (Hjelmeland et al. 1984). At 12 mm, the gut is in transition to a stomach, and ration-dependent enzyme synthesis expected under good feeding conditions (Pedersen et al. 1990) should make more digestive enzymes available. Therefore, it is reasonable that residency times should begin to decrease. Thorisson (1994) presents data showing reduced gut fullness coinciding with the period between 10 mm and 15 mm and a period of slowed growth around 12 mm. These observations and evidence of a small stomach led the researchers to conclude that a critical period in development is present around metamorphosis. The shorter gut residency times, increased metabolic costs, and high susceptibility to starvation could result in increased dependence on sufficient prey levels at the period around metamorphosis. Cod larvae may also clear their

© 2003 NRC Canada

guts at a rate related to energy need, suggesting that at 5 mm (first-feeding) and 12 mm (metamorphosis), there are additional energetic priorities (required organs, tissues) that are accompanied by efficient gut processes.

The lack of substantial larval pigmentation over the study period allows for examination of the food without removing the gut. Presumably, the white remainders are rotifer trophi and *Artemia* exoskeletons, the only known indigestible components of the prey species. Similar exoskeleton remains are described from wild cod guts in McLaren et al. (1997). This indigestible material was retained even in "empty" larvae with little or no defecation of any material. This was also observed in the 6-h experiments performed by Tilseth and Ellertsen (1984). To allow a comparison of the pattern of gut fullness in the present study with the categorical system used by McLaren et al. (1997), the gut contents progressed from a category 5 gut fullness and a category 1 level of digestion to a category 1–2 gut fullness and a category 3 level of digestion.

The gut residency times reported in this study were longer than gut evacuation times reported in the literature. It is first important to recognize that the residency or fullness reported here is different than evacuation, where passage of particles through the gut is estimated. During continuous feeding, *Artemia* nauplii have in some cases passed through the gut alive and swam away (Werner and Blaxter 1980). In no-prey conditions, the gut retains food until it has been fully digested. Second, it is conceded that there are difficulties associated with the use of cultured diets such as rotifers and *Artemia* nauplii in the study of gut processes. These prey induce longer gut residency times compared with those associated with wild zooplankton because of increased energy content accomplished through enrichment (Pedersen 1984; Arrhenius and Hansson 1994). Cultured prey are also much smaller than copepod nauplii used in other studies. The effects of size and caloric value on larval gut processes are not well understood and are recognized as a problem in extrapolating results beyond the present study.

It has been estimated that it takes 4 h for cod larvae to evacuate their guts (Lough and Mountain 1996), which is similar to values from Tilseth and Ellertsen (1984). However, McLaren et al. (1997) noted that the time of day had a significant effect on digestion and fullness and estimated that maximum fullness occurred at 19:00 hours and maximum digestion occurred at 03:00. This would suggest that 8 h of digestion time is required for cod larvae. They also note that many sampled larvae were empty or near empty and demonstrated that digestion was less complete in larvae with increased gut fullness. This suggests that increasing gut fullness reduces the level of digestion, which may mean that the 8-h digestion time is underestimated because of large numbers of larvae with low gut fullness. The feeding times associated with this experiment encouraged full guts, and larvae often ingested more than 15 rotifers. This surely elevated gut residency times over those previously reported. Despite this, large differences in gut residency over the course of the experiment indicate that age or size of larvae will affect gut fullness results and that the relationship between digestion rate and age is not linear.

The larvae in the present study appear to be prepared for short-term food deprivation, which may result from loss of feeding ability at night (Kane 1984) or small-scale patchiness (Lochmann et al. 1997). It may be helpful to interpret the present results as indicating that regular exposure to prey of adequate effective densities (including turbulence effects) is required for the entire larval period. Because a relationship between recruitment and abundance is not evident until the late larval stage (Rothschild 1986), one should be cautious about interpreting hypotheses based solely on early larval mortality (Thorisson 1994). Determining the fitness of larvae in the field will require accounting for the latency in condition factor demonstrated by Johnson and Dropkin (1995) in which 4 days were required before the effects of starvation were reflected in growth and 2 days were required to impact survival for American shad larvae (*Alosa sapidissima*). For larval cod, gut contents were digested first, followed by reduced swimming activity, sinking, and lastly reduced growth and increased mortality. If swimming activity and buoyancy are important for maintaining vertical position, then starving larvae may not be easily sampled in the field and this may result in difficulties associating poor larval condition with poor feeding conditions. Laboratory studies relating the level of starvation and associated ecological characteristics (swimming activity) to RNA–DNA ratios would be invaluable.

Although mortality due to starvation is generally linked to the transition from an endogenous to an exogenous source of nutrition, recent observations have questioned increased susceptibility of young larvae to starvation. Although, in general, the odds of survival increase with age (Houde 1997) or size (Pepin 1991), adequate prey levels are likely critical for development throughout larval life for Atlantic cod because the metabolic priority and best life-history strategy favors growth over storage of energy. As a result, the high relative importance of growth places cod at a high risk of starvation throughout the larval stage. Furthermore, larval age influences the pattern of gut fullness over time, with the periods around first-feeding and metamorphosis accompanied by the fastest rates of gut clearance. Because of these differences, using gut fullness to infer fitness or feeding success must adequately account for differences in digestion times, or residency times, before making links between feeding conditions and prey encounter rates. Information relating larval gut processes and feeding behaviour with prey concentration and caloric values, as well as how cod larvae catabolize energy reserves, both from endogenous (body tissue) and exogenous (gut contents) sources, in relation to fast growth, starvation, and development need to be better defined to properly understand the ecology of cod larvae and how optimal feeding strategies can be reached under culture conditions.

Acknowledgments

We thank Drs. V. Gotceitas and V. Puvanendran and D. Boyce for advice on experimental setup and larval rearing, Dr. W. Halteman for statistical enlightenment, and Drs. P. Pepin and V. Puvenendran and M. Bank, C. Lage, S.E. Hayhurst, and two anonymous reviewers for constructive criticism that has contributed greatly to this manuscript. This research was supported by a grant from the Natural Sciences and Engineering Research Council of Canada (NSERC)

© 2003 NRC Canada

to J.A.B. and by funding from the Canadian Centre for Fisheries Innovation (CCFI) to A.J.

References

Arrhenius, F., and Hansson, S. 1994. In situ food consumption by young-of-the-year Baltic Sea herring *Clupea harengus*: a test of the predictions of the bioenergetics model. Mar. Ecol. Prog. Ser. **110**: 145–149.

Cushing, D.H. 1990. Plankton production and year class strength in fish populations: an update of the match/mis-match hypothesis. Adv. Mar. Biol. **26**: 249–293.

Dower, J.F., Pepin, P., and Leggett, W.C. 1998. Enhanced gut fullness and an apparent shift in size selectivity by radiated shanny (*Ulvaria subbifurcata*) larvae in response to increased turbulence. Can. J. Fish. Aquat. Sci. **55**: 128–142.

Drost, M.R., and van den Boogaart, J.G.M. 1986. The energetics of feeding strikes in larval carp, *Cyprinus carpio*. J. Fish Biol. **29**(3): 371–379.

Gamble, J.C., and Houde, E.D. 1984. Growth mortality and feeding of cod (*Gadus morhua* L.) larvae in enclosed water columns and in laboratory tanks. *In* The propagation of cod *Gadus morhua* L. *Edited by* E. Dahl, E.S. Danielssen, E. Moksness, and P. Solemdal. Institute of Marine Research, Flodevigen, Norway. pp. 123–143.

Govoni, J.J., Boehlert, G.W., and Watanabe, Y. 1986. The physiology of digestion in fish larvae. Environ. Biol. Fishes, **16**: 59–77.

Hjelmeland, K., Huse, I., Jorgensen, T., Molvik, G., and Raa, J. 1984. Trypsin and tripsinogen as indices of growth and survival potential of cod (*Gadus morhua* L.) larvae. *In* The propagation of cod *Gadus morhua* L. *Edited by* E. Dahl, E.S. Danielssen, E. Moksness, and P. Solemdal. Institute of Marine Research, Flodevigen, Norway. pp. 189–202.

Hjort, J. 1914. Fluctuations in the great fisheries of northern Europe viewed in light of biological research. Rapp. P-V. Réun. Cons. Int. Explor. Mer, **20**: 1–228.

Houde, E.D. 1997. Patterns and trends in larval-stage growth and mortality of teleost fish. J. Fish Biol. **35**(Suppl. A): 52–83.

Houde, E.D., and Zastrow, C.E. 1993. Ecosystem- and taxon-specific dynamic and energetic properties of larval fish assemblages. Bull. Mar. Sci. **53**(2): 290–335.

Houlihan, D.F., Carter, G.C., and McCarthy, I.D. 1995. Protein synthesis in fish. *In* Biochemistry and molecular biology of fishes. Vol. 4. *Edited by* P.W. Hochachka and T.P. Mommsen. Elsevier, Amsterdam. pp. 191–219.

Hughes, R.N. 1997. Diet selection. *In* Behaviourial ecology of teleost fishes. *Edited by* J-G.J. Godin. Oxford University Press, New York. pp. 134–158.

Hunter, J.R. 1981. Feeding ecology and predation of marine larvae. *In* Marine fish larvae. *Edited by* R. Lasker. University Washington Press, Seattle. pp. 34–77

Hunt von Herbing, I., and Boutilier, R.G. 1996. Activity and metabolism of larval Atlantic cod (*Gadus morhua*) from Scotian Shelf and Newfoundland source populations. Mar. Biol. **124**: 607–617.

Johnson, J.H., and Dropkin, D.J. 1995. Effects of prey density and short term food deprivation on the growth and survival of American shad larvae. J. Fish Biol. **46**: 872–879.

Kane, J. 1984. The feeding habits of co-occurring cod and haddock larvae from Georges Bank. Mar. Ecol. Prog. Ser. **16**: 9–20.

Kjorsvik, E., van der Meeren, T., Kryvi, H., Arnfinnsson, J., and Kvenseth, J. 1991. Early development of the jaw and gut of cod larvae (*Gadus morhua* L.) during start-feeding. J. Fish Biol. **38**: 1–15.

Lee, E. 1992. Statistical methods for survival data analysis. John Wiley and Sons, New York.

Lochmann, S.E., Taggart, C.T., Griffin, D.A., Thompson, K.R., and Maillet, G.L. 1997. Abundance and distribution of larval cod (*Gadus morhua*) at a convergent front on Western Bank, Scotian Shelf. Can. J. Fish. Aquat. Sci. **54**: 1461–1479.

Lough, R.G., and Mountain, D.G. 1996. Effect of small-scale turbulence on feeding rates of larval cod and haddock in stratified water on Georges Bank. Deep-Sea Res. II, **43**(7–8): 1745–1772.

MacKenzie, B.R., and Leggett, W.C. 1991. Quantifying the contribution of small-scale turbulence to the encounter rates between larval fish and their zooplankton: effects of wind and tide. Mar. Ecol. Prog. Ser. **73**: 149–160.

McLaren, I.A., Avendaòo, P., Taggart, C.T., and Lochmann, S.E. 1997. Feeding of larval cod in different water-masses on Western Bank, Scotian Shelf. Fish. Oceanogr. **6**(4): 250–265.

McNamara, P.T., Calderone, E.M., and Buckley, L.J. 1999. RNA/DNA ratio and expression of 18S ribosomal RNA, actin and myosin heavy chain messenger RNAs in starved and fed larval Atlantic cod (*Gadus morhua*). Mar. Biol. **135**: 123–132.

Miller, T.J., Crowder, L.B., Rice, J.A., and Marshall, E.A. 1988. Larval size and recruitment: towards a conceptual framework. Can. J. Fish. Aquat. Sci. **45**: 1657–1670.

Morrison, C.M. 1993. Histology of the Atlantic cod, *Gadus morhua*: an atlas. Part 4. Eleutheroembryo and larvae. Can. Spec. Publ. Fish. Aquat. Sci. No. 119.

Neilson, J.D., Perry, R.I., Velerio, P., and Waiwood, K.G. 1986. Condition of Atlantic cod *Gadus morhua* larvae after the transition to exogenous feeding: morphometrics, buoyancy and predator evasion. Mar. Ecol. Prog. Ser. **32**: 229–235.

Otterlei, E., Nyhammer, G., Folkvord, A., and Stefansson, S. 1999. Temperature- and size-dependant growth of larval and early juvenile cod (*Gadus morhua*): a comparative study of Norwegian coastal cod and northeast Arctic cod. Can. J. Fish. Aquat. Sci. **56**: 2099–2111.

Pedersen, B.H. 1984. The intestinal evacuation rates of larval herring (*Clupea harengus* L.) predating on wild plankton. Dana, **3**: 21–30.

Pedersen, B.H., Ugelstad, I., and Hjelmeland, K. 1990. Effects of a transitory, low food supply in the early life of larval herring (*Clupea harengus*) on mortality, growth and digestive capacity. Mar. Biol. **102**: 61–66.

Pepin, P. 1991. Effect of temperature and size on development, mortality, and survival rates of the pelagic early life history stages of marine fish. Can. J. Fish. Aquat. Sci. **48**: 503–518.

Pepin, P., and Penney, R.W. 1997. Patterns of prey size and taxonomic composition in larval fish: are there general size-dependent models? J. Fish Biol. **51**(Suppl. A): 84–100.

Pepin, P., and Penney, R. 2000. Feeding by a larval fish community: impact on zooplankton. Mar. Ecol. Prog. Ser. **204**: 199–212.

Petersen, T., and Falk-Petersen, I.B. 1992. Morphological changes during metamorphosis in cod (*Gadus morhua* L.) with particular reference to the development of the stomach and pyloric caeca. J. Fish Biol. **41**: 449–461.

Puvanendran, V., and Brown, J.A. 1999. Foraging, growth and survival of Atlantic cod larvae reared at different prey concentrations. Aquaculture, **175**: 77–92.

Puvanendran, V., Leader, L.L., and Brown, J.A. 2002. Foraging behaviour of Atlantic cod (*Gadus morhua*) larvae in relation to prey concentration. Can. J. Zool. **80**: 689–699.

Ribeiro, L., Zambonino-Infante, J.L., Cahu, C., and Dinis, M.T. 1999. Development of digestive enzymes in larvae of *Solea senegalensis*, Kaup 1858. Aquaculture, **179**: 465–473.

© 2003 NRC Canada

Rothschild, B.J. 1986. Dynamics of marine fish populations. Harvard University Press, Cambridge, Mass.

Sclafani, M., Stirling, G., and Leggett, W.C. 1997. Osmoregulation, nutritional effects and buoyancy of marine fish: a bioassay for assessing density changes during the earliest life-history stages. Mar. Biol. **129**: 1–9.

Skiftesvik, A.B. 1992. Changes in behaviour at onset of exogenous feeding in marine fish larvae. Can. J. Fish. Aquat. Sci. **49**: 1570–1572.

Sokal, R.R., and Rohlf, F.J. 1995. Biometry. W.H. Freeman and Company, New York.

Thorisson, K. 1994. Is metamorphosis a critical interval in the early life of marine fishes? Environ. Biol. Fishes, **40**: 23–46.

Tilseth, S., and Ellertsen, B. 1984. Food consumption rate and gut evacuation processes of first feeding cod larvae (*Gadus morhua* L.). *In* The propagation of cod *Gadus morhua* L. *Edited by* E. Dahl, E.S. Danielssen, E. Moksness, and P. Solemdal. Institute of Marine Research, Flodevigen, Norway. pp. 167–182.

Townsend, D.W., and Pettigrew, N.R. 1996. The role of frontal currents in larval fish transport on Georges Bank. Deep-Sea Res. II, **43**(7–8): 1773–1792.

Werner, R.G., and Blaxter, J.H.S. 1980. Growth and survival of larval herring (*Cluplea harengus*) in relation to prey density. J. Fish Biol. **37**: 33–41.

Wieser, W. 1991. Limitations of energy acquisition and energy use in small poikilotherms: evolutionary implications. Funct. Ecol. **5**: 234–240.

Williams, P.J., Brown, J.A., Gotceitas, V., and Pepin, P. 1996. Developmental changes in escape response performance of five species of marine larvae. Can. J. Fish. Aquat. Sci. **53**: 1246–1253.

© 2003 NRC Canada

DISCUSSION / DISCUSSION

Comment on "Acoustic seabed classification: improved statistical method"[1]

J.M. Preston and R.L. Kirlin

In a discussion of methods for acoustic seabed classification, Legendre et al. (2002) claim to offer improvements over existing techniques and assert that their method "produces statistically better results than the classification method implemented in the QTC [Quester Tangent Corporation] software". Reasons for this assertion are not given in that paper but are given in an unpublished document. In this paper, we examine the basis for the assertion and discuss whether it should be accepted.

The method of Legendre et al. (2002) implements a *K*-means partitioning by an iterative process. They claim this as an advantage over QTC; however, QTC also implements a *K*-means partitioning with an iterative process (see, e.g., Preston et al. 2001), so this cannot be the explanation. Choosing the optimal number of clusters can be problematic, but Legendre et al. report differences between their methods and QTC even when both are computing with the same number of clusters, so the explanation cannot lie entirely here. What is left?

The answer, it appears, is that Legendre et al. (2002) wish to minimize the within-group sums of squares using a homogeneous measure of distance to the centre of a cluster (squared Euclidean distances), whereas QTC uses a likelihood-based measure in which the distance to the centre of any cluster is scaled by the variance of that cluster. A one-dimensional example illustrates the point at issue. Suppose we have a population that is an equal mixture of two Gaussian distributions: A, which is distributed as $N(0,(0.5)^2)$, and B ~ $N(2,(0.1)^2)$. How do we assign an observation at 1.5? Legendre et al. would say that it is a distance of 0.5 from the centre of B and 1.5 from the centre of A and therefore should be assigned to B. QTC would say that is it 5 standard deviations from the centre of B and 3 standard deviations from the centre of A and therefore should be assigned to A. In the example that we have sketched, the statement "x is from A and $x = 1.5$" has a higher probability density than "x is from B and $x = 1.5$"; that is, our method has a higher probability of making a correct assignment to a component of the mixture. Therefore, one cannot unambiguously identify Legendre et al.'s "best in the [homogeneous] least-squares sense" with best in the statistical sense. Attempts to prove the latter fail because any statistical test is also based on either homogeneous or variance-based measures; if the clustering method and the test use the same measure, the test scores will often be higher for that reason alone.

The paragraphs above summarize our comment. Legendre et al.'s (2002) claim to "statistically better results" is without support, arising as it did from applying a test that used squared Euclidean distances to two clustering methods, one using squared Euclidean distances and one using a likelihood-based measure. What remains is to provide a justification for using non-Euclidean measures for clustering and to extend this example to more dimensions.

A reasonable principle for choosing the class assignment is the maximum a posteriori probability (MAP). In other words, a vector $\mathbf{x}$ is observed and is to be assigned to one of q classes $\{\omega_1,\omega_2,\ldots,\omega_q\}$. MAP selects the class of maximum a posteriori probability from the candidates as

$$(1) \qquad \omega_k = \arg \max_{k=1,2,\cdots,q} P(\omega_k|\mathbf{x})$$

where $P(\omega_k|\mathbf{x})$ is the a posteriori probability for class ω_k. From Bayes' theorem, the a posteriori probability can be written as

$$(2) \qquad P(\omega_k|\mathbf{x}) = \frac{p(\mathbf{x}|\omega_k)P(w_k)}{p(\mathbf{x})}$$

where $p(\mathbf{x}|\omega_k)$ is the density of the data given that they are drawn from ω_k, $P(\omega_k)$ is the a priori probability for ω_k, and $p(\mathbf{x})$ is the marginal density of observed data $\mathbf{x}$. If the a priori probability $P(\omega_k)$ is uniform, the MAP rule becomes

$$(3) \qquad \omega_k = \arg \max_{k=1,2,\cdots,q} p(\mathbf{x}|\omega_k)$$

Received 10 December 2002. Accepted 15 May 2003. Published on the NRC Research Press Web site at http://cjfas.nrc.ca on 12 November 2003.
J17236

J.M. Preston.[2] Quester Tangent Corporation (QTC), 201 – 9865 West Saanich Road, Sidney, BC V8L 5Y8, Canada.
R.L. Kirlin.[3] Department of Electrical and Computer Engineering, University of Victoria, Victoria, BC V8W 3P6, Canada.

[1]Appears in Can. J. Fish. Aquat. Sci. **59**: 1085–1089 (2002).
[2]Corresponding author (e-mail: jpreston@questertangent.com).
[3]Retired.

 doi: 10.1139/F03-131 © 2003 NRC Canada

which is the maximum likelihood (ML) selection. Because $p(\mathbf{x})$ does not depend on class assignments, it drops out of the selection computations and each vector is assigned to cluster ω_i if (Cover and Hart 1967)

$$(4) \quad P(\omega_i)p(\mathbf{x}|\omega_i) > P(\omega_j)p(\mathbf{x}|\omega_j), \ \forall j \neq i$$

It is usual to assume a multivariate normal density (Fraley and Raftery 1998):

$$(5) \quad p(\mathbf{x}|\omega_i) = \frac{1}{(2\pi)^{M/2}|\mathbf{C}_i|^{1/2}} \exp[-1/2(\mathbf{x}-\mathbf{m}_i)^T\mathbf{C}_i^{-1}(\mathbf{x}-\mathbf{m}_i)]$$

where M is the dimensionality, and $\mathbf{m}_i$ and $\mathbf{C}_i$ are the estimated mean and covariance of cluster w_i. Legendre et al. (2002) and QTC both cluster in three-dimensional space called Q space, thus $M = 3$.

We can straightforwardly estimate the mean, covariance, and prior probability of the ith class if the marginal density of x,

$$(6) \quad p(\mathbf{x}) = \sum_{i=1}^{q} P(\omega_i)\frac{1}{(2\pi)^{M/2}|\mathbf{C}_i|^{1/2}} \exp[-1/2(\mathbf{x}-\mathbf{m}_i)^T\mathbf{C}_i^{-1}(\mathbf{x}-\mathbf{m}_i)]$$

can be appropriately simplified. The required simplification results when the clusters or modes of the Gaussian mixture are well separated. In that case $p(\mathbf{x})$ is well approximated in the region of the ith cluster by

$$(7) \quad p(\mathbf{x}) = \frac{P(\omega_i)}{(2\pi)^{M/2}|\mathbf{C}_i|^{1/2}} \exp[-1/2(\mathbf{x}-\mathbf{m}_i)^T\mathbf{C}_i^{-1}(\mathbf{x}-\mathbf{m}_i)], \quad \mathbf{x} \in \omega_i$$

and we can assume that all samples of $\mathbf{x}$ assigned to cluster i have been drawn only from the approximate distribution in eq. 7. In this case, we can obtain ML estimates of the required parameters using only samples of $\mathbf{x}$ assigned to cluster i.

When selecting the maximum under eq. 4, it is convenient to minimize the logarithm of the reciprocal of the left-hand side, log being a monotonic function. This gives what may be called a Bayesian metric:

$$(8) \quad d_i(\mathbf{x}) = -\log P(\omega_i) - \log(p(\mathbf{x}|\omega_i)) = -\log P(\omega_i) + \tfrac{1}{2}\log|\mathbf{C}_i| + \tfrac{1}{2}(\mathbf{x}-\mathbf{m}_i)^T\mathbf{C}_i^{-1}(\mathbf{x}-\mathbf{m}_i)$$

Two simplifications of eq. 8 deserve mention. The Euclidean metric, as used by Legendre et al. (2002), is the simplification of eq. 8 that assumes equal $P(\omega_i)$ and that the covariance matrices are equal, constant, and diagonal. Because assignments are based on minimization across classes, class-independent terms and constant factors are dropped, giving

$$(9) \quad d_i(\mathbf{x}) = (\mathbf{x}-\mathbf{m}_i)^T(\mathbf{x}-\mathbf{m}_i) \quad \text{(Euclidean)}$$

Secondly, if we continue to use equal priors $P(\omega_i)$, but now allow the covariance matrices to differ but with approximately equal determinants, we have the weighted sum of squares metric

$$(10) \quad d_i(\mathbf{x}) = (\mathbf{x}-\mathbf{m}_i)^T\mathbf{C}_i^{-1}(\mathbf{x}-\mathbf{m}_i) \quad \text{(Mahalanobis)}$$

The general case, using all terms of the Bayesian metric (eq. 8), requires estimates of the a priori probabilities, as well as the means and covariances of each cluster. QTC has implemented these estimates iteratively, with an outer loop for estimating priors and covariances and an inner K-means loop that adjusts assignments and cluster means. This is an optimal process under the MAP criterion, the only approximation being that in eq. 7 which approximates the whole density of $\mathbf{x}$ by its component due to class i alone, which is valid under the assumption of well-separated classes or mixture components.

For classifying regions of acoustic similarity, as part of acoustic sediment classification, we have described three metrics: the general case and two simplifications. Which gives optimal results? This will likely remain an open question. We have found very few statistical tests or clustering processes that work well with both simulated and real data sets and thus have come to believe that comparison with ground truth is the most meaningful basis for comparisons. However, it is unusual to have ground truth that is adequate in quantity and scope. For example, surface roughness can affect acoustic character but is destroyed when sampling with a grab. Over the years, the QTC implementation described above has repeatedly been found to give practical, useful, and accurate classes. Some recent examples are described by Morrison et al. (2001), Anderson (2001, 2002), and Ellingsen et al. (2002).

References

Anderson, J.T. 2001. Classification of marine habitats using submersible and acoustic seabed techniques. *In* Spatial processes and management of marine populations. Alaska Sea Grant College Program, AK-SG-01-02.

Anderson, J.T. 2002. Acoustic classification of marine habitats in coastal Newfoundland. ICES J. Mar. Sci. **59**: 156–167.

Cover, T.M., and Hart, P.E. 1967. Nearest neighbour pattern classification. IEEE Trans. Information Theory No. IT-13. pp. 21–27.

Ellingsen, K.E., Gray, J.S., and Bjornbom, E. 2002. Acoustic classification of seabed habitats using the QTC VIEW™ system. ICES J. Mar. Sci. **59**: 825–835.

Fraley, C., and Raftery, A.E. 1998. How many clusters? Which clustering method? Answers via model-based cluster analysis. Computer J. **41**: 578–588.

Legendre, P., Ellingsen, K.E., Bjornbom, E., and Casgrain, P. 2002. Acoustic seabed classification: improved statistical method. Can. J. Fish. Aquat. Sci. **59**: 1085–1089.

Morrison, M.A., Thrush, S.F., and Budd, R. 2001. Detection of acoustic class boundaries in soft sediment systems using the seafloor acoustic discrimination system QTC VIEW. J. Sea Res. **46**: 233–243.

Preston, J.M., Christney, A.C., Bloomer, S.F., and Beaudet, I.L. 2001. Seabed classification of multibeam sonar images. *In* Proceedings of MTS/IEEE Oceans 2001: An Ocean Odyssey, Honolulu, Hawaii, November 2001. Holland Publications, Escondido, Calif.

© 2003 NRC Canada

DISCUSSION / DISCUSSION

Reply to the comment by Preston and Kirlin on "Acoustic seabed classification: improved statistical method"[1]

Pierre Legendre

Legendre et al. (2002) described a statistical method for analysing echosounder backscatter data, which consisted of the following steps: the backscatter data were decomposed mathematically into a number of quantitative variables, which were subjected to principal component analysis (PCA). Principal components representing 95–99% of the variation were then used in a *K*-means partitioning procedure. A least-squares statistical criterion indicated the number of groups that best reflected the variability of the data. The groups were then plotted on maps of the survey area. Insofar as the mathematical decomposition of the backscatter echo produced variables that reflected the variation of the physical nature and composition of the seabed, the classes of the partition were likely to correspond to seabed types. This procedure presented several improvements over the Quester Tangent Corporation's QTC VIEW™ acoustic bottom classification method (Prager et al. 1995), and it was described in easy-to-understand terms. Free software implementing this method — *The Q Package* for Windows and *The R Package* for Macintosh — is available on the Web site http://www.fas.umontreal.ca/biol/legendre/.

J.M. Preston, from the Quester Tangent Corporation (QTC), and R.L. Kirlin wrote a comment on that paper, to which I was invited to reply. I will first address some statistical points in Preston and Kirlin's note and then go to more fundamental issues.

Statistical issues

(1) The *K*-means problem was defined by MacQueen (1967) as that of partitioning a data set in Euclidean space into *K* nonoverlapping groups in such a way as to minimize the sum (across the groups) of the within-group sums of squared Euclidean distances to the respective group centroids. The statistical problem had first been stated by Fisher (1958). What QTC seems to be doing, if I understand their description correctly, is implementing a partitioning method based on Mahalanobis distances for solving the mixture problem, like the one described by Demers et al. (1992), for instance. So they are implementing a modified form of *K*-means partitioning. This does not mean that the results produced by such an algorithm are more meaningful that those of a standard *K*-means algorithm.

The description of the classification algorithm implemented by the QTC software, provided by Preston and Kirlin, is wrapped in Bayesian language. A true Bayesian approach would require that prior probabilities be known beforehand; that is not the case in acoustic seabed classification. What is being described is simply a two-step iterative algorithm, preserving Mahalanobis distances, in which objects are assigned to the clusters and the statistical parameters of the clusters are recomputed.

(2) Preston and Kirlin (2003) criticize the closing statement of our 2002 paper, which read: "The report [Legendre, unpublished report, available at http://www.fas.umontreal.ca/biol/legendre/] shows that PCA followed by *K*-means partitioning produces statistically better results than the classification method implemented in the QTC software...". The sentence should have read: "... statistically better results *in the least-squares sense*...". The statement was based on results presented in the unpublished report and summarized in the following paragraphs.

On 16 August 1999, acoustic data were collected in the Forty Baskets Beach area of Sydney Harbour, Australia (33°48′S, 151°16′E). We used a Navisound 50 echo sounder (Navitronic Systems AS, Hasselager, Denmark) at frequency 50 kHz (transducer beam width 13.5°) connected to the QTC VIEW™ acoustic seabed classification system (CAPS version 3.25, QTC IMPACT™ ver-

Received 14 July 2003. Accepted 16 October 2003. Published on the NRC Research Press Web site at http://cjfas.nrc.ca on 12 November 2003.
J17628

P. Legendre. Département de sciences biologiques, Université de Montréal, C.P. 6128, succursale Centre-ville, Montréal, QC H3C 3J7, Canada (e-mail: pierre.legendre@umontreal.ca).

[1]Reply to J.M. Preston and T.L. Kirlin. 2003. Can. J. Fish. Aquat. Sci. **60**: 1299-1300.

 doi: 10.1139/F03-132 © 2003 NRC Canada

sion 1.0 Beta). The transducer was mounted on an over-the-side strut on the survey vessel. The positioning equipment was a differential GPS (global positioning system). After validation, the data set consisted of 1478 data lines (objects or records) and 166 QTC variables, plus geographic positions and depths. Because three of the QTC variables did not vary at all, they were eliminated from the data set, which was thus reduced to 163 variables. These data were used to illustrate the acoustic seabed classification method described in Legendre et al. (2002).

The first three principal components accounted for 96.2% of the variance in the QTC variables. Using seven principal components would have accounted for 99.2% of the variance. For fairness of comparison, I only used the first three principal components in the comparison of partitions, because this is what the QTC software uses. The data were subdivided into groups using the procedure outlined in the QTC manuals (QTC 1999, 2000). The score value was used to determine which class should be split next. As the classes were subdivided, the total score decreased; however, at split level seven (i.e., eight groups), the total score increased again. Results of the partitions into three to seven groups are reported in Table 1*a*. In an a posteriori calculation, the Calinski–Harabasz statistic (described below) selected the partition into five groups as the best one in the least-squares sense.

The same data were partitioned by *K*-means, using the first three principal components (PC1–PC3), as in the QTC procedure. The *K*-means program was asked to produce from ten to two groups; the partitioning was restarted 10 times. The best partitions into $K = 2$ to $K = 7$ groups were retained; some of these results are shown in Table 1*b*. The Calinski–Harabasz statistic (see below) selected the partition into three groups as the best one. We also computed *K*-means partitioning for all 163 QTC variables, without prior filtering by PCA. The Calinski–Harabasz statistic selected again the partition into three groups as the best one (Table 1*c*). This partition is very similar to that obtained by *K*-means on PC1–PC3.

The partitioning procedure described in the QTC manuals (QTC 1999, 2000), which we used in 1999, is not the one described by Preston and Kirlin in their Comment (see Seabed classification issues, subsection 1, below). The partitioning results of QTC IMPACT™ and *K*-means are compared in Table 1 using common measures based on least squares: the sum of within-group sums-of-squares, also called the "sum of squared errors" (SSE), and the Calinski–Harabasz statistic (C–H) (see Legendre et al. 2002 (Classification method, step 3), as well as Seabed classification issues, subsection 4, below). SSE is the global optimality criterion implemented in *K*-means algorithms. C–H is a statistical criterion indicating the best number of groups in the least-squares sense. Least-squares is a widely accepted criterion and has a long history in statistics (Legendre 1805).

By the SSE criterion, Table 1 shows that the QTC partition into three groups is not as good as the *K*-means partitions into three groups based on either the first three principal components or all 163 variables, with respect to either the first three principal components (32% larger SSE) or the 163 QTC variables (27% larger SSE). Likewise for the partitions into five groups: according to SSE, the QTC solution into five groups is much worse than the *K*-means solutions based on either PC1–PC3 or all 163 QTC variables, with respect to either the first three principal components (15% larger SSE) or the 163 variables (10% larger SSE). This shows that the QTC partitions (even the "best one" into five groups) were far from being as good, for this example and in the least-squares sense, as those obtained by *K*-means.

(3) Preston and Kirlin (2003, their paragraph 3) talk about performing an (undescribed) test of statistical significance in their partitioning method. It is not clear to what they are referring. In any case, there is nothing that can be tested for significance in *K*-means or Mahalanobis distance partitioning without invoking an external, independently obtained data set. In particular, the results of a partitioning procedure should not be tested for significance using the same data that were used to produce the partition. This would be a logical mistake, as explained by Milligan (1996, p. 366) and Legendre and Legendre (1998, p. 379).

(4) Preston and Kirlin (2003) state that "Legendre et al. (2002) and QTC both cluster in three-dimensional space". This is not what we wrote; see Legendre et al. (2002, abstract and step 1 of the Classification method). What we recommended was to use as many principal components as were necessary to explain at least 95%, and preferably 99%, of the variance of the data. In the example presented in that paper, three principal components accounted for 96.2% of the variance, so we used three for *K*-means partitioning. We also reported that in the analysis of other acoustic seabed data sets, 3–5 PCs were necessary to reach 95% of the variance and 6–10 to reach 99%. In subsection 2 above, I only used three principal components in the tables to present a fair comparison with the QTC IMPACT™ results, which are limited to three principal components by design of the program. Preston et al. (2001) present that as a feature of the QTC software, but I think it is an objectionable limitation. This point will be revisited below.

(5) Preston and Kirlin (2003, last paragraph) concluded by citing a number of papers that allegedly showed that the QTC classification method "has repeatedly been found to give practical, useful, and accurate classes". It is worth noting that the paper by Morrison et al. (2001), cited by Preston and Kirlin, was directed at developing a technique to identify habitat boundaries. Their analysis compared the accuracy of the transitions predicted by the QTC VIEW™ confidence values with those predicted by the class-dominance Berge–Parker statistic. Morrison et al. (2001) concluded that the Berge–Parker index provided a more consistent transition indicator than the QTC software confidence values.

Seabed classification issues

(1) People have long wondered what was the classification

© 2003 NRC Canada

Table 1. Comparison of partitions (least-squares statistics SSE and C–H) using two different bases: PC1–PC3 (middle) and 163 QTC variables (right).

Software and variables	No. groups *K*	Base: PC1–PC3 SSE	Base: PC1–PC3 C–H	Base: 163 QTC variables SSE	Base: 163 QTC variables C–H
(*a*)					
QTC (PC1–PC3)	3	55.16	2026	62.94	1781*
QTC (PC1–PC3)	4		1969		1678
QTC (PC1–PC3)	5*	29.85	2182*	37.00	1771*
QTC (PC1–PC3)	6		2053		1620
QTC (PC1–PC3)	7		1921		1484
(*b*)					
K-means (PC1–PC3)	3*	41.86	2904*	49.67	2453*
K-means (PC1–PC3)	5	25.97	2561	33.53	1992
(*c*)					
K-means (163 QTC var.)	3*	41.87	2903*	49.67	2453*
K-means (163 QTC var.)	5	25.97	2563	33.51	1993

Note: SSE, sum of within-group sums-of-squares (small is best, for a given number of groups); C–H, Calinski–Harabasz statistic (high is best among partitions obtained using the same data). Asterisk (*) indicates the best number of groups for that classification, according to C–H.

method used by QTC. We asked questions to that effect to the Quester Tangent Corporation in 1999 but received no answer. When they use a method, scientists need to know, and be able to describe in scientific papers, how the data are processed. However, there seems to be greater openness and QTC is now providing more details of their statistical procedure.

The Comment by Preston and Kirlin (2003) is, to my knowledge, the first published paper describing the fact that the QTC software now uses a two-step iterative algorithm preserving Mahalanobis distances. Only now are we learning from Preston and Kirlin (2003) that the QTC software is using Mahalanobis distances instead of Euclidean distances. It is not clear from Preston and Kirlin's Comment whether they state that this approach has been implemented all along the development of the QTC proprietary software, or not. In any case, the procedure used in the 1999 CLUSTER™ and the 2000 QTC IMPACT™ programs and described in the software manuals (QTC 1999, 2000) was one-dimensional (the clusters were split along the first principal component in earlier versions of the software and along a single principal component chosen by the user in the 2000 version). An evolution of the software is summarized in Preston et al. (2001), who simply described it as "an automated variant of the k-means clustering method. Clustering is done in the space of the three principal components and is iterative and stable." What is now described in the Preston and Kirlin (2003) Comment seems to be a new evolution of the QTC software, recently released or perhaps still in the testing phase. In earlier manuals provided by QTC with their statistical software (QTC 1999, 2000), there was no indication about the nature of the calculations leading to partitioning, except for the description of how to use it, which implied a lot of fiddling and left room for personal, unreplicable decisions on the part of the user.

I also applaud the fact that QTC has recently (Preston et al. 2001) released some information about the mathematical nature of the 166 variables produced by the QTC VIEW™ software. The information found in Preston et al. (2001) provides a general qualitative overview of the variables generated by QTC VIEW™ from the backscatter, but the methods by which they are derived and the quantitative nature of the information remain unexplained.

(2) In the summer of 1999, Hewitt et al. (J.E. Hewitt, National Institute of Water and Atmospheric Research, P.O. Box 11-115, Hamilton, New Zealand, unpublished data) carried out a multiresolution nested survey in Kawau Bay, located on the northeast coast of North Island, New Zealand. The spatial distribution of epibenthic communities was studied using side-scan sonar, single-beam sonar, and video. The objective was to find relationships between assemblages visible from the video and the single-beam and (or) side-scan data that would enable the researchers to use these devices to both interpolate between and extrapolate from the restricted video survey. The substrate was soft sediment in all eight 1-km^2 sites investigated. There were reasonably dense but patchy epibenthic communities. At each site, six pairs of 1-km-long transects were sampled with single-beam sonar. The transects ran down the depth gradients. Three of the eight sites could not be videoed because of the presence of shoals and subsea cables. However at the other five sites, three 1-km-long video transects were run in approximately the same positions as three of the single-beam transects. The sonar was a Simrad EA501P hydrographic sounder (Simrad AS, Horten, Norway), attached to the boat, and operated at 200 kHz, 250 W transmit power, with a ping rate of 5 s^{-1}, and a fixed beam width of 7°. This was connected to a QTC VIEW™ series 4 (Collins et al. 1996) data acquisition system. Settings for the QTC VIEW™ system were a reference depth of 14 m and a base gain of 15 dB. Sampling resolution varied from 0.37 to 3.0 m^2, depending on depth, although more generally the range was from 1.22 to 2.44 m^2. As QTC

© 2003 NRC Canada

VIEW™ uses a stack of five consecutive pings for each record, at our speed of about 5 knots (2.6 $m \cdot s^{-1}$), a ping stack (generally covering 6–12 m) was processed approximately every 8 m.

The single-beam sonar data were processed as follows: on the one hand, using the first three principal components computed by the proprietary principal component analysis procedures available in the program QTC IMPACT™ (QTC 2000), cluster splits were made in the principal component data scatter until further splits failed to reduce the overall variance in an important way. Splitting decisions were made as detailed in Morrison et al. (2001) using inflexion points of the total scores and the QTC cluster performance index. On the other hand, principal component analysis was applied to the 166 variables produced by the QTC VIEW™ system using the data from all five sites; the number of principal components required to explain 95% of the variance was five. Ping scores along those five axes were used in the *K*-means partitioning procedure of *The Q Package* freeware. The Calinski–Harabasz statistic was used as a stopping criterion to determine the best number of groups for each data set, in the least-squares sense.

The QTC IMPACT™ classification into seven groups was more related to depth than was the six-group *K*-means classification. Discriminant analysis identified that 53% of the points could be allocated correctly to the QTC IMPACT™ groups based on depth alone, compared with 34% for the *K*-means classification. As a consequence, the rest of the analyses reported by Hewitt et al. (J.E. Hewitt, National Institute of Water and Atmospheric Research, P.O. Box 11-115, Hamilton, New Zealand, unpublished data) were based on the *K*-means classification, on which depth had less of an influence.

The first principal component of the 166 QTC variables was highly correlated with depth (Spearman's $r = -0.91$). The relationship found between depth and partition was not totally avoidable in that study because the transects ran down depth gradients and the size of the sonar footprint is a function of depth. Obviously, the fact that QTC IMPACT™ only uses three axes in determining its partition makes it especially sensitive to depth. By opposition, Legendre et al.'s (2002) *K*-means partitioning uses the number of axes necessary to explain 95% (or 99% in other studies) of the variability in the data; that explains the differences between the results of the two methods. There is certainly an advantage in using more than three principal components as the basis for classification.

(3) Preston and Kirlin (2003) argue that elongated (hyperellipsoidal) clusters, produced by their Mahalanobis-based clustering method, are more natural than, and thus preferable to, the hyperspherical clusters produced by *K*-means. There is no particular reason why the data points (sonar backscatters, decomposed into QTC-generated variables) should be structured in any particular way in multivariate space, or in a reduced space of principal components. Within the range of variation of the 166 QTC variables, any intermediate value is possible, so that observations may be found anywhere within the convex envelope surrounding the data points in multivariate space. Natural separation of clusters is predicted, for instance, by the theory of biological evolution, which was the starting point for the development of many of the methods of numerical classification (Sokal and Sneath 1963), but I do not think any theory predicts the existence of regions occupied by points, in the space of acoustic variables, separated by regions where no observations are possible. Nor do we have a theory that predicts that the clusters should have any particular shape. We only want to empirically divide the sonar backscatters into groups, to simplify their multivariate description. These groups will be useful if they are found to correspond to characteristics of the seabed. A division of the space into multivariate boxes of equal sizes would produce a perfectly good classification of the seabed. This can easily be done, for example, in the two-dimensional space of RoxAnn™ variables E1 and E2 developed by Marine Micro Systems Ltd. (Chivers et al. 1990; E1 and E2 are often referred to as "hardness" and "roughness"), but it would be impractical to attempt doing it in a space with 166 dimensions. The reason that we resort to partitioning methods in that space is because we only need to define boxes that are occupied by a sufficient number of points; in particular, we do not want boxes (or classes) containing no point at all. So it is perfectly reasonable to look for spherical or hyperspherical *K*-means clusters in that space. Because they have borders forming flat interfaces, their shape is actually hyperpolyhedric rather than hyperspherical. On these grounds, any other cluster shape is also perfectly acceptable, including those produced by the Mahalanobis-based QTC algorithm. In summary, I believe that the particular metric used for partitioning is not a key point to insure a useful partition of the data points. The choice of the variables derived from the sonar backscatter, and the number of principal components retained for partitioning (see above), are much more important.

(4) There are computational and statistical reasons to prefer a solution implementing a least-squares criterion. The first one is that it runs faster than a Mahalanobis-based algorithm. So, the available computing time can be used to try more random starts of the algorithm; this, in turn, increases the chances of finding an optimal partition (in the least-squares sense). The second reason is that least squares go well with least squares: because *K*-means is a partitioning method optimizing the least-squares criterion, as in multiple regression, it allows the application of a criterion based on least squares to determine the "best" number of clusters. In the *K*-means algorithm incorporated in *The Q Package* and *The R Package*, we are using the Calinski–Harabasz (1974) criterion (C–H), which is a least-squares criterion. This criterion is simply an *F* statistic of multivariate analysis of variance; the partition displaying the highest value of this criterion is the best one in the least-squares sense. Actually, the partitions corresponding to the various maxima of the graph of the C–H statistics against the number of

© 2003 NRC Canada

groups may be worth examining and mapping. There is no direct equivalent of this criterion in Mahalanobis space, at least none that I know of. I encourage the Quester Tangent Corporation to offer our procedure as an option in their computer package. We published our procedure in the scientific literature (Legendre et al. 2002), so it is not proprietary.

(5) The relative usefulness of the partitions produced by QTC VIEW™ and our software should be judged by ground truthing. Because our *K*-means software is freely available, users in governmental and private research institutions, as well as universities, should be encouraged to analyse QTC data using the QTC VIEW™ classification software (based on three PCA axes) and our *K*-means software (using a sufficient number of PCA axes to account for 95% or 99% of the variation in the QTC data) and to compare the results to ground-truthing data, as was done by Hewitt et al. (unpublished data; see subsection 2 above). Comparisons of this kind are part of the scientific process needed to determine the usefulness of acoustics for mapping features of the seabed and, in particular, the horizontal distribution of ecological communities.

Conclusion

This debate does point to a more general dilemma, where technological innovation leads to proprietary products that are used and should be scrutinized by the scientific community. Although science is supposed to be based on free and open communication and debate, companies may choose to act differently in commercial activities. There is clearly a need for new and cost-effective surveying devices that enable us to image and map large areas of the seafloor in a routine and timely fashion. Every surveying device has its limitation and it is important that we recognize them so that technologies can continue to be developed and improved. This note is meant to contribute to that process. I also hope that our paper (Legendre et al. 2002) and freeware (*The Q Package* for Windows and *The R Package* for Macintosh) will be used for seafloor management, especially by researchers in underdeveloped countries, who can benefit from freely available software implementing sound statistical procedures.

References

Calinski, T., and Harabasz, J. 1974. A dendrite method for cluster analysis. Commun. Stat. **3**: 1–27.

Chivers, R.C., Emerson, N., and Burns, D.R. 1990. New acoustic processing for underway surveying. The Hydrographic Journal, **56**: 9–17.

Collins, W., Gregory, R., and Anderson, J. 1996. A digital approach to seabed classification. Sea Technol. **37**: 83–87.

Demers, S., Kim, J., Legendre, P., and Legendre, L. 1992. Analyzing multivariate flow cytometric data in aquatic sciences. Cytometry, **13**: 291–298.

Fisher, W.D. 1958. On grouping for maximum homogeneity. J. Am. Statist. Assoc. **53**: 789–798.

Legendre, A.M. 1805. Nouvelles méthodes pour la détermination des orbites des comètes. Courcier, Paris.

Legendre, P., and Legendre, L. 1998. Numerical ecology. 2nd English ed. Elsevier Science BV, Amsterdam.

Legendre, P., Ellingsen, K.E., Bjørnbom, E., and Casgrain, P. 2002. Acoustic seabed classification: improved statistical method. Can. J. Fish. Aquat. Sci. **59**: 1085–1089.

MacQueen, J. 1967. Some methods for classification and analysis of multivariate observations. *In* Proceedings of the fifth Berkeley symposium on mathematical statistics and probability. Vol. 1. *Edited by* L.M. Le Cam and J. Neyman. University of California Press, Berkeley. pp. 281–297.

Milligan, G.W. 1996. Clustering validation — results and implications for applied analyses. *In* Clustering and classification. *Edited by* P. Arabie, L.J. Hubert, and G. De Soete. World Scientific Publ. Co., River Edge, N.J. pp. 341–375.

Morrison, M.A., Thrush, S.F., and Budd, R. 2001. Detection of acoustic class boundaries in soft sediment systems using the seafloor acoustic discrimination system QTC VIEW. J. Sea Res. **46**: 233–243.

Prager, B.T., Caughey, D.A., and Poeckert, R.H. 1995. Bottom classification: operational results from QTC View. *In* Proceedings of the MTS/IEEE Oceans 1995: Challenges of Our Changing Global Environment, San Diego, Calif., 9–12 Oct. 1995. Vol. 3. pp. 1827–1835.

Preston, J.M., and Kirlin, T.L. 2003. Comment on "Acoustic seabed classification: improved statistical method". Can. J. Fish. Aquat. Sci. **60**: 1299–1300.

Preston, J.M., Christney, A.C., Bloomer, S.F., and Beaudet, I.L. 2001. Seabed classification of multibeam sonar images. *In* Proceedings of MTS/IEEE Oceans 2001: An Ocean Odyssey, Honolulu, Hawaii, Nov. 2001. Holland Publications, Escondido, Calif.

Quester Tangent Corporation (QTC). 1999. CLUSTER operator's manual. 24 March 1999. Quester Tangent Corporation, Sidney, B.C.

Quester Tangent Corporation (QTC). 2000. QTC IMPACT™ acoustic seabed classification, user guide version 2.00. Integrated mapping, processing and classification toolkit. Revision 2. Quester Tangent Corporation, Sidney, B.C.

Sokal, R.R., and Sneath, P.H.A. 1963. Principles of numerical taxonomy. W.H. Freeman, San Francisco, Calif.

© 2003 NRC Canada

ERRATUM / ERRATUM

Erratum: A size-based model of the impacts of bottom trawling on benthic community structure

Daniel E. Duplisea, Simon Jennings, Karema J. Warr, and Tracy A. Dinmore

Ref.: Can. J. Fish. Aquat. Sci. **59**: 1785–1795 (2002).

The production (*P*) curve of Fig. 7 in the published paper came from model runs showing only the productivity of a portion of the community. This curve is therefore inconsistent with the other values from total fauna baseline runs presented. The actual baseline (total community) productivity decline with increasing trawling frequency is not as great as depicted by the *P* curve in the original Fig. 7.

A new Fig. 7 is presented with the correct *P* curve and the published paper text should be changed in two places to reflect this new *P* curve: (1) on page 1791, 2nd column, line 2, "more" should be changed to "also" and (2) on page 1791, 2nd column, line 3, in the same sentence "tenfold" should be changed to "twofold". The corrected sentence should read

> "Total production was *also* sensitive to trawling, showing a decline of more than *twofold* over the same trawling frequency range."

Fig. 7. Modelled biomass and productivity of the benthic community versus trawling intensity: solid line and circles, total biomass; short-dashed line and triangles, biomass in organism sizes >1 g wet weight (wwt); long-dashed lines and crosses, production. Lines are spline smoothers through modelled data points.

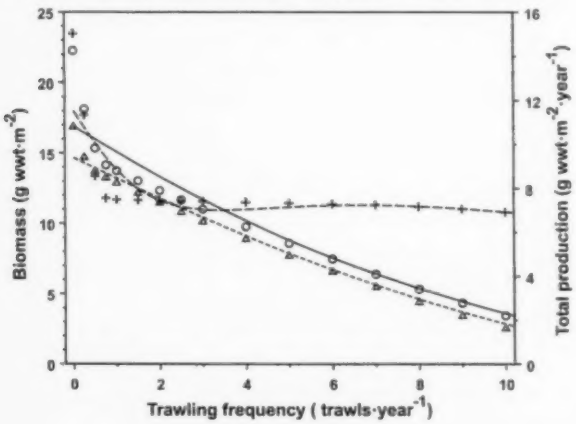

Accepted 14 August 2003. Received at NRC 16 October 2003. Published on the NRC Research Press Web site at http://cjfas.nrc.ca on 12 November 2003.
J16854E

D.E. Duplisea,[1,2] S. Jennings, K.J. Warr, and T.A. Dinmore. Centre for Environment, Fisheries and Aquaculture Science (CEFAS), Lowestoft Laboratory, Pakefield Road, Lowestoft, Suffolk, NR33 0HT, United Kingdom.

[1]Corresponding author (e-mail: duplisead@dfo-mpo.gc.ca).
[2]Present address: Institut Maurice-Lamontagne, CP 1000, Mont-Joli, QC G5H 3Z4, Canada.

 doi: 10.1139/F03-122 © 2003 NRC Canada

ERRATUM ERRATUM

Daniel E. Duplisea, Simon Jennings, Karema J. Warr, and Tracy A. Dinmore **1306** Erratum: A size-based model of the impacts of bottom trawling on benthic community structure

National Research Council Canada
Ottawa, Canada K1A 0R6

Conseil national de recherches Canada
Ottawa, Canada K1A 0R6

Postage paid at Ottawa
Publications mail
Registration No. 40062591

Port payé à Ottawa
Poste-publication
Enregistrement n° 40062591

USPS periodical postage paid at Champlain, N.Y.

Canadian Journal of Fisheries and Aquatic Sciences

Volume 60, Number 10, October 2003

Journal canadien des sciences halieutiques et aquatiques

Volume 60, numéro 10, octobre 2003

ARTICLES

Darren G. Bos and Brian F. Cumming	**1177–1189**	Sedimentary Cladoceran remains and their relationship to nutrients and other limnological variables in 53 lakes from British Columbia, Canada
Ross Claytor and Jacques Allard	**1190–1203**	Change-in-ratio estimates of lobster exploitation rate using sampling concurrent with fishing
Mark N. Maunder and Richard B. Deriso	**1204–1216**	Estimation of recruitment in catch-at-age models
Andre E. Punt	**1217–1228**	Extending production models to include process error in the population dynamics
Christian S. Reiss, Ian A. McLaren, and Patricia Avendaño	**1229–1244**	Horizontal and vertical distribution patterns, retention rates, and population dynamics of zooplankton on Western Bank, Scotian Shelf
Christine Barnard, Jean-Jacques Frenette, and Warwick F. Vincent	**1245–1257**	Planktonic invaders of the St. Lawrence estuarine transition zone: environmental factors controlling the distribution of zebra mussel veligers
Gary D. Marty, Terrance J. Quinn II, Greg Carpenter, Theodore R. Meyers, and Neil H. Willits	**1258–1265**	Role of disease in abundance of a Pacific herring (*Clupea pallasi*) population
Joseph L. Ebersole, William J. Liss, and Christopher A. Frissell	**1266–1280**	Thermal heterogeneity, stream channel morphology, and salmonid abundance in northeastern Oregon streams
Jean-Michel Weber, Gérard Brichon, and Georges Zwingelstein	**1281–1288**	Fatty acid metabolism in rainbow trout (*Oncorhynchus mykiss*) tissues: differential incorporation of palmitate and oleate
Adrian Jordaan and Joseph A. Brown	**1289–1298**	The risk of running on empty: the influence of age on starvation and gut fullness in larval Atlantic cod (*Gadus morhua*)

DISCUSSION

J.M. Preston and R.L. Kirlin	**1299–1300**	Comment on "Acoustic seabed classification: improved statistical method"
Pierre Legendre	**1301–1305**	Reply to the comment by Preston and Kirlin on "Acoustic seabed classification: improved statistical method"

Continued on inside back cover / Suite au verso

Canada

Printed in Canada by / Imprimé au Canada par
University of Toronto Press Inc.
Page production by / Mise en page par
NRC Research Press / Presses scientifiques du CNRC

0706-652X(200310)60:10;1-5